Deliverable D6.7

PRHYDE Results as Input for Standardisation

Report Status: FINAL

Report Date: 05 April 2023 (Revision 1.2)

Authors:

Nick Hart (ITM Power), Claus Due Sinding (Nel), Steve Mathison (First Element Fuel), Spencer Quong (Quong & associates, Inc. on behalf of Toyota Motor North America), Vincent Mattelaer (Toyota Motor Europe), Antonio Ruiz, Alexander Grab (Nikola), Alexander Kvasnicka, Christian Spitta (ZBT), Fouad Ammouri, Elena Vyazmina, Vincent Ren, Guillaume Lodier (Air Liquide), Quentin Nouvelot, Thomas Guewouo, Julien Martin, Dorine Crouslé, Nicola Benvenuti (ENGIE), Benoit Poulet (Shell), Christopher Kutz, Martin Zerta (Ludwig-Bölkow-Systemtechnik)

Confidentiality Level: PU – Public

Acknowledgement:

This project has received funding from the Fuel Cells and Hydrogen 2 Joint Undertaking (now Clean Hydrogen Partnership) under Grant Agreement No 874997. This Joint Undertaking receives support from the European Union's Horizon 2020 Research and Innovation programme, Hydrogen Europe and Hydrogen Europe Research.

Clean Hydrogen Partnership

Co-funded by the European Union

R E P O R T

Disclaimer

PRHYDE Deliverable D6.7 – PRHYDE Results as Input for Standardisation

Authors:

Nick Hart (ITM Power), Claus Due Sinding (Nel), Steve Mathison (First Element Fuel), Spencer Quong (Quong & associates, Inc. on behalf of Toyota Motor North America), Vincent Mattelaer (Toyota Motor Europe), Antonio Ruiz, Alexander Grab (Nikola), Alexander Kvasnicka, Christian Spitta (ZBT), Fouad Ammouri, Elena Vyazmina, Vincent Ren, Guillaume Lodier (Air Liquide), Quentin Nouvelot, Thomas Guewouo, Julien Martin, Dorine Crouslé, Nicola Benvenuti (ENGIE), Benoit Poulet (Shell), Christopher Kutz, Martin Zerta (Ludwig-Bölkow-Systemtechnik)

Revision History

Revision	Revision date	Summary of changes
1	**05.12.2022**	**Final version for publication**
1.1	**10.03.2023**	**Corrected Version** Correction in Eq. A. 46
1.2	**05.04.2023**	**Corrected Version** Corrections in Eq. A. 48, 51, 52 and explanations in B.2.2.2 and B.2.2.3

Checked by

Name	Company	Date
Christopher Kutz	**LBST**	**08.12.2022**

Approved by

Name	Company	Date
Nick Hart WP6 leader	**ITM Power**	**09.12.2022**
Christopher Kutz PRHYDE coordinator team	**LBST**	**09.12.2022**

CONTENTS

TABLES IX

FIGURES XI

EXECUTIVE SUMMARY XIV

REFERENCES XIX

DEFINITIONS XX

ABBREVIATIONS AND SYMBOLS XXI

1 INTRODUCTION 1

1.1 Modelling supporting the Fuelling Protocol Specification development 2

1.2 Experimentation supporting the Modelling and the Fuelling Protocol Specification development 3

2 FUELLING PROTOCOL TYPES 4

2.1 Protocol levels of communication usage 4

2.2 Protocol approach to fuelling parameters 4

2.3 Protocol fill control 5

2.4 Protocol types nomenclature 5

3 FINAL PROTOCOL 7

3.1 Advanced MC Formula Framework Fuelling Concepts 7

3.2 Description of each Fuelling Concept 9

3.2.1 Type 2-PR-S – Static Data 9

3.2.1.1 t_{final} Table Selection 9

3.2.1.2 t_{final} Vector Calculation 9

3.2.2 Type 3-PR-S – Dynamic Data T_{gas} Initial 9

3.2.2.1 t_{final} Table Selection 10

3.2.2.2 t_{final} Vector Calculation 10

3.2.3 Type 3-PR-S – Dynamic Data T_{gas} Initial+ 10

3.2.3.1 t_{final} Table Selection 10

3.2.3.2 t_{final} Vector Calculation 11

3.2.4 Type 3-PR-S – Dynamic Data T_{gas} Throttle 11

3.2.5 SOC Taper 15

3.2.6 Data Fluctuations 20

3.2.7 Final Notes on the Fuelling Protocol Development 27

4 GENERAL ASSUMPTIONS FOR PROTOCOL DEVELOPMENT 29

4.1 Components 29
4.1.1 Components for performance estimates 31
4.2 Communication 31
5 PERFORMANCE ESTIMATE 32
5.1 CHSS System Performance 32
5.1.1 Fuelling Protocols Compared 32
5.1.2 Simulation Results 33
5.1.3 Key Takeaways from Simulations 35
5.2 Single Tank Performance 36
5.2.1 Testing Results 36
5.2.2 Key Takeaways from Single Tank Testing 38
5.3 Interpretation of performance estimates 38
6 IMPLEMENTATION OF PRHYDE FUELLING CONCEPTS 39
6.1 Type 2-PR-S – Static 42
6.2 Type 3-PR-S – T_{gas} Initial 43
6.3 Type 3-PR-S – T_{gas} Initial+ 44
6.4 Type 3-PR-S – T_{gas} Throttle 45
7 HOW TO DERIVE T_{FINAL} VALUES 46
7.1 Fuelling model 46
7.2 Validation of the Fuelling Model 47
7.3 Model Capabilities 47
7.3.1 Pressure Ramp Rate 47
7.3.2 Simulation Conditions 47
7.3.3 Model Output 48
7.3.4 Automated Capabilities 48
7.4 Considerations 49
7.5 Inputting the CHSS configuration and properties to the fuelling model 50
7.6 Inputting the station side fuelling components to the fuelling model 51
7.7 Selecting the conditions used in the fuelling simulations 54
7.7.1 Common conditions 54
7.7.2 Specific conditions unique to each fuelling concept 55
7.7.2.1 Static fuelling concept 55
7.7.2.2 T_{gas} initial fuelling concept 56
7.7.2.3 T_{gas} initial+ fuelling concept 58

7.7.2.4 T_{gas} Throttle fuelling concept 60
7.8 Conducting the simulations and deriving the t_{final} values 61
7.8.1 Setting up the simulations 61
7.8.2 Generating the t_{final} tables....64
8 BRIEF PRESENTATION OF MODELLING TOOLS FOR PROTOCOL DEVELOPMENT 65
8.1 Simple Engineering models 65
8.2 SOFIL by Air Liquide 65
8.3 HyFill by Engie 66
8.4 H2FillS by NREL....66
8.5 H2-Fill by Wenger Engineering 68
8.6 Benchmark brief presentation, results and recommendations....68
8.7 CFD approach 69
9 EXPERIMENTAL VALIDATION OF THE MODELS.... 70
9.1 Experimental data....70
9.1.1 Tests performed at ZBT on the H70 240 L tank 70
9.1.2 Tests performed at ZBT on the 350 L H50 tank 71
9.1.3 Tests performed at ZBT on the 322 L H35 tank 72
9.1.4 Tests performed at Nikola on the 165 L H70 tank 73
9.2 Validation of engineering models....74
9.2.1 240 L type IV H70 tank at ZBT 74
9.2.2 350 L type IV H50 tank at ZBT 77
9.2.3 322 L type III H35 tank at ZBT 78
9.2.4 165 L type IV H70 tank at Nikola....79
9.3 Validation of CFD results 80
10 OUTCOME FROM MODELLING PERFORMED IN THE PRHYDE PROJECT 84
10.1 Conclusions (performance of the models)....84
10.2 Recommendations on modelling approach....84
10.2.1 Simple Engineering models 84
10.2.2 CFD 85
10.3 Recommendations on experimental measurements 86
11 PHASE 1 TESTING CAMPAIGN: PROVISION OF EXPERIMENTAL DATA FOR MODELLING VERIFICATION.... 87

11.1 Phase 1 ZBT Test Campaign....87
11.1.1 Test Matrix....87
11.1.2 Test Results....90
11.2 Phase 1 Nikola Test Campaign....93
11.2.1 Test Matrix....93
11.2.2 Test Results....94
12 PHASE 2 TESTING CAMPAIGN: PROTOCOL CONCEPT IMPLEMENTATION AND COMPARISON TESTING....95
12.1 Phase 2 ZBT Test Campaign....95
12.1.1 Test setup....95
12.1.2 Test Matrix....96
12.1.3 Test results....97
12.2 Phase 2 Nikola Test Campaign....98
12.2.1 Test Matrix....99
12.2.2 Test Results....100
13 FINDINGS AND RECOMMENDATIONS FROM EXPERIMENTAL WORK IN PHASES 1 & 2....101
13.1 Internal Gas Temperature Measurements....101
13.2 T_{gas} Throttle Parameters....102
13.3 Internal Gas Temperature Stratification....103
14 OVERALL SUMMARY OF WORK PERFORMED IN THE PRHYDE PROJECT AND KEY FINDINGS....104
APPENDIX A : FUELLING PROTOCOL ALGORITHMS....105
A.1 Fuelling Control....105
A.1.1 Advanced MC Formula Control Subroutines....105
A.1.1.1 Subroutine – Determine Initial Parameters....105
A.1.1.2 Subroutine – Parameter Initialization....106
A.1.1.3 Subroutine – Selection of t_{final} Table for Static Fuelling Concept....111
A.1.1.4 Subroutine – Selection of t_{final} Table for T_{gas} Initial Fuelling Concept....112
A.1.1.5 Subroutine – Selection of t_{final} Table for T_{gas} Initial+ Fuelling Concept....114
A.1.1.6 Subroutine – Selection of t_{final} Table for T_{gas} Throttle Fuelling Concept....121
A.1.1.7 Subroutine - t_{final} Vector Interpolation....122

A.1.1.8 Subroutine - Mass Average Calculation of the Fuel Delivery Temperature 123
A.1.1.9 Subroutine - Calculation of t_{final} 125
A.1.1.10 Subroutine - Calculation of PRR and P_{ramp} 126
A.1.1.11 Subroutine - Determine Communication Pressure Target 131
A.1.1.12 Subroutine - Evaluate End of Fill Criteria 132
A.1.1.13 Subroutine - Process Check 132
A.1.1.14 Subroutine - Advance Counters 133

APPENDIX B : LEARNINGS FROM PROTOCOL IMPLEMENTATION 135

B.1 Learnings from testing 135
B.2 Changes made to the fuelling protocol control specification............... 135
B.2.1 Changes made to Equation A.46 135
B.2.1.1 Original Equation 135
B.2.1.2 Revised Equation... 135
B.2.1.3 Explanation of changes.................................... 136
B.2.2 Changes made to Equation A.48 136
B.2.2.1 Original Equation 136
B.2.2.2 Revised Equation... 137
B.2.2.3 Explanation of changes.................................... 138
B.2.3 Changes made to Equation A.49 139
B.2.3.1 Original Equation 139
B.2.3.2 Revised Equation... 139
B.2.3.3 Explanation of changes.................................... 140
B.2.4 Changes made to Equation A.50 140
B.2.4.1 Original Equation 140
B.2.4.2 Revised Equation... 141
B.2.4.3 Explanation of changes.................................... 142
B.2.5 Changes made to Equation A.53 142
B.2.5.1 Original Equation 142
B.2.5.2 Revised Equation... 142
B.2.5.3 Explanation of changes.................................... 143

APPENDIX C : TEST FACILITIES AND EQUIPMENT UTILISED DURING THE PRHYDE PROJECT 144

C.1 General 144
C.2 Test layout at ZBT HYDROGEN TESTFIELD 144
C.3 Summary of Nikola's Contracted Test Facility (TesTneT Gmbh)......... 145

APPENDIX D : TEST RESULTS 147

D.1 ZBT Phase 1 testing results 147
D.2 Nikola Phase 1 testing results 150
D.3 ZBT Phase 2 testing results 151
D.4 Nikola Phase 2 testing results 157

APPENDIX E : RISK ASSESSMENT 159

E.1 Executive Summary 159
E.2 Acronyms and Abbreviations 161
E.3 Introduction 162
E.4 Methodology 163
E.4.1 Scope 163
E.4.2 Bowtie Framework 163
E.4.3 LOPA Framework 165
E.5 Output 167
E.5.1 Threat – Wrong Pressure Ramp Rate resulting in high tank temperature 167
E.5.1.1 T_{Fuel} Error 168
E.5.1.2 Mass Flow Error 169
E.5.1.3 Station Pressure Error 170
E.5.1.4 Ambient Temperature Error 171
E.5.1.5 T_{gas} (Vehicle) for fuelling history error 172
E.5.1.6 T_{gas} (Vehicle) for fuelling history and T_{soak} error 173
E.5.1.7 T_{gas} (Vehicle) error 174
E.5.2 Preventive Barriers 175
E.5.2.1 Redundant Sensor Monitoring (Station) 175
E.5.2.2 Redundant Sensor Monitoring (Vehicle) 175
E.5.2.3 High MT / Vehicle Abort Signal 175
E.5.2.4 Shut-off Valve (Vehicle) 175
E.5.2.5 Safety Max PRR Limit 175
E.5.2.6 Qualify the CHSS to 95°C 176
E.5.2.7 Vehicle record last refuelling 176
E.5.2.8 Integrity barrier 176
E.5.3 Modifiers (Left Side of Bowtie) 177
E.5.3.1 Probability of loss of containment for single event exposures 177
E.5.3.2 Maximum CHSS Gas Temperature due to Initiating Events 178

E.5.3.3 Probability of loss of containment for repeated exposures 181
E.5.4 Mitigative Barriers, Modifiers 184
E.5.4.1 Mitigative Barriers general 184
E.5.4.2 Hydrogen detector (Station) 184
E.5.4.3 Hydrogen detector (Vehicle) 184
E.5.4.4 Ultrasonic leak detector (Station) 184
E.5.5 Tolerability 185
E.5.5.1 Modifiers (Consequence): 186
E.5.5.2 Consequences: 186
E.5.5.3 Jet fire from the vehicle tank leading to single fatality 187
E.5.5.4 Flash fire / explosion leading to multiple fatalities 187
E.6 Output of Bowtie-LOPA 188
E.6.1 Static 188
E.6.2 T_{gas} initial 188
E.6.3 T_{gas} initial + ... 188
E.6.4 T_{gas} throttle 189
E.6.4.1 Additional barriers to achieve the target probability 189
E.7 Non-scored threats 190
E.7.1 Development, implementation and maintenance of Fuelling Parameters 190
E.8 Highlights of specific risks 192
E.9 Conclusion 193

TABLES

Table 1: Summary of PRHYDE concepts xv
Table 2: Protocol levels of communication usage 4
Table 3: Protocol approach 4
Table 4: Protocol fill control 5
Table 5: Example of a t_{final} table 8
Table 6: Data type for each fuelling protocol approach 31
Table 7: Fuelling simulations common to all fuelling concepts 54
Table 8: Fuelling simulations unique to the Static fuelling concept 55
Table 9: Parameters utilized for each t_{final} table with Static fuelling concept 56
Table 10: Fuelling simulations unique to the T_{gas} Initial fuelling concept 56
Table 11: Parameters utilized for each t_{final} table with T_{gas} Initial fuelling concept 57
Table 12: Fuelling simulations unique to the T_{gas} Initial+ fuelling concept 58
Table 13: Parameters utilized for each t_{final} table with T_{gas} Initial+ fuelling concept 59
Table 14: Fuelling simulations unique to the T_{gas} Throttle fuelling concept 60
Table 15: Parameters utilized for each t_{final} table with T_{gas} Throttle fuelling concept 61
Table 16: Test matrix for 240 L H70 tank at ZBT 70
Table 17: Test matrix for the 350 L H50 tank at ZBT 71
Table 18: Test matrix for the 322 L H35 tank at ZBT 72
Table 19: Test matrix for the 165 L H70 tank at Nikola 73
Table 20: Test matrix for ZBT test campaign (Phase 1) 87
Table 21: Test Results for the ZBT test campaign (Phase 1) 90
Table 22: Test matrix for Nikola test campaign (Phase 1) 93
Table 23: Test Results for Nikola test campaign (Phase 1) 94
Table 24: Test matrix for ZBT test campaign (Phase 2) 96
Table 25: Test Results for ZBT test campaign (Phase 2) 97
Table 26: Test matrix for Nikola test campaign during (Phase 2) 99
Table 27: Test Results for Nikola test campaign (Phase 2) 100
Table 28: Overview of applicable Initiating Events for each of the Fuelling Concepts 167
Table 29: Preventive barriers identified for Fuel Temperature Error 168
Table 30: Preventive barriers identified for Mass Flow Error 169
Table 31: Preventive barriers identified for Station Pressure Error 170
Table 32: Preventive barriers identified for Ambient Temperature Error 171
Table 33: Preventive barriers identified for Gas Temperature for Fuelling History Error 172
Table 34: Preventive Barriers Identified for Gas Temperature for Fuelling History and Soak Error 173
Table 35: Preventive Barriers Identified for Gas Temperature Error 174
Table 36: Probabilities of Loss of Containment for three cases 177

Table 37: Enabling factors for fuelling concepts 183
Table 38: Excerpt of UK HSE Process Safety Leadership Group Final Report 185
Table 39: Bowtie-LOPA output for Fuelling Concept: Static....188
Table 40 Bowtie-LOPA output for Fuelling Concept: Tgas Initial 188
Table 41 Bowtie-LOPA output for Fuelling Concept: Tgas Initial+ 188
Table 42 Bowtie-LOPA output for Fuelling Concept: Tgas throttle....189
Table 43 Required additional PFD to achieve target for fuelling concept: Tgas Throttle....189
Table 44 T-final implementation - Potential Threats and Potential Mitigative Barriers....190

FIGURES

Figure 1: Protocol Types Nomenclature with PRHYDE fuelling concepts xvi
Figure 2: Protocol Types Nomenclature with PRHYDE fuelling concepts 6
Figure 3 Derivation of t_{final} values 8
Figure 4: Throttle approach 12
Figure 5: Sensitivity of the original T_{gas} Throttle concept to $T_{threshold}$ 13
Figure 6: Control logic for revised adaptable T_{gas} Throttle 14
Figure 7: Performance and variables for revised adaptable T_{gas} Throttle 15
Figure 8: Derivation of t_{final} with maximum dispenser pressure constraint 16
Figure 9: Derivation of t_{final} without maximum dispenser pressure constraint and illustration of P_{ramp} hold approach using this t_{final} value 17
Figure 10: Illustration of the SOC Taper Concept 18
Figure 11: Comparison between No SOC Taper (left) and SOC Taper approach (right) 20
Figure 12: Fluctuations in CHSS gas temperature for four LD FCVs 21
Figure 13: Illustration of noise function in NREL's H2FillS fuelling model 21
Figure 14: Illustration of triple moving average smoothing function 22
Figure 15: Example of PRR control with TMA applied to noisy T_{gas_high} 23
Figure 16: Illustration of the measurement of T_{gas_diff} and $T_{gas\_diff\_max}$ 24
Figure 17: Throttling region where T_{gas_high} and T_{gas_smooth} are relatively flat 25
Figure 18: Illustration of self-adjusting parameters in T_{gas} Throttle 26
Figure 19: Fuelling Time Comparison: T_{amb} = 35 °C, T_{soak} = 40 °C 34
Figure 20: Fuelling Time Comparison: T_{amb} = 35 °C, T_{soak} = 35 °C 34
Figure 21: Fuelling Time Comparison: T_{amb} = 35 °C, T_{soak} = 30 °C 35
Figure 22: Fuelling Time Comparison: Tamb = 35 °C, T_{gas} Initial = 35 °C 37
Figure 23: Fuelling Time Comparison: T_{amb} = 35 °C, T_{gas} Initial= 25 °C 37
Figure 24: Flow Diagram for Type 2-PR-S Static Data Fuelling Concept 42
Figure 25: Flow Diagram for Type 3-PR-S T_{gas} Initial Fuelling Concept 43
Figure 26: Flow Diagram for Type 3-PR-S T_{gas} Initial+ Fuelling Concept 44
Figure 27: Flow Diagram for Type 3-PR-S T_{gas} Throttle Fuelling Concept 45
Figure 28: GUI for NREL's H2FillS model (Source: H2FillS) 47
Figure 29: "Set fill profile" window from NREL's H2FillS model (Source: H2FillS) 49
Figure 30: Example of fuelling model inputs for a "pipe" element in the CHSS (Source: H2FillS) 50
Figure 31: Example of fuelling model inputs for a "pipe" element in the CHSS (Source: H2FillS) 50
Figure 32: Example of fuelling model inputs for a "hand valve" element in the CHSS (Source: H2FillS) 51

Figure 33: Example of fuelling model inputs for a “tank” element in the CHSS (Source: H2FillS) 51
Figure 34: Example of fuelling model inputs for the breakaway fitting (Source: H2FillS) 52
Figure 35: Example of fuelling model inputs for the hose (Source: H2FillS) 53
Figure 36: Example of fuelling model inputs for the nozzle/receptacle coupling (Source: H2FillS) 53
Figure 37: Example of setting the model inputs for a complete set of simulations (Source: H2FillS)....62
Figure 38: Example of setting the model inputs for generating $APRR_{max}$ (Source: H2FillS) 63
Figure 39: P&ID of the experimental setup for the H70 tank at ZBT....71
Figure 40: P&ID of the experimental setup for the H50 tank at ZBT....72
Figure 41: P&ID of the experimental setup for the H35 tank at ZBT....73
Figure 42: P&ID of the experimental setup for the H70 tank at Nikola 74
Figure 43: HyFill model outputs and experimental measurements for test #2 on the 240 L type IV H70 tank at ZBT facilities....75
Figure 44: Comparison between experimental temperature and HyFill output temperature in the tank for 15 filling tests on the 240 L type IV H70 tank at ZBT 76
Figure 45: HyFill model outputs and experimental measurements for test #26 on the 350 L type IV H50 tank at ZBT facilities....77
Figure 46: Comparison between experimental temperature and SOFIL output gas temperature in the tank for 18 filling tests on the 322 L type III H35 tank at ZBT....78
Figure 47: Comparison between experimental temperature and SOFIL output gas temperature in the tank for 18 filling tests on the 165 L type IV H70 tank at Nikola 79
Figure 48: Positions of the temperature probes on the thermocouple tree inside the tank 80
Figure 49: Temperature measured at the different probes during the test#2. Refer to the previous Figure 48 for the color legend....80
Figure 50: Temperature measured at the different probes during the test#14. Refer to the previous Figure 48 for the color legend....81
Figure 51: Expected fluid behavior during the filling for both experiments....81
Figure 52: Two different turbulence models lead to two different flow organizations and thus to two thermal behaviors within the tank 83
Figure 53: Sun Protection on the 70 MPa ZBT Tank (Source: ZBT) 95
Figure 54: Figures showing the difference between temperature reading with different OTV-tank combinations 102
Figure 55: Experimental setup ZBT test site (Source: ZBT)....144
Figure 56: 35MPa type 3 tank (322L) (Source: ZBT) 144
Figure 57: 50MPa type 4 tank (341L) (Source: ZBT) 145
Figure 58: 70MPa type 4 tank (240L) (Source: ZBT) 145
Figure 59: Experimental Set-up Nikola test site (Source: Nikola)....146

Figure 60: ZBT Tank Test #17 147
Figure 61: ZBT Tank Test #19 148
Figure 62: ZBT Tank Test #47 149
Figure 63: Nikola Test #1 150
Figure 64: ZBT Tank Test #1 151
Figure 65: ZBT Tank Test #2 152
Figure 66: ZBT Tank Test #3 153
Figure 67: ZBT Tank Test #4 154
Figure 68: ZBT Tank Test #5 155
Figure 69: ZBT Tank Test #6 156
Figure 70: Nikola Protocol Concept Test #1 157
Figure 71: An example bowtie 163
Figure 72: LOPA methodology 165
Figure 73: LOPA residual risk frequency calculation 165
Figure 74: Effect of error on T_{fuel} (or Mass Flow) 179
Figure 75: Effect of error on T_{amb} measurement 15°C, but actual is 30°C 180
Figure 76: Effect of error on T_{amb} measurement 15°C, but actual is 50°C 180

Executive Summary

The **PRHYDE project (PRotocol for heavy duty HYDrogEn refuelling)**, running between January 2020 and September 2022, had the aim to develop recommendations for a non-proprietary heavy duty refuelling protocols used for future standardization activities for trucks and other heavy duty transport systems applying hydrogen technologies. It has received funding from the Fuel Cells and Hydrogen 2 Joint Undertaking (now Clean Hydrogen Partnership) under Grant Agreement No 874997.

The **PRHYDE consortium** involved partners from Europe and America, namely Air Liquide, Commissariat à l'énergie atomique et aux énergies alternatives (CEA), ENGIE, ITM Power, Ludwig-Bölkow-Systemtechnik (LBST), Nikola Cooperation, Nel, Shell, Toyota Motor Europe (TME), Toyota Motor North America (TMNA), and Zentrum für BrennstoffzellenTechnik (ZBT).

Based on existing fuelling protocols and current state of the art for compressed gaseous hydrogen fuelling, **different hydrogen fuelling protocol concepts were developed** for large tank systems with 35, 50, and 70 MPa nominal working pressures using simulations, as well as, experimental verification. A broad industry perspective was captured via an intense **stakeholder participatio**n process with several workshops throughout the project. In this context, the PRHYDE consortium thanks the following companies and institutions for their contribution to the project (in alphabetical order): Bennett Pump, Daimler Truck, FirstElement Fuel, Hexagon Purus, Honda, LifteH2, Luxfer, National Renewable Energy Laboratory (NREL), National Technology & Engineering Solutions of Sandia, LLC (NESS), Risktec, Savannah River National Laboratory (SRNL) and TÜV SÜD Rail.

The work summarized in this document will enable the widespread deployment of hydrogen for heavy duty applications in road, train, and maritime transport. The results are a valuable guidance for station design but also the prerequisite for the deployment of a standardized, cost-effective hydrogen infrastructure.

The PRHYDE project has formulated **new fuelling protocol concepts for heavy duty segment**. These PRHYDE fuelling concepts & methodologies target high performance hydrogen fuelling of heavy duty (HD) vehicles by optimizing the refuelling time, the amount of real H_2 refuelling quantity and the energy efficiency by reducing demand for pre-cooling requisite.

The PRHYDE protocol concepts are based on the MC Formula Framework known from SAE J2601 standard, allowing a number of previously defined parameters to be reused and referenced. A shift in use of communicated data prepares the PRHYDE protocol concepts to be adaptable to future component and technology advances in the hydrogen automotive industry. Key element of the PRHYDE H_2 refuelling concepts considers advanced communication between HRS and vehicle which results in an increasingly relying on the data communicated from vehicle to station.

A map of Protocol Types was developed based on Protocol Levels (of communication usage), Protocol Approach (to fuelling parameters) and Protocol Fill Control. Out of

the various Protocol Types available, four concepts were defined. Following the applied nomenclature presented in Figure 1, these concepts can be described as follows:

Table 1: Summary of PRHYDE concepts

Concept	Summary
Type 2-PR-S Static Data	CHSS gas temperature is <u>not</u> taken into account. CHSS temperature is assumed to be at hot-soak conditions.
Type 3-PR-S Dynamic Data – T_{gas} Initial	CHSS gas temperature is used to screen for fuelling history, which if absent allows higher P_{min} values to be used based on $P_{initial}$.
Type 3-PR-S Dynamic Data – T_{gas} Initial+	CHSS gas temperature is taken into account. CHSS gas temperature is used to choose a set of t_{final} tables with different CHSS soak temperatures in combination with different P_{min} values based on $P_{initial}$.
Type 3-PR-S Dynamic Data – T_{gas} Throttle	CHSS gas temperature is taken into account. The actual CHSS gas temperature (T_{gas_high}) is used to reduce the pressure ramp rate (PRR) when a threshold temperature is reached. The t_{final} table is derived with a higher CHSS gas temperature (e.g. 95 C) facilitating faster fuelling in the early portion of the fill.

PR = Prescriptive: A fuelling protocol whereby the fuelling rate and end of fill conditions are specifically defined as a function of the fuelling conditions.

PB = Performance: A fuelling protocol whereby the fuelling rate and end of fill conditions are not always fully defined and the implementor must determine them such that the vehicle and station systems stay within the allowed operational limits.

The four concepts were described in great detail in this project. The concepts increasingly rely on the data communicated from vehicle to station. Accordingly, this increased reliance on data between vehicle and station must be countered with increased reliability of communication loop, as discussed in a provisional Risk Assessment performed in PRHYDE.

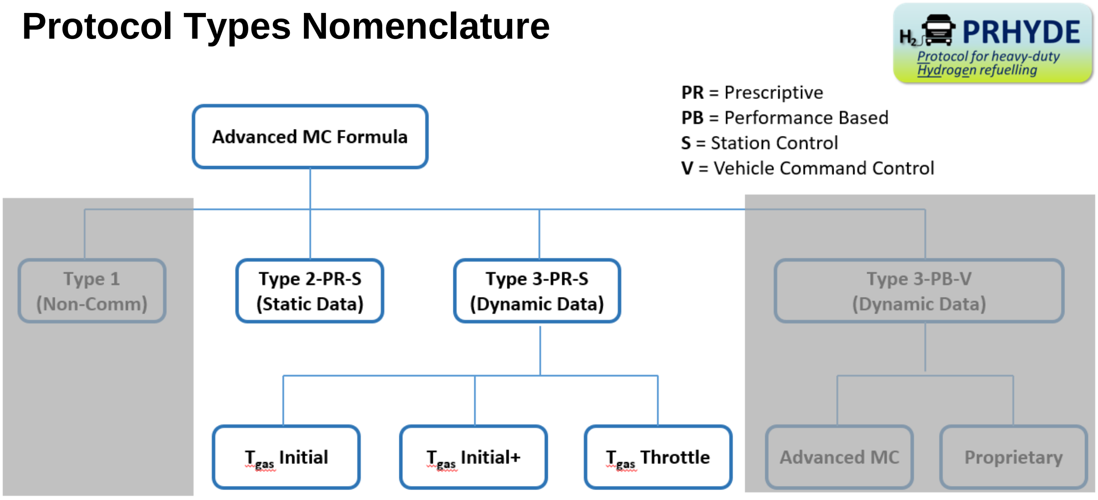

Figure 1: Protocol Types Nomenclature with PRHYDE fuelling concepts

As mentioned above, all the fuelling concepts operate within a common control framework denoted as Advanced MC Formula. This means that a vehicle can choose which fuelling concept to utilize and the station can implement the MC Formula control logic under this unified framework. Each of these concepts have advantages and disadvantages, so by providing a variety of concepts, a vehicle OEM can utilize the concept that best meets their objectives.

Complementary to the four PRHYDE fuelling concepts, a protocol feature that can apply to all concepts was also developed. This feature, the so-called SOC Taper, can adjust the fuelling speed when station meets non-ideal situations such as low storage capacity or high flow restrictions.

Testing to validate the simulation tools, and field tests proving the refuelling concepts were conducted at different test facilities . Field tests and further analysis led to optimizations of the PRHYDE concepts; especially for the T_{gas} Throttle concept.

The development of a refuelling protocol requires a **validated approach by applying different simulation approaches**. Due to the limited time and budget, the experimental data cannot cover the whole possible ranges of protocol parameters such as initial pressure P, temperature T, ambient and precooling temperatures, pressure ramp, refuelling time, hardware specifications etc.

In the context of PRHYDE project, two numerical approaches are applied:

1. Thermodynamic modelling which gives the heat parameters estimation in the gas (volume average temperature) and 1D temperature distribution in the tank wall. In the PRHYDE projects, two in-house engineering numerical tools (0D in the gas and 1D in the tank walls) are used: SOFIL by Air Liquide and HyFill by Engie. In addition, the H2FillS modelling software by NREL supported the modelling efforts.

2. Computational Fluid Dynamics (CFD) approach gives a detailed temperature, pressure, velocity 3D mapping of the spatial distribution inside the tank (both gas and walls). However, this approach is very expensive in terms of the CPU

calculation time. Therefore, it was only used as a complementary approach on selected cases to better understand physical behaviour of the flow and the associated heat distribution inside the tank.

Both of these approaches, however, also require a careful validation versus the experimental data in the conditions similar to the final usage: shapes of tank (the aspect ratio of the tank's length to its diameter), temperature ranges (initial and pre-cooling), pressure ramps and mass flow rates etc.

Therefore, an **experimental test campaign on different test sites** was conducted to validate the modelling efforts and provide proof-of-concept that the protocol concepts work as intended. In the context of the PRHYDE project, four single hydrogen tanks were tested at two different test sites (at ZBT's test facility in Duisburg, Germany and a test facility commissioned by Nikola) under different fuelling conditions.

ZBT tested three single tanks: a 70 MPa nominal pressure Type IV tank, a 50 MPa nominal pressure Type IV tank and a 35 MPa nominal pressure Type III tank. In addition, Nikola tested another 70 MPa nominal pressure Type IV tank. Each of the four tanks was instrumented with a thermocouple tree (TC) containing up to 16 thermocouples, providing detailed insights on the thermal behaviour of the gas during fuelling.

Two discrete testing phases were conducted during the PRHYDE project:

- Phase 1 (May 2021 – April 2022) focused on generating experimental data for model verification purposes.
- Phase 2 (May 2022 – August 2022) focused comparison of experimental results to the performance simulations, and for protocol implementation testing.

Please note: Due to time constraints and supply chain issues, an additional testing phase, Phase 3, focussing on full system testing of the PRHYDE protocol concepts could not be started and will be conducted after the end of the PRHYDE project. The tests will be performed at NREL's and possibly other testing facilities.

Ultimately **performance estimates** of the developed PRHYDE protocol concepts were conducted based on simulations and referenced for implications on how these fuelling concepts can improve fuelling time in the heavy duty segment. Although there are still some unknowns which will influence the absolute fuelling performance (such as the thermophysical properties of the station side fuel dispensing components), the simulations and testing have demonstrated the positive impact of PRHYDE fuelling concepts on fuelling performance. The simulations indicated the concepts to have significant reductions in fuelling time due to the elimination of many of the inherent embedded worst-case assumptions. Fuelling times less than 10 minutes can be realized under all fuelling conditions and with the Type 3 PRHYDE fuelling concepts (T_{gas} Initial, T_{gas} Initial+ and T_{gas} Throttle). Furthermore, fuelling times less than five minutes can be realized under many typical fuelling conditions.

To ensure information transfer of the PRHYDE results into ongoing **standardization activities**, several members of the PRHYDE consortium and also members of the external expert group are involved in different committees, including ISO TC 197/WG24, SAE FCEV Interface Task Force (ITF), CEN/TC 268 WG5 and others, see PRHYDE **Deliverable 6.8**. This PRHYDE Deliverable D6.7 will serve as main project output for further standardization activities.

References

Documents

SAE J2601 202005	Fueling Protocols for Light Duty Gaseous Hydrogen Surface Vehicles
PRHYDE D2.1	Performance metrics for refuelling protocols for heavy duty hydrogen vehicles
PRHYDE D2.2	State of the Art on Refuelling Risk Assessment
PRHYDE D2.3	Gap analysis of existing heavy duty gaseous hydrogen vehicle refuelling protocol
PRHYDE D2.4	Gap analysis of existing hardware used for heavy duty gaseous hydrogen vehicle refuelling
PRHYDE D2.6	Requirements for a future refuelling protocol
PRHYDE D6.2	Final dissemination and exploitation plan
PRHYDE D6.8	PRHYDE: Topics for Further Work

All public deliverables of the PRHYDE project are available here: https://prhyde.eu.

Tools

H2FillS	Simulation tool by NREL – National Renewable Energy Laboratory. H2FillS: Hydrogen Filling Simulation | Hydrogen and Fuel Cells | NREL
NIST	National Institute of Standards and Technology Thermophysical Properties of Fluid Systems (nist.gov)

DEFINITIONS

Fuelling Protocol types:

- Prescriptive: A fuelling protocol whereby the fuelling rate and end of fill conditions are specifically defined as a function of the fuelling conditions.
- Performance: A fuelling protocol whereby the fuelling rate and end of fill conditions are not always fully defined and the implementor must determine them such that the vehicle and station systems stay within the allowed operational limits.

Definitions related to the MC Formula Framework are defined in SAE J2601[1].

1 S. I. W. Group, „SAE J2601-2020 Fueling Protocols for Light Duty Gaseous Hydrogen Surface Vehicles," SAE International, Detroit, 05/2020.

Abbreviations and Symbols

0D	Zero-Dimensional
1D	One-Dimensional
2D	Two-Dimensional
3D	Three-Dimensional
APRR	Average Pressure Ramp Rate (MPa/min)
CFD	Computational Fluid Dynamics
CFL	Courant-Friedrichs-Levy
CFRP	Carbon Fiber Reinforced Polymer
CHSS	Compressed Hydrogen Storage System
CPU	Central Processing Unit
ECU	Electronic Control Unit
FCEV	Fuel Cell Electric Vehicle
FCV	Fuel Cell Vehicle
H_2	Hydrogen
HRS	Hydrogen Refuelling Station
IrDA	Infrared Data Association
LES	Large Eddy Simulation
MAT	Mass Average of Tfuel
MAWP	Maximum Allowable Working Pressure
NIST	National Institute of Standards and Technology
NREL	National Renewable Energy Laboratory
NWP	Nominal Working Pressure
OEM	Original Equipment Manufacturer
OTV	On Tank Valve
P&ID	Piping and Instrumentation Diagram
PRR	Pressure Ramp Rate
RSM	Reynolds Stress Model
SAE	Society of Automotive Engineers
SAS	Scale Adaptive
SOC	State of Charge
SOCRR	SOC Ramp Rate
SST	Shear Stress Transport
TC	Thermocouple
TMA	Triple Moving Average
WP	Work Package
ZBT	Zentrum für BrennstoffzellenTechnik

ΔP	A value representing the calculation of the current ramp pressure P_{ramp} minus the current CHSS pressure MP
ΔP_{max}	The maximum ΔP measured during the fill up to and including the current timestep.
ΔP_{tol_high}	A delta pressure added to P_{ramp} to define P_{limit_high}. Also used in calculating β
$\dot{m}$	The mass flow rate of dispensed hydrogen
a	A parameter utilized only in the T_{gas} Throttle fuelling concept. The recommended values are provided in Appendix A.
AD	A parameter utilized only in the T_{gas} Throttle fuelling concept and represents an input value to the $PRR_{throttle}$ equation.
b	A parameter utilized only in the T_{gas} Throttle fuelling concept. The recommended value is provided in Appendix A.
j	A calculation time step counter, which advances every second
m	The total mass dispensed from the beginning of the main fuelling time up to the current time
MAT_0	The mass average of $T_{fuel\text{-}inst}$ calculated from the start of the main fuelling time (i.e., t = 0 seconds)
MAT_{30}	The mass average of $T_{fuel\text{-}inst}$ calculated starting after a total of 30 seconds of mass flow have elapsed
MAT_C	A mathematical combination of $MAT_{expected}$, MAT_{30}, and MAT_0 utilized as the control input for the t_{final} equation
$MAT_{expected}$	The expected mass average of the fuel delivery temperature at the end of the fill
MP	The CHSS measured pressure communicated via IRDA according to SAE J2799
n	A counter which advances at the same frequency as time step counter j, but only if there is mass flow. It is utilized to determine the point in the fill at which the calculation of MAT_{30} commences
P_{final}	The final pressure used in the derivation of the t_{final} equation coefficients, set at 1.25 x NWP
$P_{initial}$	Initial pressure of hydrogen in the CHSS as per the definition in Section 3.11.3 in SAE J2601
P_{limit_high}	The upper boundary of the pressure corridor which $P_{station}$ must stay within
P_{min}	The initial pressure used in the derivation of the t_{final} equation coefficients
P_{ramp}	The pressure upon which the PRR is based and which defines the station target pressure for each time step. Also used to define P_{limit_high}

P_{ramp_target}	This is a setpoint value in the dispenser and represents the maximum ramp pressure that the dispenser can achieve. It is utilized in the SOC Taper approach. It is typically set slightly lower than the MAWP.
PRR	The pressure ramp rate used to calculate the ramp pressure for the next time step. It is the minimum of PRR_{MC}, PRR_{SOC} (when it is calculated) and $PRR_{throttle}$ (when it is calculated). Units are MPa/sec.
PRR_{MC}	A pressure ramp rate calculated using the MC Formula pressure ramp rate equation.
PRR_{SOC}	A pressure ramp rate calculated using the SOC Taper pressure ramp rate equation.
$PRR_{threshold}$	A parameter utilized only in the T_{gas} Throttle fuelling concept and represents an input value to the $PRR_{throttle}$ equation. It is a function of P_{final}, P_{min}, and t_{final}.
$PRR_{throttle}$	A pressure ramp rate calculated using the T_{gas} Throttle pressure ramp rate equation.
$P_{station}$	Fuelling pressure as measured by station at the dispenser outlet
P_{target_comm}	The target end of fill pressure for communication fills
$P_{threshold}$	A parameter utilized in the SOC Taper approach. It is a function P_{ramp_target} and ΔP.
P_{trans}	A parameter which determines the weighting of MAT_0 and MAT_{30} in the MAT_C equation
RR_{max}	The maximum calculated pressure ramp rate throughout the fill
RR_{min}	The minimum calculated pressure ramp rate throughout the fill
SOC_{target}	The end of fill target SOC, used in calculating P_{target_comm}. Expressed in percentage
t	Fuelling time, representing the total time elapsed since the initiation of the main fuelling time, including the time elapsed during intended non-fuelling events
T_{amb}	Ambient temperature as measured by fuelling station, not in direct sunlight
t_{final}	The time required to fill from P_{min} to P_{final}. Input to the PRR equation. Units are in minutes.
t_{final_sec}	The t_{final} value represented in seconds.
T_{fuel}	Fuel Delivery Temperature
T_{fuel_inst}	Instantaneous fuel delivery temperature measured at the dispenser outlet
$T_{fuel\_inst\_A}$, $T_{fuel\_inst\_B}$	Two independent measurements of the instantaneous fuel delivery temperature for redundancy

T_{gas_diff} A measurement of the difference between the current Tgas_high and the current T_{gas_smooth}. This measurement is only conducted in the T_{gas} Throttle fuelling concept with self-adjusting parameters utilized.

$T_{gas\_diff\_factor}$ A parameter utilized only in the T_{gas} Throttle fuelling concept with self-adjusting parameters utilized. The recommended value is provided in Appendix A.

$T_{gas\_diff\_max}$ The maximum T_{gas_diff} measured during the fill up to and including the current timestep.

T_{gas_high} The highest value of the bulk average gas temperature in a multi-tank CHSS.

T_{gas_low} The lowest value of the bulk average gas temperature in a multi-tank CHSS.

T_{gas_max} A parameter utilized only in the T_{gas} Throttle with self-adjusting parameters fuelling concept which represents the maximum T_{gas_high} value the vehicle allows. This value is typically 85 °C, although the vehicle can communicate a higher value.

$T_{gas\_offset\_multiplier}$ A parameter utilized only in the T_{gas} Throttle fuelling concept with self-adjusting parameters utilized. The recommended value is provided in Appendix A.

T_{gas_smooth} A parameter utilized only in the T_{gas} Throttle fuelling concept with self-adjusting parameters utilized. It is a triple moving average of T_{gas_high} where the moving average length is defined by TMAL.

$T_{gas\_smooth\_offset}$ A parameter utilized only in the T_{gas} Throttle fuelling concept with self-adjusting parameters utilized. The recommended value is provided in Appendix A.

T_{gas_target} A parameter utilized only in the T_{gas} Throttle fuelling concept which represents the maximum T_{gas_high} value the dispenser utilizes in the control algorithm. When self-adusting parameters are utilized, T_{gas_target} is a function of T_{gas_max}. When self-adjusting parameters are not utilized, T_{gas_target} represents T_{gas_max}.

T_{hot_soak} A temperature typically warmer than the ambient temperature that represents the warmest temperature the CHSS is expected to be soaked at (gas, liner walls) prior to fuelling. This temperature is defined in SAE J2601 by an equation.

$t_{lookback\_SOC}$ A setpoint value in the dispenser which represents the number of timesteps backwards that a previous SOC value is compared with the SOC value for the current timestep. This value is utilized in the SOC Taper approach.

TMAL A parameter utilized only in the T_{gas} Throttle fuelling concept with self-adjusting parameters utilized. The recommended value is provided in Appendix A.

t_{remain_SOC}	A parameter utilized in the SOC Taper approach. It represents the time remaining for the SOC to reach SOC_{target} at the current rate of change. It is utilized as an intermediary calculation in determining PRR_{SOC}.
$T_{threshold}$	A parameter utilized only in the T_{gas} Throttle fuelling concept. It is a function of the parameters T_{gas_target}, a, and ΔP_{max} and determines when the T_{gas} Throttle method is activated.
α	A parameter which is multiplied by t_{final} to compensate for non-linearity in the PRR during the fill
β	A parameter which is multiplied by t_{final} to allow tolerance on pressure, i.e., the pressure corridor

Additional symbols not defined in SAE J2601 are listed below:

T_{gas_high}	The highest value of the bulk average gas temperature in a multi-tank CHSS.
T_{gas_low}	The lowest value of the bulk average gas temperature in a multi-tank CHSS.

1 INTRODUCTION

This report documents the final output of the PRHYDE (Protocol for Heavy Duty Hydrogen Refuelling) project, combining:

1. The final Fuelling Protocol Specification developed during the PRHYDE Project;
2. Modelling supporting the Fuelling Protocol Specification development;
3. Experimentation supporting the Modelling and the Fuelling Protocol Specification development.

Specific proposals for future work necessary are captured in the PRHYDE **Deliverable 6.8**[2] that accompanies this report.

Following on from the initial analysis of the State of the Art of refuelling protocols for the refuelling of hydrogen powered heavy duty vehicles, published in PRHYDE Deliverables 2.1 to 2.6, this report provides detail on the approach that the PRHYDE consortium believes to be appropriate to take forward to the Standards Development Organisations identified in PRHYDE **Deliverable 2.3** (and PRHYDE **Deliverable 2.4**) to contribute to the development of standards for the refuelling of gaseous hydrogen powered heavy duty vehicles.

The PRHYDE consortium have followed a programme of modelling and experimental work to support the development of the Fuelling Protocol Specification, and a summary of this activity is also provided in this report.

Chapters 1.1 to 1.3 below give a short summary for each of these areas of activity within the project, with Chapters 2 to 7 providing an in-depth explanation of the Fuelling Protocol Specification, Chapters 8 to 10 describing the supporting modelling and Chapters 11 to 13 describing the supporting experimental work. The overall project summary with final conclusions is included in Chapter 14.

Further relevant information is included in the Appendices referred to within the relevant parts of the document.

The current SAE J2601 fuelling protocols for gaseous fuel cell electric vehicles is based on the philosophy that:

- The hydrogen fuelling station is fully responsible for safe fuelling of the vehicle.
- Limited information is communicated from the vehicle that can be used for safety related functions (i.e. only used for improving fill quality).
- Worst case boundary conditions are assumed.

[2] All public PRHYDE Deliverables are available for download here: https://prhyde.eu.

The combination of these elements results in a significant margin between the estimated and final CHSS temperature and the end of fuelling. This causes the fuelling to either take longer than needed or pre-cooling to be colder than needed which could result in higher station cost.

Furthermore, the assumptions and boundary conditions cannot easily be changed to accommodate future vehicle and station designs.

The PRHYDE Project set out to develop a protocol which:

- Has performance appropriate for primarily MD/HD vehicles, but also facilitate other applications, such as rail and maritime.
- Is adaptable to future technology change, such as novel tank design (e.g., different or no liners, etc.).

The HD vehicle market is still immature, so there are no legacy vehicles or stations that needs backwards compatibility, hence this segment offers a new opportunity for a change in thinking.

1.1 Modelling supporting the Fuelling Protocol Specification development

Development of a protocol requires a validated approach. Due to the limited time and budget, the experimental data cannot cover the whole possible ranges of protocol parameters such as initial P, T, ambient and precooling temperatures, pressure ramp, refuelling time, hardware specifications etc. Hence, a validated numerical tool is essential for a safe and efficient protocol development.

In the frame of PRHYDE project, two numerical approaches are used:

1. Quick engineering model which gives the heat parameters estimation in the gas (volume average temperature) and 1D temperature distribution in the tank wall. In the PRHYDE projects, two in-house engineering numerical tools (0D in the gas and 1D in the tank walls) are used: SOFIL by Air Liquide and HyFill by Engie.
2. Computational Fluid Dynamics (CFD) approach gives a detailed temperature, pressure, velocity 3D mapping of the spatial distribution inside the tank (both gas and walls). However, this approach is very expensive in terms of the CPU calculation time. Therefore, it is used as a complementary approach to better understand physical behaviour of the flow and the associated heat distribution inside the tank.

Both of these approaches require a careful validation versus the experimental data in the conditions similar to the final usage: shapes of tank (the aspect ratio of the tank's length to its diameter), temperature ranges (initial and pre-cooling), pressure ramps and mass flow rates etc. Sections 8, 9 and 10 are dedicated to the validation of engineering tools and CFD approaches for the conditions considered during PRHYDE project.

Chapter 8 addresses a brief description of modelling tools used in PRHYDE , including a comparison to models by external partners (H2FillS by NREL and H2-Fill by Wenger Engineering). Chapter 9 is focused on the comparison and validation of the results obtained by the engineering models of SOFIL and HyFill as well as CFD modelling with the experimental data. Chapter 10 gives the overall conclusions of the modelling work and recommendations for the future projects.

1.2 Experimentation supporting the Modelling and the Fuelling Protocol Specification development

This document also describes the testing that was performed by WP5 in the PRHYDE project.

In this context, four different single hydrogen tanks were tested at two different test sites (by ZBT and Nikola) in different fuelling conditions. A brief description of the test facilities and equipment utiliesed can be found in APPENDIX C of this document.

ZBT tested three single tanks: a 70 MPa nominal pressure Type IV tank, a 50 MPa nominal pressure Type IV tank and a 35 MPa nominal pressure Type III tank. In addition, Nikola tested another 70 MPa nominal pressure Type IV tank. Each of the four tanks was instrumented with a thermocouple tree (TC) containing up to 16 thermocouples, providing detailed insights on the thermal behaviour of the gas during fuelling.

Two discrete testing phases were conducted on the tanks at ZBT and the tank at Nikola.

- Phase 1 focused on generating experimental data for model verification purposes (see description in chapter 11 and detailed test results in APPENDIX D).
- Phase 2 focused comparison of experimental results to the performance simulations, and for protocol implementation testing (see description in chapter 12 and detailed test results in APPENDIX D).

Please note: Due to time constraints and supply chain issues, an additional testing phase, Phase 3, focussing on full system testing of the PRHYDE protocol concepts will be conducted after the end of the PRHYDE project. The tests will be performed at NREL's and possibly other testing facilities.

Chapter 13 summarizes some key findings and recommendations derived from the testing campaign.

2 Fuelling Protocol Types

2.1 Protocol levels of communication usage

PRHYDE identified three levels of applying Vehicle CHSS Information:

Table 2: Protocol levels of communication usage

Vehicle CHSS Information Used	Gas Temp. Margin	Performance Acceptable?	Pre-cooling Temp.	Station Costs	Vehicle Costs	Non-Comm Fuelling	Comment
1: None	↑	Maybe	T40	↑	↓	Yes	▪ J2601 philosophy ▪ Worst case assumptions about most things ▪ Fuelling history assumed ▪ Station fully responsible
2: Static data	↔	Yes	T30?	↔	↔	Yes	▪ CHSS assumptions eliminated ▪ Worst case assumptions about some things ▪ Fuelling history assumed ▪ Station and vehicle share responsibility although most is still on station side
3: Dynamic data (CHSS gas temp.)	↓	Yes	T20	↓	↑	Maybe	▪ Fewer assumptions need to be made ▪ The gas temp can be used in different ways ▪ Direct use or to screen for fuelling history ▪ Station and vehicle share responsibility

It is important to note that the increased use of Vehicle CHSS Information puts further demands on the reliability of the communication, as investigated in APPENDIX E

2.2 Protocol approach to fuelling parameters

Another factor is the protocol's approach to fuelling parameters, i.e. how fast the vehicle can be fuelled and when to stop.

Roughly put, the protocol approach can either be prescriptive or performance-based:

Table 3: Protocol approach

Protocol Approach	Advantages	Disadvantages
Prescriptive	▪ **Consistency of fuelling performance** for the end customer ▪ Much **easier to validate** stations because only need to validate the implementation, not validate the fuelling method itself ▪ Already developed, so **no development costs** ▪ Open and fair to all companies both small and large	▪ Less room for innovation ▪ More difficult to get a fuelling method approved (e.g., effort for MC Formula)
Performance based	▪ More **room for innovation** ▪ Allows for **competition** between companies	▪ High development costs ▪ Less fair for small companies (must spend on development) ▪ Allows companies to corner the market through IP

2.3 Protocol fill control

Finally, there is the control issue:

a. Station controls the fill
b. Vehicle controls the fill
c. Station and Vehicle cooperates to control the fill

Table 4: Protocol fill control

Command Control	Advantages	Disadvantages
Station (Type 1, 2, or 3)	▪ **May not require advanced bi-directional communication** (lower cost) ▪ **One-stop shop**—station determines both command and physical control ▪ **Lower functional safety** requirements **on vehicle** (lower cost)	▪ **Higher functional safety** requirement on station (higher cost) ▪ **Stations typically have lower processing power** than vehicles so it may be more difficult to implement a complex algorithm on station PLC ▪ **Station has more responsibility**
Vehicle (Type 3 only)	▪ **Vehicles inherently have high processing power** on-board—it may be easier and lower cost to implement a complex algorithm on vehicle ▪ **Lower functional safety requirements** on station (lower cost)	▪ **Higher functional safety** requirement **on vehicle** (higher cost) ▪ **Vehicle has more responsibility**

2.4 Protocol types nomenclature

When combining the above aspects, a map of protocol types can be visualized.

As shown in Figure 2, the focus of this project are concepts in the Type 2-PR-S and Type 3-PR-S subdomains.

Type 1

This type is defined as using no communication so there can be no prescriptive or performance-based subdomains.

Concepts in Type 1 were not considered in this project as its focus was on advancing the state-of-the-art. Further detail on current developments in Type 1 refuelling protocols can be found in PRHYDE Deliverable D6.8.

Type 2

This type is defined as using only Static Data so there can be no Performance-based subdomain.

One concept was developed in subdomain Type 2-PR-S.

Type 3

Three concepts were developed in subdomain Type 3-PR-S.

Concepts in Type-3-PR-V and Type 3-PB-V subdomains were not considered in this project. Type 3-PB-V was discussed early in the PRHYDE Project, but it was then dropped as it was difficult to harmonize with the other Type 2 and 3 PR-S protocols and was also completely open ended, since performance-based, by definition means the protocol control methodology is not defined. This subdomain type could be considered in the future as the respective original equipment manufacturers (OEMs) can decide the logic on the vehicle, inspired by the Type 3-PR-S concepts or not.

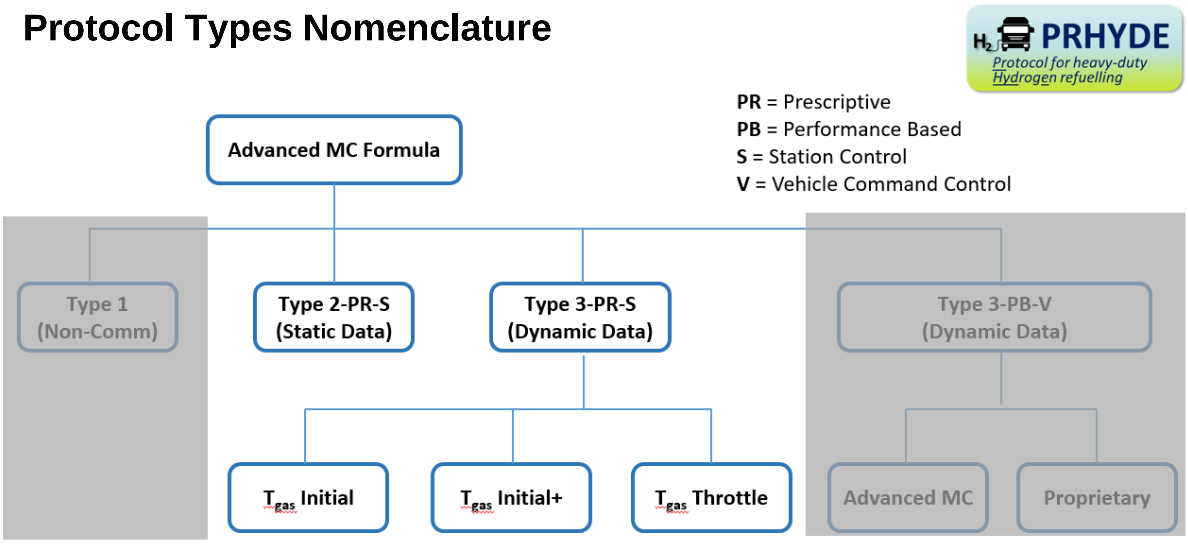

Figure 2: Protocol Types Nomenclature with PRHYDE fuelling concepts

3 FINAL PROTOCOL

With the protocol types defined in Section 2.4, the full list of final fuelling concepts developed in the context of the PRHYDE Project is provided:

- Type 2-PR-S Static Data
- Type 3-PR-S Dynamic Data – T_{gas} Initial
- Type 3-PR-S Dynamic Data – T_{gas} Initial+
- Type 3-PR-S Dynamic Data – T_{gas} Throttle

All the fuelling concepts operate within a common control framework denoted as Advanced MC Formula (see following section). This means that a vehicle can choose which fuelling concept to utilize and the station can implement the MC Formula control logic under this unified framework. Each of these concepts have advantages and disadvantages, so by providing a variety of concepts, a vehicle and station provider can utilize the concept that best meets their objectives.

3.1 Advanced MC Formula Framework Fuelling Concepts

All of the fuelling concepts in PRHYDE are advancements of the MC Formula method, “Advanced MC Formula Framework”, which utilize the same approach to derive the t_{final} values used in the protocol. These t_{final} values are stored in a set of t_{final} tables in the vehicle electronic control unit (ECU). The vehicle determines the appropriate t_{final} table to utilize based on the ambient temperature, initial pressure and in some fuelling concepts, the initial gas temperature in the CHSS. The OEM is responsible for the derivation of the t_{final} values based on a validated fuelling model.

The fuelling model used must be able to reflect accurately the CHSS design of the considered vehicle (individual tank sizes, fuelling line diameters and wall thicknesses, lengths, junctions, manifolds, valves, etc) and thermophysical properties. This fuelling model must also be able to reflect the dispenser fuelling component design and thermophysical properties (based on consensus assumptions, to be defined in a fuelling protocol standard).

The fuelling model is then run over a range of input conditions where the fuel delivery temperature (T_{fuel}), ambient temperature (T_{amb}), minimum CHSS pressure (P_{min}), and initial CHSS soak temperature (T_{soak}) are varied over a defined range of values. The output from each of these simulations is a t_{final} value. These t_{final} values are then arranged in a set of t_{final} tables, delineated by T_{amb} and MAT (MAT is the mass average of T_{fuel}), which are stored in the vehicle ECU and called upon during each fuelling event. Figure 3 illustrates how the derivation of the t_{final} tables is conducted.

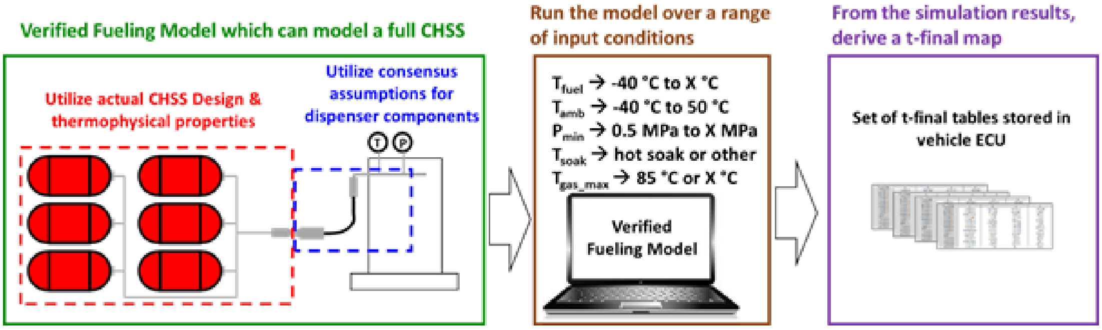

Figure 3 **Derivation of t_{final} values**

The advantage of this approach is that many of the vehicle CHSS assumptions can be eliminated, while other assumptions can be more precise. This allows the optimization of fuelling performance to the characteristics and capabilities of the CHSS, resulting in significantly improved performance when compared to a Type 1 fuelling concept which utilizes worst case assumptions. Section 7 provides a thorough explanation and specification of the t_{final} derivation process.

Table 5 illustrates the formatting of a t_{final} table. The values are stored at T_{amb} increments of 5 °C and MAT increments of 2 °C, as MM.M, which is in minutes to the tenth of a minute. This provides a t_{final} resolution of 6 seconds. The range of MAT values is shown from –40 °C to –10 °C, however, the OEM can choose a wider range of values, up to and including ambient temperatures.

Table 5: **Example of a t_{final} table**

MAT_C / T_{amb}	-40	-38	-36	-34	-32	-30	-28	-26	-24	-22	-20	-18	-16	-14	-12	-10
50	xx.x	xx.x	xx.x	xx.x	xx.x	xx.x	xx.x	xx.x	xx.x	xx.x	xx.x	xx.x	xx.x	xx.x	xx.x	xx.x
45	xx.x	xx.x	xx.x	xx.x	xx.x	xx.x	xx.x	xx.x	xx.x	xx.x	xx.x	xx.x	xx.x	xx.x	xx.x	xx.x
40	xx.x	xx.x	xx.x	xx.x	xx.x	xx.x	xx.x	xx.x	xx.x	xx.x	xx.x	xx.x	xx.x	xx.x	xx.x	xx.x
35	xx.x	xx.x	xx.x	xx.x	xx.x	xx.x	xx.x	xx.x	xx.x	xx.x	xx.x	xx.x	xx.x	xx.x	xx.x	xx.x
30	xx.x	xx.x	xx.x	xx.x	xx.x	xx.x	xx.x	xx.x	xx.x	xx.x	xx.x	xx.x	xx.x	xx.x	xx.x	xx.x
25	xx.x	xx.x	xx.x	xx.x	xx.x	xx.x	xx.x	xx.x	xx.x	xx.x	xx.x	xx.x	xx.x	xx.x	xx.x	xx.x
20	xx.x	xx.x	xx.x	xx.x	xx.x	xx.x	xx.x	xx.x	xx.x	xx.x	xx.x	xx.x	xx.x	xx.x	xx.x	xx.x
15	xx.x	xx.x	xx.x	xx.x	xx.x	xx.x	xx.x	xx.x	xx.x	xx.x	xx.x	xx.x	xx.x	xx.x	xx.x	xx.x
10	xx.x	xx.x	xx.x	xx.x	xx.x	xx.x	xx.x	xx.x	xx.x	xx.x	xx.x	xx.x	xx.x	xx.x	xx.x	xx.x
5	xx.x	xx.x	xx.x	xx.x	xx.x	xx.x	xx.x	xx.x	xx.x	xx.x	xx.x	xx.x	xx.x	xx.x	xx.x	xx.x
0	xx.x	xx.x	xx.x	xx.x	xx.x	xx.x	xx.x	xx.x	xx.x	xx.x	xx.x	xx.x	xx.x	xx.x	xx.x	xx.x
-10	xx.x	xx.x	xx.x	xx.x	xx.x	xx.x	xx.x	xx.x	xx.x	xx.x	xx.x	xx.x	xx.x	xx.x	xx.x	xx.x
-20	xx.x	xx.x	xx.x	xx.x	xx.x	xx.x	xx.x	xx.x	xx.x	xx.x	xx.x	xx.x	xx.x	xx.x	xx.x	xx.x
-30	xx.x	xx.x	xx.x	xx.x	xx.x	xx.x	xx.x	xx.x	xx.x	xx.x	xx.x	xx.x	xx.x	xx.x	xx.x	xx.x
-40	xx.x	xx.x	xx.x	xx.x	xx.x	xx.x	xx.x	xx.x	xx.x	xx.x	xx.x	xx.x	xx.x	xx.x	xx.x	xx.x

3.2 Description of each Fuelling Concept

3.2.1 Type 2-PR-S – Static Data

This fuelling concept is characterized by using the static data from communications to optimize the fuelling parameters accounting for vehicle CHSS characteristics such as the CHSS design and thermophysical properties. The Static Data fuelling concept uses two sets of t_{final} tables, each with a different minimum pressure assumption (referred to as P_{min}). These t_{final} tables are stored in the vehicle ECU. As in SAE J2601, t_{final} tables are developed for two different P_{min} values, the first (t_{final} table A) being the minimum operating pressure of the CHSS, and the second being approximately 5 MPa above the first (t_{final} table B) This fuelling concept assumes that fuelling history is present, since it cannot screen for fuelling history by using the CHSS gas temperature. This is why even if $P_{initial}$ = 20 MPa (for example), the minimum pressure P_{min} used in the derivation of t_{final} is 6 MPa. This approach prevents overheat risk if there has been fuelling history.

3.2.1.1 t_{final} Table Selection

The vehicle selects the t_{final} table to utilize based on the initial pressure in the CHSS. If $P_{initial} \geq P_{min}$ then t_{final} table A is utilized. If $P_{initial} < P_{min}$ then t_{final} table B is utilized.

3.2.1.2 t_{final} Vector Calculation

The t_{final} tables provide t_{final} values for each MAT value based on discrete ambient temperature values (see Table 5). The ambient temperature, however, is rarely measured to be exactly at one of these discrete values in the t_{final} table. Therefore, it is necessary to interpolate each row in the t_{final} table on ambient temperature. After interpolation, a vector is calculated which provides the precise t_{final} value at each MAT value for the ambient temperature.

3.2.2 Type 3-PR-S – Dynamic Data T_{gas} Initial

This fuelling concept is characterized by using dynamic data before the filling to optimize the fuelling parameters accounting for vehicle CHSS characteristics such as the CHSS design and thermophysical properties, and fuelling history.

The T_{gas} Initial fuelling concept differs from the Static Data fuelling concept in that it has t_{final} tables for additional P_{min} values. Whereas the Static Data fuelling concept uses two P_{min} values, (e.g. 1 MPa, and 6 MPa), the T_{gas} Initial fuelling concept can utilize multiple P_{min} values, typically separated by pre-determined increments, for example: P_{min} = 1, 6, 11, 16, 21 MPa, etc. There is no limit to the number of P_{min} values, or to the spacing of these values – this is left up to the vehicle OEM to decide. The benefit of being able to utilize higher P_{min} values is that the t_{final} values become progressively shorter as P_{min} increases, and thus fuelling times can be significantly reduced. The reason that the T_{gas} Initial fuelling concept can utilize higher P_{min} values is that this fuelling concept uses the initial CHSS gas temperature T_{gas} to screen for fuelling history. If $T_{gas} \leq T_{hot\_soak}$ (the hot soak temperature utilized in SAE J2601), then the t_{final} table with the highest P_{min} value – which is less than the initial CHSS pressure $P_{initial}$ – can be utilized. If $T_{gas} > T_{hot\_soak}$, then the t_{final} table with the lowest P_{min} value will be used.

As an example, if the initial CHSS pressure is measured to be 18 MPa and $T_{gas} \leq T_{hot\_soak}$, then the t_{final} table corresponding to a P_{min} value of 16 MPa can be utilized. Using this same example, if $T_{gas} > T_{hot\_soak}$, then the t_{final} table corresponding to the minimum P_{min} value (e.g. 1 MPa) must be utilized, because in this case, fuelling history is likely to have occurred, meaning that the vehicle may have recently been fuelled with a much lower initial pressure. By utilizing this approach, fuelling performance can be greatly improved under typical conditions, and in those rare instances where fuelling history is present, this concept utilizes conservative t_{final} values to prevent overheating from occurring.

3.2.2.1 t_{final} Table Selection

The vehicle stores multiple t_{final} tables, the first t_{final} table with a P_{min} value equal to the minimum operating pressure of the CHSS and each subsequent t_{final} table with a P_{min} value approximately 5 MPa above the previous value. The vehicle selects the t_{final} table to utilize based on the initial pressure P_{initial} in the CHSS and the initial gas temperature in the CHSS T_{gas_high} (the highest gas temperature measured in each tank within the CHSS). If $T_{gas\_high} \leq T_{hot\_soak}$ then the t_{final} table selected is the t_{final} table with the highest P_{min} value that is less than P_{initial}. If $T_{gas\_high} > T_{hot\_soak}$ then the t_{final} table selected is the t_{final} table with the lowest P_{min} value.

3.2.2.2 t_{final} Vector Calculation

Same as subsection 3.2.1.2

3.2.3 Type 3-PR-S – Dynamic Data T_{gas} Initial+

This fuelling concept is characterized by using dynamic data before the filling to optimize the fuelling parameters accounting for vehicle CHSS characteristics such as the CHSS design and thermophysical properties, and eliminates the initial CHSS soak temperature assumptions. A key difference of the T_{gas} Initial+ concept vs the T_{gas} Initial concept (see section 3.2.2) is: the initial CHSS gas temperature T_{gas_high} is used a) to screen for fuelling history; and b) to determine the initial CHSS soak temperature assumption to use. This fuelling concept therefore has even more t_{final} tables, where the t_{final} tables derived are based on a multitude of initial pressure (P_{min}) and a multitude of CHSS soak temperatures. The P_{min} values and CHSS soak temperatures (T_{soak}) utilized in the t_{final} table derivations are determined by the vehicle OEM. As an example, the vehicle OEM may utilize P_{min} = 1, 6, 11, 16, 21 MPa, and $T_{\mathrm{soak}} = T_{\mathrm{hot\_soak}}$, $T_{\mathrm{soak}} = T_{\mathrm{hot\_soak}}$ - 5 °C, and $T_{\mathrm{soak}} = T_{\mathrm{hot\_soak}}$ - 10 °C, which would be a total of fifteen t_{final} tables. The soak temperature used in the derivation of each t_{final} table must be referenced to the hot soak temperature, i.e. a constant ΔT below the hot soak temperature for each t_{final} table. A practical set of values for ΔT is 5 °C and 10 °C, but the choice is ultimately left to the OEM.

3.2.3.1 t_{final} Table Selection

The vehicle stores multiple t_{final} tables, the first set of t_{final} tables with a P_{min} value equal to the minimum operating pressure of the CHSS and each subsequent set of t_{final} tables with a P_{min} value approximately 5 MPa above the previous value. For each P_{min} value, a number of different CHSS soak temperatures can be utilized (forming a set of t_{final} tables at that P_{min} value). The vehicle selects the t_{final} table to utilize based on the initial pressure P_{initial} in the CHSS and the initial CHSS temperature $T_{\mathrm{gas\_high}}$. The set of t_{final} tables is first selected based on the set with the highest P_{min} value that is less than P_{initial}. This results in a set of t_{final} tables with the same P_{min} value, but each with a different T_{soak} value. To select the t_{final} table to use, the T_{soak} value associated with each t_{final} table is compared to the initial value of T_{gas_high}. The t_{final} table used is the t_{final} table with the lowest soak temperature where the following condition is satisfied: $T_{gas\_high} < 2\ T_{soak} - T_{hot\_soak}$.

3.2.3.2 t_{final} Vector Calculation

Same as subsection 3.2.1.2

3.2.4 Type 3-PR-S – Dynamic Data T_{gas} Throttle

This fuelling concept is characterized by using both static and dynamic data from the communications to optimize the fuelling parameters accounting for vehicle CHSS characteristics such as the CHSS design and thermophysical properties and to actively monitor the T_{gas_high} temperature and reduce the PRR once the T_{gas_high} temperature rises above a threshold temperature.

With this approach, a t_{final} table is derived but only using a single P_{min} value representing the lowest pressure allowed in the CHSS, e.g. 1 MPa. This approach is simple as there is only a single t_{final} table. In regard to the t_{final} table derivation, the key difference is in the peak CHSS gas temperature limit utilized in the fuelling simulations. In the Static, T_{gas} Initial and T_{gas} Initial+ approaches, the maximum CHSS gas temperature utilized in the simulations for the derivation of the t_{final} values is 85 °C, which is the current limit for fuelling protocols, such as SAE J2601, due to the CHSS qualification standards and regulations such as GTR No. 13. In the T_{gas} Throttle fuelling concept, the maximum CHSS gas temperature utilized in the fuelling simulations during derivation of the t_{final} tables is chosen by the OEM. Although the OEM could choose 90 °C, 95 °C, 100 °C, or even some higher value, fuelling simulations conducted under PRHYDE demonstrated that there is not a significant performance improvement in choosing a maximum gas temperature above 95 °C. The t_{final} vector is calculated exactly the same as described in Section 3.2.3.2.

The initial concept for T_{gas} throttle is simple, as shown in Figure 4. When the CHSS gas temperature T_{gas} reaches a threshold temperature $T_{threshold}$, the pressure ramp rate *PRR* is reduced to prevent the gas temperature from exceeding 85 °C. The reduction in *PRR* is a function of the *PRR* at $T_{threshold}$ (referred to as $PRR_{threshold}$) and T_{gas}. As T_{gas} continues to rise above $T_{threshold}$, the *PRR* is gradually reduced using Equation 1.

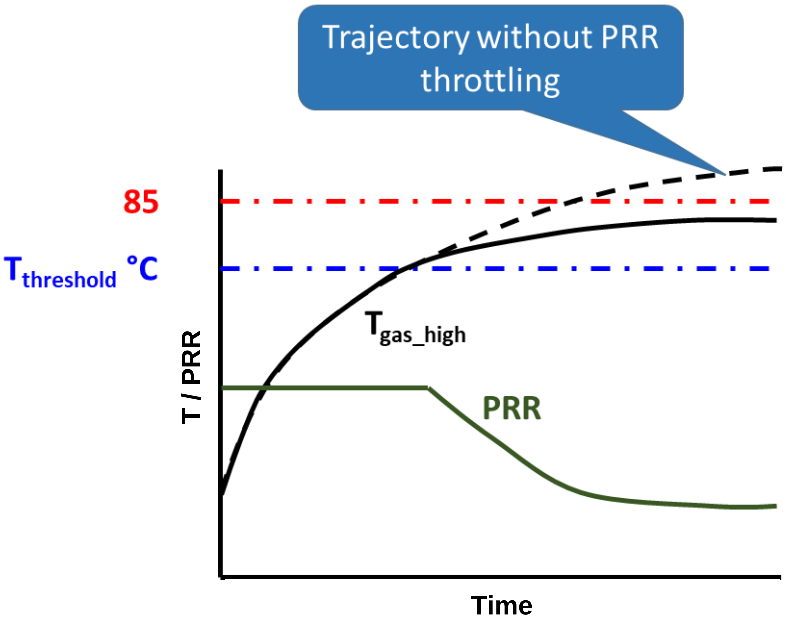

Figure 4: Throttle approach

$$if\ T_{gas\_high} \geq T_{threshold}, \quad PRR = \frac{(85 - T_{gas\_high})PRR_{threshold}}{85 - T_{threshold}} \qquad \text{(Eq. 1)}$$

Where,

PRR = the pressure ramp rate

T_{gas_high} = the CHSS gas temperature (highest value in a multi-tank system)

$T_{threshold}$ = the CHSS gas temperature at which the throttling equation is activated

$PRR_{threshold}$ = the PRR when T_{gas_high} = $T_{threshold}$.

Fuelling simulations, however, demonstrated that if the $T_{threshold}$ value is too high, T_{gas_high} can momentarily rise above 85 °C. This can be prevented by lowering the $T_{threshold}$ value, but when this is done, the fuelling time increases. Fuelling simulations demonstrated that the selection of an appropriate $T_{threshold}$ value is highly dependent on the pressure drop between the dispenser pressure and CHSS pressure. The higher this pressure drop, the lower the $T_{threshold}$ value has to be set to prevent T_{gas_high} from overshooting the maximum gas temperature limit of 85 °C. This characteristic is not optimal because the $T_{threshold}$ value must be set sufficiently low to prevent the CHSS gas temperature from overshooting the limit temperature, which causes fuelling times to increase. This is illustrated in Figure 5.

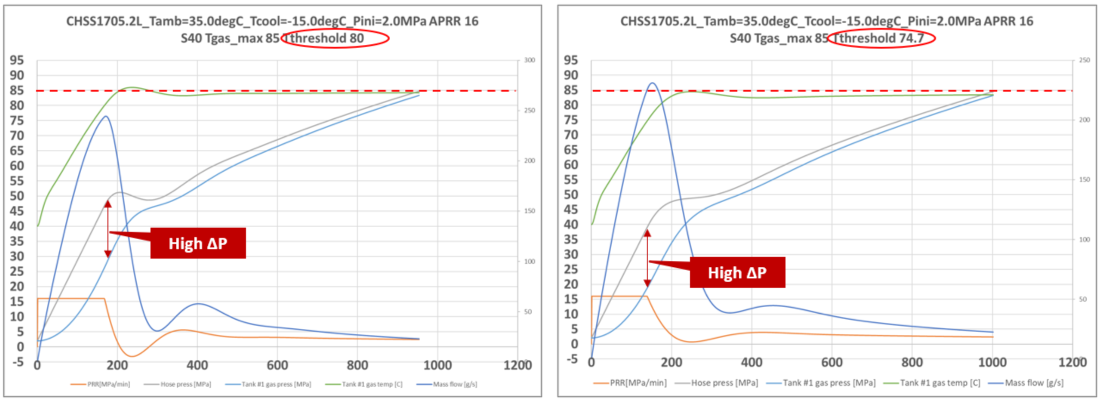

• $T_{threshold}$ is set at 80 °C • T_{gas_high} (tank #1) overshoots and reaches 86 °C • Fueling time = 15.9 minutes	• $T_{threshold}$ is set at 74.7 °C • T_{gas_high} (tank #1) stays below 85 °C (peak is 84.5 °C) • Fueling time = 16.7 minutes (~ 1 minute longer)

Figure 5: Sensitivity of the original T_{gas} Throttle concept to $T_{threshold}$

Further development of the T_{gas} Throttle fuelling concept resulted in an adaptable method whereby the $T_{threshold}$ value automatically adapts to the measured pressure drop. This prevents the CHSS gas temperature from overshooting the limit temperature. Furthermore, the denominator of the $PRR_{throttle}$ equation was changed so that it too adapts to the pressure drop. When the pressure drop is high, the denominator is larger, reducing the pressure ramp rate (PRR). As the pressure drop decreases (which naturally occurs later in the fill), the denominator gets smaller, increasing the PRR. By utilizing this approach, gas temperature overshoot is avoided without sacrificing fuelling time performance. This revised “adaptable” T_{gas} Throttle concept control logic is shown in Figure 6.

$\Delta P = P_{ramp} - P_{CHSS}$

IF $\Delta P > \Delta P_{max}$, then $\Delta P_{max} = \Delta P$

$T_{threshold} = T_{gas\_target} - a\Delta P_{max}$

IF $T_{gas\_high} \geq T_{threshold}$

THEN

Set i=1

$P_{ramp(i)} = P_{ramp}$

$\Delta P_{(i)} = P_{ramp(i)} - P_{CHSS(i)}$

$$PRR_{threshold(i)} = \frac{P_{final} - P_{min}}{t_{final(i)}}$$

$$AD_{(i)} = MAXIMUM\left[\, b\,, \left(a\Delta P_{(i)}\right)\right]$$

$$PRR_{throttle(i)} = \mathrm{MAXIMUM}\left[0, \frac{PRR_{threshold}\, x \left(T_{gas\_target} - T_{gas\_high(i)}\right)}{AD_{(i)}}\right]$$

$$PRR_{(i)} = MINIMUM\left[\, PRR_{MC(i)}, PRR_{SOC(i)}, PRR_{throttle(i)}\right]$$

i = i +1

"a" and "b" are tuning parameters

In simulations, the following settings work well:

IF $T_{gas\_initial} < T_{hot\_soak}$ and $P_0 < 10$ MPa, a = 3, ELSE a = 4
b = 4

Figure 6: Control logic for revised adaptable T_{gas} Throttle

In Figure 6, T_{gas_target} is the gas temperature that should not be exceeded, which would typically be set to 85 °C, but a more general term is used for flexibility (e.g., it could be set higher or lower). P_{ramp} is the ramp pressure (the pressure the dispenser is targeting for each time step throughout the fill) and P_{CHSS} is the pressure in the CHSS communicated to the dispenser from the vehicle. As noted in the figure, parameters "a" and "b" are values used to tune the behaviour of control. The "a" parameter is primarily used as a multiplier on ΔP to determine $T_{threshold}$, and thus when the PRR throttling begins. The "a" parameter is also used in the "adjustable denominator" parameter AD. Therefore, the larger the value "a" is, the sooner the PRR throttling begins, and the greater the PRR is reduced with increasing gas temperature. The "b" parameter is simply a minimum value for the AD parameter. This ensures that towards the end of the fill when the pressure drop is very low, the AD value is still sufficiently large so that the PRR throttling does not get overly sensitive to changes in the gas temperature. Figure 7 illustrates the fuelling performance and change in variables over the course of the fill for the revised adaptable T_{gas} Throttle concept.

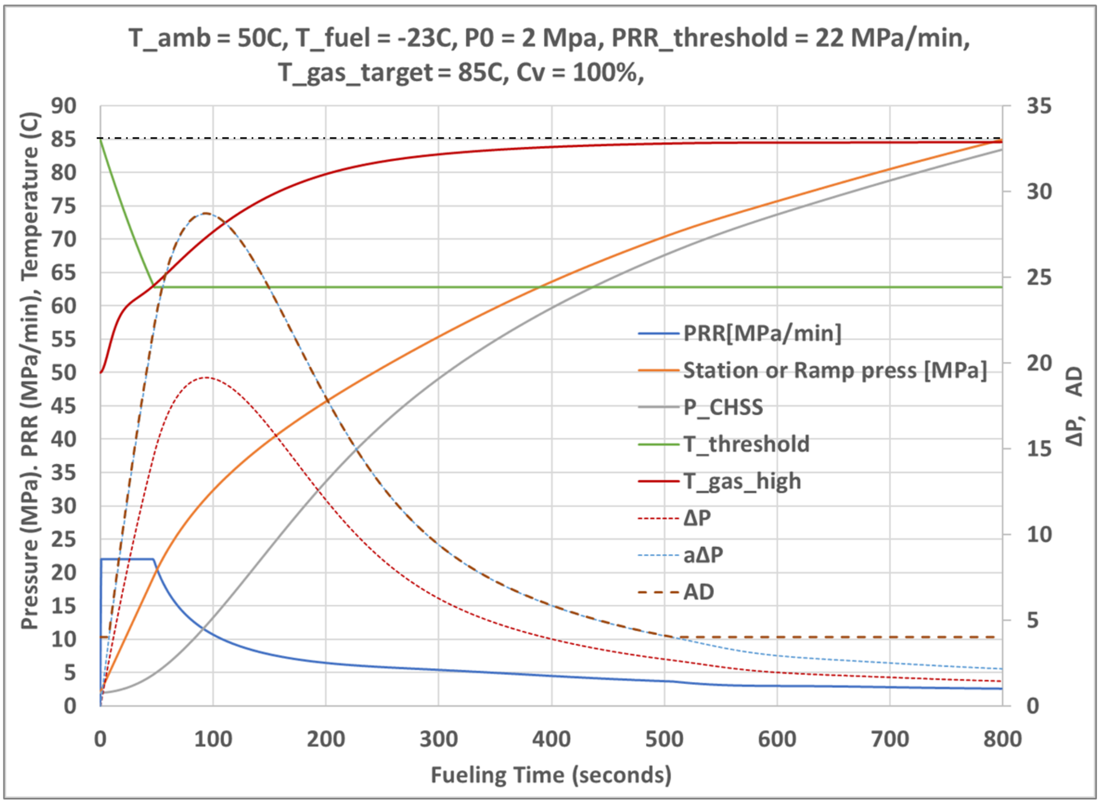

Figure 7: **Performance and variables for revised adaptable T_{gas} Throttle**

3.2.5 SOC Taper

Another feature developed within the PRHYDE project is an approach that reduces the PRR when necessary, so that the target SOC can be achieved. This feature is called SOC Taper[3]. SOC Taper is not a stand-alone fuelling concept. Rather it is a methodology that is applied to all the PRHYDE fuelling concepts and only activates when it is needed.

When deriving the t_{final} values, the dispenser pressure is not constrained (see Section 7). In other words, when running the fuelling model at different ambient temperatures and fuel delivery temperatures, the model determines the fastest APRR where the CHSS gas temperature (T_{gas_high}) and the flow rate is less than the maximum allowed. In some cases, especially if the system level flow coefficient (K_v) is not sufficiently high, the dispenser pressure at the end of the fill will be above the maximum (1.25 X NWP). This is especially an issue for H35 fills because the maximum pressure drop during the fill typically occurs near the ending pressure (whereas, for H70 fills the pressure drop can be substantially lower near the end of the fill due to the compressibility of hydrogen causing the mass flow rate to decrease). Under these

[3] In previous PRHYDE working documents, this feature is called “SOC Throttle”. The PRHYDE group decided to change the feature name to “SOC Taper” to avoid confusion between a feature and the fuelling concept “T_{gas} Throttle”.

cases, the ramp pressure P_{ramp} will reach its maximum value before the CHSS achieves the target SOC.

To counteract this, one approach would be to implement a constraint on the dispenser pressure during the derivation of the t_{final} values. However, in some cases, this can cause the fuelling times to be substantially longer. Figure 8 illustrates the first approach where the H35 dispenser pressure is constrained to 43.75 MPa during the derivation of t_{final} values. In this case the fuelling time is 14.2 minutes.

Another approach would be to, during the fill, hold P_{ramp} constant until the CHSS achieves the target SOC. However, once P_{ramp} is held constant, there is no more pressure ramp rate control as described below (Figure 11). Also, the pressure ramp rate cannot be slowed to reduce the fuel delivery temperature (MAT value). This is undesirable and, in some rare circumstances, could result in overheating.

In the first graph of Figure 9, t_{final} values are derived without a maximum dispenser constraint imposed. In this case, the dispenser pressure substantially exceeds 43.75 MPa, but the fuelling time is only 6 minutes. In the second graph of Figure 9, the fuelling starts with the same t_{final} value of 6 minutes, and when P_{ramp} reaches 43.75 MPa, it is held constant until the SOC target is achieved. In this case, there are over 300 seconds where there is no PRR control.

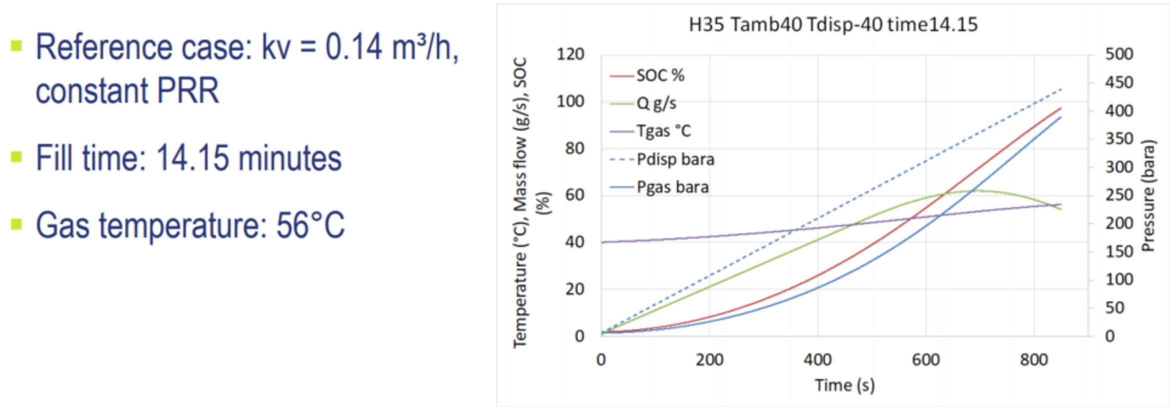

Figure 8: **Derivation of t_{final} with maximum dispenser pressure constraint**

- Unconstrained dispenser pressure: constant PRR until 87.5 MPa for determining a ramp rate
- Fill time: 6 minutes
- Gas temperature: 71°C

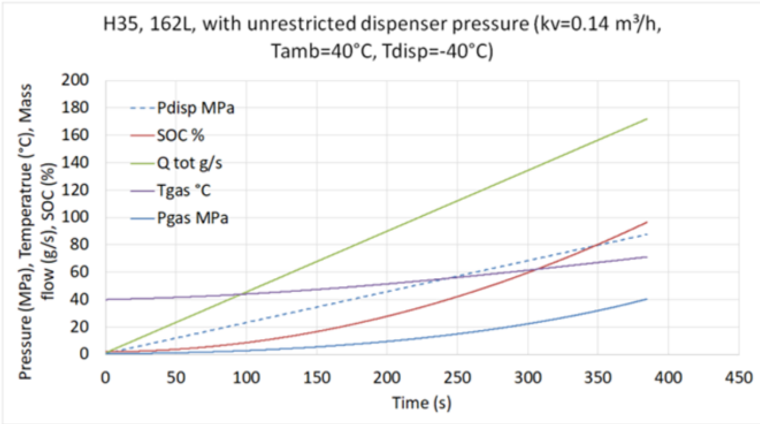

- Same PRR as previous case, but holding the dispenser pressure at 1.25 NWP
- Fill time: 8.4 minutes
- Gas temperature: 59°C

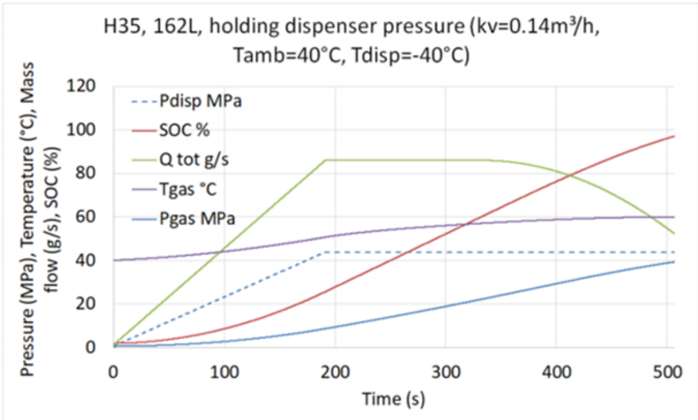

Figure 9: Derivation of t_{final} without maximum dispenser pressure constraint and illustration of P_{ramp} hold approach using this t_{final} value

SOC Taper was developed as an approach to allow t_{final} to be derived without a maximum dispenser constraint, but during fuelling, retain pressure ramp rate control throughout the fill. It essentially slows the ramp rate if the pressure limit is reached before the SOC limit. The SOC Taper concept is illustrated in Figure 10.

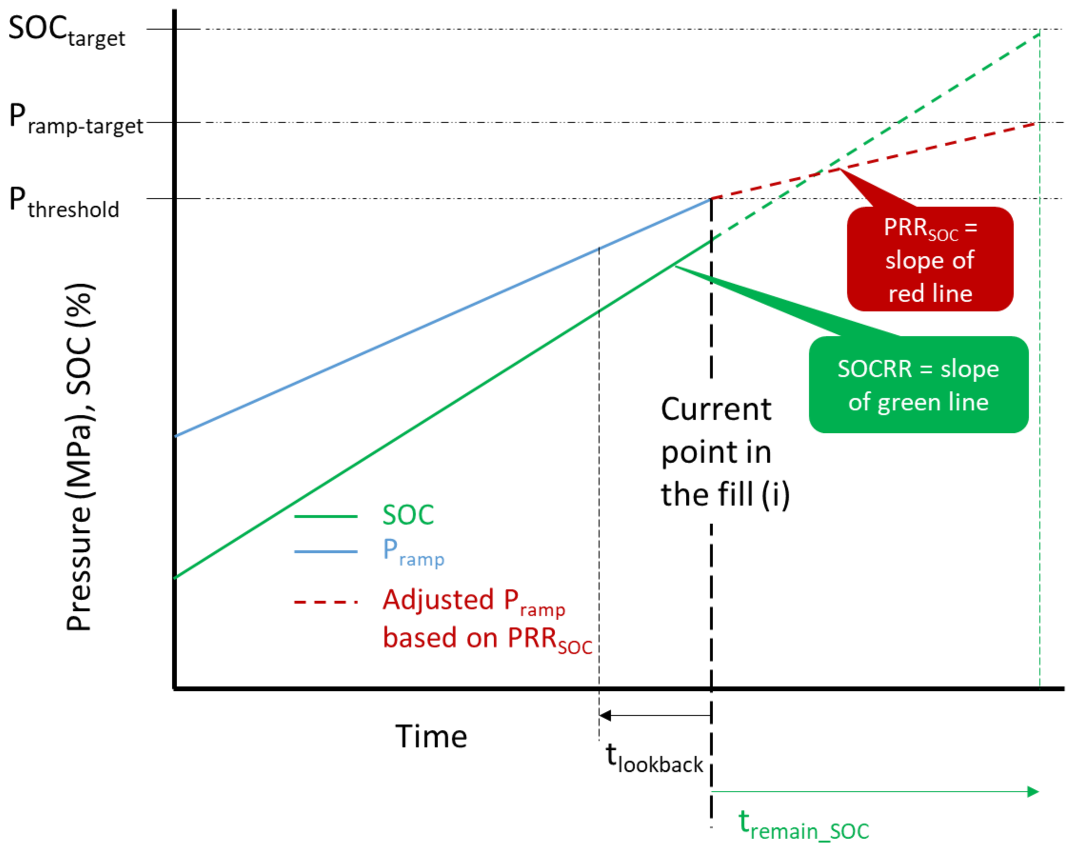

Figure 10: Illustration of the SOC Taper Concept

In Figure 10, once P_{ramp} exceeds $P_{threshold}$, the SOC Taper concept is applied. A lookback period $t_{lookback}$ is defined in seconds. This is a discretionary value, but a typical value is $t_{lookback}$ = 30 seconds, and this has been shown to work well in fuelling simulations. Throughout the fill, the SOC for each time step is logged. Once SOC Taper is active, the following steps are applied:

1) Calculate a SOC Ramp Rate (SOCRR) by subtracting the SOC value $t_{lookback}$ seconds ago from the current SOC value and this is divided by $t_{lookback}$.
2) Calculate time remaining for SOC to achieve the target SOC. This is done by subtracting the target SOC value from the current SOC value and dividing this by SOCRR. This time remaining is called t_{remain_SOC}.
3) Determine a SOC pressure ramp rate (PRR_{SOC}) which causes the ramp pressure P_{ramp} to achieve its target value P_{ramp_target} at the same time that SOC achieves its target value. This is calculated by subtracting P_{ramp_target} from the current P_{ramp} value and dividing this by t_{remain_SOC}.
4) For each time step, the PRR_{SOC} is compared to the PRR normally calculated by MC Formula (under any of the fuelling concepts).
    a. If PRR_{SOC} is greater than the MC Formula calculated PRR, then PRR_{SOC} is not applied, and the normal PRR is used.

b. If PRR_{SOC} is less than the MC Formula calculated PRR, the PRR for that time step is set to PRR_{SOC}.

There are only two parameter settings for SOC Taper: $P_{threshold}$ and $t_{lookback}$. $P_{threshold}$ is an adaptable parameter, in other words, it is calculated as a function of the pressure difference between P_{ramp} and P_{CHSS}. That is, for each time step,

1) Calculate $\Delta P = P_{ramp} - P_{CHSS}$.
2) Then $P_{threshold} = P_{ramp\_target} - \Delta P$,

   where P_{ramp_target} is the maximum ramp pressure setting (typically a couple of MPa below the MAWP of the dispenser).

Because $P_{threshold}$ is calculated automatically, the only discretionary setting for SOC Taper is $t_{lookback}$. As mentioned, a recommended value for $t_{lookback}$ is 30 seconds, although this concept should be robust to a range of $t_{lookback}$ values, for example, 30 +/- 15 seconds.

The dynamic data P_{CHSS} is used in SOC Taper, which is implemented in all fuelling concepts even the static one. It can be done because SOC Taper is made to increase fuelling performance but is typically not safety relevant. The only situation where it could cause issues is if SOC Taper is not triggered and P_{ramp} reaches P_{ramp_target}, so the PRR is zero for the rest of the fuelling. If the MAT warms during this time, overheating could occur because the pressure ramp rate cannot be reduced anymore. However, this will only happen if P_{CHSS} is reading high, so the ΔP calculation is low and SOC Taper is not triggered. But if P_{CHSS} is reading high, the fill will end early anyway, reducing any overheating risk.

Another important benefit of implementing the SOC Taper concept is that it allows the fuelling protocol control to adapt to the station's PRR capability. For example, if the station cannot achieve the ramp pressure P_{ramp} calculated by the Advanced MC Formula fuelling protocol, SOC Taper automatically adjusts the ramp pressure so that pressure ramp rate control remains active throughout the fill until the SOC target is reached. This is illustrated in Figure 11. Without the utilization of SOC Taper, if the dispenser pressure $P_{station}$ falls behind P_{ramp}, P_{ramp} will hit P_{ramp_target} well before the target SOC is achieved and P_{ramp} will have to be held constant, meaning there is no pressure ramp rate control. As illustrated in the graph on the right, with the utilization of SOC Taper, when the dispenser pressure falls behind the ramp pressure, this will cause ΔP to be relatively large and $P_{threshold}$ to be relatively low, and therefore, SOC Taper will be activated early in the fill, reducing the ramp pressure just enough so that the station can fill the vehicle in the fastest time it is capable of, all while keeping pressure ramp rate control to the end of the fill.

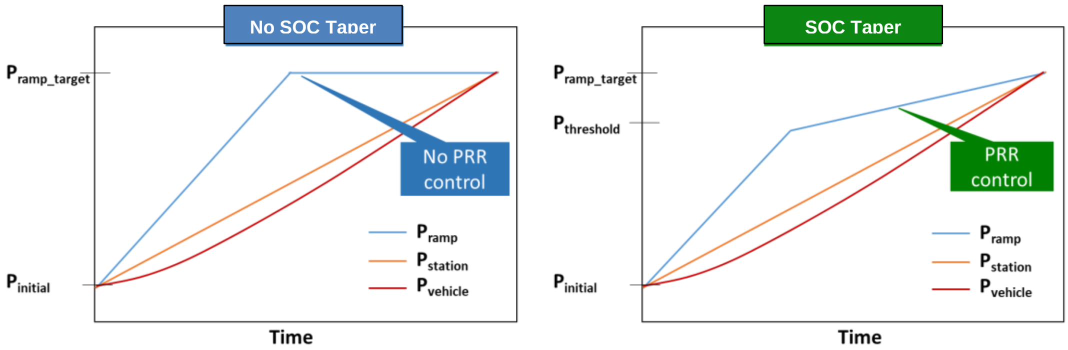

Figure 11: Comparison between No SOC Taper (left) and SOC Taper approach (right)

3.2.6 Data Fluctuations

The fast fuelling performance and smooth PRR throttling of the revised adaptable T_{gas} Throttle was demonstrated using a special version of NREL's H2FillS fuelling model. This fuelling model calculates the bulk average gas temperature of the CHSS, and this is used as the input to the T_{gas} Throttle equations. In the real world, however, the temperature measurement in the CHSS will not be this smooth – it is prone to fluctuations in temperature from gradients in the CHSS that develop due to imperfect mixing. Fuelling data, both from the PRHYDE testing and data from light duty FCV measurements shows that the temperature measurement, typically at or near the OTV (on-tank-valve) can fluctuate by many degrees up and down. Figure 12 illustrates CHSS gas temperature data collected from four different light duty FCVs. Note that the amplitude of the fluctuations differs from vehicle to vehicle.

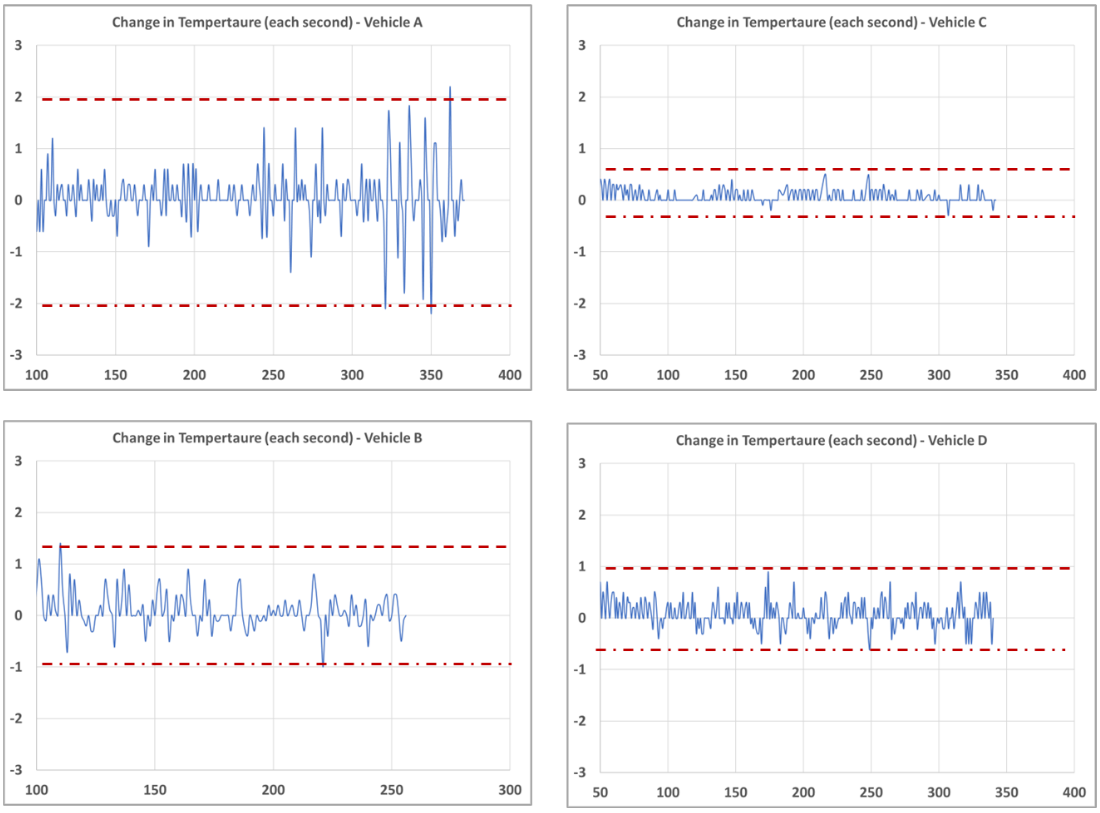

Figure 12: Fluctuations in CHSS gas temperature for four LD FCVs

To simulate this real-world environment, NREL added a noise function (a random number generator that is constrained to upper and lower bounds) to the CHSS gas temperature. See Figure 13 for an illustration of this noise function. When the revised T_{gas} Throttle fuelling concept was run with noisy T_{gas_high} of various amplitudes, this caused the PRR to fluctuate as well. As shown in the PRR equation in Figure 6, the PRR is directly a function of T_{gas_high} so fluctuations in this value cause similar fluctuations in PRR. These fluctuations in PRR are not desirable because they make it more difficult for the dispenser pressure or flow control valve to follow.

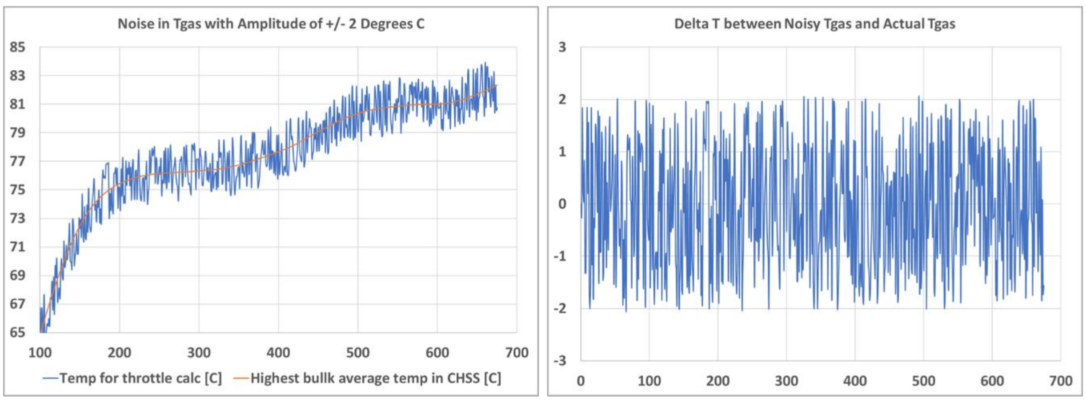

Figure 13: Illustration of noise function in NREL's H2FillS fuelling model

To reduce the fluctuations in the PRR caused by the noise in the CHSS gas temperature, a noise filter was added to smooth these fluctuations. A number of different noise filters were investigated, but a triple moving average (TMA) of the CHSS gas temperature demonstrated the best combination of effectiveness and simplicity. Figure 14 illustrates the TMA (orange line), which is a reasonable approximation of the bulk average CHSS gas temperature (blue line). The TMA does introduce a time lag, but this does not have a material effect on the control since the precision of the PRR throttling is most important after the CHSS gas temperature has reached an asymptote during the latter part of the fill. The TMA is simply a moving average of a moving average of a moving average of the CHSS gas temperature. The length or periodicity of each moving average can be different, e.g., 15, 10, 5, or it can be the same, e.g. 10, 10, 10. Extensive simulations were conducted and it was determined that a TMA of equal periodicities of 10 worked well. This should be further confirmed in actual testing.

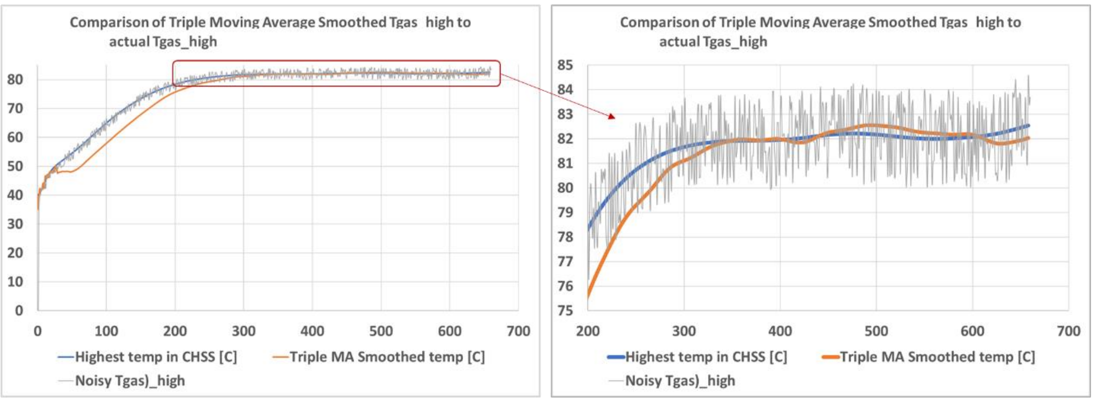

Figure 14: Illustration of triple moving average smoothing function

The effectiveness of the TMA in smoothing the CHSS gas temperature and consequently the PRR is illustrated in Figure 15.

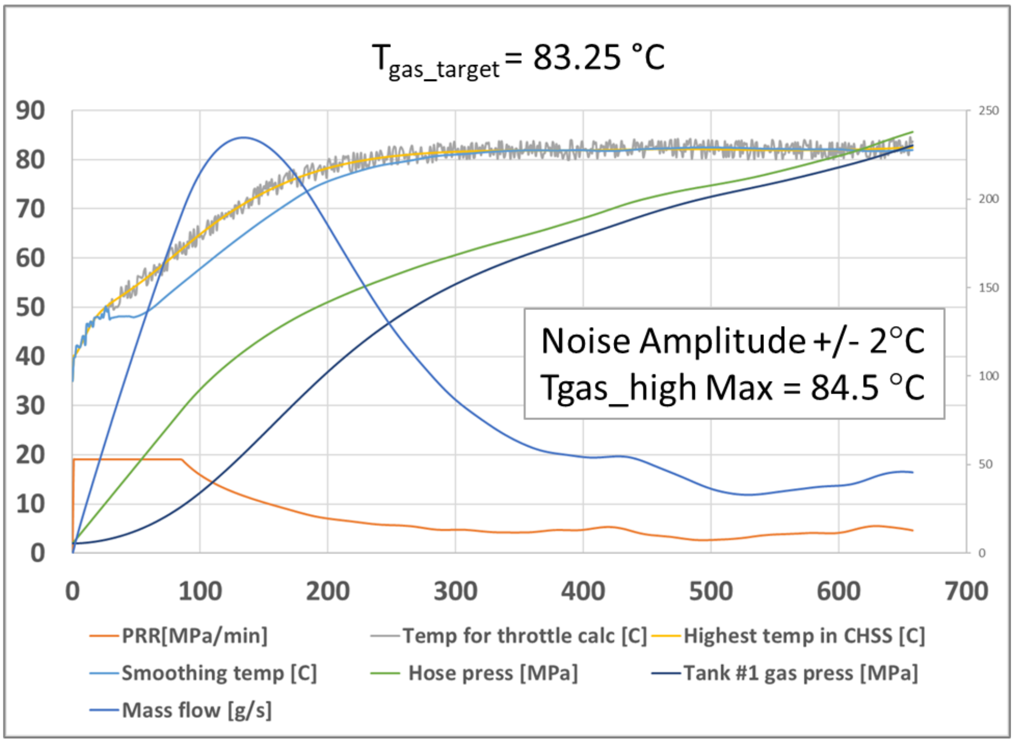

Figure 15: Example of PRR control with TMA applied to noisy T_{gas_high}

Note in Figure 15 that the T_{gas_target} value had to be set lower than 85 °C to avoid the CHSS gas temperature from momentarily spiking above the temperature limit. In this case, T_{gas_target} was set to 83.25 °C, which resulted in a peak T_{gas_high} value of 84.5 °C. Although this methodology is effective, a shortcoming of it is that each vehicle will have different levels of fluctuations in T_{gas_high}. So how should T_{gas_target} be set if the level required depends on the magnitude of these fluctuations? One way to deal with this is to set T_{gas_target} sufficiently low so that it is effective against all expected fluctuation levels in T_{gas_high} (e.g. a noise level of +/- 5 °C). However, this approach increases the fuelling time substantially, because the lower T_{gas_target} is set, the more the PRR is reduced, lengthening the fuelling time. An alternative is for the vehicle OEM to measure the fluctuations in T_{gas_high} under a variety of fuelling conditions and determine an appropriate T_{gas_target} value, which can then be communicated from the vehicle to the dispenser. A third approach is to develop an approach whereby the T_{gas_target} value automatically adjusts to the fluctuations inherent in T_{gas_high}. This third approach was developed in PRHYDE.

There are two control parameters in the adaptable T_{gas} Throttle fuelling concept which need to be adjusted due to fluctuations in T_{gas_high}: T_{gas_target} and AD. T_{gas_target} is explained above in Figure 6. AD is the denominator in the PRR Throttle equation. The smaller the value of AD, the more sensitive PRR is to changes in T_{gas_high}, or T_{gas_smooth} (which is the result after applying TMA to T_{gas_high}). Therefore, with higher amplitude in the fluctuations of T_{gas_high}, T_{gas_target} needs to be reduced and the minimum value of AD needs to be increased. Recall that the minimum value of AD is determined by the parameter "*b*".

To determine the inherent fluctuations in T_{gas_high}, the difference between T_{gas_high} and T_{gas_smooth} is measured. This parameter is named T_{gas_diff}. T_{gas_diff} is measured after T_{gas_smooth} crosses above a threshold temperature named $T_{gas\_smooth\_threshold}$. Once T_{gas_diff} begins to be measured, the maximum value is recorded as $T_{gas\_diff\_max}$. This process is illustrated in Figure 16 .

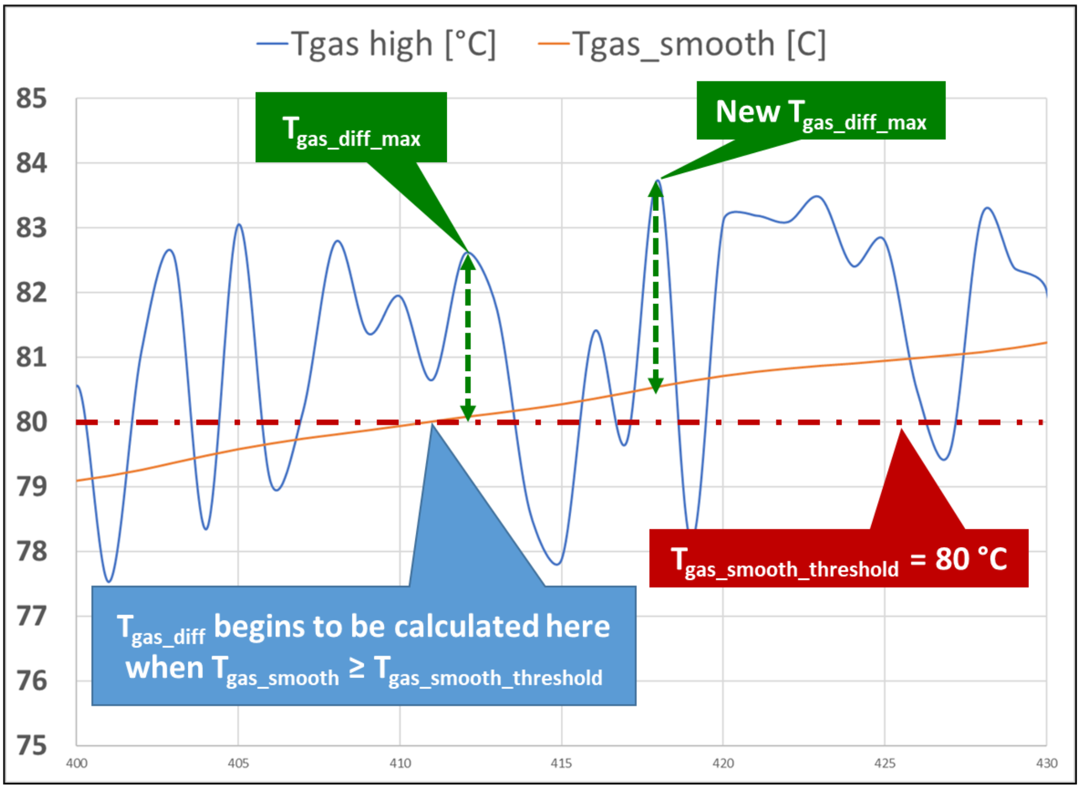

Figure 16: Illustration of the measurement of T_{gas_diff} and $T_{gas\_diff\_max}$

The reason that T_{gas_diff} is measured only after T_{gas_smooth} rises above $T_{gas\_smooth\_threshold}$ is because early in the fill, the CHSS gas temperature is rising rapidly. As noted previously, T_{gas_smooth} lags due to the TMA smoothing function. If T_{gas_diff} is measured from the beginning of the fill, $T_{gas\_diff\_max}$ will be artificially high due to this lag. Therefore, the objective is to set the $T_{gas\_smooth\_threshold}$ value at a value where the CHSS gas temperature is naturally beginning to asymptote. Fuelling simulations showed that a value of 75 °C to 80 °C works well (see Chapter 9). Fuelling performance is relatively insensitive to the $T_{gas\_smooth\_threshold}$ value utilized within this range. This asymptote behaviour in the CHSS gas temperature is illustrated in Figure 17. This region where T_{gas_high} and T_{gas_smooth} are relatively flat is referred to as the throttling region and it is where the PRR throttling is most critical to avoid exceeding the maximum gas temperature.

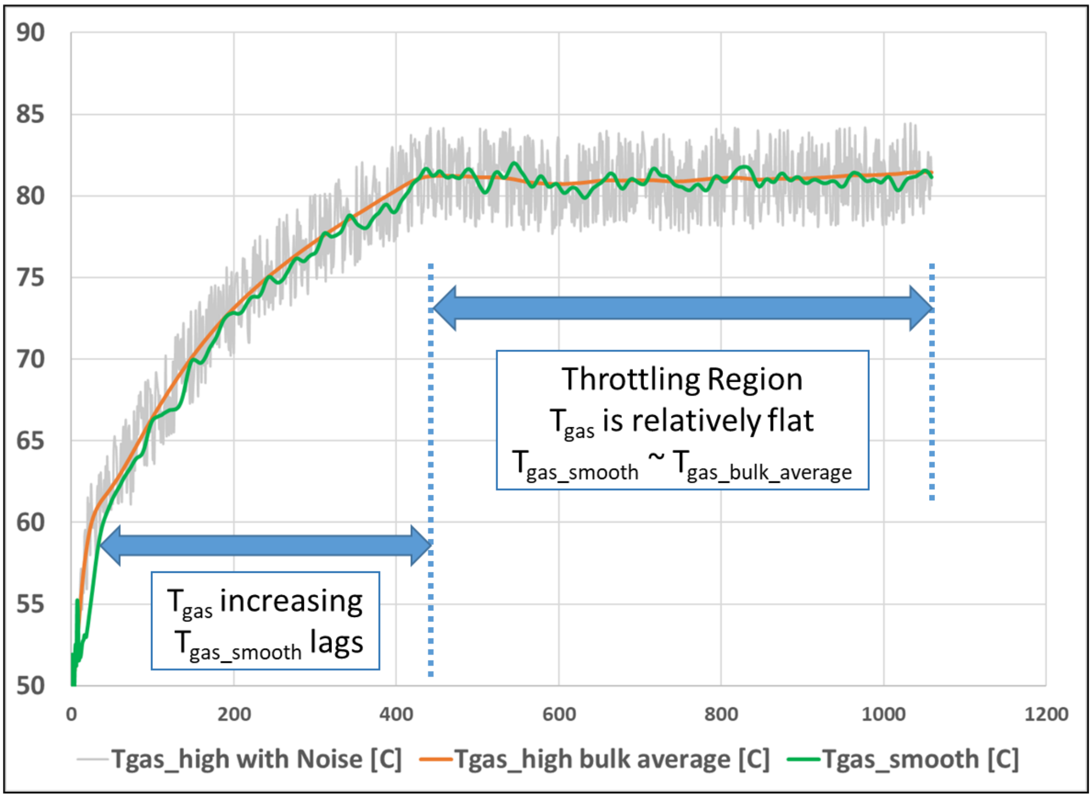

Figure 17: Throttling region where T_{gas_high} and T_{gas_smooth} are relatively flat

$T_{gas\_diff\_max}$ is a measurement of the magnitude of fluctuation inherent in T_{gas_high}. Its purpose is to determine an appropriate setting for T_{gas_target} and the parameter "*b*". To utilize $T_{gas\_diff\_max}$ in this manner, a derivative parameter T_{gas_offset} is calculated. T_{gas_offset} is calculated by multiplying $T_{gas\_diff\_max}$ by a parameter named $T_{gas\_offset\_factor}$, i.e. $T_{gas\_offset} = T_{gas\_diff\_max} \times T_{gas\_offset\_factor}$. T_{gas_target} is then calculated as follows: $T_{gas\_target} = T_{gas\_max} - T_{gas\_offset}$. T_{gas_max} is the maximum CHSS gas temperature allowed (typically 85 °C). When $T_{gas\_smooth\_threshold}$ has not yet been reached, $T_{gas\_target} = T_{gas\_max}$. "b" is calculated as follows: $b = MAXIMUM\ [4,\ (T_{gas\_offset\_multiplier} \times T_{gas\_offset})]$. When $T_{gas\_smooth\_threshold}$ has not yet been reached, b=4. $T_{gas\_offset\_factor}$ and $T_{gas\_offset\_multiplier}$ are both tuning parameters. Multiple fuelling simulations were conducted and appropriate settings for these two parameters were determined to be $T_{gas\_offset\_factor} = 0.6$ and $T_{gas\_offset\_multiplier} = 5$. These settings should be confirmed with actual testing.

To summarize, the adaptable T_{gas} Throttle concept with self-adjusting parameters utilizes the control logic illustrated in Figure 6 whereby T_{gas_target} and "b" automatically adjust during fuelling according to the equations above. To illustrate the self-adjusting parameters in action, see Figure 18. This graph shows how T_{gas_target} changes based on $T_{gas\_diff\_max}$ and thus T_{gas_offset}.

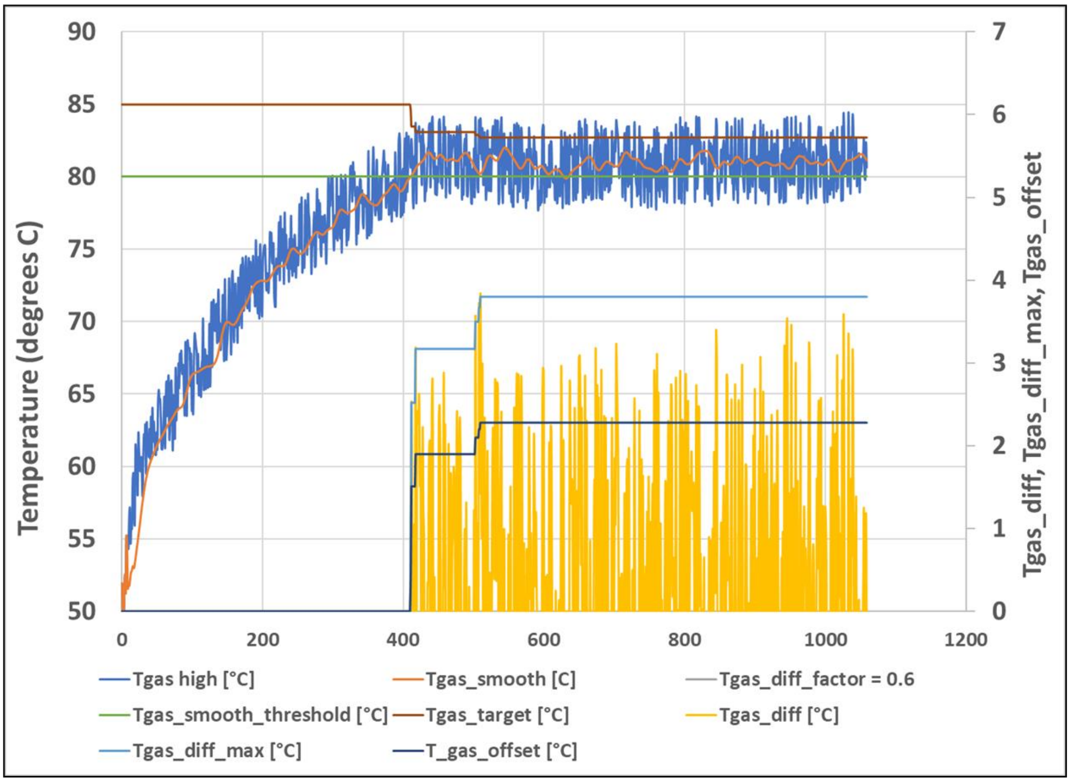

Figure 18: Illustration of self-adjusting parameters in T_{gas} Throttle

To demonstrate the robustness of the adaptable T_{gas} Throttle with self-adjusting parameters, approximately 150 fuelling simulations were conducted at different ambient temperatures, fuel delivery temperatures, noise amplitudes in T_{gas_high}, initial CHSS pressures, CHSS K_v values, CHSS type 4 liner thermal conductivity values, CHSS type 3 liner properties, and CHSS surface to volume ratios. In other words, to test the robustness of this approach, all relevant parameters were varied over a wide range. In every simulation, the peak CHSS gas temperature T_{gas_high} was kept below 85 °C. The highest peak gas temperature observed was 84.7 °C. Although these fuelling simulations show the methodology to be robust, this should be confirmed with testing.

The final version of the T_{gas} Throttle fuelling concept allows the self-adjusting parameters to be activated or inactivated via a flag variable SELFADJUST. When SELFADJUST = TRUE, the self-adjusting parameters are activated. When SELFADJUST = FALSE, the self-adjusting parameters are inactivated.

It is important to note that the filtering of noise from the vehicle should be discussed further within industry prior to implementation, as the unintended consequences could occur by modifying the measured temperature of the CHSS. Also, filtering may work differently if the station is not operating as expected.

3.2.7 Final Notes on the Fuelling Protocol Development

The PRHYDE project provided the opportunity to research many aspects of fuelling medium and heavy-duty vehicle CHSS at high flow rates. Although the thermodynamics of fuelling medium/heavy-duty vehicles at high flow rates is fundamentally the same as fuelling light duty vehicles at lower flow rates, the influence of various factors is different and important to note.

The first factor to note is the importance of the global flow coefficient of the combined station and vehicle fuelling components from the break-away to the tank inlets. This flow coefficient affects the pressure drop and the pressure drop greatly influences the gas temperature development in the CHSS. The larger the pressure drop, the more reverse Joule-Thomson heating that occurs, resulting in a higher internal gas temperature, everything else being equal. Therefore, it is important for vehicle OEMs and CHSS manufacturers to focus on the components that influence the global flow coefficient so that it is sufficiently large. This will be impactful on the fuelling times which can be achieved for a given fuel delivery temperature. Additionally, as noted in the SOC Taper Section (3.2.5), a large pressure drop will also cause the pressure ramp rate to be reduced, even under conditions where the gas temperature is not approaching its maximum. For both of these reasons, minimizing the pressure loss is very important for excellent high flow fuelling performance.

A second factor to note is the relatively lower influence of the thermal mass of the fuelling components on fuelling time performance for medium/heavy-duty vehicle high flow fuelling compared to light-duty vehicle fuelling. With the larger CHSS used in medium/heavy-duty vehicles, the relative amount of heat stored in the fuel delivery components compared with the enthalpy of the hydrogen dispensed is substantially lower for medium/heavy-duty vehicles than for light-duty vehicles. In SAE J2601, there is something called “cold dispenser” fuelling for both the table-based and MC Formula protocols. With “cold dispenser” the initial temperature of the fuel delivery components is assumed to be cold due to a previous fuelling. This results in the initial temperature of these components being substantially colder than the normal assumption that they are soaked at ambient temperature. Therefore, the amount of heat stored in the components and transferred to the hydrogen during fuelling is substantially less and this results in substantially faster fuelling times. Originally PRHYDE had considered including “cold dispenser” t_{final} tables, whereby the vehicle derives and stores a set of warm dispenser t_{final} tables and cold dispenser t_{final} tables. However, fuelling simulations which were conducted with a variety of assumptions for the thermal mass of the fuel delivery components showed relatively little difference in the derived t_{final} value. The small reduction in t_{final} with a “cold dispenser” did not look to be sufficient to warrant the added complexity of another set of t_{final} tables. Furthermore, “cold dispenser” fuelling has, to date, not been implemented by stations following SAE J2601, primarily due to the difficulty of determining if the station side fuel delivery components are adequately cold to qualify for the use of the “cold dispenser” fuelling. For the above reasons, PRHYDE partners decided not to implement the use of “cold dispenser” fuelling for the PRHYDE fuelling concepts.

A third factor to note is the importance of the injector design and the location of the temperature sensor in large CHSS. The CHSS of medium/heavy-duty vehicles typically use tanks with substantially larger length to diameter aspect ratios than light-duty CHSS. This makes mixing of the gas during fuelling more difficult and can result in large temperature gradients. Because the PRHYDE fuelling concepts utilize a one-dimensional fuelling model to derive the t_{final} tables, which can only calculate a bulk average gas temperature, it is important for the vehicle OEM or CHSS designer to pay special attention to the design of the hydrogen gas injector into the tank, the diameter, angle and length, to promote the best mixing possible. Furthermore, the placement of the gas temperature sensor within the tank is also important so that it represents the bulk average gas temperature as closely as possible. Testing and CFD modelling can be utilized to confirm temperature gradients and temperature sensor placement under different flow and fuel delivery temperature conditions.

4 General Assumptions for Protocol Development

The following classes of assumptions were made to enable simulation work and performance estimates. These assumptions are subject to further work needed, which will be discussed in PRHYDE Deliverable D6.8.

4.1 Components

Flow coefficient and thermal mass of the components are key parameters used by the fuelling model when deriving the t_{final} tables. The section below describes how component characteristics should be chosen for their use in the fuelling model depending on their belonging to the vehicle (components after the receptacle) or to the station (components including the nozzle / receptacle coupling, hose, and breakaway):

- Vehicle components (downstream of the receptacle all the way to the inlet(s) of the onboard storage system): Real vehicle component characteristics should be used when deriving the t_{final} table with the fuelling model, avoiding to use conservative hypothesis.
- Station components (piping, break-away, hose, nozzle / receptacle coupling,):
  - As the t_{final} table will be calculated by the OEM and stored onboard the vehicle, a set of conservative station component parameters have to be defined in a fuelling protocol standard that will be used by every OEM in the model used to derive the t_{final} table. These assumptions must be conservative in order to guarantee that all the stations on which the vehicle will fuel will have higher flow coefficient and lower specific heat capacity, as if it is not the case, there is a significant risk to overheat the CHSS.
  - As a consequence, it is important that the conservative parameters that will be defined in a future fuelling protocol standard are aligned with the recommendations made for station components.
  - One possibility is that the future fuelling protocol standard could include two sets of assumptions, one less conservative than the other. This could facilitate stations with larger, higher flow rate components and those with smaller, lower flow rate systems. Of course, it would also double the number of t_{final} tables, but would allow stations with better components to have better performance.

Recommendation on conservative parameters on station components :

Flow coefficient :

- Preliminary PRHYDE research has showed that for a specific case (fuelling of a 100 kg capacity CHSS of 7 type 4 350 L tank in 8 minutes at 15°C without precooling) estimating values for the minimum fuelling line flow coefficient.
- These values correspond to the entire fuelling line and therefore the K_v values of each components in the fuelling line should be higher than these values.
- The previous case is a specific case but could be used as a reference case to established a first recommendation of conservative set of parameters.
- Note that at the time of this writing the components available for the hydrogen automotive industry facilitates up to 120 g/s for H35 (60 g/s for H70) which could differ strongly from the previous recommendation.

Thermal mass:

- H70 high-flow components are still under development and there is currently no public information on the specifications of the prototypes. Therefore, it is difficult to estimate a conservative thermal mass value. NREL currently has the only H70 high-flow station known, although this station uses hard tubing connections to connect the dispenser to the CHSS. One approach would be to use a thermal mass of 2 times this value as the conservative hypothesis until better information is available.
- For large CHSS found on medium-duty/heavy-duty vehicles, modelling showed that the variation of thermal mass has a much smaller impact on the gas temperature development than for light-duty vehicles (typically less than 1 °C). This is because the ratio of the stored thermal energy in the components to the enthalpy of hydrogen dispensed is much smaller.

Notes on station components parameters used for deriving the ***t_{final}*** **table implemented and tested in PRHYDE for the fuelling protocol experimental validation campaign:**

In order to derive the t_{final} tables that have been implemented in the test equipment PLC for the fuelling protocol tests, flow coefficient and thermal mass hypothesis were made based on real component characteristics as both vehicle and station components were known. This situation and approach differ from the situation in which every OEM deriving t_{final} table will be as they will use standard hypothesis on station component. Nevertheless, the approach for the experimental validation is still valid.

4.1.1 Components for performance estimates

The components for performance estimates were based on NREL's heavy-duty station and heavy-duty vehicle simulator. As noted above, the station side components used are hard tubing and unions, and are not necessarily representative of the properties (K_v and thermal mass) of actual components which are still under development. Discussion on the specifications for future heavy-duty components will be discussed in PRHYDE Deliverable D6.8.

4.2 Communication

The focus of the PRHYDE team was fuelling protocols, and vehicle to dispenser communications was outside the scope of the project. Table 6 shows the type of data necessary for each fuelling protocol approach described in Section 3.2.

Table 6: Data type for each fuelling protocol approach

Fuelling protocol approach	Data type	Data transmitted
Type 2-PR-S Static	Static	t_{final} tables
Type 3-PR-S T_{gas} Initial	Static and Dynamic	t_{final} tables
Type 3-PR-S T_{gas} Initial+	Static and Dynamic	t_{final} tables, initial CHSS temperature
Type 3-PR-S T_{gas} Throttle	Static and Dynamic	t_{final} table, CHSS temperature

The Static, T_{gas} Initial, Initial + and Throttle fuelling processes require safety-critical communication of the vehicle-specific t_{final} tables from the vehicle to the dispenser before fuelling can begin; The T_{gas} Throttle fuelling requires communication of safety-critical real-time sensor data during the fuelling process. If a vehicle initiated fuelling abort signal is required (or implemented) as a safety mitigation, then special consideration must also be given to the safety-critical requirements for communication of the abort signal.

This has been assessed in APPENDIX E.

5 PERFORMANCE ESTIMATE

To estimate the performance of the PRHYDE fuelling concepts, computer fuelling simulations, as well as laboratory tests, were conducted. Fuelling simulations were conducted by WP4 and laboratory testing was conducted by WP5. The computer fuelling simulations modeled a full CHSS whereas the laboratory tests were conducted on single tanks. The fuel delivery temperatures utilized for the modeling and testing were based on achieving an approximately 10 minute fuelling time from the minimum CHSS pressure and SAE J2601 hot soak temperature at an ambient temperature of 35 °C. Although the absolute fuelling performance of these fuelling concepts can be inferred from the simulation and test results, it is the relative fuelling performance that is of the most interest. All of the PRHYDE fuelling concepts have potential to achieve sub 10-minute fuelling under all ambient temperature conditions, but the fuel delivery temperature required to do so will vary, depending on a number of factors, including the K_v of the station side fuel delivery components, K_v of the CHSS components, the thermal mass or effective heat capacity of these components, and the thermophysical properties of the individual tanks within the CHSS.

5.1 CHSS System Performance

A number of CHSS system fuelling simulations were conducted by WP4 using different CHSS, assumptions, and two different fuelling models. The focus of this section will be on simulation results obtained from the National Renewable Energy Laboratory's (NREL's) H2FillS model. This model facilitated the simulation of not only the PRHYDE fuelling concepts but also two additional fuelling protocols to provide a relative comparison of the fuelling time improvement achieved with the PRHYDE fuelling concepts.

5.1.1 Fuelling Protocols Compared

Currently, there is only one published standard fuelling protocol for heavy duty vehicles with CHSS volumes greater than 250 liters, SAE J2601 CHSS Capacity Category D. This protocol is applicable to vehicles with 70 MPa CHSS and a total water volume capacity of 250 liters and above. A limitation of this fuelling protocol is that it is constrained to peak mass flow rates of less than 60 g/s.

A new fuelling protocol document has been initiated within the SAE Fuel Cell Standards Committee Interface Task Force, TIR J2601/5. This fuelling protocol document is expected to first be published as a technical information report, and will include fuelling protocols with flow rates greater than 60 g/s. It is currently anticipated that this will include higher flow versions of the Category D protocol as well as a new general-purpose high-flow MC Formula fuelling protocol (MCF-HF-G). [4] The MCF-HF-G fuelling protocol is the most relevant comparison to the PRHYDE fuelling concepts because it is expected to have the same maximum peak flow rate (i.e. 300 g/s for H70). Because it is a general-purpose fuelling protocol, it is expected to be a Type 1, see Section 3 structured similar to the SAE J2601 fuelling protocol utilized for LD fuelling. This means it will likely have CHSS volume categories and will likely

[4] The MCF-HF-G is a preliminary protocol that has not been fully developed, so the results are provided as an example, and should not be taken as final.

utilize worst-case assumptions regarding the pressure drop between the dispenser and CHSS, the thermal mass and surface areas of both station side and vehicle side components, the thermophysical properties of the tanks within the CHSS, and fuelling history will be assumed. There are two potential parameters communicated from the vehicle which can be utilized in this protocol to improve the fuelling performance. The first is the tank volume (TV), which is the total CHSS volume. This parameter can be checked independently by the dispenser by implementing a volume measurement algorithm. The second parameter is the largest single tank volume within the CHSS. This parameter can be communicated via the optional data field (OD) in the SAE J2799 communication protocol, but the dispenser is not able to check or verify it. It allows the protocol to utilize a more accurate t_{final} table derived based a boundary tank which is similar in size and thermodynamic behaviour. In comparing the PRHYDE fuelling concepts to the MCF-HF-G, the modelling assumed that the vehicle communicates both the total CHSS volume and the largest single tank volume. If these parameters are not communicated or not known, fuelling times will be slower.

Because the MCF-HF-G fuelling protocol is still under development, many of the assumptions and boundary conditions are preliminary, meaning they could change between now and when the protocol is published in a standard. Conservative assumptions were made regarding the Kv and thermal mass for the fuel dispensing components on the station and vehicle CHSS. The Kv was set to 0.65 of the default value and the thermal mass was set to 3 times the default value. The default values are based on the design of the experimental dispenser and CHSS (heavy-duty vehicle simulator or HDVS) integrated into NREL's Hydrogen Infrastructure Testing and Research Facility (HITRF). NREL's HDVS is a CHSS designed to emulate that of a real-world Class 8 truck. It consists of seven Type IV 243.5 L tanks for a total CHSS volume of 1705 L (68.5 kg of hydrogen at full density). Because representative high flow fuel dispensing components (nozzle, receptacle, hose, breakaway) are not yet available, the high-flow dispenser and HDVS CHSS are the best representation of a real-world system currently available. For the PRHYDE fuelling concepts, the Kv and thermal mass were based on the default values.

5.1.2 Simulation Results

The simulation results are shown in Figure 19 through Figure 21. The ambient temperature utilized is 35 °C and the fuel delivery temperature utilized for all the simulations is -21 °C. The ambient temperature was chosen to represent performance on a warm summer day and the fuel delivery temperature was chosen as the temperature at which the PRHYDE fuelling concepts can achieve a 10 minute fill from minimum CHSS pressure (2 MPa) and the CHSS soaked at the J2601 hot-soak temperature. In each figure, there are five initial pressures (2, 5, 10, 15, and 20 MPa) to illustrate the fuelling time performance at different starting pressures. Figure 19 illustrates the fuelling time when the CHSS is initially at the hot-soak temperature. In Figure 20 and Figure 21, the initial soak temperature of the CHSS is °5 C and °10 C colder, respectively.

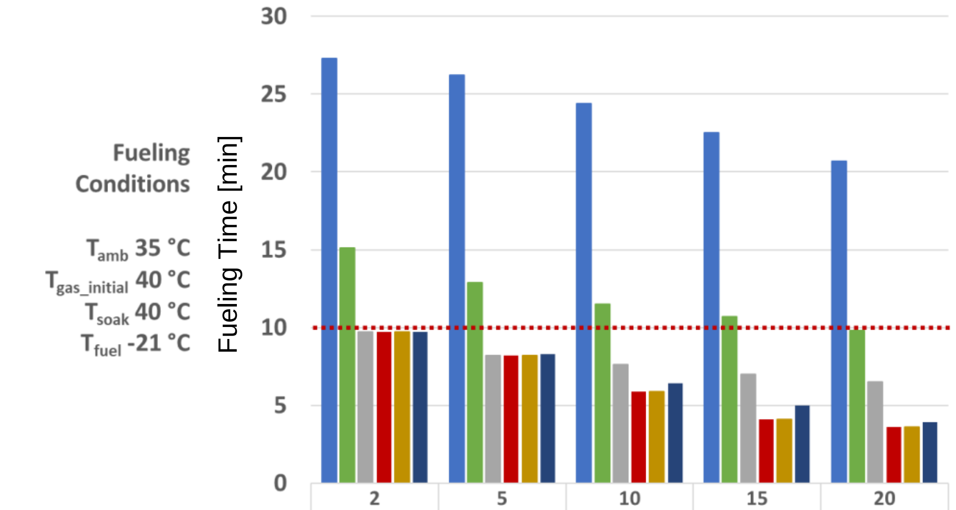

	2	5	10	15	20
SAE J2601 Category D	27.3	26.2	24.4	22.5	20.7
MC Formula High Flow General	15.1	12.9	11.5	10.7	9.8
Static	9.7	8.2	7.6	7	6.5
Tgas Initial	9.7	8.2	5.9	4.1	3.6
Tgas Initial+	9.7	8.2	5.9	4.1	3.6
Tgas Throttle Adaptable	9.7	8.3	6.4	5	3.9

Figure 19: Fuelling Time Comparison: T_{amb} = 35 °C, T_{soak} = 40 °C

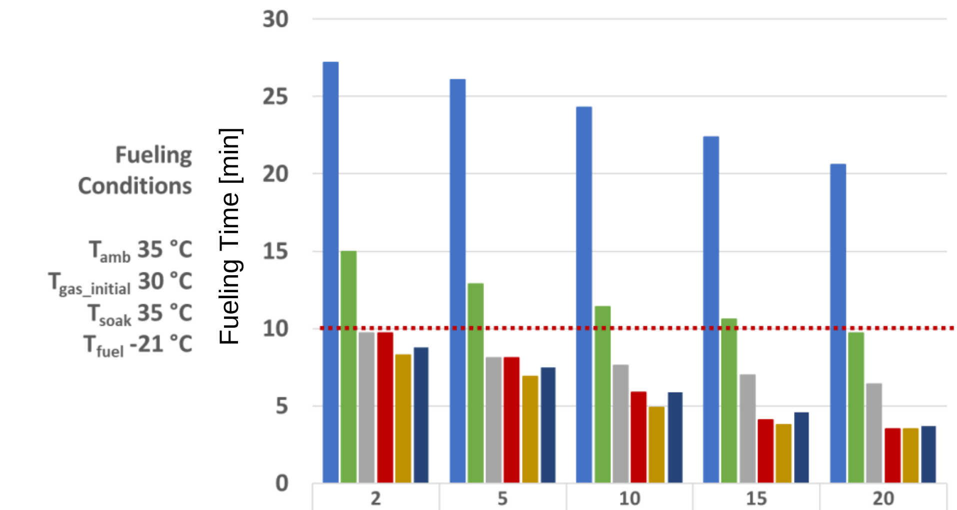

	2	5	10	15	20
SAE J2601 Category D	27.2	26.1	24.3	22.4	20.6
MC Formula High Flow General	15	12.9	11.4	10.6	9.7
Static	9.7	8.1	7.6	7	6.4
Tgas Initial	9.7	8.1	5.9	4.1	3.5
Tgas Initial+	8.3	6.9	4.9	3.8	3.5
Tgas Throttle Adaptable	8.8	7.5	5.9	4.6	3.7

Figure 20: Fuelling Time Comparison: T_{amb} = 35 °C, T_{soak} = 35 °C

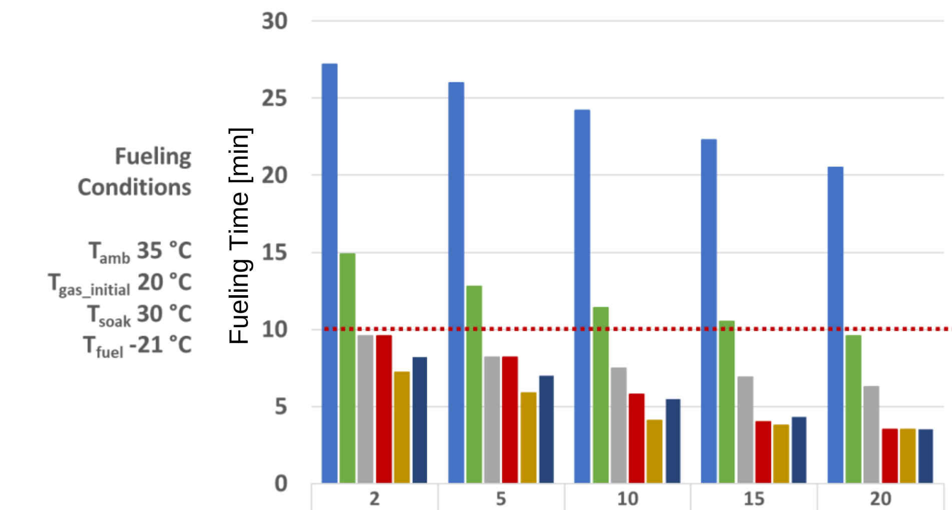

	2	5	10	15	20
SAE J2601 Category D	27.2	26	24.2	22.3	20.5
MC Formula High Flow General	14.9	12.8	11.4	10.5	9.6
Static	9.6	8.2	7.5	6.9	6.3
Tgas Initial	9.6	8.2	5.8	4	3.5
Tgas Initial+	7.2	5.9	4.1	3.8	3.5
Tgas Throttle Adaptable	8.2	7	5.5	4.3	3.5

Figure 21: Fuelling Time Comparison: T_{amb} = 35 °C, T_{soak} = 30 °C

5.1.3 Key Takeaways from Simulations

All of the PRHYDE fuelling concepts can achieve sub-10-minute fuelling with a fuel delivery temperature of -21 °C, which in SAE J2601 parlance falls within the "T20" fuel delivery temperature category. Such achievement was one of the objectives of PRHYDE **Deliverable D2.6** because less pre-cooling generally translates into lower capital and operational costs of the station, resulting in lower fuel costs to the customer. At an initial CHSS pressure of 2 MPa and CHSS hot-soak (conditions which result in the longest fuelling times), the MCF-HF-G fuelling protocol takes approximately 50% longer than the PRHYDE fuelling concepts. This is due to a combination of worst-case assumptions, including the CHSS pressure drop (lower K_v), higher CHSS thermal mass, and a conservative boundary tank (the largest tank in the CHSS) which has a lower surface to volume ratio than that of the tanks in actual CHSS. And finally, at these same conditions, the SAE J2601 Category D fuelling protocol takes 173% (17.3 minutes) longer to fill than the PRHYDE fuelling concepts. This is due primarily to the 60 g/s flow rate limit, but even without this limit (for example, a Category D protocol with a 90 or 120 g/s flow rate limit), at T20 fuel delivery temperatures, the fuelling time would be constrained to about 23 minutes.

When looking at the fuelling performance of the PRHYDE concepts at conditions which have higher initial pressures and/or lower initial gas temperatures, the relative performance improvement over SAE J2601 Category D and the MCF-HF-G fuelling protocols is even more stark. This is because the T_{gas} Initial, T_{gas} Initial+ and T_{gas} Throttle fuelling concepts all take advantage of a higher initial CHSS pressure, and T_{gas} Initial+ and T_{gas} Throttle take advantage of a lower initial CHSS gas temperature to give fuelling performance that exceeds the PRHYDE 10 minute goal. For example, as illustrated in Figure 19, even under hot soak conditions, when the initial CHSS pressure is 10 MPa (~ 20% SOC), the fuelling time for T_{gas} Initial, T_{gas} Initial+ and T_{gas} Throttle is approximately 6 minutes. And at an initial CHSS pressure of 20 MPa (~ 35% SOC), the fuelling concepts all deliver fuelling times less than four minutes. Referencing Figure 21, when the initial gas temperature is substantially colder than the ambient temperature, the T_{gas} Initial+ fuelling concept can deliver 4-minute fuelling times at an initial CHSS pressure as low as 10 MPa.

Considering that most fills occur at an initial CHSS pressure > 10 MPa and with an initial gas temperature lower than ambient (due to the gas cooling under the depressurization that occurs during driving), these fuelling simulations indicate that the PRHYDE fuelling concepts should be able to deliver typical fuelling times that are faster than gasoline and diesel for medium duty and heavy duty trucks.

In terms of the best overall fuelling performance, it appears that the T_{gas} Initial+ and T_{gas} Throttle Concepts offer the best overall fuelling performance, with a slight edge perhaps going to T_{gas} Initial+. These simulations only considered conditions where the initial CHSS pressure and initial CHSS gas temperature were higher and lower, respectively. There may be other conditions where T_{gas} Throttle may have a slight edge over T_{gas} Initial+, such as if the station side fuel delivery components have a lower pressure drop (higher K_v) than the default value utilized in the t_{final} derivation or when the fuel delivery components are cold from a previous fuelling.

5.2 Single Tank Performance

Single tank tests were conducted by WP5 at two laboratories. TestNet conducted testing of a Nikola sourced 165 L Type IV H70 tank and ZBT conducted (among other tanks) testing of a 244 L Type IV H70 tank. The TestNet facility was able to tightly control the temperature of the tank via a temperature-controlled chamber. ZBT conducted testing in an outdoor facility where the temperature could not be controlled. The focus of this section will be on the testing results obtained from the TestNet laboratory, because of the temperature-controlled conditions.

5.2.1 Testing Results

The testing results are shown in Figure 22 and Figure 23. The ambient temperature utilized was 35 °C and the fuel delivery temperature utilized for tests with an initial pressure of 2 MPa was approximately -18 °C and for tests with an initial pressure of 15 MPa was approximately -15 °C. The ambient temperature was chosen to represent performance on a warm summer day and the fuel delivery temperature was chosen as the temperature at which the PRHYDE fuelling concepts can achieve an approximately 10-minute fill from minimum CHSS pressure (2 MPa) and the CHSS soaked at the ambient temperature. In each figure, there are two initial pressures (2 and 15 MPa) to illustrate the fuelling time performance at different starting pressures. Figure 22 illustrates the fuelling time when the tank is initially soaked at the ambient temperature. In Figure 23, the tank is defueled prior to the test so that the initial gas temperature is °10 C colder. Because the Static and T_{gas} Initial fuelling concepts use the same t_{final} tables, regardless of the initial gas temperature, only T_{gas} Initial+ and T_{gas} Throttle fuelling concepts were tested with a colder initial gas temperature.

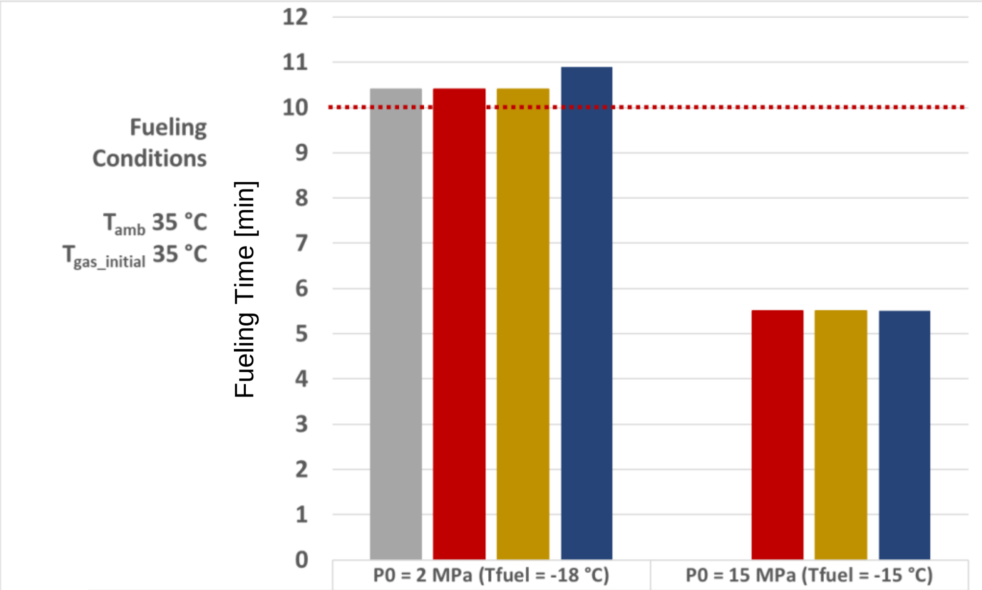

	P0 = 2 MPa (Tfuel = -18 °C)	P0 = 15 MPa (Tfuel = -15 °C)
Static	10.4	
Tgas Initial	10.4	5.5
Tgas Initial+	10.4	5.5
Tgas Throttle Adaptable	10.9	5.5

Figure 22: Fuelling Time Comparison: Tamb = 35 °C, T_{gas} Initial = 35 °C

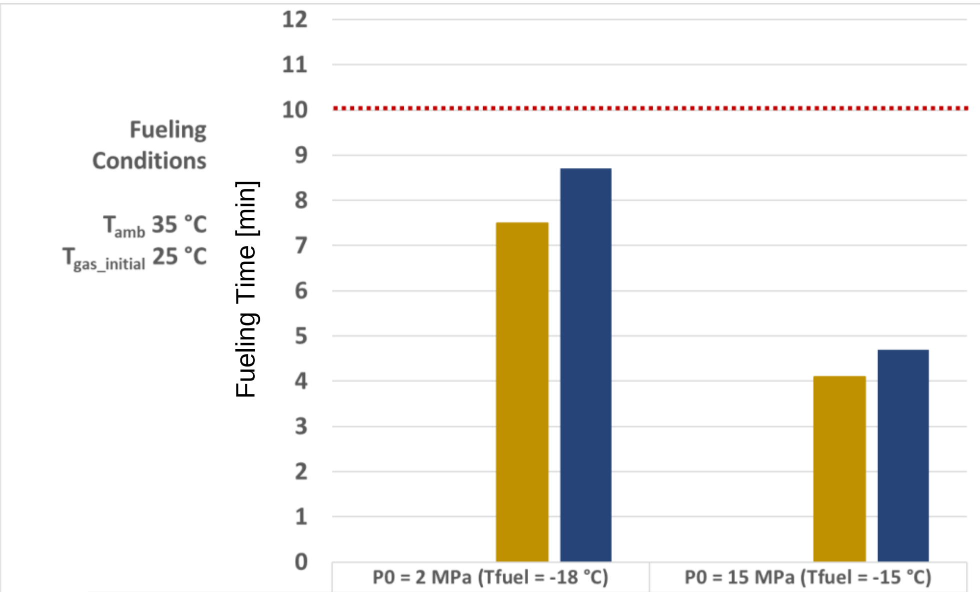

	P0 = 2 MPa (Tfuel = -18 °C)	P0 = 15 MPa (Tfuel = -15 °C)
Static		
Tgas Initial		
Tgas Initial+	7.5	4.1
Tgas Throttle Adaptable	8.7	4.7

Figure 23: Fuelling Time Comparison: T_{amb} = 35 °C, T_{gas} Initial= 25 °C

5.2.2 Key Takeaways from Single Tank Testing

The key takeaways from a review of the testing results are primarily that they confirm the modelling that was done on a full CHSS in Section 7.1. In other words, the single tank testing at an ambient temperature and initial CHSS gas temperature of 35 °C and initial CHSS pressure of 2 MPa demonstrated an approximate 10-minute fuelling time, similar to that of the fuelling simulations of the full CHSS. Comparing the relative fuelling time improvement at a higher initial CHSS pressure of 15 MPa, a similar ~ 40% reduction in fuelling time was realized. And comparing the fuelling time reduction at an initial CHSS pressure of 2 MPa and a lower initial gas temperature, the reduction was 20 to 25%, and with an initial CHSS pressure of 15 MPa, the reduction was 55 to 60%. These results also correlate well with the reduction in fuelling times demonstrated by the simulation results shown in Figure 20 and Figure 21.

5.3 Interpretation of performance estimates

Although there are still some unknowns which will influence the absolute fuelling performance (such as the thermophysical properties of the station side fuel dispensing components), the fuelling simulations and testing have demonstrated the PRHYDE fuelling concepts to have drastic reductions in fuelling time due to the elimination of many of the inherent embedded worst-case assumptions. Fuelling times less than 10 minutes can be realized under all fuelling conditions and with the Type 3 PRHYDE fuelling concepts (T_{gas} Initial, T_{gas} Initial+ and T_{gas} Throttle), fuelling times less than five minutes can be realized under many typical fuelling conditions.

6 Implementation of PRHYDE Fuelling Concepts

This section provides the flow diagrams and APPENDIX A details the subroutines for the fuelling concepts described in this document.

The Static, T_{gas} Initial, and T_{gas} Initial+ fuelling concepts are essentially identical in the way the control algorithm is implemented, and the control framework is almost identical to MC Formula in SAE J2601. The only thing that differentiates these three approaches is the selection of the t_{final} table, and this is done by the vehicle at the beginning of the fuelling. Once the t_{final} table is selected and the t_{final} vector is calculated for that fill, then all three fuelling concepts operate identically. The T_{gas} Throttle fuelling concept also functions identically, except an additional throttling PRR is calculated and can reduce the PRR when T_{gas} throttling is active.

Flow diagrams are provided for each of the fuelling concepts. These flow diagrams make reference to subroutines in APPENDIX A and are provided to illustrate the order of operation of the subroutines for each fuelling concept. All of the subroutines, except for the selection of the t_{final} table subroutine, are common to all fuelling concepts. In some subroutines, there may be elements which are only activated for certain fuelling concepts, in which case, these are called out in the subroutine.

The flow diagrams illustrate the order in which the subroutines are implemented, and also provide a callout with a short description of each subroutine. A high-level description of each subroutine is also provided below. For a more detailed explanation of each subroutine and its function, refer to the appropriate subsection of APPENDIX A which describes each subroutine in detail.

Subroutine A.1.1.1 - Determine Initial Parameters.

This subroutine determines the initial conditions of many important parameters such as the initial CHSS pressure $P_{initial}$, the ambient temperature T_{amb}, and the expected end of fill mass average fuel delivery temperature $MAT_{expected}$.

Subroutine A.1.1.2 - Parameter Initialization.

Many of the parameters used by the control algorithm need to have initial values assigned to them. This subroutine assigns those initial values. There are parameters that are initialized with non-discretionary values – these parameters must be initialized by the values specified in the subroutine. There are also parameters that are initialized with discretionary values – these values are determined by the dispenser manufacturer or testing laboratory. An example is the target state of charge (SOC_{target}). This can be set between 95 and 100 percent.

Subroutines A.1.1.3 through A.1.1.6 - Selection of t_{final} table.

These subroutines are unique to each fuelling concept:

- Subroutine A.1.1.3 applies to the Type 2 Static Data Fuelling Concept,
- Subroutine A.1.1.4 applies to the Type 3 T_{gas} Initial Fuelling Concept,
- Subroutine A.1.1.5 applies to the Type 3 T_{gas} Initial+ Fuelling Concept, and
- Subroutine A.1.1.6 applies to the Type 3 T_{gas} Throttle Fuelling Concept.

This subroutine selects the appropriate t_{final} table and P_{min} value. The t_{final} table and P_{min} value are selected based on initial conditions.

Subroutine A.1.1.7 - t_{final} Vector Interpolation.

This subroutine interpolates the t_{final} values from the selected t_{final} table based on the ambient temperature. Each row of the t_{final} table provides a set of t_{final} values for a particular ambient temperature. Because the actual ambient temperature will usually be at a value between two values in the t_{final} table, it is necessary to interpolate on the ambient temperature to derive the set of t_{final} values utilized in the control algorithm. This set of t_{final} values is referred to as the t_{final} vector. This vector is a set of t_{final} values associated with an MAT value. This vector is stored and called up in the Calculation of t_{final} Subroutine (A.1.1.9) to precisely calculate a t_{final} based on the control value of the mass average fuel delivery temperature MAT_C.

Subroutine A.1.1.8 - Mass Average Calculation of the Fuel Delivery Temperature.

This subroutine calculates three mass average fuel delivery temperatures, MAT_0, MAT_{30}, and MAT_C. MAT_C is derived from MAT_{30} and MAT_0.

Subroutine A.1.1.9 - Calculation of t_{final}.

This subroutine calculates the t_{final} value for each time step throughout the fill. t_{final} is the primary control variable used to calculate the pressure ramp rate PRR in the Calculation of PRR and P_{ramp} Subroutine (A.1.1.10). In this subroutine, t_{final} is calculated from the t_{final} vector. Linear interpolation is used to calculate the t_{final} value by utilizing MAT_C and the two MAT vector values above and below MAT_C.

Subroutine A.1.1.10 - Calculation of PRR and P_{ramp}.

This subroutine calculates the pressure ramp rate PRR and ramp pressure P_{ramp}. The ramp pressure is the pressure the dispenser targets for each timestep throughout the fill. An upper pressure limit value is also calculated based on P_{ramp}, which enforces a process limit on the dispenser pressure. P_{ramp} advances each timestep in an amount equal to the PRR. This subroutine also calculates a reduced PRR for the T_{gas} Throttle fuelling concept once the gas temperature T_{gas_high} exceeds a threshold temperature value $T_{threshold}$.

Subroutine A.1.1.11 - Determine Communication Pressure Target.

This subroutine calculates the pressure target as a function of the lowest gas temperature in the CHSS, T_{gas_low}, and the SOC target value, SOC_{target}.

Subroutine A.1.1.12 - Evaluate End of Fill Criteria.

This subroutine compares the dispenser pressure $P_{station}$ to the pressure target and if the dispenser pressure is greater than or equal to the pressure target, the fill is terminated. This subroutine is unique from the others in that the frequency is 10 Hz, in other words, the comparison of the dispenser pressure to the pressure target is conducted 10 times per second or timestep.

Subroutine A.1.1.13 - Process Check.

This subroutine is used to check if temperature, pressure, and mass flow rate are within the process limits. If any of the process condition checks are not satisfied, the

Process Check Subroutine fails, and the fill shall terminate as soon as possible, but within five seconds.

Subroutine A.1.1.14 - Advance Counters.

This subroutine marks the end of a single timestep within the control algorithm. It advances the counters “n” and “j” by one and then loops back to Subroutine A.1.1.8.

6.1 Type 2-PR-S – Static

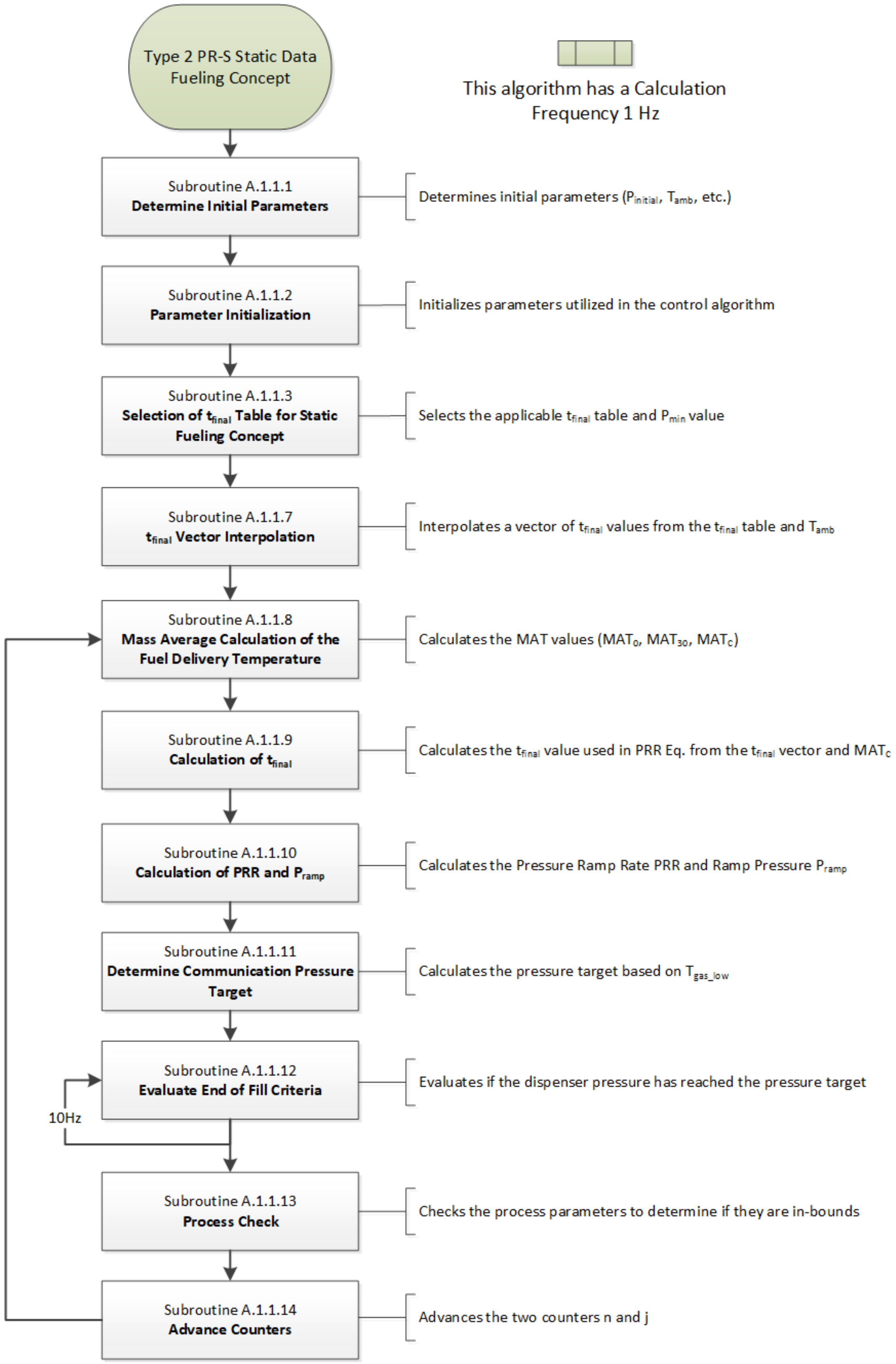

Figure 24: Flow Diagram for Type 2-PR-S Static Data Fuelling Concept

6.2 Type 3-PR-S – T_{gas} Initial

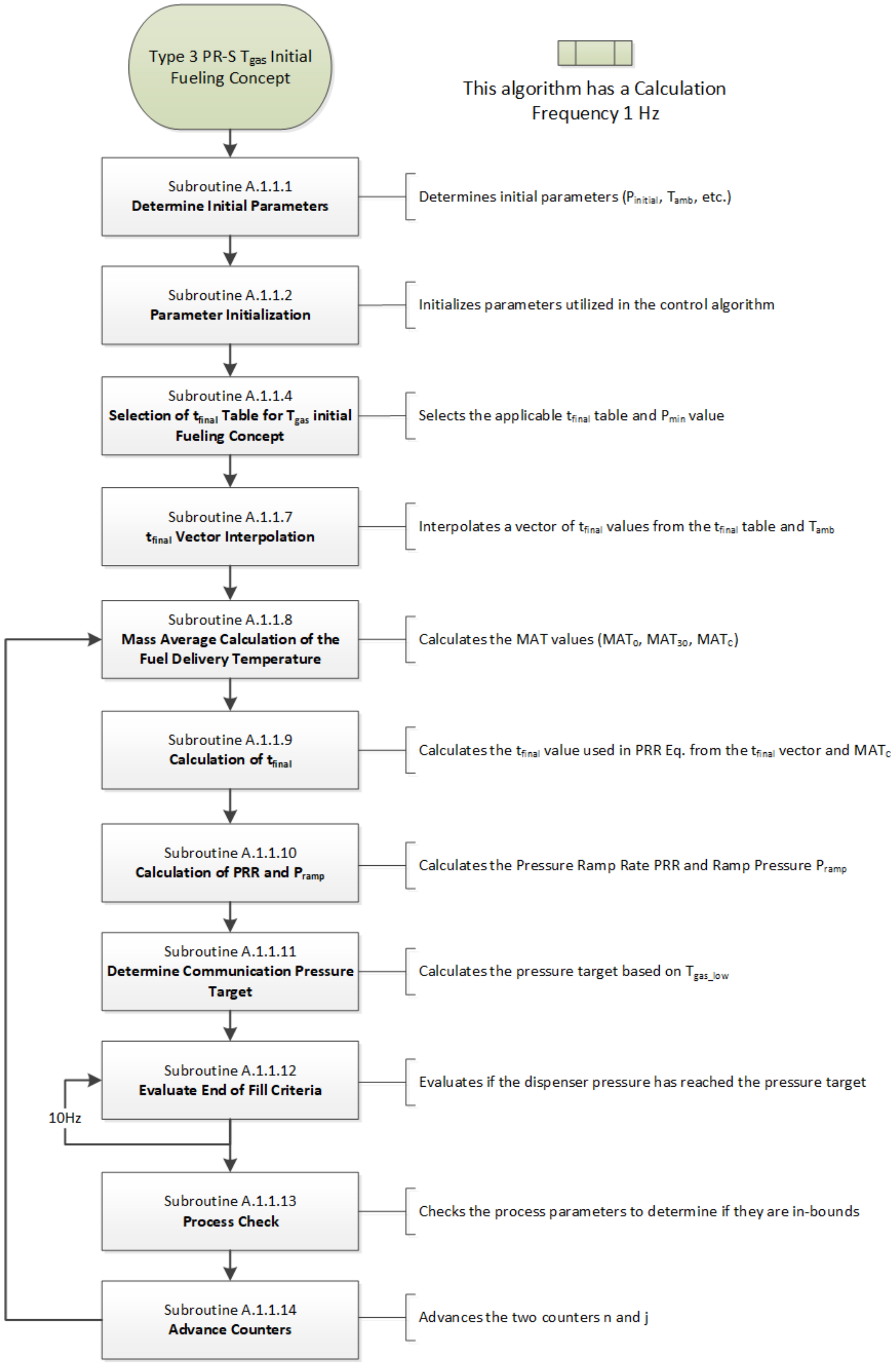

Figure 25: Flow Diagram for Type 3-PR-S T_{gas} Initial Fuelling Concept

6.3 Type 3-PR-S – T_{gas} Initial+

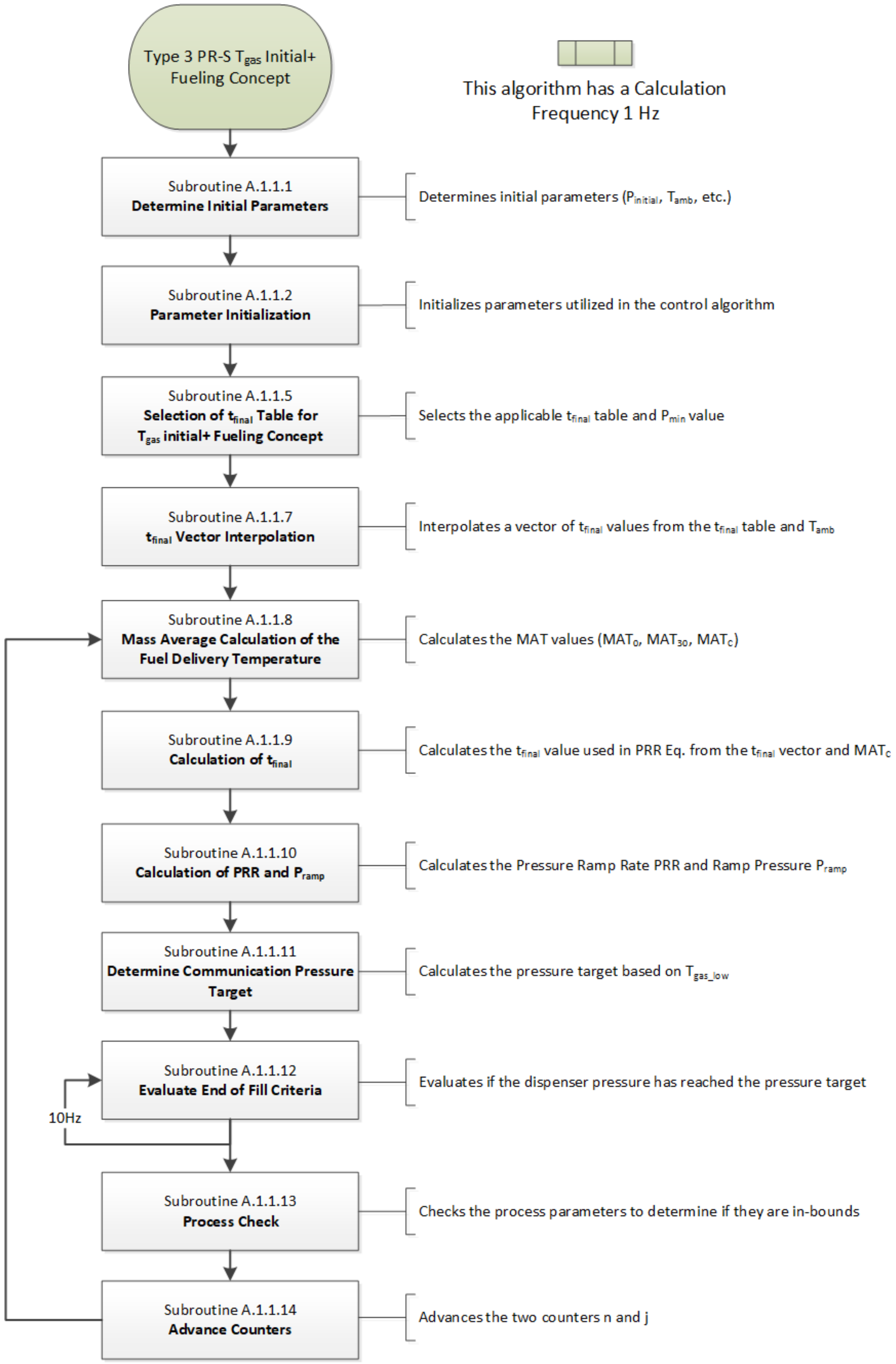

Figure 26: Flow Diagram for Type 3-PR-S T_{gas} Initial+ Fuelling Concept

6.4 Type 3-PR-S – T_{gas} Throttle

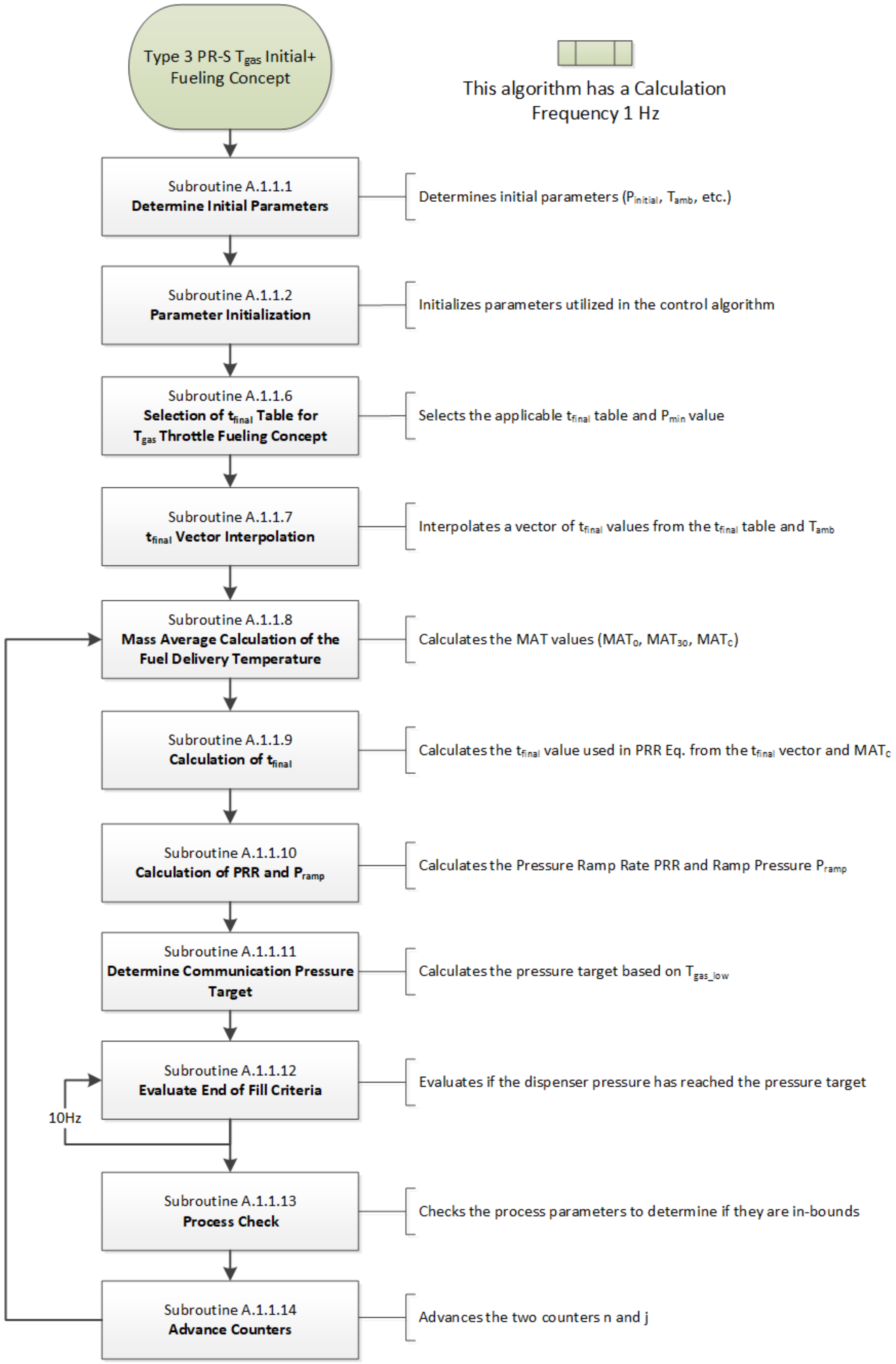

Figure 27: Flow Diagram for Type 3-PR-S T_{gas} Throttle Fuelling Concept

7 How to derive t_{final} values

All of the PRHYDE fuelling concepts utilize a set of t_{final} tables. A t_{final} value is calculated from these t_{final} tables, and is utilized in the PRR equation. The t_{final} table consist of t_{final} values which are a function of the ambient temperature and the mass average of the fuel delivery temperature at discrete intervals. t_{final} tables are also a function of the minimum pressure P_{min} and there can be multiple t_{final} tables for discrete P_{min} values. Therefore, these t_{final} tables provide a control map for determining the correct fuelling rate continuously during the fuelling process (see Section 3).

Because the PRHYDE fuelling concepts utilize t_{final} tables which are tailored to the vehicle CHSS, the vehicle OEM is responsible for the derivation of the t_{final} tables specific to the vehicle. Therefore, it is paramount that each vehicle OEM utilize the correct process for deriving the t_{final} tables. This document will provide a step-by-step explanation of that correct process.

7.1 Fuelling model

A prerequisite to the derivation of t_{final} tables is the use of a validated fuelling model. The fuelling model should be capable of accurately modelling the gas temperature development in the CHSS. Typically, this is done using a model which calculates the bulk-average gas temperature in each tank of the CHSS. The model should include the heat transfer of the stored thermal energy and heat from the environment from the fuel dispensing components to the hydrogen gas. The fuel dispensing components consist of all the components downstream of the dispenser outlet temperature and pressure measurement locations, including the breakaway fitting, hose, nozzle, receptacle, piping, joints, manifolds and valves. The model should have the fidelity to input the thermophysical properties of these components (internal and external surface areas, heat capacity, thermal conductivity, flow coefficient, etc.) and conduct a mass and energy balance from the dispenser outlet to inlet of each CHSS tank. An alternative but less preferred approach that can be used is to treat these components globally whereby the total surface area, heat capacity, and thermal conductivity is utilized, along with a global C_v or K_v coefficient. This approach can only be used when all of the tanks in the CHSS are identical.

An example of a fuelling model with this capability is the H2FillS model developed and published by the National Renewable Energy Laboratory (NREL). Figure 28 illustrates the GUI for this model that facilitates the input of all the necessary parameters.

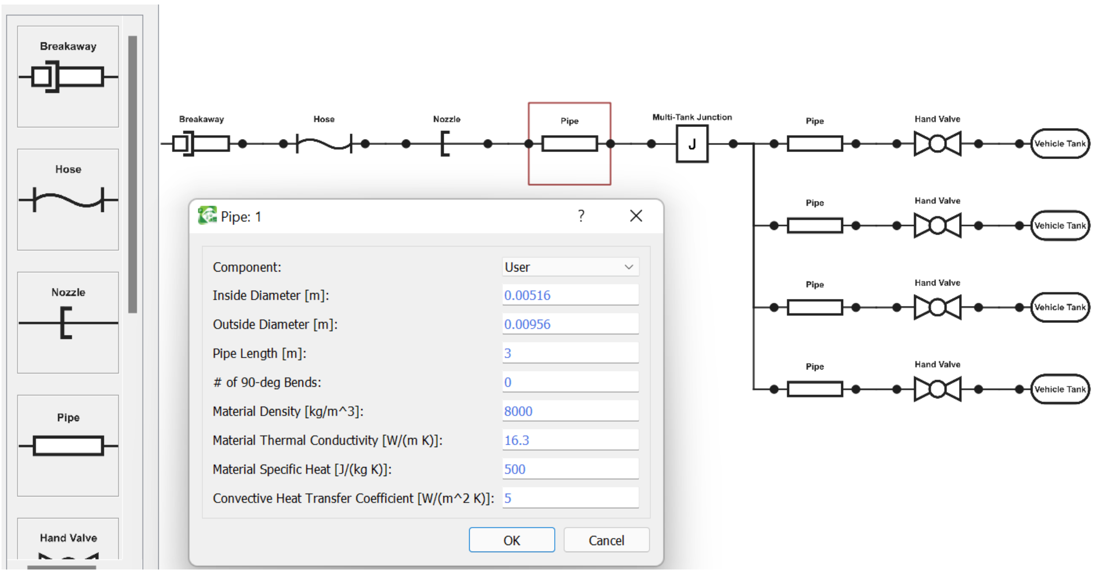

Figure 28: GUI for NREL's H2FillS model (Source: H2FillS)

7.2 Validation of the Fuelling Model

A validated fuelling model is one which has gone through a thorough verification process whereby the model output results are compared to experimental results and found to be sufficiently accurate. Typically, this means that the bulk average gas temperature from the model and experiments have an agreement within +/- 3 to 5 K. The verification process should include confirming the model results under high-flow and low-flow conditions, cold and warm fuel delivery temperatures, and a wide range of ambient temperatures.

7.3 Model Capabilities

In addition to accurately calculating the bulk-average gas temperature in each of the tanks within the CHSS, the model should have some other features which are amenable to the derivation of the t_{final} tables.

7.3.1 Pressure Ramp Rate

The fuelling model should be capable of conducting simulations where the pressure at the dispenser outlet is increased at a constant rate throughout the fill. This is called the pressure ramp rate (PRR) of the fill. This can be a user specified value, or the model can automatically calculate this value iteratively based on user specified end of fill conditions, the latter feature being highly desirable.

7.3.2 Simulation Conditions

The fuelling model should allow the user to specify the ambient temperature, the fuel delivery temperature, and the ending SOC. In a multi-tank CHSS, the ending SOC should be based on the lowest calculated SOC for each of the tanks in the CHSS.

7.3.3 Model Output

The fuelling model should, at a minimum, output the bulk-average gas temperature and pressure for each of the tanks in the CHSS.

7.3.4 Automated Capabilities

In order to generate the t_{final} tables, the model should be capable of automating the process as much as possible. At a minimum, this requires the fuelling model to be capable of calculating a PRR that results in specified end conditions, such as a maximum gas temperature and SOC. The model then solves for the pressure ramp iteratively. Additionally, the model should allow the user to specify a maximum peak flow rate. In this case, the model solves for the PRR that achieves the SOC target and does not exceed the maximum gas temperature or maximum peak flow rate.

Ideally, the model should be capable of iteratively solving for the PRR by stepping through a range of ambient temperatures and fuel delivery temperatures. This allows the t_{final} tables to be derived automatically, which can result in significant time savings and reduce the chance of errors.

The NREL H2FillS model has all of these capabilities. Figure 29 shows an example of the “set fill profile” window within H2FillS whereby the user can specify the ambient temperature range and increment, the fuel delivery temperature range and increment, the CHSS initial range and increment, the APRR range (used to set bounds for the iterative solution), the peak mass flow rate, the peak dispenser outlet pressure (or breakaway inlet pressure), the fuel delivery (hose) temperature profile (flat or 30 second cool-down from ambient temperature), the maximum vehicle tank temperature (this is the maximum temperature in any individual tank in the CHSS), the initial CHSS tank soak temperature (defined as an initial temperature for the gas, liner, and tank walls), and the end of fill condition, which can be either a pressure or SOC (for t_{final} derivation, it is the SOC).

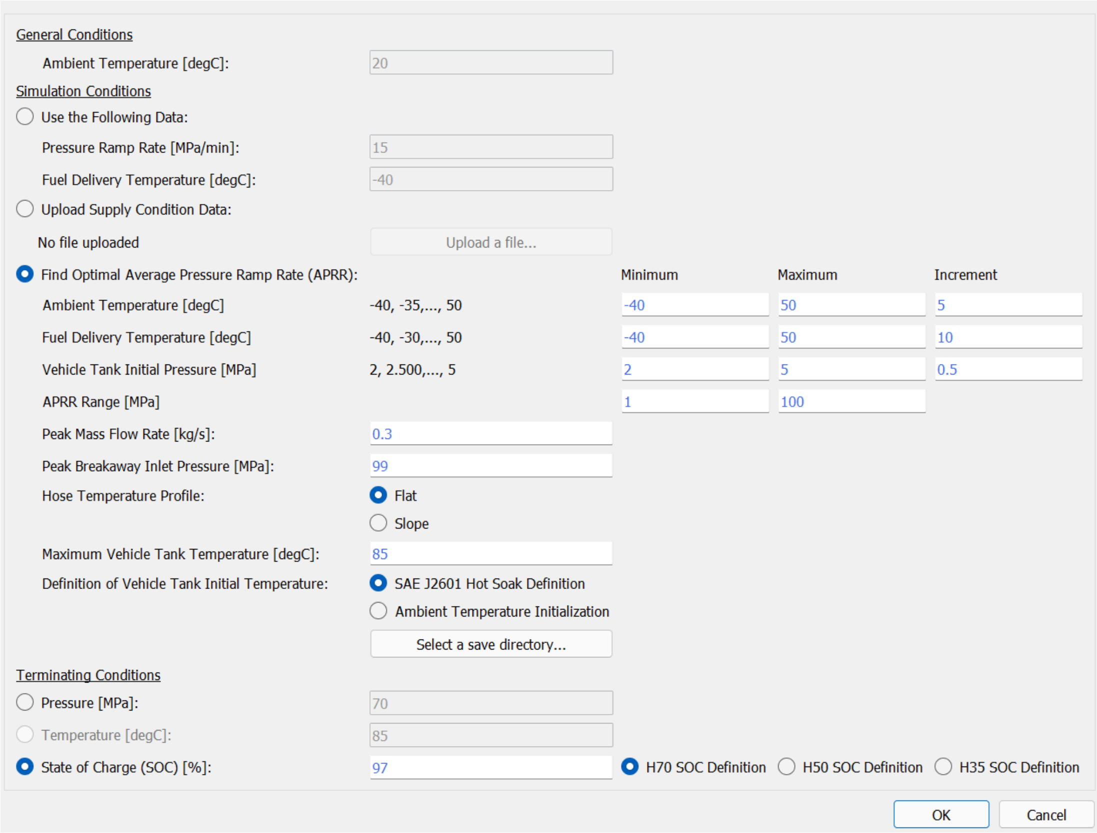

Figure 29: “Set fill profile” window from NREL’s H2FillS model (Source: H2FillS)

7.4 Considerations

The use of a 0D fuelling model does have some limitations, especially for modelling heavy duty vehicle tanks where the length to diameter ratio is relatively long (compared to vehicle tanks used in light duty vehicles). Experiments conducted in the PRHYDE project show that there can be significant gas temperature stratification. The stratification developed is strongly influenced by the mixing (or lack thereof) of the cold gas entering the tank with the rest of the gas in the tank. The HyTransfer project[5] showed that if the inlet velocity of the gas is above approximately 5 m/s, mixing is promoted and stratification is reduced. PRHYDE experimental results confirmed this as well. In addition to the inlet velocity, the profile of the injector into the tank also influences the mixing and temperature stratification.

The vehicle OEM needs to be cognizant of these factors when utilizing a 0D model to derive the t_{final} tables. Under fuelling conditions where it is known that significant temperature stratification can occur, the vehicle OEM may choose to factor this into the settings for the maximum gas temperature of the 0D model to provide additional temperature margin.

---

5 HyTransfer - Pre-Normative Research for Thermodynamic Optimization of Fast Hydrogen Transfer, see https://cordis.europa.eu/project/id/325277.

7.5 Inputting the CHSS configuration and properties to the fuelling model

The first step is to input each component of the CHSS into the fuelling model. The fuelling model should accurately represent the detailed design of the CHSS, including the piping, junctions and valves from the receptacle to each of the individual tanks in the CHSS. Figure 28 shows an example GUI of a multi-tank CHSS. Figure 30 through Figure 33 show examples of the inputs for each of these components. These values should be further refined in the standards organizations where PRHYDE will be documented.

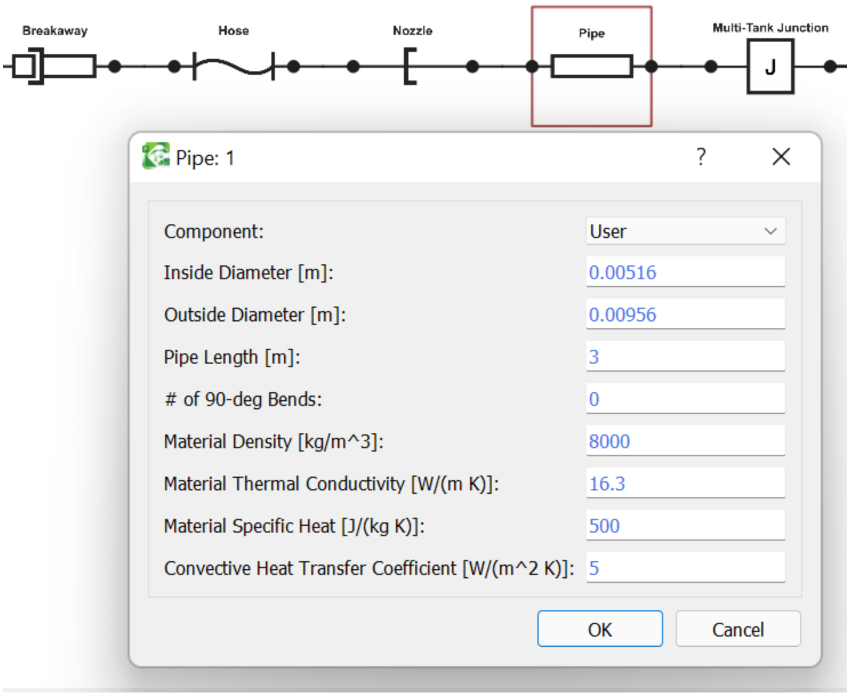

Figure 30: Example of fuelling model inputs for a "pipe" element in the CHSS (Source: H2FillS)

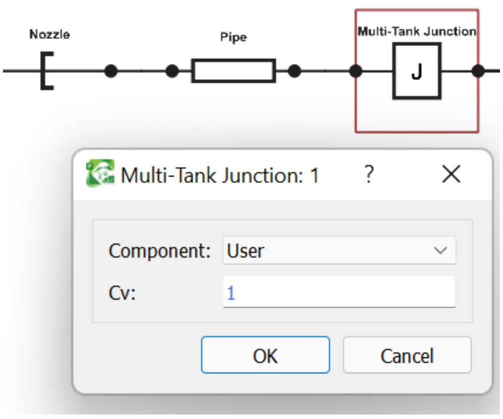

Figure 31: Example of fuelling model inputs for a "pipe" element in the CHSS (Source: H2FillS)

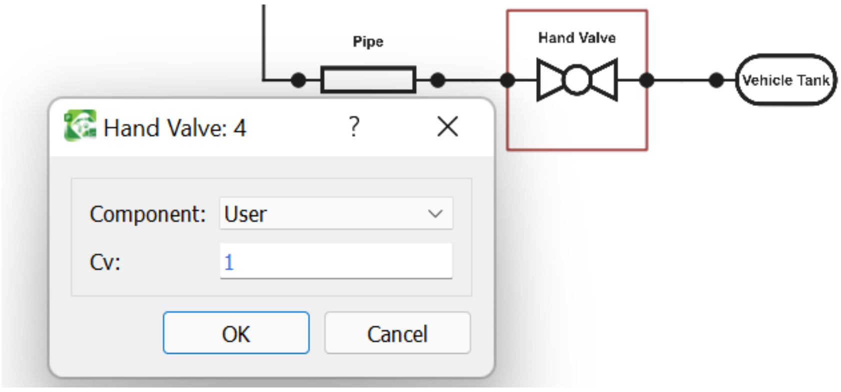

Figure 32: Example of fuelling model inputs for a "hand valve" element in the CHSS (Source: H2FillS)

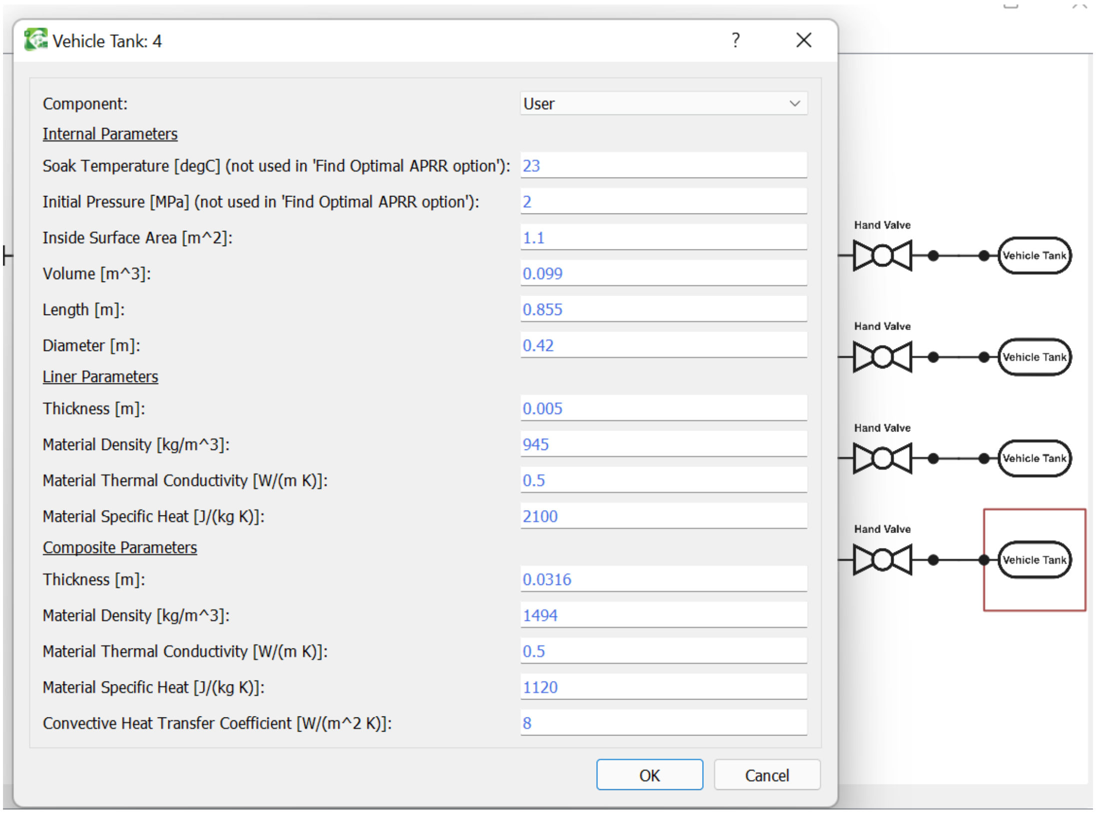

Figure 33: Example of fuelling model inputs for a "tank" element in the CHSS (Source: H2FillS)

7.6 Inputting the station side fuelling components to the fuelling model

In addition to the CHSS, the station side fuel delivery components must be input to the fuelling model. These include the breakaway fitting, the hose, and nozzle. These components are not unique to the vehicle CHSS. These components are common to the derivation of the t_{final} tables by all vehicle OEMs. The properties for these components should be conservative since there are a number of manufacturers of these components in the marketplace. The fuelling protocol standard should specify the values to use for the thermophysical properties of these components. Figure 34 through Figure 36 show examples of the inputs for each of these components. The values populated in these figures are just examples, not the actual values that should be used.

The PRHYDE project cannot provide these values since these components are still under development, so the boundary conditions specifying the thermophysical properties required for these components cannot yet be determined.

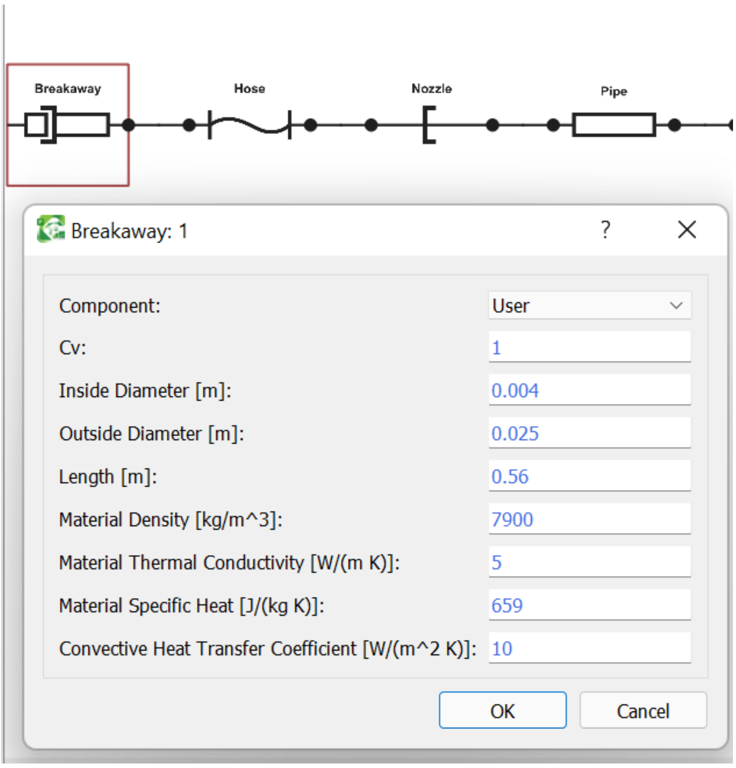

Figure 34: Example of fuelling model inputs for the breakaway fitting (Source: H2FillS)

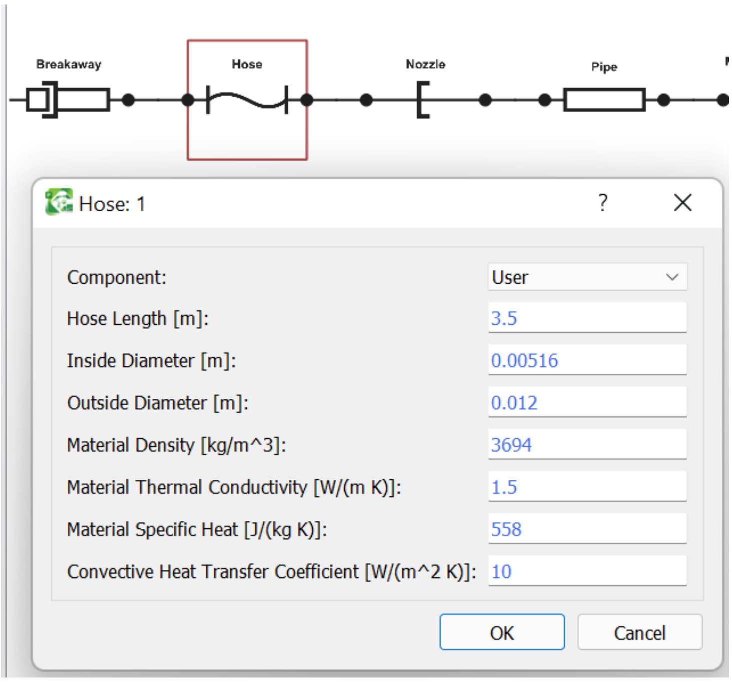

Figure 35: **Example of fuelling model inputs for the hose (Source: H2FillS)**

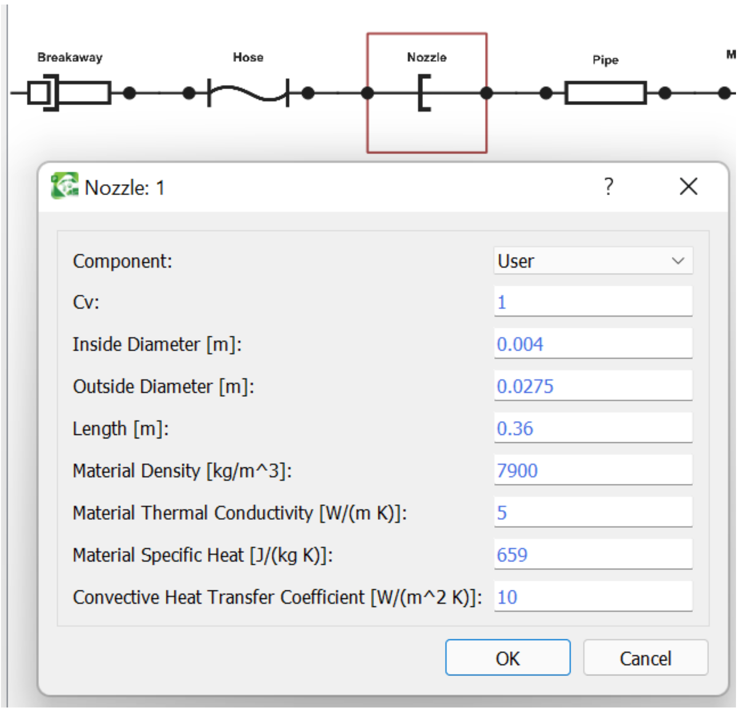

Figure 36: **Example of fuelling model inputs for the nozzle/receptacle coupling (Source: H2FillS)**

7.7 Selecting the conditions used in the fuelling simulations

There are common elements to the derivation of the t_{final} tables and there are also unique elements which depend on the fuelling concept.

7.7.1 Common conditions

Conditions which are common to the t_{final} derivation for all of the fuelling concepts presented in Section 3 are shown in Table 7.

Table 7: Fuelling simulations common to all fuelling concepts

Condition	Range and Increments
Ambient Temperature	-40 °C to 50 °C (10 °C increments below 0 °C and 5 °C increments above 0 °C)
Fuel Delivery Temperature	-40 °C to -10 °C @ 2 °C increments (note that OEM can determine the upper range value – it could be higher than – 10 °C if OEM deems this appropriate)
CHSS Hot Soak Temperature	If T_{amb} ≤ 0 °C, Then T_{hot_soak} = 15 °C Else If 35 °C ≤ T_{amb} < 40 °C, Then T_{hot_soak} = 40 °C Else If T_{amb} ≥ 40 °C, Then T_{hot_soak} = T_{amb} Else If 0 °C < T_{amb} ≤ 10 °C, Then T_{hot_soak} = 15 + T_{amb} Else If 10 °C < T_{amb} ≤ 20 °C, Then T_{hot_soak} = 25 + 0.5* (T_{amb} – 10) Else T_{hot_soak} = 30 + 2* (T_{amb} – 20)/3
Peak mass flow rate	This is determined by the vehicle and station based on the receptacle geometry used and vehicle specific limitations.
Ending SOC	97% to 100% (choosing a lower value will result in shorter t_{final} values, but will result in a lower maximum pressure.)

The ambient temperature range is -40 °C to 50 °C with 10 °C increments below 0 °C and 5 °C increments above 0 °C.

The fuel delivery temperature range is – 40 °C to an upper value determined by the OEM with 2 °C increments. The upper value would typically be -10 °C, but can be higher if the OEM deems it to be acceptable for the CHSS. Values higher than -10 °C will typically result in quite slow fuelling times, so consideration should be given to gas temperature stratification in the CHSS.

The CHSS hot soak temperature T_{hot_soak} is provided by the formula in Table 7. All fuelling concepts utilize this hot soak temperature in the derivation of the t_{final} tables.

The peak mass flow rate is chosen by the vehicle OEM, but is typically a function of the receptacle geometry used, along with any design limitations the OEM may impose. For H35 high flow, the peak mass flow rate is typically 120 g/s. For H70 high flow, the peak mass flow rate is typically 300 g/s. The OEM should not utilize a value higher than the flow rate associated with the receptacle geometry as the station may utilize the maximum flow rate as a process limit.

Ending SOC can be chosen by the vehicle OEM, but typical values are between 97% to 100%. Choosing a lower value (e.g. 97%) will result in slightly shorter t_{final} values, but also in a lower maximum pressure that can be used by the dispenser. Typically the t_{final} tables would be defined using an SOC of 100%. Where a lower SOC is used, the vehicle must communicate a maximum pressure corresponding to the pressure at the SOC target and the maximum gas temperature used in the derivation. For example, for a 70 MPa CHSS, if an SOC target of 97% is used with a maximum gas temperature of 85 °C, the maximum pressure will be 83.5 MPa. With an SOC target of 98%, the maximum pressure will be 84.8 MPa, with an SOC target of 99%, the maximum pressure will be 86 MPa, and with an SOC target of 100%, the maximum pressure will be 87.5 MPa. The dispenser will use this maximum pressure as a limit. If the dispenser calculates SOC based on dispenser pressure, then it will impose this maximum pressure as a constraint on the dispenser pressure. If the dispenser calculates SOC based on the vehicle communicated pressure, then it will impose this maximum pressure as a constraint on the communicated vehicle pressure.

7.7.2 Specific conditions unique to each fuelling concept

The following sections describe the conditions which are unique to each of the fuelling concepts presented in chapter 3.

7.7.2.1 Static fuelling concept

This section describes the conditions which are unique to the Static fuelling concept. These conditions are combined with the common conditions described in Section 7.7.1 and Table 7.

Conditions which are unique to the Static fuelling concept are shown in Table 8.

Table 8: Fuelling simulations unique to the Static fuelling concept

Condition	Range and Increments
Minimum Operating Pressure P_{min}	Two values should be used. The first value corresponds to the minimum operating pressure of the CHSS, which is determined by the OEM. The second value is described in the text below.
Maximum gas temperature T_{gas_max}	The maximum gas temperature of the CHSS for the PRHYDE program was 85 °C because almost all tanks are currently qualified to this temperature. In the future, if the CHSS is qualified to a higher temperature, it can be used.

The P_{min} value is the initial pressure utilized in the fuelling simulations. The Static fuelling concept uses two P_{min} values. The first corresponds to the minimum operating pressure of the CHSS as determined by the OEM. The second is set approximately 5 MPa above the first value. So if the minimum pressure is 1 MPa, then the first P_{min} would be 1 MPa, and the second would be 6 MPa. The spread of 5 MPa mimics the spread used on SAE J2601 where the two P_{min} values are 0.5 MPa and 5 MPa, respectively. Because it is very rare for the initial pressure to be below the second P_{min} value, the assumption of no fuelling history can be applied. Furthermore, in those rare instances where there is fuelling history, the time difference between the t_{final} value using P_{min} of the lower value and P_{min} of the higher value is lower than the additional time it would take the user to re-initiate the fuelling process.

The vehicle communicates the maximum gas temperature to the station and this is used as a safety shutdown by the station. If a value higher than 85 °C is utilized, this may cause a lower SOC than desired under some circumstances. Once 85 °C is exceeded 100% SOC is no longer possible.

Table 9 shows the parameters utilized for each t_{final} table. For the Static fuelling concept, there are two t_{final} tables.

Table 9: Parameters utilized for each t_{final} table with Static fuelling concept

Parameter Settings	T_{amb}	T_{fuel}	CHSS Soak T	P_{min}	SOC	T_{gas} Max	Flow Rate Max
t_{final} Table A	T_{amb} Range A	T_{fuel} Range A	T_{hot_soak}	$CHSS_{min}$	OEM set	OEM set	OEM set
t_{final} Table B	T_{amb} Range B	T_{fuel} Range B	T_{hot_soak}	$CHSS_{min}$ + X (e.g. X = 5 MPa)	OEM set	OEM set	OEM set

For the Static fuelling concept, the following parameters associated with the derivation of the t_{final} tables are communicated from the vehicle to the station: t_{final} table or t_{final} vector and associated P_{min}, T_{gas_max} , maximum pressure, maximum flow rate.

7.7.2.2 T_{gas} initial fuelling concept

This section describes the conditions which are unique to the T_{gas} Initial fuelling concept. These conditions are combined with the common conditions described in Section 7.7.1 and Table 7.

Conditions which are unique to the T_{gas} Initial fuelling concept are shown in Table 10.

Table 10: Fuelling simulations unique to the T_{gas} Initial fuelling concept

Condition	Range and Increments
Minimum Operating Pressure P_{min}	Multiple values, as described in the text below, are used and these values are determined by the vehicle OEM.
Maximum gas temperature T_{gas_max}	The maximum gas temperature of the CHSS for the PRHYDE program was 85 °C because almost all tanks are currently qualified to this temperature. In the future, if the CHSS is qualified to a higher temperature, it can be used.

The P_{min} value is the initial pressure utilized in the fuelling simulations. The T_{gas} Initial fuelling concept uses multiple P_{min} values. The first corresponds to the minimum operating pressure of the CHSS as determined by the vehicle OEM. The other values are typically set at a spacing of 5 MPa. For example, if the minimum operating pressure of the CHSS is 1 MPa, the vehicle OEM may choose P_{min} values of 1, 6, 11, 16, and 21 MPa. Typically, there is little benefit to utilizing P_{min} values higher than about 20 MPa.

The maximum gas temperature used is determined by the vehicle OEM based on the qualification temperature of the CHSS. This is typically 85 °C, but can be higher if the OEM has qualified the CHSS accordingly. The vehicle communicates the maximum gas temperature to the station, and this is used as a safety shutdown by the station. If a value higher than 85 °C is utilized, this may cause a lower SOC than desired under some circumstances. Once 85 °C is exceeded 100% SOC is no longer possible.

Table 11shows the parameters utilized for each t_{final} table. For the T_{gas} Initial fuelling concept, there are typically five t_{final} tables (depending on the increments of P_{min} the vehicle OEM utilizes). In this example, the increment X is constant, however it may be chosen differently by the OEM.

Table 11: Parameters utilized for each t_{final} table with T_{gas} Initial fuelling concept

Parameter Settings	T_{amb}	T_{fuel}	CHSS Soak T	P_{min}	SOC	T_{gas} Max	Flow Rate Max
t_{final} table A	T_{amb} Range A	T_{fuel} Range A	Hot Soak T	$CHSS_{min}$	OEM set	OEM set	OEM set
t_{final} table B	T_{amb} Range B	T_{fuel} Range B	Hot Soak T	$CHSS_{min}$ + X	OEM set	OEM set	OEM set
t_{final} table C	T_{amb} Range C	T_{fuel} Range C	Hot Soak T	$CHSS_{min}$ + 2X	OEM set	OEM set	OEM set
t_{final} table D	T_{amb} Range D	T_{fuel} Range D	Hot Soak T	$CHSS_{min}$ + 3X	OEM set	OEM set	OEM set
t_{final} table E	T_{amb} Range E	T_{fuel} Range E	Hot Soak T	$CHSS_{min}$ + 4X	OEM set	OEM set	OEM set

For the T_{gas} Initial fuelling concept, the following parameters associated with the derivation of the t_{final} tables are communicated from the vehicle to the station: t_{final} table or t_{final} vector and associated P_{min}, T_{gas_max}, maximum pressure, maximum flow rate.

7.7.2.3 T_{gas} initial+ fuelling concept

This section describes the conditions which are unique to the T_{gas} Initial+ fuelling concept. These conditions are combined with the common conditions described in Section 7.7.1 and Table 7.

Conditions which are unique to the T_{gas} Initial fuelling concept are shown in Table 12.

Table 12: Fuelling simulations unique to the T_{gas} Initial+ fuelling concept

Condition	Range and Increments
Minimum Operating Pressure P_{min}	Multiple values, as described in the text below, are used and these values are determined by the vehicle OEM.
Maximum gas temperature T_{gas_max}	The maximum gas temperature of the CHSS for the PRHYDE program was 85 °C because almost all tanks are currently qualified to this temperature. In the future, if the CHSS is qualified to a higher temperature, it can be used.
CHSS Soak Temperature T_{hot_soak}	Multiple CHSS soak temperatures, as described in the text below, are utilized.

The P_{min} value is the initial pressure utilized in the fuelling simulations. The T_{gas} Initial fuelling concept uses multiple P_{min} values. The first corresponds to the minimum operating pressure of the CHSS as determined by the vehicle OEM. The other values are typically set at a spacing of 5 MPa. For example, if the minimum operating pressure of the CHSS is 1 MPa, the vehicle OEM may choose P_{min} values of 1, 6, 11, 16, and 21 MPa. Typically, there is little benefit to utilizing P_{min} values higher than about 20 MPa.

The maximum gas temperature used is determined by the vehicle OEM based on the qualification temperature of the CHSS. This is typically 85 °C, but can be higher if the OEM has qualified the CHSS accordingly. The vehicle communicates the maximum gas temperature to the station and this is used as a safety shutdown by the station. If a value higher than 85 °C is utilized, this may cause a lower SOC than desired under some circumstances. Once 85 C is exceeded 100% SOC is no longer possible.

Three CHSS soak temperatures are typically utilized. The first is the hot soak temperature. The second is the hot soak temperature minus 5 °C. The third is the hot soak temperature minus 10 °C. The vehicle OEM may choose fewer of more CHSS soak temperature values, but they must be at a constant ΔT value below the hot soak temperature. The magnitude of ΔT is also at the discretion of the vehicle OEM.

Table 13 shows the parameters utilized for each t_{final} table. For the T_{gas} Initial+ fuelling concept, there are typically fifteen t_{final} tables (depending on the increments of P_{min} the vehicle OEM utilizes and the number of soak temperature increments utilized). In this example, the increment X is constant (e.g. 5 MPa), however it may be chosen differently by the OEM.

Table 13: Parameters utilized for each t_{final} table with T_{gas} Initial+ fuelling concept

Parameter Settings	T_{amb}	T_{fuel}	CHSS Soak T	P_{min}	SOC	T_{gas} Max	Flow Rate Max
t_{final} table A	T_{amb} Range A	T_{fuel} Range A	Hot Soak T	$CHSS_{min}$	OEM set	OEM set	OEM set
t_{final} table B	T_{amb} Range B	T_{fuel} Range B	Hot Soak T	$CHSS_{min}$ + X	OEM set	OEM set	OEM set
t_{final} table C	T_{amb} Range C	T_{fuel} Range C	Hot Soak T	$CHSS_{min}$ + 2X	OEM set	OEM set	OEM set
t_{final} table D	T_{amb} Range D	T_{fuel} Range D	Hot Soak T	$CHSS_{min}$ + 3X	OEM set	OEM set	OEM set
t_{final} table E	T_{amb} Range E	T_{fuel} Range E	Hot Soak T	$CHSS_{min}$ + 4X	OEM set	OEM set	OEM set
t_{final} table F	T_{amb} Range F	T_{fuel} Range F	Hot Soak T - 5 °C	$CHSS_{min}$	OEM set	OEM set	OEM set
t_{final} table G	T_{amb} Range G	T_{fuel} Range G	Hot Soak T - 5 °C	$CHSS_{min}$ + X	OEM set	OEM set	OEM set
t_{final} table H	T_{amb} Range H	T_{fuel} Range H	Hot Soak T - 5 °C	$CHSS_{min}$ + 2X	OEM set	OEM set	OEM set
t_{final} table I	T_{amb} Range I	T_{fuel} Range I	Hot Soak T - 5 °C	$CHSS_{min}$ + 3X	OEM set	OEM set	OEM set
t_{final} table J	T_{amb} Range J	T_{fuel} Range J	Hot Soak T - 5 °C	$CHSS_{min}$ + 4X	OEM set	OEM set	OEM set
t_{final} table K	T_{amb} Range K	T_{fuel} Range K	Hot Soak T - 10 °C	$CHSS_{min}$	OEM set	OEM set	OEM set
t_{final} table L	T_{amb} Range L	T_{fuel} Range L	Hot Soak T - 10 °C	$CHSS_{min}$ + X	OEM set	OEM set	OEM set
t_{final} table M	T_{amb} Range M	T_{fuel} Range M	Hot Soak T - 10 °C	$CHSS_{min}$ + 2X	OEM set	OEM set	OEM set
t_{final} table N	T_{amb} Range N	T_{fuel} Range N	Hot Soak T - 10 °C	$CHSS_{min}$ + 3X	OEM set	OEM set	OEM set
t_{final} table O	T_{amb} Range O	T_{fuel} Range O	Hot Soak T - 10 °C	$CHSS_{min}$ + 4X	OEM set	OEM set	OEM set

For the T_{gas} Initial+ fuelling concept, the following parameters associated with the derivation of the t_{final} tables are communicated from the vehicle to the station: t_{final} table or t_{final} vector and associated P_{min}, T_{gas_max}, maximum pressure, maximum flow rate.

7.7.2.4 T_{gas} Throttle fuelling concept

This section describes the conditions which are unique to the T_{gas} Throttle fuelling concept. These conditions are combined with the common conditions described in Section 7.7.1 and Table 7.

Conditions which are unique to the T_{gas} Throttle fuelling concept are shown in Table 14.

Table 14: Fuelling simulations unique to the T_{gas} Throttle fuelling concept

Condition	Range and Increments
Minimum Operating Pressure P_{min}	A single value, as described in the text below, corresponding to the minimum operating pressure of the CHSS is used.
Maximum gas temperature T_{gas_max}	For the derivation of the t_{final} table, the maximum gas temperature is determined by the vehicle OEM, but should not exceed 95 °C.

The P_{min} value is the initial pressure utilized in the fuelling simulations. The T_{gas} Throttle fuelling concept uses a single P_{min} value. This value corresponds to the minimum operating pressure of the CHSS as determined by the vehicle OEM.

The maximum gas temperature used in the derivation of the t_{final} table is determined by the vehicle OEM, but should not exceed 95 °C. 95 °C is the typical maximum gas temperature utilized and provides the best overall fuelling performance, but the vehicle OEM can choose a value less than this.

It should be noted that if the vehicle OEM utilizes 95 °C as the maximum gas temperature, then the Ending SOC from Table 7 must be set to 98.2%. This is the maximum SOC achievable at this temperature without exceeding the MAWP of the CHSS. In this case, the maximum pressure is the MAWP (e.g. 87.5 MPa for an H70 CHSS).

Table 15 shows the parameters utilized for the t_{final} table. For the T_{gas} Throttle fuelling concept, there is one t_{final} table.

Table 15: Parameters utilized for each t_{final} table with T_{gas} Throttle fuelling concept

Parameter Settings	T_{amb}	T_{fuel}	CHSS Soak T	P_{min}	SOC	T_{gas} Max	Flow Rate Max
t_{final} table A	T_{amb} Range A	T_{fuel} Range A	Hot Soak T	$CHSS_{min}$	OEM set	OEM set	OEM set

For the T_{gas} Throttle fuelling concept, the following parameters associated with the derivation of the t_{final} tables are communicated from the vehicle to the station: t_{final} table or t_{final} vector and associated P_{min}, T_{gas_max}, maximum pressure, maximum flow rate.

7.8 Conducting the simulations and deriving the t_{final} values

This section explains the process for conducting the simulations and subsequent derivation of the t_{final} table values.

7.8.1 Setting up the simulations

Figure 37 shows an example of setting the conditions in the fuelling model to generate all the simulations required for a complete set of t_{final} tables. The settings shown are examples that can be used to generate the five t_{final} tables for the T_{gas} Initial fuelling concept. Each of the inputs used is explained below.

Note the box circled in red. This instructs the model to run in "batch" mode where it conducts simulations automatically over the range of input values specified and finds the optimal average pressure ramp rate (APRR) (i.e. the highest PRR that complies with the constraints on peak mass flow rate, maximum temperature and final SOC).

Ambient Temperature: The range is -40 °C to 50 °C in 5 °C increments.

Fuel Delivery Temperature: The range is -40 °C to -10 °C in 2 °C increments.

Vehicle Tank Initial Pressure: In this case, 2 MPa to 22 MPa in 5 MPa increments is selected. This results in five P_{min} values for five t_{final} tables (2, 7, 12, 17, 22 MPa).

APRR Range: In this case 1 to 100 MPa/min is selected (this just defines the range that model uses in the iteration process to solve for the optimal APRR).

Peak Mass Flow Rate: In this case 0.3 kg/s (300 g/s) is selected

Peak Breakaway Inlet Pressure: In this case 99 MPa (this is an example value which should be a sufficiently high setting so that it is not a constraint in the t_{final} derivation process. This value can be set higher if needed.)

Hose Temperature Profile: Flat needs to be chosen (this means there is no cool-down period. It is important to utilize a flat fuel delivery of the hose temperature profile because this ensures that the mass average fuel delivery temperature will be equal to the fuel delivery temperature specified)

Maximum Vehicle Tank Temperature: In this case, the value is set to 85 °C. It can be set lower by the OEM, for instance to take into account the model uncertainties.

Definition of Vehicle Tank Initial Temperature: This is the soak temperature of the CHSS. In this case, the hot soak temperature from SAE J2601 is selected (see Table 7). The model automatically calculates the hot soak temperature as a function of the ambient temperature.

Terminating Conditions: The model is instructed to end the fill based on reaching the SOC target value without exceeding the other constraints of peak mass flow rate and maximum vehicle tank temperature. As noted in Section 7.7.1, the SOC setting can be a value between 97 and 100. In this case, 100 is selected. The NWP of the CHSS must also be selected. In this case, it is H70.

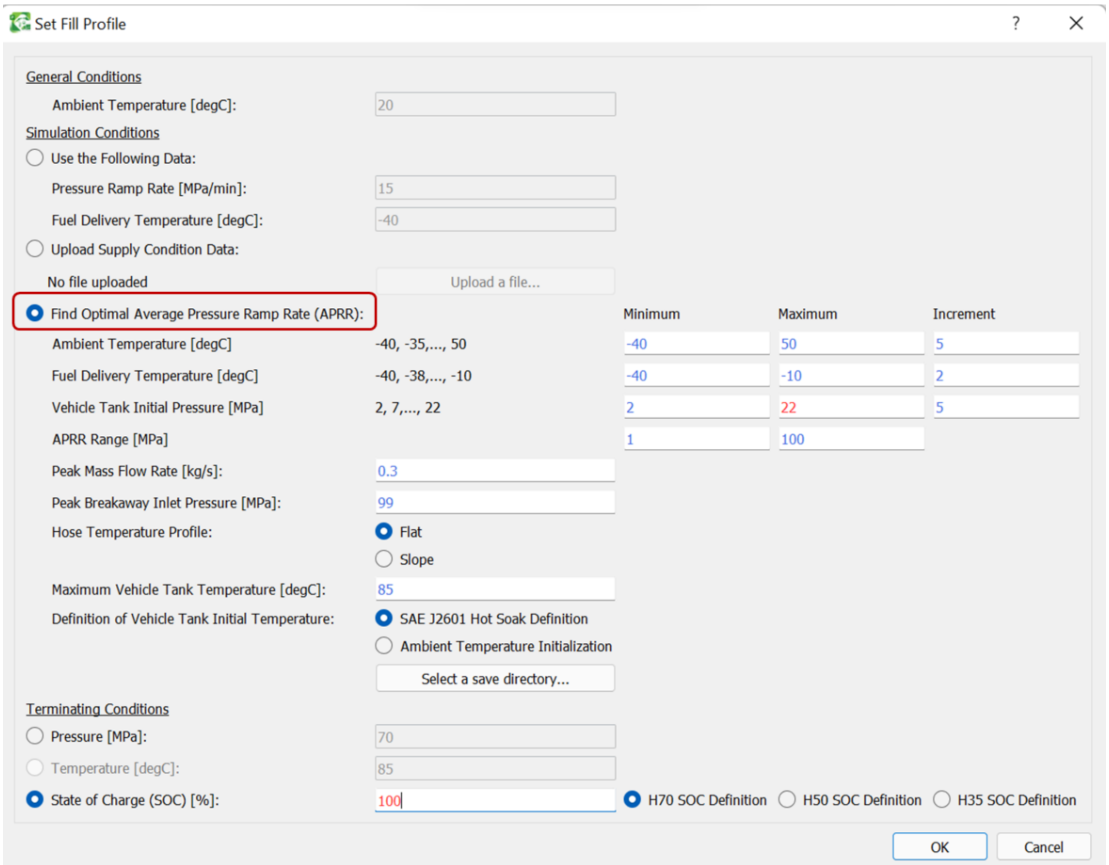

Figure 37: Example of setting the model inputs for a complete set of simulations (Source: H2FillS)

Iterative Solution: After the settings have been entered, the model is run. The model solves for the optimal APRR, referred to as $APRR_{optimal}$ and defined as the fastest APRR that ends at the SOC value, does not exceed the mass flow limit and the maximum vehicle tank temperature. The model has the following built-in tolerance for each of these criteria: SOC +0–0.1%; maximum mass flow +0 –0.1 g/s, and maximum vehicle tank temperature +0–0.01 °C. (Note: NREL has indicated that in a future version of H2FillS, the user will be able to input these tolerances). The model solves for $APRR_{optimal}$ for range of T_{amb}, T_{fuel}, and P_{min} values specified. In this case, there are five P_{min} values specified, so the output can be used to generate five t_{final} tables, with P_{min} of 2 MPa, 7 MPa, 12 MPa, 17MPa and 22 MPa, respectively.

When generating t_{final} tables for the T_{gas} Initial and T_{gas} Initial+ fuelling concepts, in addition to the simulations run with the above settings, there is one more important set of simulations to run. They are run with the settings shown in Figure 38. Note that there are two differences from the settings from Figure 37. First, there is only a single Vehicle Tank Initial Pressure value used (or P_{min}), corresponding to the minimum CHSS pressure, in this case 2 MPa. The second difference is the maximum gas temperature. This time, the maximum gas temperature is set to 95 °C. This will generate a set of APRR values for each T_{amb} and T_{fuel} with a maximum gas temperature of 95 °C. These APRR values are referred to as $APRR_{max}$. This is an important feature of the t_{final} derivation for the T_{gas} Initial and T_{gas} Initial+ fuelling concepts because it provides a bound on the maximum gas temperature. This means that if the CHSS temperature is grossly wrong, the gas temperature in the CHSS can never exceed 95 °C. If the CHSS were qualified to 95 °C, then the CHSS temperature is not safety critical, and even if the CHSS is not qualified to 95 °C, by limiting the overtemperature potential, the probability of damage to the CHSS resulting in a leak is reduced (see also Appendix E.5.2.5 and E.5.2.6).

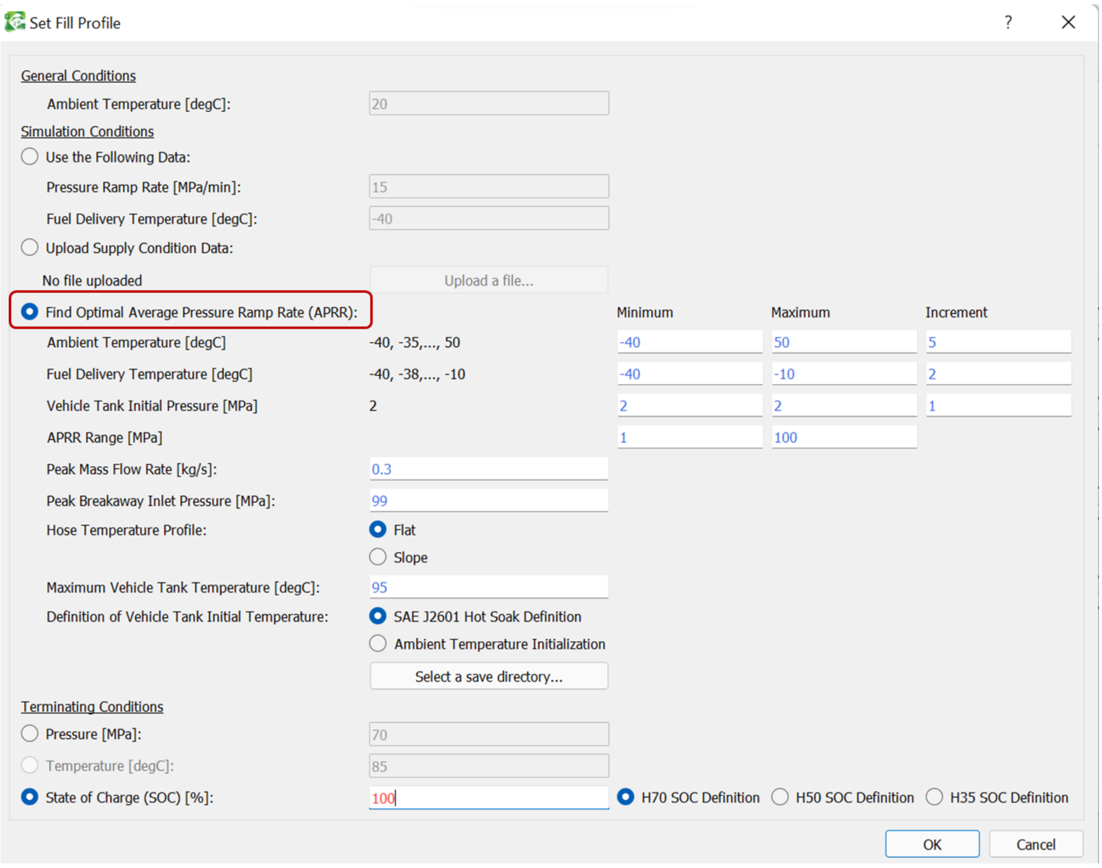

Figure 38: Example of setting the model inputs for generating $APRR_{max}$ (Source: H2FillS)

7.8.2 Generating the t_{final} tables

Once the $APRR_{optimal}$ has been calculated (and the $APRR_{max}$ for T_{gas} Initial and T_{gas} Initial+ fuelling concepts), the t_{final} table values can be derived. Equation 2 is used to derive the t_{final} value for each fuelling simulation.

$$t_{final} = MAXIMUM\left[\frac{(1.25 \times NWP - P_{min\_table})}{APRR_{optimal}}, \frac{(1.25 \times NWP - P_{min\_table})}{APRR_{max}}\right] \qquad \text{(Eq. 2)}$$

t_{final} tables are constructed as shown in the example in Table 5.

8 BRIEF PRESENTATION OF MODELLING TOOLS FOR PROTOCOL DEVELOPMENT

8.1 Simple Engineering models

Simple 0D-1D models are developed in order to predict the average gas properties in hydrogen tanks during their refuelling.

Such models can compute pressure and temperature increases in the tank rapidly and accurately during the filling. It allows to test multiple refuelling conditions numerically, thus reducing the need for experimental campaigns. These simple engineering models are the kind of models that are used in the derivation of fuelling protocol tables. The engineering models that were used during PRHYDE project are presented below. All these models assume that the gas temperature is isothermal (0D) inside the tank volume at each time step, which is not always the case. In fact in some specific conditions during refuelling, thermal stratifications can occur. Computational Fluid Dynamics (CFD) simulations can only address these situations.

8.2 SOFIL by Air Liquide

The SOFIL model (developed by Air Liquide R&D since 2010) assumes homogeneous gas temperature and pressure in the tank, and linear evolution of the tank wall. The 0D-gas/1D-wall approach has proven to be predictive in comparison to experiments, allowing to estimate the gas as well as the tank wall temperature accurately[6].

The model solves mass and energy balance equations to estimate gas temperature and pressure. A real gas equation is used to obtain gas properties. The model takes into account, if present, the tank bosses. The piping, from dispenser to FCEV tank, can be modelled through a lumped thermal mass or a more precise 2D (radially and longitudinally) discretization.

The pressure drop formula used to determine the mass flow into the tank is presented in the following for the sonic conditions ($P_1 > 2\ P_2$) and for the subsonic conditions ($P_1 \leqslant 2\ P_2$):

$$\frac{dm_g}{dt} = C\ k_v P_1 \sqrt{\frac{\rho_N}{T_1}} \quad \text{(for sonic conditions: } P_1 > 2\ P_2\text{)}$$

$$\frac{dm_g}{dt} = 2\ C\ k_v \sqrt{\frac{\rho_N\ (P_1 - P_2) P_2}{T_1}} \quad \text{(for subsonic conditions: } P_1 \leqslant 2\ P_2\text{)}$$

where m_g is the mass of gas in the tank (kg), *a* constant C equal to 257, k_v the flow coefficient (m^3/h), P_1 the upstream pressure (bara) at the dispenser, P_2 the downstream pressure (bara) in the tank, ρ_N the gas density at normal conditions 0°C, 1 atm (kg/Nm^3) and T_1 the upstream temperature (K).

6 For more details see: Bourgeois T, Brachmann T, Barth F, Ammouri F, Baraldi D, Melideo D, Acosta-Iborra B, Zaepffel D, Saury D, and Lemonnier D. 2017. Optimization of hydrogen vehicle refuelling requirements. International Journal of Hydrogen Energy 42:13789–809 **and**
Bourgeois T, Ammouri F, Weber M, Knapik C. Evaluating the temperature inside a tank during a filling with highly-pressurized gas. International Journal of Hydrogen Energy 2015;40:11748-55.

8.3 HyFill by Engie

Engie Lab CRIGEN developed the HyFill tool to contribute to the reflexion on hydrogen mobility and more particularly on hydrogen refuelling stations. HyFill allows to simulate fast filling and emptying of hydrogen tanks, in order to predict the final temperature reached by hydrogen. HyFill is a pseudo-1D model. It considers the gas temperature is uniform at each instant in the tank (0D), and heat transfer between the gas and the outside is modelled by discretizing the wall to capture accurately the temperature fluctuations in it.

Heat transfer in the piping system is modelled using longitudinal discretization for the gas, and radial discretization in the pipe wall. The thermal weight of all the components is taken into account in the model. The piping model allows to compute the gas temperature at the inlet of the tank.

The mass flow and pressure drop are computed thanks to the flow coefficient k_v of the system.

To have access to the temperature, mass and pressure of the gas in the tank, a system of equations – mass balance, energy balance, equation of state - is solved at each time step. The thermodynamic properties are calculated using the GERG-2008 equation of state, valid for pressure from 0 to 3000 bar and temperatures from 77 to 473 K, thus covering the range of temperatures and pressures reached when filling or emptying a tank. Conduction equations are implemented in the wall. At the inner boundary, convective heat transfer between the tank and the wall is modelled using a mixed-convection correlation to find the convective heat transfer coefficient. At the outer boundary, the external convective heat transfer coefficient is assumed constant, and radiative heat transfer is also considered. Finally, heat transfer in the bosses of the tank is also considered when relevant.

8.4 H2FillS by NREL

The tank model described in the following two papers: Monde, M. et al 2012 and Monde, M. et al 2013[7], has been implemented in the H2FillS software.

Initially, the FCEV tank is given a pressure, temperature, internal volume, internal surface area, internal diameter, and the thermal properties of the liner and carbon fiber reinforced polymer (CFRP). After the values are set to the tank model, the mass and energy balances are calculated with the assumption that the tank volume does not increase with the pressure rise. The governing equations for the mass and energy balances are shown as follows:

$$\frac{d}{dt}(m) = \dot{m}_{in}$$

$$\frac{d}{dt}(mu) = \dot{m}_{in}h_{in} + A_{wall}\alpha_{in}(T_{wall}|_{x=0} - T)$$

[7] Monde, M, Woodfield P, Takano T and Kosaka M. 2012. Estimation of temperature change in practical hydrogen pressure tanks being filled at high pressures of 35 and 70 MPa. International Journal of Hydrogen Energy 37:5723-34 and Monde, M. and Kosaka, M., "Understanding of Thermal Characteristics of Fueling Hydrogen High Pressure Tanks and Governing Parameters," SAE Int. J. Alt. Power. 2(1):61-67, 2013, https://doi.org/10.4271/2013-01-0474.

where m is the hydrogen mass, u is the specific internal energy, m_{in} is the mass flow rate, h_{in} is the specific enthalpy, A_{wall} is the inner surface area in the tank, α_{in} is the heat transfer coefficient at the inner surface, T is the hydrogen temperature, $T_{wall}|_{x=0}$ is the inner surface wall temperature, dt is the time step, and t is the time.

When the energy and mass balances are solved by the equations, the state inside the tank is assumed to be a lumped model; thus, the acquired temperature and pressure are treated as mean values calculated by the bulk specific internal energy and density. The heat conduction in the wall is assumed to be one-dimensional. It is assumed that the tank wall is a flat plate, even though the tank shape is cylindrical. This is because the curvature radius of the tank is large compared to the wall thickness. (The effectiveness of this assumption has been examined). Hence, the following unsteady heat conduction equation and boundary conditions are applied to obtain the temperature distribution in the wall:

$$\frac{\partial T_{wall}}{\partial t} = a_{wall} \frac{\partial^2 T_{wall}}{\partial x^2}$$

$$-\lambda_{wall} \frac{\partial T_{wall}}{\partial x}\bigg|_{x=0} = \alpha_{in}(T - T_{wall}|_{x=0})$$

$$-\lambda_{wall} \frac{\partial T_{wall}}{\partial x}\bigg|_{x=l} = \alpha_{out}(T_{wall}|_{x=l} - T_{amb})$$

Where a_{wall} is the thermal diffusivity, x is the position at which $x = 0$ is the inner wall surface and $x = l$ is the total thickness of the wall, λ_{wall} is the thermal conductivity, α_{out} is the heat transfer coefficient at the outer surface, and T_{amb} is the ambient temperature. The value of α_{out} was set to 8.0 W/(K·m^2). The value of α_{in} was derived from a Nusselt number correlation based on the Reynolds number at the tank inlet and Rayleigh number inside the tank.

The equations implemented in the model for the mass flow calculation are based on two steps:

Volumetric flow rate (m³/h) calculation: calculates the volumetric flow rate based on the differential pressure at the inlet and outlet of the valve ($P_{upstream}$ and $P_{downstream}$), temperature at the inlet of the valve $T_{upstream}$, and specific gravity to air G.

If $P_{upstream} \geq 0.5 * P_{downstream}$ (non-choked flow):

$$\dot{V} = 2930\, C_v \sqrt{\frac{(P_{upstream} - P_{downstream})(P_{upstream} + P_{downstream})}{P_{upstream} G T_{upstream}}}$$

If $P_{upstream} < 0.5 * P_{downstream}$ (choked flow):

$$\dot{V} = 2538 C_v \frac{P_{upstream}}{G T_{upstream}}$$

Conversion to mass flow rate (kg/s): Converts the volumetric flow rate (m³/h) to the mass flow rate (kg/s) using density at 0.1 MPa and 15.6 °C and a coefficient β, developed to handle the unsteady flow during the fuelling process:

$$\dot{m} = \frac{\beta \rho \dot{V}}{3600}$$

8.5 H2-Fill by Wenger Engineering[8]

In the context of the project, the models applied in PRHYDE (i.e., SOFIL; HyFill, and H2FillS) were benchmarked to another model called H2-Fill (see Section 8.6). H2-Fill calculates gas pressure and temperature curves in a vehicle tank for refuelling and defuelling with gaseous hydrogen.

An individual vehicle tank system size, configuration and type can be used for simulation with H2-Fill. The tank starts with initial conditions for gas pressure (Initial gas pressure) and gas respectively vessel wall temperature (Initial tank temperature).

The fuel gas is delivered by the station with a given pressure and a given fuel temperature (Precooling temperature). For fuelling simulation, the station either ramps up pressure with a linear rate (Ramp rate) starting from the initial tank pressure and using a fixed standard pressure drop coefficient to derive a certain mass flow or directly uses a prescribed constant mass flow (Mass flow).

Heat transfer to ambience from idealized station and car components including vessel depends on Ambient temperature. Fuel from the station exchanges heat with the thermal masses constituted by the fuelling hose, pipes, and vehicle line components. Each thermal mass is characterized by its mass, specific heat capacity, and thermal conductivity. They exchange heat with the environment at ambient temperature.

The fuel gas enters the tank vessel and mass and energy balance are solved in order to obtain the gas temperature and pressure curves over time. It is assumed that the gas inside the tank is always perfectly mixed.

All properties of the gas inside the vessel are computed from the gas equation of state. The heat transfer rate between gas and vessel internal surface (liner) is calculated from a set of Nusselt equations for various geometries and for forced and free convection. The vessel wall is discretized in radial direction and the transient heat conduction equation is solved in one dimension. This yields the temperature profile inside the vessel. On the outer surface, the vessel wall exchanges heat with the environment, the heat transfer coefficient is again based on a set of Nusselt equations for various geometries and for free convection.

8.6 Benchmark brief presentation, results and recommendations

The four models from Air Liquide, Engie, NREL and Wenger Engineering are described and compared on three benchmark cases for H35, H50 and H70 tanks in a scientific paper[9].

All models are in good general agreement. The end-of-fill properties of the gas were very similar in each prediction, with end-of-fill temperature predictions within less than a 2 °C range. This range is in accordance with the expected accuracy of the models

8 The PRHYDE consortium thanks Wenger Engineering for the contribution to this modeling benchmark.

9 Charolais, A., Ammouri, F. , Vyazmina, E., Nouvelot, Q., Guewouo, T., Greisel, M., Gebhard, M., Kuroki, T. and Mathison, S., Protocol for heavy duty hydrogen refuelling: a modeling benchmark, ICHS conference 2021.
Publications in the context of the PRHYDE project are available for download here: https://lbst.de/prhyde/.

and it could therefore be deduced that all models are acceptable to the use of refuelling simulations. The differences observed may be explained by the real gas equations used to compute the gas properties, the bosses' presence in the models, the simplified tank geometry implemented and the pressure drop formula leading to slightly different simulated mass flows.

These models give quick results on average gas temperature in the tank and are useful for rapid, safe and efficient protocol development. They can provide quick feedback on different approaches as well as give an estimation of the influence of each parameter. In Section 9, in addition to CFD results on two filling cases, only the results of engineering models of SOFIL and HyFill will be presented as these 2 models were used for the whole test results carried out within PRHYDE.

8.7 CFD approach

For the CFD modeling approach, the commercial software Ansys/Fluent was used for 165L type 4 H70 tank and for two filling conditions where significant thermal stratifications occur inside the tank.

Simulations with different meshes were tested for the gas volume inside the tank and the tank walls. At the end, the most appropriate mesh was used (after mesh refinement the results would not change).

For the turbulence modeling, different models proposed by Ansys/Fluent were tested. The best one is Reynolds Stress Model (RSM). It represents mostly the exact behavior of the impacting cold jet on the tank internal walls. Consequently, it also reproduces the best the thermal stratifications inside the tank during filling.

9 EXPERIMENTAL VALIDATION OF THE MODELS

In a first step, the different models used for simulations in PRHYDE WP4 (i.e. SOFIL model by Air Liquide and HyFill Model by ENGIE) were validated with experimental data collected during the test campaigns in WP5.

The experimental data described in Section 9.1 are used to test the accuracy of the thermodynamic models: the actual experiment parameters are taken as the inputs of the simulation, and the difference between simulation outputs and measurements is analysed. Indeed, it is important to check the accuracy of the models, in particular their ability to model the pressure and temperature of the gas, because they will be used to establish the fuelling protocols.

The validation work for SOFIL and HyFill models is detailed in Section 9.2.

For the CFD models, only two experimental cases were investigated for the filling of the 165L type IV H70 tank due to the extensive computing time (few months) needed to run these simulations. The validation work conducted with the CFD models is detailed in Section 9.3.

9.1 Experimental data

Experimental test campaigns were conducted in WP5 during the PRHYDE project. Several fillings were monitored on four different single tanks:

- 240 L type IV H70 tank, at ZBT
- 350 L type IV H50 tank, at ZBT
- 322 L type III H35 tank, at ZBT
- 165 L type IV H70 tank, at Nikola

The test conditions are summarized below in Sections 9.1.1 to 9.1.4.

9.1.1 Tests performed at ZBT on the H70 240 L tank

These tests were performed at the ZBT facility in Duisburg, Germany, in November 2021. The tank used is a type IV tank of 240L. Table 16 presents the test matrix that was carried out, and Figure 39 shows the P&ID of the experimental setup.

Table 16: Test matrix for 240 L H70 tank at ZBT

Test Number	Initial P (bar)	Dispenser Temperature Profile	Dispenser Pressure Profile
#1 (ref)	20	-40°C	Constant PRR 8 MPa/min
#2	20	-20°C	Constant PRR 8 MPa/min
#3	20	-10°C	Constant PRR 8 MPa/min
#4	20	0°C	Constant PRR 8 MPa/min
#5	20	-40°C for 5 min, then no cooling	Constant PRR 8 MPa/min
#6	20	No cooling for 4 min 30, then -40°C	Constant PRR 8 MPa/min
#7	20	-40°C for 5 min, then -20°C	Constant PRR 8 MPa/min
#8	70	-40°C	Constant PRR 8 MPa/min
#9	350	-40°C	Constant PRR 8 MPa/min
#10	20	-40°C	Constant PRR 5 MPa/min
#10bis	20	-40°C	Constant PRR 1 MPa/min
#11	20	-40°C	16 MPa/min for 3.85 min, transitions to 1 MPa/min

#12	20	-40°C	16 MPa/min for 3.85 min, transitions to 3 MPa/min
#13	20	-40°C	Constant PRR 3 MPa/min
#14	20	-40°C	Constant PRR 16 MPa/min
#17 (ref)	20	-40°C	Constant PRR 8 MPa/min

Note that the ambient temperature cannot be controlled at the ZBT facility.

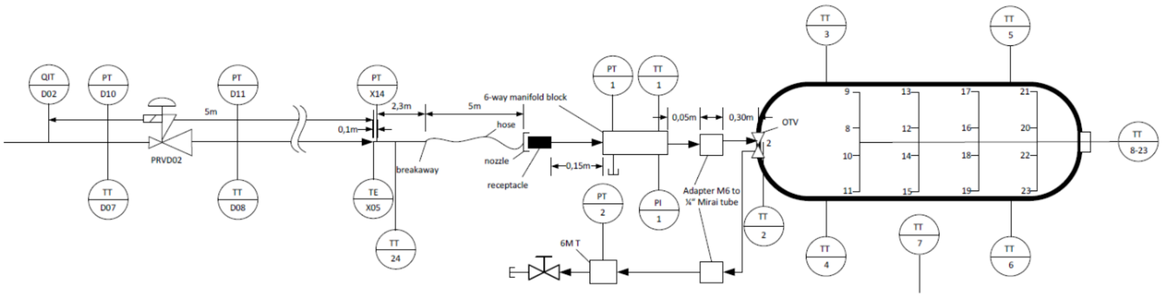

Figure 39: P&ID of the experimental setup for the H70 tank at ZBT

9.1.2 Tests performed at ZBT on the 350 L H50 tank

These tests were performed at the ZBT facility in Duisburg, Germany, in February 2022. The tank used is a type IV tank of 350L. Table 17 presents the test matrix that was executed, and Figure 40 shows the P&ID of the experimental setup.

Table 17: Test matrix for the 350 L H50 tank at ZBT

Test Number	Initial P (bar)	Dispenser Temperature Profile	Dispenser Pressure Profile
#18 (ref)	20	0°C	Constant PRR 5.5 MPa/min
#19	20	-40°C	Constant PRR 5.5 MPa/min
#20	20	Ambient	Constant PRR 5.5 MPa/min
#22	50	0°C	Constant PRR 5.5 MPa/min
#23	250	0°C	Constant PRR 5.5 MPa/min
#24	20	0°C	Constant PRR 3.5 MPa/min
#25	20	0°C	Simulate T_{gas} Throttle with initial PRR 12 MPa/min
#26	20	0°C	Simulate T_{gas} Throttle with initial PRR 10 MPa/min
#27	20	0°C	Simulate T_{gas} Throttle with initial PRR 8 MPa/min
#28	20	Ambient (as high as possible)	Constant PRR 5.5 MPa/min

Note: test #21 with a customized temperature profile was cancelled, as no proposal was deemed satisfactory. The ambient temperature cannot be controlled at the ZBT facility.

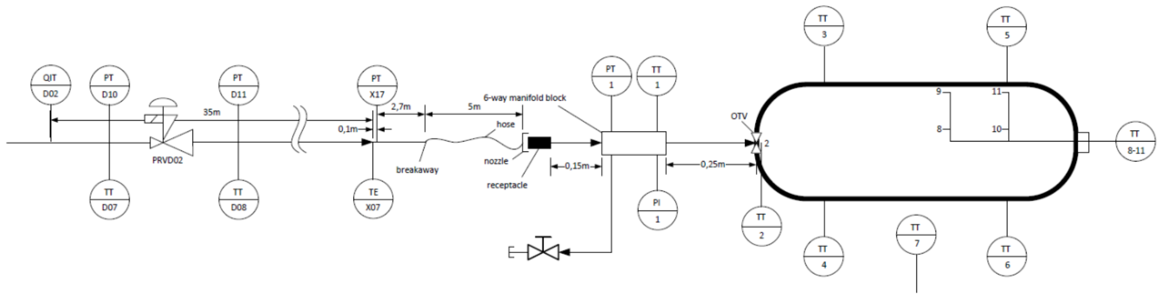

Figure 40: P&ID of the experimental setup for the H50 tank at ZBT

9.1.3 Tests performed at ZBT on the 322 L H35 tank

These tests were performed at the ZBT facility in Duisburg, Germany, in March and April 2022. The tank used is a type III tank of 322 L. Table 18 presents the test matrix that was executed, and Figure 41 shows the P&ID of the experimental setup.

Table 18: Test matrix for the 322 L H35 tank at ZBT

Test Number	Initial P (bar)	Dispenser Temperature Profile	Dispenser Pressure Profile
#1 (ref)	20	-20°C	Constant PRR 8 MPa/min
#2	20	-40°C	Constant PRR 8 MPa/min
#3	20	-10°C	Constant PRR 8 MPa/min
#4	20	0°C	Constant PRR 8 MPa/min
#5	20	no cooling	Constant PRR 8 MPa/min
#6	20	-40°C for 5 min, then no cooling	Constant PRR 8 MPa/min
#8	70	-20°C	Constant PRR 8 MPa/min
#9	150	-20°C	Constant PRR 8 MPa/min
#10	20	-20°C	Constant PRR 4 MPa/min
#11	20	-20°C	Constant PRR 3 MPa/min
#12	20	-20°C	Constant PRR 14 MPa/min
#13	20	-20°C	PRR 14 MPa/min for 2.75 min, then 1 MPa/min
#14	20	-20°C	PRR 14 MPa/min for 2.5 min, then 3 MPa/min
#15	20	-20°C	Simulate T_{gas} Throttle with initial PRR 12 MPa/min
#16	20	-20°C	Simulate T_{gas} Throttle with initial PRR 10 MPa/min
#17	20	-20°C	Simulate T_{gas} Throttle with initial PRR 8 MPa/min
#18 (ref)	20	-20°C	Constant PRR 8 MPa/min

Note: test #7 was dismissed because changing the dispenser temperature mid-fill was not easily possible at the facility for the H35 case. The ambient temperature cannot be controlled at the ZBT facility.

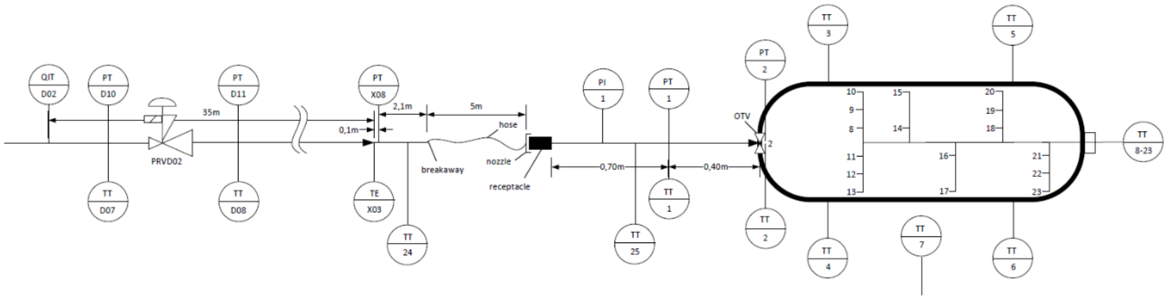

Figure 41: P&ID of the experimental setup for the H35 tank at ZBT

9.1.4 Tests performed at Nikola on the 165 L H70 tank

These tests were performed at the Nikola facility in May 2021. The tank used is a type IV tank of 165 L. Table 19 presents the test matrix that was executed, and Figure 42 shows the P&ID of the experimental setup.

Table 19: Test matrix for the 165 L H70 tank at Nikola

Test Number	Ambient Temperature (°C)	Initial P (bar)	Dispenser Temperature Profile (°C)	Dispenser Pressure Profile
1	15	20	-40	Constant PRR 8 MPa/min
2	50	20	-40	Constant PRR 8 MPa/min
3	40	20	-40	Constant PRR 8 MPa/min
4	-30	20	-40	Constant PRR 8 MPa/min
5	-15	20	-40	Constant PRR 8 MPa/min
6	0	20	-40	Constant PRR 8 MPa/min
7	15	20	-33	Constant PRR 8 MPa/min
8	15	20	-26	Constant PRR 8 MPa/min
9	15	20	-17.5	Constant PRR 8 MPa/min
10	15	50	-40	Constant PRR 8 MPa/min
11	15	250	-40	Constant PRR 8 MPa/min
12	15	20	-40	Constant PRR 5 MPa/min
13	15	20	-40	Constant PRR 16 MPa/min
14	15	20	-40	Constant PRR 20 MPa/min
15	15	20	-40	20 MPa/min for 3.85 min, transition to 1 MPa/min
16	15	20	-40	20 MPa/min for 3.85 min, transition to 3 MPa/min
17	15	20	-40	20 MPa/min for 3.33 min, transition to 1 MPa/min with pulse of 8 MPa/min for 10s every 30s
18	40	20	-17.5	Constant PRR 8 MPa/min

Note: ambient temperature was controlled at the Nikola facility.

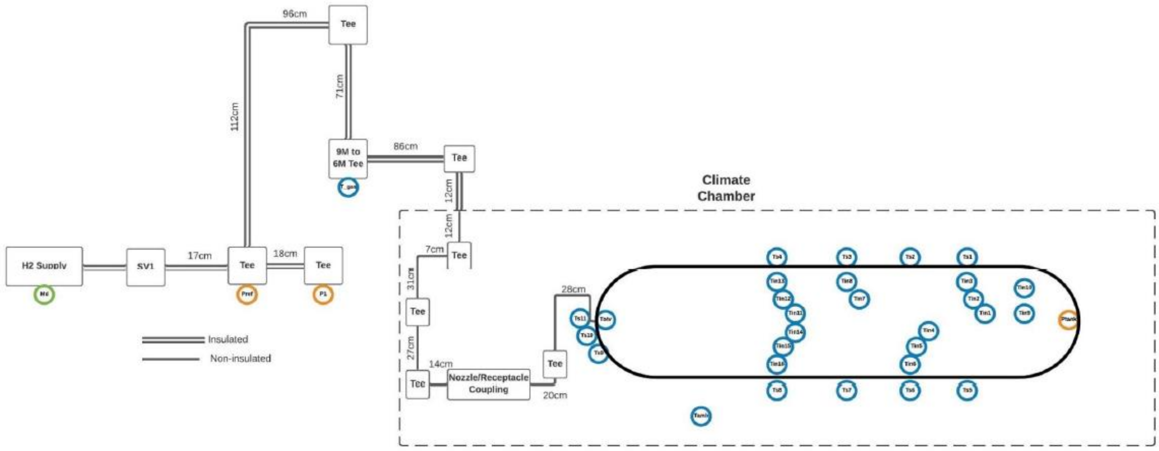

Figure 42: P&ID of the experimental setup for the H70 tank at Nikola

This test matrix illustrates the various conditions that can be tested. The same kind of test matrix was applied on the other tanks. For the ZBT experiments, it was not possible to control the ambient temperature, while the climate chamber at Nikola facility allows changing this parameter.

9.2 Validation of engineering models

HyFill and SOFIL models were both validated on all the tests conducted on the four tanks. Some of the validation results for the two models are displayed in the next sections.

9.2.1 240 L type IV H70 tank at ZBT

The example below shows temperature, pressure, velocity and mass flow development computed by HyFill during test #2 on the 240 L type IV H70 tank at ZBT facilities. More precisely,

- “exp” variables (in black or red) denote experimental data.
- “calc” variables (in blue) denote HyFill outputs.
- Δ variables (in yellow) show the difference between the calculated and experimental values. They have to be read on the right axis.
- The location “inlet pipe” corresponds to the values at the dispenser.
- The location “outlet pipe” corresponds to the location of the last measurements before the tank, for tests conducted at ZBT.

The inputs of the model were “$T_{inlet\ pipe}$ exp” and “$P_{inlet\ pipe}$ exp”, the measured temperature and pressure at the dispenser. The calculated values “T_{tank} calc” and “P_{tank} calc” can be compared to the measured quantities “T_{tank} exp” and “P_{tank} exp”. Note that the quantity considered as the reference experimental temperature “T_{tank} exp” is the average value of all thermocouples in the tank, but there are temperature heterogeneities up to 9°C in the tank.

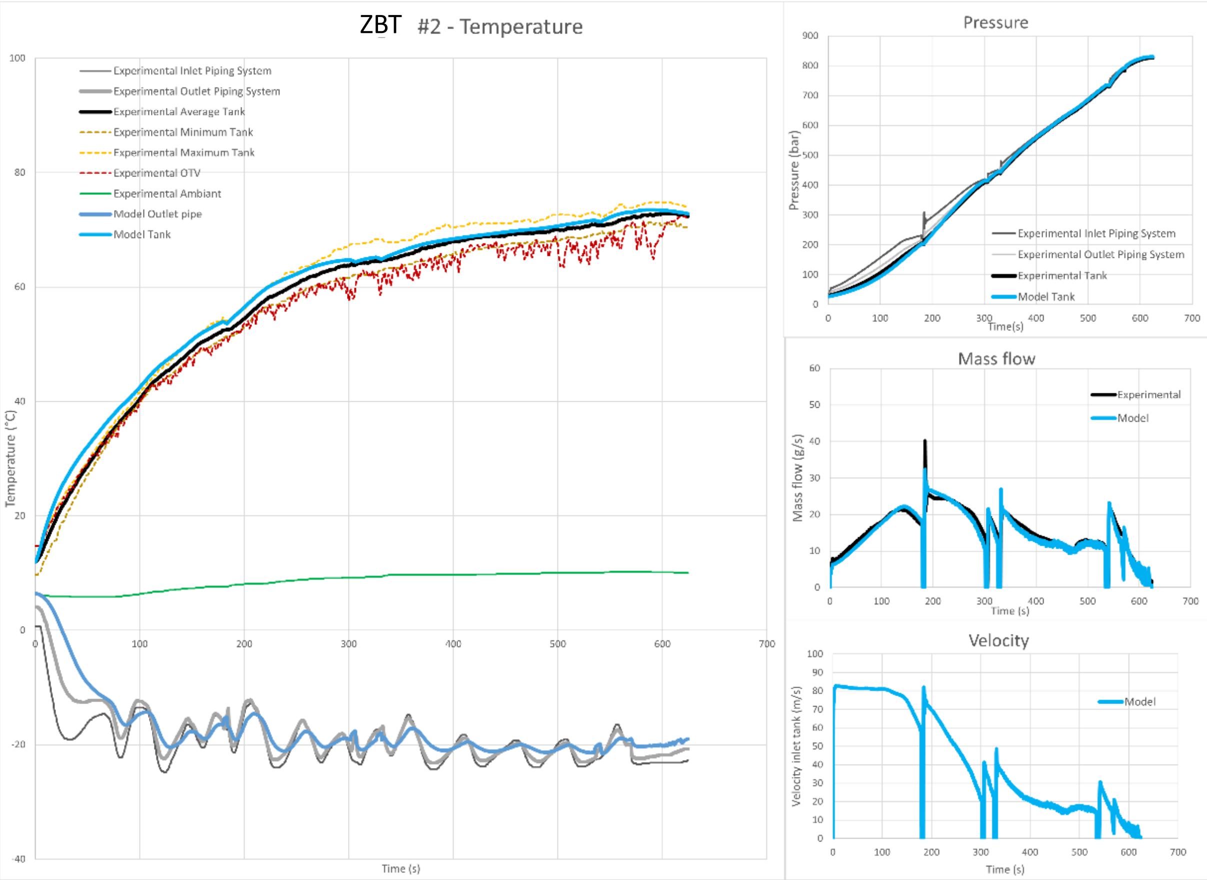

Figure 43: **HyFill model outputs and experimental measurements for test #2 on the 240 L type IV H70 tank at ZBT facilities**

It can be seen on Figure 43 that the temperature and pressure in the tank are very well predicted by HyFill model. The maximum temperature difference between the measured and experimental data in the tank is 3.88°C, and the maximum pressure difference in the tank is 12.9 bar. Moreover, it is important to be accurate on the final state of the tank to be able to know if the safety constraints are respected. HyFill is very accurate to model the final part of the refuelling: the final temperature is predicted here with 0.32°C accuracy.

Figure 44 summarizes the differences between the temperature predicted by the model and the experimental temperature for all experiments on one tank. It shows three quantities:

- Mean absolute temperature difference:

$$\Delta T_{\text{mean}} = \frac{1}{N}\sum_{t=1}^{t_{final}} |T_{tank,calc}(t) - T_{tank,exp}(t)|$$

- Maximum absolute temperature difference:

$$\Delta T_{max} = \max_{t}\left(\left|T_{tank,calc}(t) - T_{tank,exp}(t)\right| \right)$$

- Final temperature difference

$$\Delta T_{end} = T_{tank,calc}\left(t = t_{final}\right) - T_{tank,exp}\left(t = t_{final}\right)$$

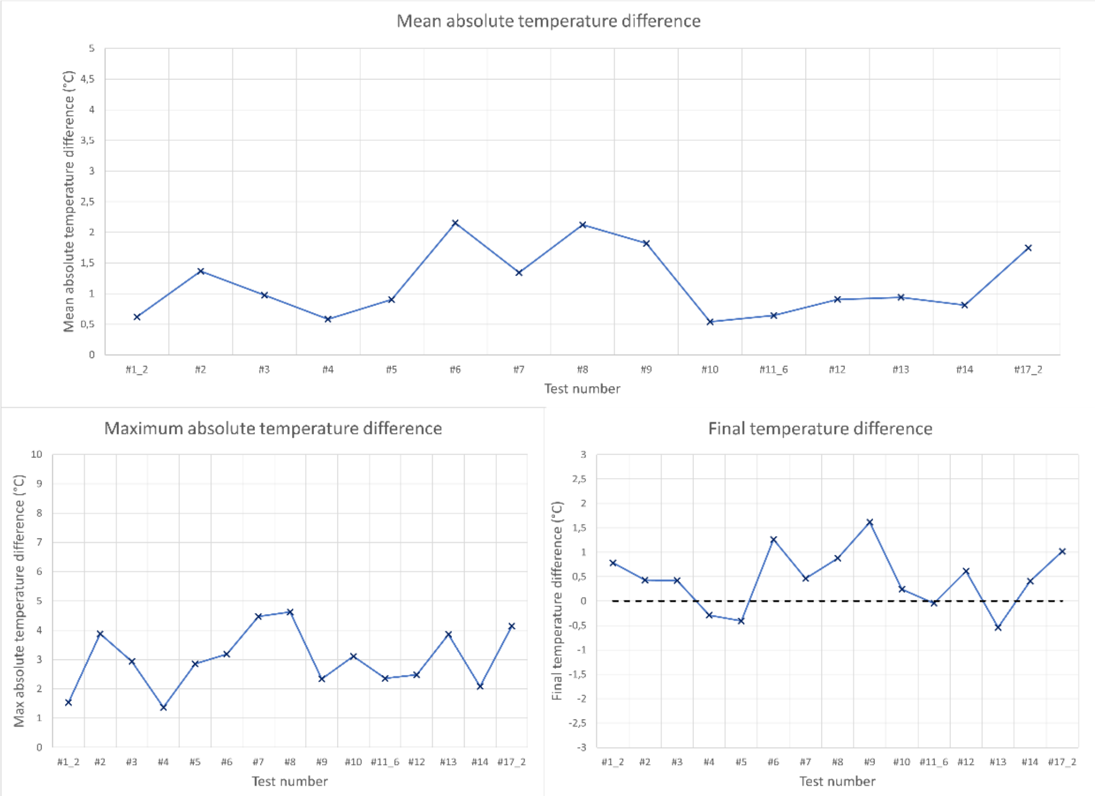

Figure 44: **Comparison between experimental temperature and HyFill output temperature in the tank for 15 filling tests on the 240 L type IV H70 tank at ZBT**

The HyFill model gives very accurate results when reproducing the ZBT experiments on the 240 L type IV H70 tank: the mean absolute temperature difference between the experiments and the model is less than 2.5°C for all experiments, and the final temperature is predicted with +/- 2°C accuracy. This accuracy is satisfying: it is of the same order of magnitude than the accuracy of the mean experimental temperature.

9.2.2 350 L type IV H50 tank at ZBT

Figure 45 shows HyFill results using inputs corresponding to the 350 L type IV H50 tank test #26.

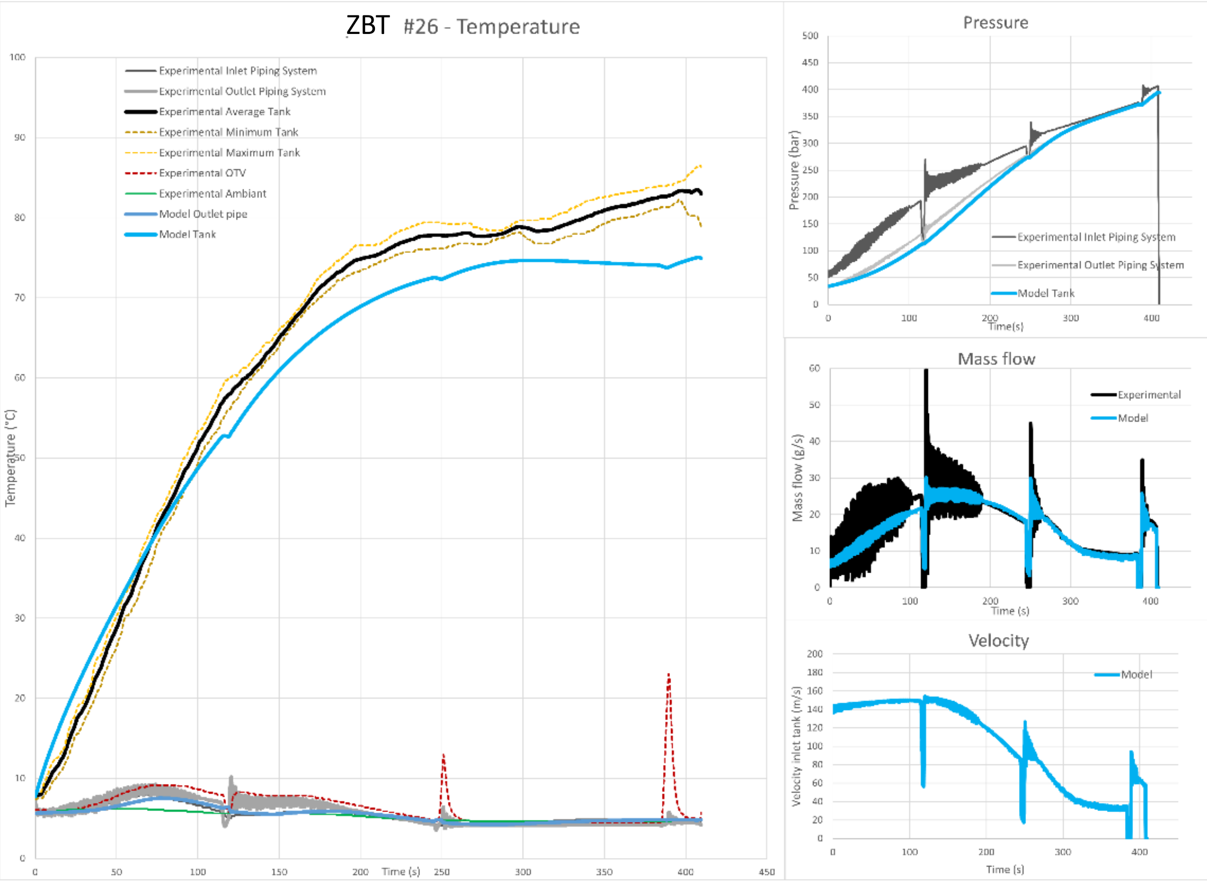

Figure 45: HyFill model outputs and experimental measurements for test #26 on the 350 L type IV H50 tank at ZBT facilities

HyFill succeeds in modelling the general evolution of pressure and temperature when reproducing the ZBT 350 L type IV H50 tank experiments. However, the quantitative results are less accurate than for the experiments using the ZBT 240 L type IV H70 tank, the ZBT 322 L type III H35 tank or the Nikola 165 L type IV H70 tank. For test #26 displayed here, the final temperature difference is -9°C. On the complete set of twelve tests, the final temperature is always underpredicted, from -2°C to -14°C. These large differences are probably due to the location of the functional sensors: there are only four functional thermocouples during the 350 L type IV H50 tank experiments, all located in the top of the tank opposite to the injector, which is one of the hottest zones of a tank during refuelling. Moreover, the difference between predicted and experimental temperature tends to increase at the end of the fills when the velocity is slower. It is consistent because a lower velocity implies less forced convection, and therefore a higher development of vertical stratification due to buoyancy effects, and a bigger difference between temperature at the top of the tank and average gas temperature.

Therefore, the "experimental average" derived from the values of these four thermocouples is not representative of the whole temperature field because there are thermal heterogeneities in the tank and the thermocouples are not evenly distributed in this tank. Thus, the measured temperature overestimates the real average gas temperature, which is consistent with the model finding a lower temperature.

9.2.3 322 L type III H35 tank at ZBT

The results for simulation using SOFIL software for the 18 filling tests done with the 322 L type III H35 tank are summarized in the following figure.

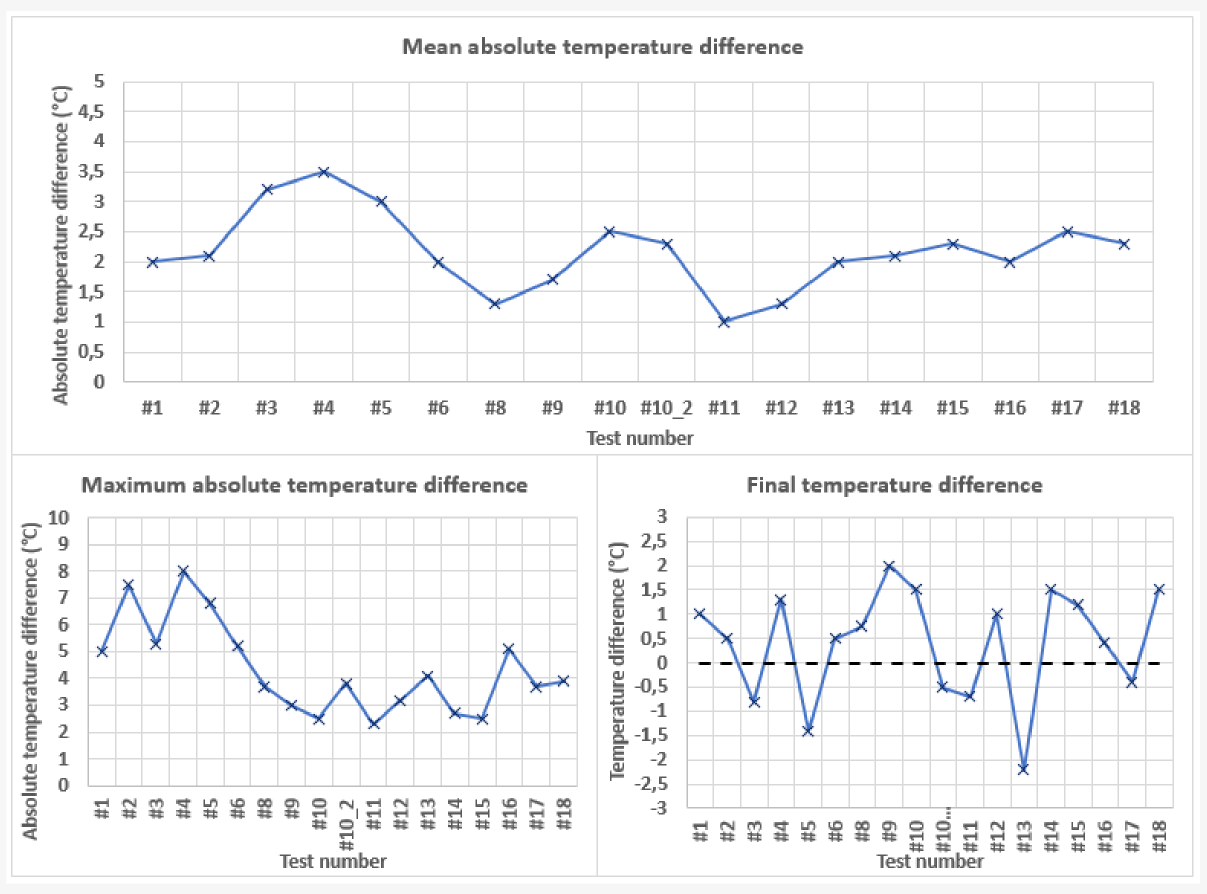

Figure 46: Comparison between experimental temperature and SOFIL output gas temperature in the tank for 18 filling tests on the 322 L type III H35 tank at ZBT

The mean absolute gas temperature difference is less than 3.5°C for all the tests as well as the gas temperature at the filling end.

Thus, the agreement between the modelling results from SOFIL and the experiments for gas temperature is good for the 322 L tank.

9.2.4 165 L type IV H70 tank at Nikola

The results for simulation using SOFIL software for the 18 filling tests done with the 165 L type IV tank are summarized in the following figure.

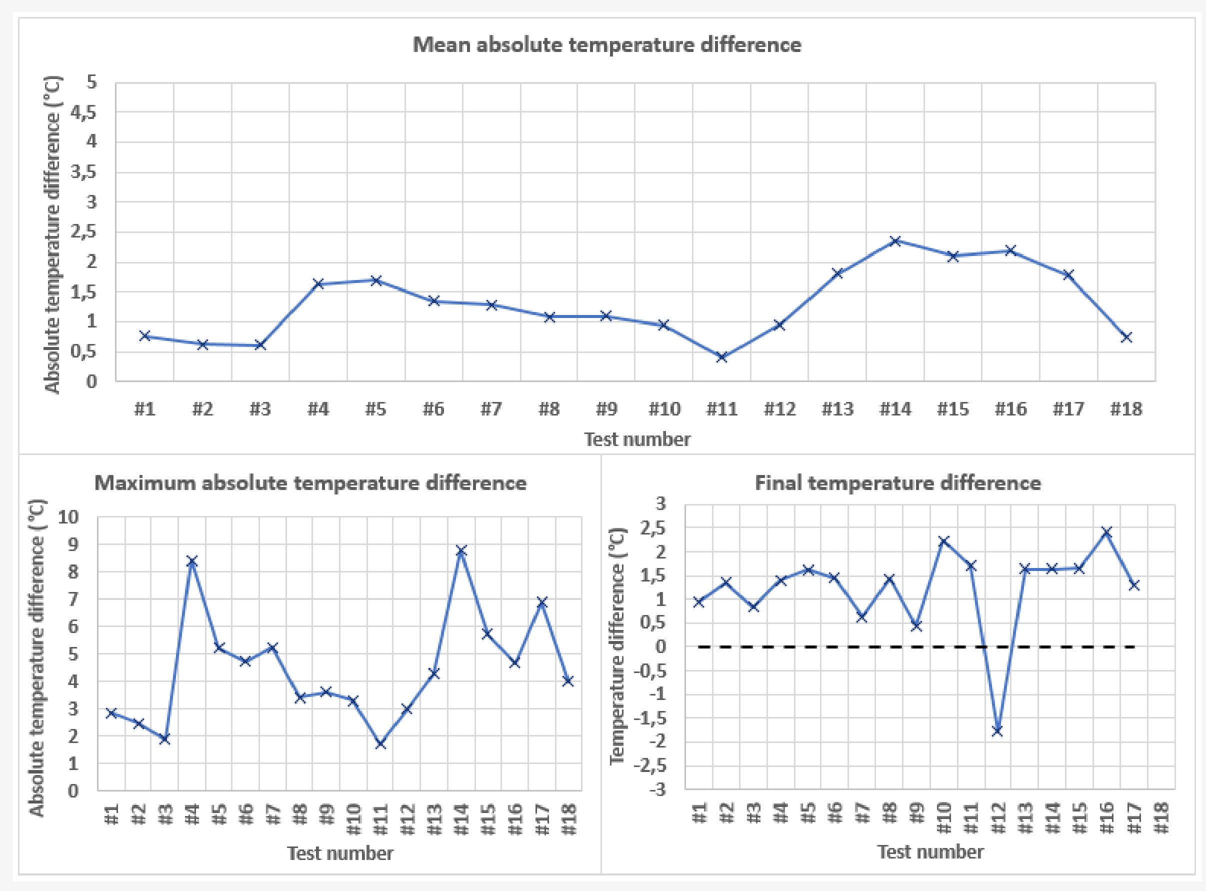

Figure 47: Comparison between experimental temperature and SOFIL output gas temperature in the tank for 18 filling tests on the 165 L type IV H70 tank at Nikola

The mean absolute gas temperature difference is less than 2.5°C for all the tests as well as the gas temperature at the filling end.

Consequently, the agreement between the modelling results from SOFIL and the experiments for gas temperature is good for the 165L tank.

9.3 Validation of CFD results

As CFD computing time for one tank filling takes many weeks to be completed, only two refuelling cases were launched.

This concerns 165L type 4 H70 tank and for test #2 and test #14. In these two cases, thermal stratifications (horizontal and vertical) occur during filling.

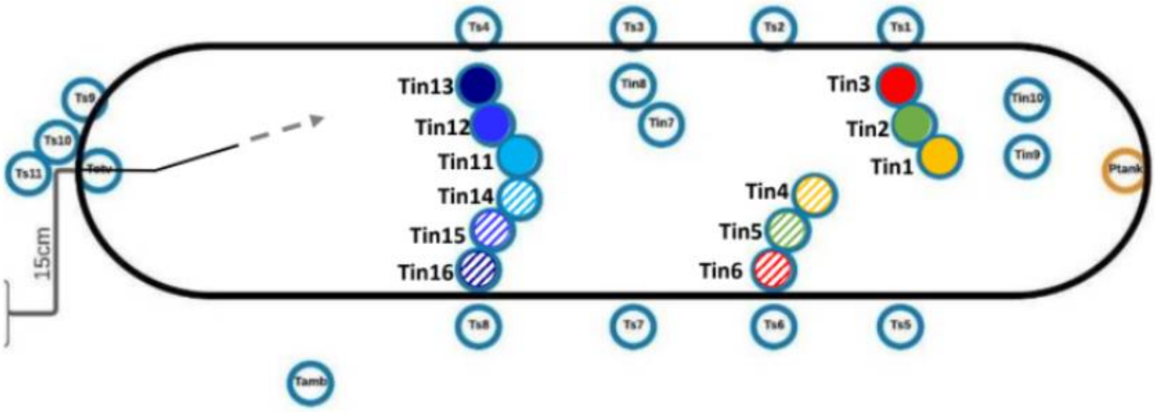

Figure 48: Positions of the temperature probes on the thermocouple tree inside the tank

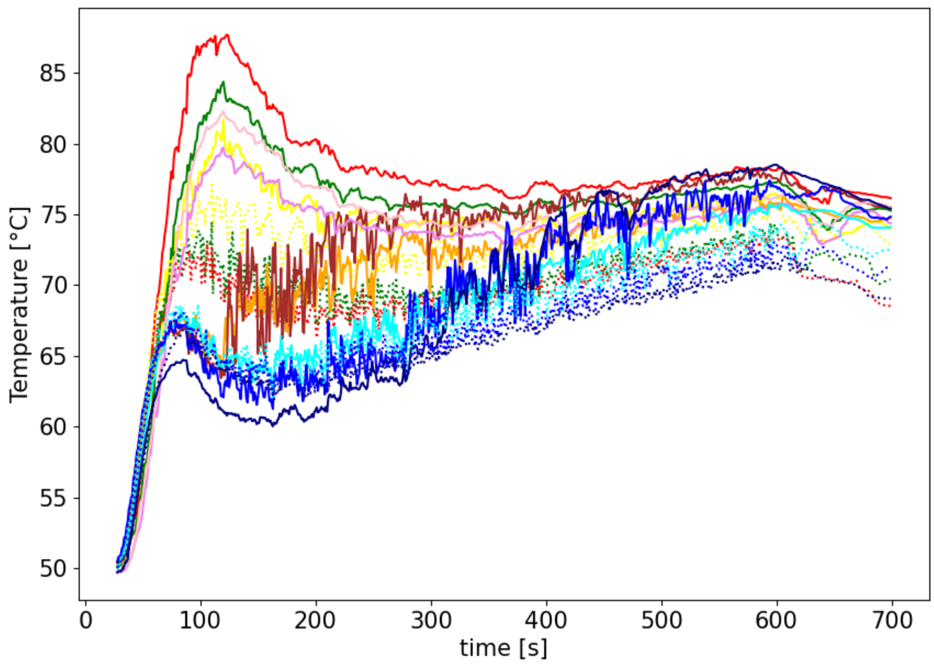

Figure 49: Temperature measured at the different probes during the test#2. Refer to the previous Figure 48 for the color legend

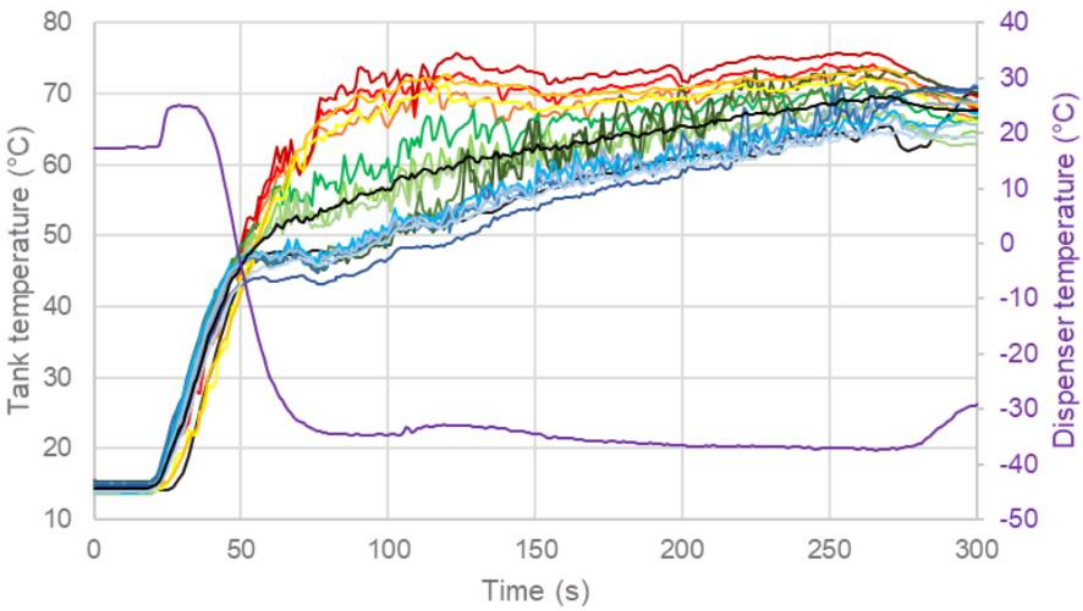

Figure 50: **Temperature measured at the different probes during the test#14. Refer to the previous Figure 48 for the color legend**

Hot temperatures are measured in the back of the tank (TC1, 2 and 3) while the front of the tank remains cold. A general flow pattern can be deduced from these measurements (see Figure 51):

- The precooled gas injected towards the top recirculate in the front part of the tank. The front part of the tank remains cold.
- The gas at the end of the tank mixes little with the precooled jet and undergoes an adiabatic-like compression. The end of the tank is thus hotter. A vertical temperature stratification is observed in the area where buoyancy forces play a determinant role.

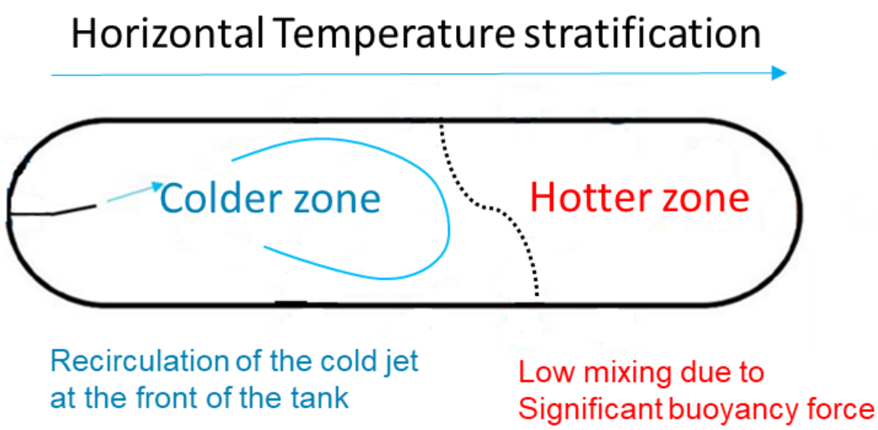

Figure 51: **Expected fluid behavior during the filling for both experiments**

This pattern can be explained by the fact that the jet has enough impulsion to reach the top of the tank but falls down before reaching the end of the tank, as the cold jet coming out of the injector has a higher density than the surrounding gas. Thus, there is a competition between the buoyancy forces due to the temperature gradient and the impulsion of the jet. In order to reproduce this flow pattern correctly, several phenomena should be well modelled:

- the cold jet coming out of the injector,
- the interaction of the jet with the top wall of the tank, and
- the mixing between the cold zone and the hot zone at the interface.

The choice of the turbulence model is of prime importance to capture the balance between convective and buoyancy forces, as illustrated in Figure 51 below, where two different models lead to significantly different flow behaviour and temperature gradients within the tank.

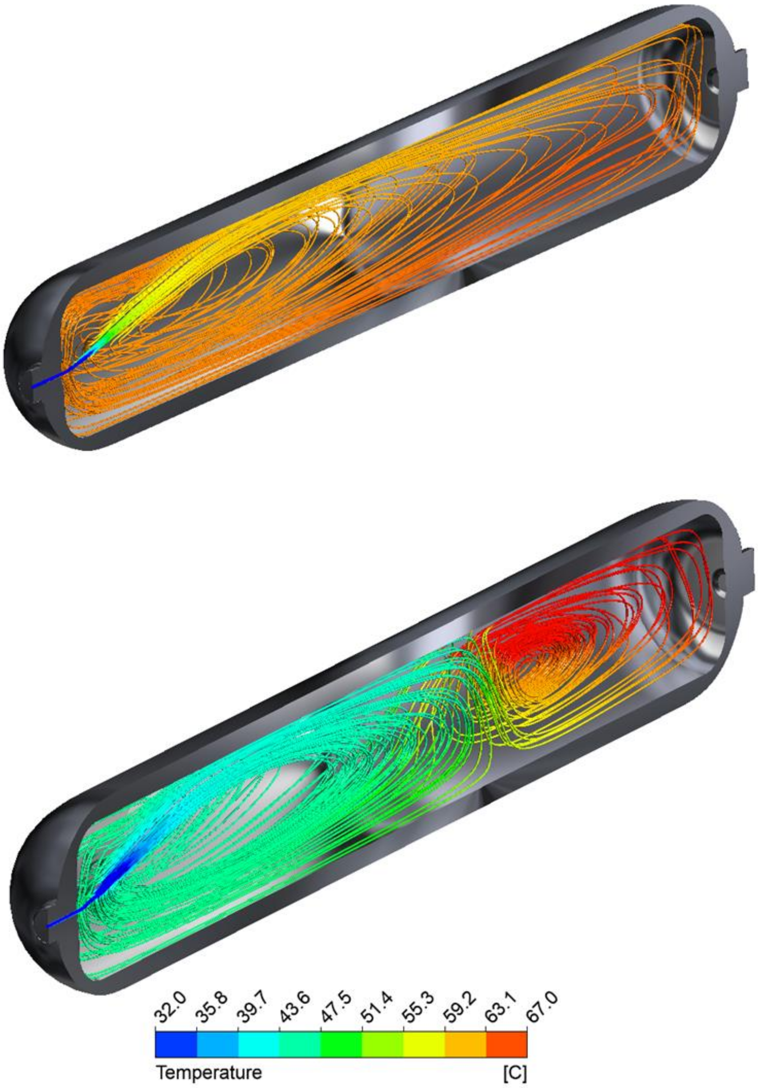

Figure 52: **Two different turbulence models lead to two different flow organizations and thus to two thermal behaviors within the tank**

Among the different turbulence models (k- ε, k-ω SST, SAS and RSM) that were tested, **RSM (Reynolds Stress Model) model seems the best to reproduce the behaviour of the impacting jet.** Large Eddy Simulation (LES) model could not be used due to the huge computing time needed.

10 OUTCOME FROM MODELLING PERFORMED IN THE PRHYDE PROJECT

10.1 Conclusions (performance of the models)

Engineering models studied in PRHYDE project reach an accuracy of +/-3°C on the spatial average gas and wall temperatures. These models run in a few minutes. Nevertheless they cannot represent/evaluate the presence of thermal gradient. However, they can be used to develop refuelling protocols when thermal stratifications are well mitigated by tank/OTV design or taken into account with additional margin.

The CFD models studied in PRHYDE project reach an accuracy on +/-5°C on the maximal local temperature reached in the tank when the right choice of turbulence model was made. Nevertheless, these models are time extensive with one run taking several weeks. Still, they are required to better understand thermal stratification phenomena but are not usable for protocol development due to the high number of simulations needed and the very long computing time.

10.2 Recommendations on modelling approach

For the future protocol development, numerical tools such as Engineering models as well as CFD can be used. However, these models should be validated using experimental data under different tank refuelling conditions.

10.2.1 Simple Engineering models

Nowadays, all simple models give only the volume average gas temperatures, they are not able to correctly model the temperature stratification (maximum and minimum temperature). However, they can suggest that the stratification is possible by estimating the gas velocity at the inlet. According to previous studies with axial injections in horizontal tanks, potential appearance of thermal stratification occurs below 5 m/s.

The most important advantage of simple models is the calculation time, which is in the order of several minutes.

In the absence of thermal gradients, these models can be used for the direct protocol development in the future under the conditions that they are validated versus experimental data for

- the whole range of temperatures investigated within the protocol (minimum and maximum possible temperatures). For instance, in the context of PRHYDE, the minimum T=-40°C and maximum T=+85°C. If the protocol targets a different or larger temperature range, it should be validated for the targeted range;
- the whole possible range of pressures (minimum and maximum values);
- the whole range of tank types (III, IV, V or others) and geometries (aspect ratios between length and diameter, wall thicknesses, thermal properties of the tank material etc.);
- the whole range of the injector geometries (orientation, length, diameter, material properties);

- the whole range of connection devices (hose, receptacle/nozzle coupling, on-board piping, valves etc.), which can create a pressure drop within the system dispenser/tank, and the range of thermal mass, which can contribute to the heat exchange with the gas and influence the temperature within the tanks;
- gas (hydrogen) properties (density, specific heat capacity, viscosity etc.) within the whole range of the considered temperatures and beyond.

The thermal gradient appearance during tank refuelling should be minimized by design, but thermal stratification may occur and can be sometimes significant (around 20°C for some Type III tank experiments). In case of doubts, CFD or experimental approached should be used.

For experimental measurements of gas temperature within the tank to see stratification, it is recommended to put several thermocouples in the height of the tank (thermocouple tree in the vertical axial plan of the tank), to measure vertical thermal stratification, as well as in the length, to measure horizontal stratification, as both can occur. Thermocouples should be as far away as possible from the injector to not alter the jet in front of the injector.

The CFD recommendations are listed in the section below.

10.2.2 CFD

In comparison to simple engineering models, CFD models can predict 3D phenomena within the tank: temperature stratification, injection jet behaviour etc. However, because the physics in the tank during filling is very complex (fluid mechanics, impacting jet on a wall etc...), it is challenging to get an accurate modelling. The work done in PRHYDE has shown that special attention should be paid to:

- The turbulence models: very different results have been obtained with k-eps and RSM models for example. RMS model gives better prediction for impacting jet-angled injector.
- The mesh, especially at the outlet of the injector (recommendation: 5 to 10 cells within the injector diameter) and in boundary layers when dealing with impacting jets (recommendation: maximum for the dimensionless distance y+ values of 10 at impacting point).
- The computational time: the order of magnitude is several weeks to simulate a full filling. CFL numbers less than 100 give a good trade-off between results and computational time with implicit methods.

Similarly to the simple engineering models, it is recommended that the CFD models should first be validated against experimental data under similar conditions to which it will be used – ” similar conditions” being the points listed above, plus considering:

- the injector geometry: diameter, orientation / angle, length, etc. and
- whether it is horizontal or vertical filling. For instance, a 2D axisymmetric model could be used for vertical filling models. However, a 3D approach must be applied for horizontal tanks.

Finally, by applying the recommendation above, it has been found that an accuracy of 5°C on the maximum gas hydrogen temperature can be expected from simulations that take approximately a couple of weeks of computational time, even in high thermal stratification cases. This accuracy seems reasonable for using modelling approach in the future for the protocol development.

10.3 Recommendations on experimental measurements

In the following, the different recommendations for gas temperature measurements inside a tank are listed in order to get a good representation of the volume average temperature for the gas during the tank refuelling.

The temperature measured on the On Tank Valve (OTV) may not represent the volume average for gas temperature. In many test cases within PRHYDE, this measured temperature (on the OTV) underestimates the average gas temperature (measured by the thermocouple tree inserted inside the tank) by 5 to 7°C. In some other cases, this temperature was almost equal to the precooled inlet gas temperature which is much less than the average gas temperature inside the tank, see PRHYDE Deliverable D6.8. **Consequently, the position of the temperature sensor on the OTV should be carefully studied and then properly positioned using either tests with different temperature sensor positions or CFD simulations in some specific cases.** The final objective for this sensor is to measure a temperature that is the closest possible to the average gas temperature for different filling conditions.

When performing model validation and/or checking for thermal stratification inside the tank, it is recommended to install a thermocouple tree inside the tank volume to be inserted from the opposite side of the gas inlet inside the tank. It is recommended that all the thermocouples stay in the vertical axial plan for a horizontal tank. Around 16 thermocouples are necessary to get a good indication of the gas temperature distribution inside the tank. Half of the thermocouples should be located in the upper vertical axial plan of the tank and the other half in the lower part of the same plan. The front part of the thermocouple tree should stay at a sufficient distance from the injection system to not disturb the gas jet entering inside the tank volume, as in fact in normal situation, the tank is not equipped with thermocouple tree.

Under some refuelling conditions for the same tank, thermal stratification can occur inside the tank. In these cases, the gas and wall temperatures can exceed 85°C locally, while the gas average temperature may stay below this limit. This can be observed with the thermocouple tree. In order to prevent these situations **in case of axial injection and horizontal tank**, inlet gas velocity should stay above 5 m/s during the whole period of tank filling (HyTransfer European project results[10]). However, **for cases with non-axial injections and horizontal tank**, the conditions without thermal stratification are not well defined. This should be investigated with specific tests with a thermocouple tree and/or with CFD calculations after validation in some dedicated cases.

---

[10] For details, see Pre-Normative Research for Thermodynamic Optimization of Fast Hydrogen Transfer | HYTRANSFER Project https://cordis.europa.eu/project/id/325277 and
D. Melideo, D. Baraldi, B. Acosta-Iborra, R. Ortiz Cebolla, P. Moretto: CFD simulations of filling and emptying of hydrogen tanks, International Journal of Hydrogen Energy, 42(11) 7304-7313, 2017. https://doi.org/10.1016/j.ijhydene.2016.05.262

11 Phase 1 Testing Campaign: Provision of Experimental Data for Modelling Verification

Testing was required from WP5 to generate fuelling data for the purpose of model verification (1D and 3D / CFD modelling) in WP4. As such, the Phase 1 Testing Campaign was defined to test a reference test case (ex. Test Number 1), and then vary key parameters to provide a comprehensive set of data on the respective tank under test.

A description of the test facilities and equipment used in the PRHYDE project is provided in APPENDIX C.

A summary of the results of this testing is available in APPENDIX D.

11.1 Phase 1 ZBT Test Campaign

11.1.1 Test Matrix

The following test matrix details the tests that were performed at the ZBT facility.

Table 20: Test matrix for ZBT test campaign (Phase 1)

Test Number	Tank	Initial Pressure (bar)	Ambient Temperature (°C)	Dispenser Temperature Profile	Dispenser Pressure Profile	End of Fill Criteria
#1 (ref)	Type IV 240L	20	-	-40°C	Constant PRR 8MPa/min	97-100% SoC
#2	Type IV 240L	20	-	-20°C	Constant PRR 8MPa/min	97-100% SoC[11]
#3	Type IV 240L	20	-	-10°C	Constant PRR 8MPa/min	97-100% SoC[12]
#4	Type IV 240L	20	-	0°C	Constant PRR 8MPa/min	To be determined with simulation
#5	Type IV 240L	20	-	for 5min -40°C and then cooling off	Constant PRR 8MPa/min	97-100% SoC
#6	Type IV 240L	20	-	for 5min no cooling and then cooling -40°C	Constant PRR 8MPa/min	97-100% SoC
#7	Type IV 240L	20	-	for 5min -40°C cooling and then cooling -20°C	Constant PRR 8MPa/min	97-100% SoC
#8	Type IV 240L	70	-	-40°C	Constant PRR 8MPa/min	97-100% SoC

Test Number	Tank	Initial Pressure (bar)	Ambient Temperature (°C)	Dispenser Temperature Profile	Dispenser Pressure Profile	End of Fill Criteria
#9	Type IV 240L	350	-	-40°C	Constant PRR 8MPa/min	97-100% SoC
#10	Type IV 240L	20	-	-40°C	Constant PRR 5MPa/min	97-100% SoC
#11	Type IV 240L	20	-	-40°C	16MPa/min for 3.85min, transitions to 1MPa/min	97-100% SoC
#12	Type IV 240L	20	-	-40°C	16MPa/min for 3.85min, transitions to 3 MPa/min	97-100% SoC
#13	Type IV 240L	20	-	-40°C	Constant PRR 3MPa/min	97-100% SoC
#14	Type IV 240L	20	-	-40°C	Constant PRR 16MPa/min	97-100% SoC
#15	Type IV 240L	20	As high as possible[13]	-40°C	Constant PRR 8MPa/min	97-100% SoC
#16	Type IV 240L	20	-	-	Customized pressure profile	97-100% SoC
#17(ref)	Type IV 240L	20	-	-40°C	Constant PRR 8MPa/min	97-100% SoC
#18 (ref)	Type IV 350 L	20	-	0°C	Constant PRR 5.5MPa/min	97-100% SoC
#19	Type IV 350 L	20	-	-40°C	Constant PRR 5.5MPa/min	97-100% SoC
#20	Type IV 350 L	20	-	Ambient	Constant PRR 5.5MPa/min	97-100% SoC
#21	Type IV 350 L	20	-	Customized temperature profile	Constant PRR 5.5MPa/min	97-100% SoC
#22	Type IV 350 L	50	-	0°C	Constant PRR 5.5MPa/min	97-100% SoC
#23	Type IV 350 L	250	-	0°C	Constant PRR 5.5MPa/min	97-100% SoC
#24	Type IV 350 L	20	-	0°C	Constant PRR 3.5MPa/min	97-100% SoC
#25	Type IV 350 L	20	-	0°C	PRR 12MPa/min with linearization	97-100% SoC

Test Number	Tank	Initial Pressure (bar)	Ambient Temperature (°C)	Dispenser Temperature Profile	Dispenser Pressure Profile	End of Fill Criteria
#26	Type IV 350 L	20	-	0°C	PRR 10MPa/min with linearization	97-100% SoC
#27	Type IV 350 L	20	-	0°C	PRR 8MPa/min with linearization	97-100% SoC
#28	Type IV 350 L	20	As high as possible	Ambient	Constant PRR 5.5MPa/min	97-100% SoC
#29 (ref)	Type IV 350 L	20	-	0°C	Constant PRR 5.5MPa/min	97-100% SoC
#30 (ref)	Type III 322 L	20	-	-20°C	Constant PRR 8.0MPa/min	97-100% SoC
#31	Type III 322 L	20	-	-40°C	Constant PRR 8.0MPa/min	97-100% SoC
#32	Type III 322 L	20	-	-10°C	Constant PRR 8.0MPa/min	97-100% SoC
#33	Type III 322 L	20	-	0°C	Constant PRR 8.0MPa/min	97-100% SoC
#34	Type III 322 L	20	-	Ambient	Constant PRR 8.0MPa/min	97-100% SoC
#35	Type III 322 L	20	-	For 5min -40°C and then cooling off	Constant PRR 8.0MPa/min	97-100% SoC
#36	Type III 322 L	20	-	For 5min no cooling and then -40°C	Constant PRR 8.0MPa/min	97-100% SoC
#37	Type III 322 L	70	-	-20°C	Constant PRR 8.0MPa/min	97-100% SoC
#38	Type III 322 L	150	-	-20°C	Constant PRR 8.0MPa/min	97-100% SoC
#39	Type III 322 L	20	-	-20°C	Constant PRR 4.0MPa/min	97-100% SoC
#40	Type III 322 L	20	-	-20°C	Constant PRR 3.0MPa/min	97-100% SoC
#41	Type III 322 L	20	-	-40°C	Constant PRR 14.0MPa/min	97-100% SoC
#42	Type III 322 L	20	-	-20°C	14.0MPa/min for 2,75min then 1MPa/min	97-100% SoC
#43	Type III 322 L	20	-	-20°C	14.0MPa/min for 2,5min then 3MPa/min	97-100% SoC

Test Number	Tank	Initial Pressure (bar)	Ambient Temperature (°C)	Dispenser Temperature Profile	Dispenser Pressure Profile	End of Fill Criteria
#44	Type III 322 L	20	-	-20°C	12.0MPa/min with linearization	97-100% SoC
#45	Type III 322 L	20	-	Ambient	10.0MPa/min with linearization	97-100% SoC
#46	Type III 322 L	20	-	Ambient	8.0MPa/min with linearization	97-100% SoC
#47 (ref)	Type III 322 L	20	-	-20°C	Constant PRR 8.0MPa/min	97-100% SoC
#XX	Additional test at the end of PRHYDE project to test refuelling protocol developed in WP3 in specific condition					

11.1.2 Test Results

The following table show the test results for the PRHYDE simulation validation tests at the ZBT site. The End of Fill SOC was calculated from the average gas temperature in the tank (average mean of the TC Tree temperature measurements) and not from the OTV temperature sensor. Since the measured OTV temperatures were generally below the mean gas temperatures in the tank, the calculated SOC values are below the advised level. The Peak Mass Flow Rate shown does not consider the maximum mass flow peaks during a pressure bank changeover.

Table 21: Test Results for the ZBT test campaign (Phase 1)

Test Number	Fill Duration (min)	Peak Tank Temperature OTV || TC-Tree (°C)	Peak Pressure / End Pressure (MPa)	End of Fill SOC (%)	Peak Mass-Flow Rate (g/s)
#1	9.87	59.9 (OTV) 63.4 (TT21)	79.416	98.18	23.49
#2	10.63	72.3 (OTV) 74.8 (TT17)	82.863	96.79	24.82
#3	10.43	79.8 (OTV) 82.63 (TT17))	82.208	96.38	23.53
#4	8.30	84.0 (OTV) 86.14 (TT21)	66.80	85.90	22.52
#5	10.47	73.6 (OTV) 75.97 (TT21)	84.00	97.48	23.65
#6	4.98	83.3 (OTV) 86.85 (TT21)	39.49	61.45	21.92
#7	10.58	64.1 (OTV) 66.64 (TT21)	82.76	96.72	23.91
#8	9.55	57.6 (OTV) 59.51 (TT21)	78.04	93.72	20.91

Test Number	Fill Duration (min)	Peak Tank Temperature OTV || TC-Tree (°C)	Peak Pressure / End Pressure (MPa)	End of Fill SOC (%)	Peak Mass-Flow Rate (g/s)
#9	6.23	38.7 (OTV) 40.72 (TT13)	81.99	96.19	15.24
#10	16.72	56.4 (OTV) 58.03 (TT21)	82.42	96.51	15.41
#11	20.27	64 (OTV) 68.22 (TT21)	81.62	101.76	31.62
#12	9.92	61.9 (OTV) 65.31 (TT21)	81.26	95.78	30.92
#13	27.32	49.4 (OTV) 50.73 (TT09)	82.55	96.59	9.45
#14	5.67	67.1 (OTV) 69.8 (TT21)	81.37	95.86	31.97
#15			Test Not Completed		
#16			Test Not Completed		
#17	10.52	60.2 (OTV) 62.81 (TT21)	82.66	96.66	21.99
#18	10.31	-8.58 (OTV min. during filling) 65.85 (OTV max. after filling) 86.43 (TT11)	58.19	94.87	23.44
#19	10.43	-39.26 (OTV min) 46.78 (OTV max) 68.12 (TT11)	57.95	98.48	24.64
#20	5.69	7.31 (OTV min) 66.45 (OTV max) 86.13 (TT09)	31.84	58.34	22.27
#21			Test Not Completed		
#22	10.03	-2.72 (OTV min) 66.45 (OTV max) 86. 5 (TT11)	57.50	93.99	20.8
#23	14.37	2.3 (OTV min) 43.01 (OTV max) 58.32 (TT09)	60.47	104.07	13.57
#24	6.83	-6.65 (OTV min) 63.57 (OTV max) 86.26 (TT11)	53.82	89.50	14.89
#25	7.72	-16.85 (OTV min) 61.81 (OTV max) 87.07 (TT09)	49.58	83.98	36.3
#26	7.04	3.48 (OTV min) 61.84 (OTV max) 86.47 (TT09)	39.16	69.60	Noisy mass flow
#27	11.14	-16.63 (OTV min) 55.87 (OTV max) 86.71 (TT11)	51.25	86.22	26.16
#28	5	9.46 (OTV min) 61.27 (OTV max) 86.19 (TT09)	26.13	49.16	20.81

Test Number	Fill Duration (min)	Peak Tank Temperature OTV || TC-Tree (°C)	Peak Pressure / End Pressure (MPa)	End of Fill SOC (%)	Peak Mass-Flow Rate (g/s)
#30	4.88	64.5 (OTV) 78.29 (TT23)	37.90	92.15	31.54
#31	4.70	48.9 (OTV) 62.59 (TT23)	34.89	89.30	33.83
#32	4.46	51.9 (OTV) 65.78 (TT23)	35.22	88.94	31.2
#33	4.63	48.4 (OTV) 62.68 (TT23)	33.50	86.34	33.05
#34	5.52	71.8 (OTV) 73.85 (TT23)	39.30	95.87	30.05
#35	7.27	44.2 (OTV) 55.82 (TT23)	39.15	99.94	28.12
#36			Test Not Completed		
#37	4.33	57.4 (OTV) 71.46 (TT23)	36.69	91.29	28.26
#38	4.01	52.7 (OTV) 64.72 (TT23)	38.82	97.23	29.18
#39	9.30	44.9 (OTV) 52.41 (TT23)	37.94	97.29	21.46
#40	12.49	59.7 (OTV) 64.95 (TT23)	38.84	96.13	18.44
#41	2.53	49.4 (OTV) 71.23 (TT23)	24.11	64.67	41.3
#42	2.76	51.2 (OTV) 74.08 (TT23)	23.97	63.94	47.3
#43	4.58	66.2 (OTV) 83.42 (TT23)	38.78	94.02	43.02
#44	5.16	67.5 (OTV) 80.37 (TT23)	38.77	93.81	35.47
#45	5.69	76.5 (OTV) 84.64 (TT23)	39.37	93.74	32.54
#47	5.06	63.4 (OTV) 78.14 (TT23)	36.92	90.45	31.48

The given peak mass flow rate was determined before first bank switchover. Maximum values after bank switching can also be significantly higher.

11.2 Phase 1 Nikola Test Campaign

11.2.1 Test Matrix

The following test matrix show all tests that were performed at Nikola's contracted facility (TesTneT Gmbh.).

Table 22: Test matrix for Nikola test campaign (Phase 1)

Test Number	Tank	Initial P (MPa)	Ambient T (°C)	Dispenser Temperature Profile	Dispenser Pressure Profile	End of Fill Criteria
#1 (ref)	Type IV 165L	2	15	-40°C	Constant PRR 8MPa/min	97-100% SoC
#2	Type IV 165L	2	50	-40°C	Constant PRR 8MPa/min	97-100% SoC
#3	Type IV 165L	2	40	-40°C	Constant PRR 8MPa/min	97-100% SoC
#4	Type IV 165L	2	-30	-40°C	Constant PRR 8MPa/min	97-100% SoC
#5	Type IV 165L	2	-15	-40°C	Constant PRR 8MPa/min	97-100% SoC
#6	Type IV 165L	2	0	-40°C	Constant PRR 8MPa/min	97-100% SoC
#7	Type IV 165L	2	15	-33°C	Constant PRR 8MPa/min	97-100% SoC
#8	Type IV 165L	2	15	-26°C	Constant PRR 8MPa/min	97-100% SoC
#9	Type IV 165L	2	15	-17.5°C	Constant PRR 8MPa/min	97-100% SoC
#10	Type IV 165L	5	15	-40°C	Constant PRR 8MPa/min	97-100% SoC
#11	Type IV 165L	25	15	-40°C	Constant PRR 8MPa/min	97-100% SoC
#12	Type IV 165L	2	15	-40°C	Constant PRR 5MPa/min	97-100% SoC
#13	Type IV 165L	2	15	-40°C	Constant PRR 16MPa/min	97-100% SoC
#14	Type IV 165L	2	15	-40°C	Constant PRR 20MPa/min	97-100% SoC
#15	Type IV 165L	2	15	-40°C	20MPa/min for 3.85min, transitions to 1MPa/min	97-100% SoC
#16	Type IV 165L	2	15	-40°C	20MPa/min for 3.85min, transitions to 3MPa/min	97-100% SoC

Test Number	Tank	Initial P (MPa)	Ambient T (°C)	Dispenser Temperature Profile	Dispenser Pressure Profile	End of Fill Criteria
#17	Type IV 165L	2	15	-40°C	20MPa/min for 3.33min, transitions to 1MPa/min with an 8MPa/min pulse for 10s, every 30s	97-100% SoC
#18	Type IV 165L	2	40	-17.5°C	Constant PRR 8MPa/min	97-100% SoC

11.2.2 Test Results

The following table show the test results for the PRHYDE simulation validation tests at Nikola's contracted facility (TesTneT Gmbh).

Table 23: Test Results for Nikola test campaign (Phase 1)

Test Number	Fill Duration (min)	Peak Tank Temperature (°C)	Peak Pressure (MPa)	End of Fill SOC (%)	Peak Mass-Flow Rate (g/s)
#1	10.2	61.7	83.02	102	16.6
#2	10.6	92.2	85.9	100	15.1
#3	10.5	81.02	84.6	100	15.6
#4	9.75	43.2	77.9	102	17.8
#5	9.9	51.0	79.4	101	17.6
#6	10.0	57.0	80.7	101	17.1
#7	10.3	68.9	83.8	101	16.2
#8	10.4	70.4	84.5	102	18.4
#9	10.5	76.6	84.7	100	15.9
#10	9.6	60.5	81.2	102	15.4
#11	6.7	54.5	79.3	101	11.9
#12	15.5	56.6	79.1	100	10.8
#13	5.2	74.1	82.2	99	33.2
#14	4.35	75.8	83.9	100	77.8
#15	7.6	74.5	83.3	102	42.2
#16	5.1	75.8	82.9	100	42.2
#17	8.2	71.7	82.2	102	43.0
#18	10.7	88.7	85.4	98	15.6

12 PHASE 2 TESTING CAMPAIGN: PROTOCOL CONCEPT IMPLEMENTATION AND COMPARISON TESTING

The Phase 2 testing campaign was defined for two primary objectives. Firstly, to test the successful implementation of the protocol concepts, and secondly to confirm the results of the performance simulation campaign conducted by WP3 (Protocol Development) and WP4 (Simulations). A summary of the results of this testing is available in APPENDIX D.

12.1 Phase 2 ZBT Test Campaign

12.1.1 Test setup

Since the measurements under Section 11.1.2 showed that the influence of direct solar radiation on the tanks leads to enormous temperature differences within the tank, a sun protection was set up for the protocol validation. This issue was observed for the first time during Phase 2 tests as they were performed in late spring to early summer time. Otherwise, the measurement setup was identical to Phase 1 testing that one described in PRHYDE Deliverable D5.1 - Report on Test Specification.

In the absence of advanced communication the t_{final} tables were programmed directly into the dispensing system programmable logic controller (PLC).

Figure 53: Sun Protection on the 70 MPa ZBT Tank (Source: ZBT)

12.1.2 Test Matrix

The following test matrix shows the tests performed at ZBT test site to validate the protocol concepts developed and described by WP3 in PRHYDE Deliverable D3.5 – Final Fuelling Protocols Specification. In total, four different protocol concepts have been tested at different conditions: Static, T_{gas} Initial+, T_{gas} Throttle, and Adjustable T_{gas} Throttle.

Table 24: Test matrix for ZBT test campaign (Phase 2)

Test Number	Tank	Protocol Concept	Initial Pressure (bar)	Ambient Temperature (°C)	Initial Gas Temperature (°C)	Dispenser Pre-cooling Temperature	Fuelling Rate
#1	Type IV 240L	Static	150	29.5	ambient	-20°C	T_{gas} Static P_{min}=50bar T_{hot_soak}
#2	Type IV 240L	T_{gas} Initial +	150	30.1	ambient	-20°C	T_{gas} Initial + P_{min}=20bar T_{hot_soak} -5
#3	Type IV 240L	T_{gas} Throttle	150	27	ambient	-20°C	P_{min}=150bar
#4	Type IV 240L	T_{gas} Throttle self-adjusting	150	22.4	ambient	-20°C	P_{min}=20bar
#5	Type IV 240L	T_{gas} Initial +	20	30.4	ambient	-20°C	P_{min}=20bar
#6	Type IV 240L	T_{gas} Throttle	20	23.5	ambient	-20°C	T95 table P_{min}=20bar a=4
#7	Type IV 240L	T_{gas} Throttle self-adjusting	20	26.7	ambient	-20°C	95 table P_{min}=20bar *a*=4; *b*=4

12.1.3 Test results

Table 25: Test Results for ZBT test campaign (Phase 2)

Test Number	Fill Duration (min)	Peak Tank Temperature (°C)	Peak Pressure (MPa)	End of Fill SOC (%)	Peak Mass Flow Rate (g/s)
#1	6.49	68.3 (OTV) 71.43 (TT21)	78.83	96.18	28.1
#2	4.08	71.7 (OTV) 76.16 (TT21)	77.97	94.55	34.2
#3	4.34	68.9 (OTV) 72.72 (TT21)	77.54	94.72	33.81
#4	4.39	63.4 (OTV) 66.62 (TT21)	75.59	94.27	35.42
#5	8.13	76.3 (OTV) 79.25 (TT21)	80.26	95.69	28.92
#6	5.83	77.5 (OTV) 81.53 (TT17)	79.17	94.69	36.63
#7[1]					

[1]: Test #7 needed to be repeated due to programming issues. Results were not available at time of this report.

12.2 Phase 2 Nikola Test Campaign

The Phase 2 testing campaign for Nikola was focused on evaluating the implementation of the protocol concepts and comparing the protocol concepts against each other under similar conditions to verify the results of the performance simulation campaign conducted in WP4.

- The ambient or chamber temperature was held constant for all test cases.
- The initial gas temperature was varied for between being soaked at the ambient temperature, to being 10°C less than ambient temperature to compare the performance of the T_{gas} Initial+ and T_{gas} Throttle protocol concepts with each other. This was accomplished by rapidly defuelling the vessel, pausing at the initial pressure target, and starting the test once the measured gas temperature warmed to the target start temperature.
- Tin9, the thermocouple on the thermocouple tree located at the aft end (opposite to the OTV) of the tank was used for control of the T_{gas} Throttle protocol concept. This was done as it was known from the Phase 1 testing campaign that there was significant thermal stratification from front to aft, with the aft end of the tank getting much hotter than the front. In this fashion, the T_{gas} Throttle tests conducted at Nikola were controlled using a gas temperature closer to the peak or maximum temperature inside of the tank, rather than the bulk average temperature.

As the results show, the PRHYDE protocol concepts were successful in achieving full fills (>97% SOC) is very competitive fuelling times (<15 minutes) even under strenuous boundary conditions. Some insights were attained, such as:

- All protocols concepts resulted in peak gas temperature measurements that exceeded 85°C by a small margin. This can possibly be attributed to:
  - Inaccuracies between WP4's model and the actual experimental implementation resulting in excessive fuelling rates or t_{final} values.
  - Excessive thermal stratification of the gas inside of the tank.
  - Improper selection of protocol concept fuelling parameters or improper implementation of the fuelling protocol concepts at the test facility.
  - The inherent tolerance / accuracy of the temperature sensors.

12.2.1 Test Matrix

Table 26: Test matrix for Nikola test campaign during (Phase 2)

Test Number	Tank	Protocol Concept	Initial Pressure (MPa)	Ambient / Chamber Temperature (°C)	Initial Gas Temperature (°C)	Dispenser Pre-cooling Temperature	Fuelling Rate (as calculated by WP4)
#1	Type IV 165L	T_{gas} Initial +	2	35+2/-2C	35+0/-4C	-17.5+0/-4C	T_{gas} Initial + Hot Soak
#2	Type IV 165L	T_{gas} Throttle	2	35+2/-2C	35+0/-4C	-17.5+0/-4C	T_{gas} Throttle
#3	Type IV 165L	T_{gas} Initial +	2	35+2/-2C	25+0/-4C	-17.5+0/-4C	T_{gas} Initial + Hot Soak -10
#4	Type IV 165L	T_{gas} Throttle	2	35+2/-2C	25+0/-4C	-17.5+0/-4C	T_{gas} Throttle
#5	Type IV 165L	Static	15	35+2/-2C	35+0/-4C	-17.5+0/-4C	T_{gas} Static
#6	Type IV 165L	T_{gas} Initial +	15	35+2/-2C	35+0/-4C	-17.5+0/-4C	T_{gas} Initial + Hot Soak
#7	Type IV 165L	T_{gas} Throttle	15	35+2/-2C	35+0/-4C	-17.5+0/-4C	T_{gas} Throttle
#8	Type IV 165L	T_{gas} Initial +	15	35+2/-2C	25+0/-4C	-17.5+0/-4C	T_{gas} Initial + Hot Soak -10
#9	Type IV 165L	T_{gas} Throttle	15	35+2/-2C	25+0/-4C	-17.5+0/-4C	T_{gas} Throttle

12.2.2 Test Results

Table 27: Test Results for Nikola test campaign (Phase 2)

Test number	Fill Duration (min)	Peak Tank Temperature (°C)	Peak Pressure (MPa)	End of Fill SOC (%)	Peak Mass Flow Rate (g/s)
#1	10.4	87.8	85.0	98.6	18.8
#2	10.9	90.1	83.5	97.9	31.2
#3	7.5	87.5	84.5	98	21.9
#4	8.7	88.8	84.7	99.2	79.2
#5	5.5	87.4	84.6	98.9	31.9
#6	4.9	87.7	84.6	98.7	33.9
#7	5.5	86.9	84.2	98.9	36.0
#8	4.1	86.1	84.9	99.3	61.0
#9	4.7	83.4	85.1	99.8	36.2

13 FINDINGS AND RECOMMENDATIONS FROM EXPERIMENTAL WORK IN PHASES 1 & 2

13.1 Internal Gas Temperature Measurements

In some of the tests conducted at ZBT, the gas temperature measured by the OTV was impacted by the incoming pre-cooled gas and rendered inaccurate. The cause of this can be due to several reasons and is likely specific to the OTV and tank combination. As most tanks utilize only one temperature sensor inside of the tank which is typically located on the OTV, this is key finding that should be considered by the industry. Steps should be taken to ensure that the temperature sensor(s) accurately represent the bulk gas temperature. This is especially important for the T_{gas} Throttle protocol concept, which required dynamic measurement and control using the gas temperature measurement. The following figures show an inaccurate and accurate example of temperature measurement via OTV sensor during a T40 fuelling.

Due to the large number of thermocouples in the tanks, we assume that the average TC tree temperature corresponds approximately to the average bulk gas temperature. During all test even for the good OTV tank combinations, the measured OTV temperature was always below this temperature.

Additionally, the temperature as measured by the OTV was consistently shown to be lower by varying margins than the gas temperature as measured by the thermocouples on the thermocouple tree. This is explained further in Section 13.3.

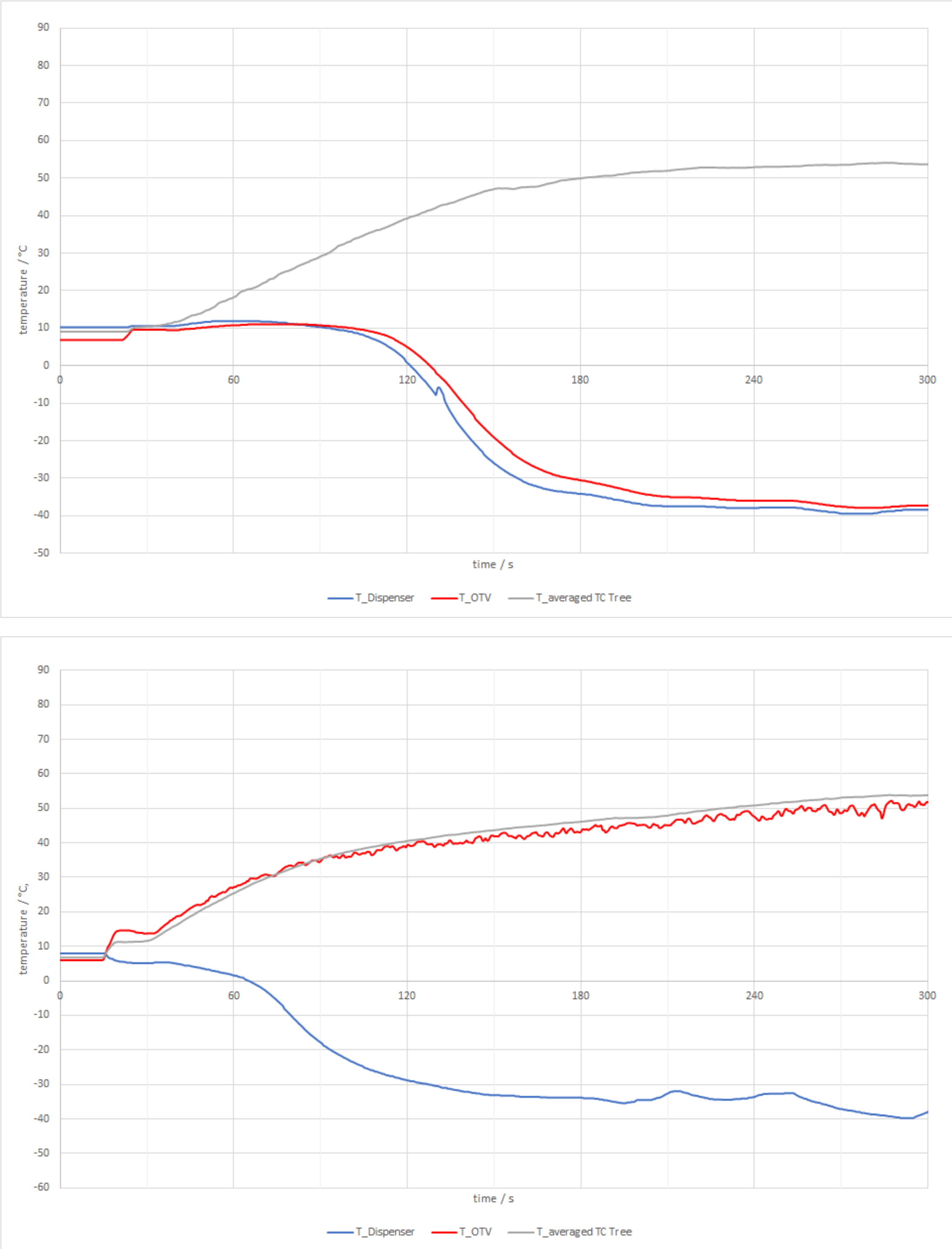

Figure 54: Figures showing the difference between temperature reading with different OTV-tank combinations

13.2 T_{gas} Throttle Parameters

As experienced in the test campaigns conducted at ZBT and Nikola, the parameters selected and utilized for the T_{gas} Throttle protocol concept must be optimized for the specific tank or CHSS being fuelled. Improper selection of these parameters can lead to reduced performance of the protocol concept, or possible temperature overshoot.

13.3 Internal Gas Temperature Stratification

The utilization of the thermocouple trees inside of the tested tanks provided great insight into the heterogenous behaviour of the gas temperature inside of the tanks during fuelling. In one of the tests conducted and under worst-case conditions, the gas temperature varied by as much as 27°C inside of the tank during fuelling. This stratification of temperature is heavily influenced by the aspect ratio (length over diameter) of the tank, OTV injector characteristics (angle, inner diameter, insertion depth), and needs to be considered by the industry for the generation of the fuelling tables (t_{final} values) and other fuelling protocol concepts.

14 OVERALL SUMMARY OF WORK PERFORMED IN THE PRHYDE PROJECT AND KEY FINDINGS

The PRHYDE protocol development work has further developed the MC Formula Framework in a way that enables conservatisms inherent in the SAE J2601 approach for refuelling of light duty vehicles to be reduced by the utilisation of data communicated from the vehicle to the dispenser by the protocol.

Out of the various protocol types initially explored during the project, four concepts were developed, which are described in this final PRHYDE deliverable. Applying the nomenclature presented in this report, these concepts can be described as follows:

- Type 2-PR-S Static Data
- Type 3-PR-S Dynamic Data – T_{gas} Initial
- Type 3-PR-S Dynamic Data – T_{gas} Initial+
- Type 3-PR-S Dynamic Data – T_{gas} Throttle

Developing these protocol concepts was largely based on thermodynamical modelling. 0D modelling was used to estimate fuelling speed and end-of-fill statistics. Computational Fluid Dynamics was used to examine phenomena inside the tank systems. The modelling supporting the concepts has been summarized in this report.

Furthermore lab testing was conducted on suitable setups. The lab tests were used to validate the modelling efforts and provide proof-of-concept that the protocol concepts works as intended. A few workarounds were needed to overcome the limitation that current day communication cannot communicate the fuelling parameters from vehicle to station.

Ultimately performance estimates based on simulations were conducted and referenced for implications on how the PRHYDE protocol concepts can improve fuelling time in the heavy duty segment. Based on the results, a few general comments are summarized:

- PRHYDE fuelling concepts T_{gas} initial+ and T_{gas} Throttle shows improvement over Static and T_{gas} initial concepts
- T_{gas} Throttle tends to have better fuelling performance, at lower initial pressure P_o
- T_{gas} initial+ tends to have better fuelling performance, at higher initial pressure P_o and lower initial gas temperature
- T_{gas} Throttle (100 °C) slightly faster than T_{gas} Throttle (95 °C), most notably at higher P_0
- T_{gas} Throttle is significantly less affected by fuelling history
- Sub 4 minute fills are possible at high P_0 using T_{gas} Initial+
- Static data fill times are notably longer, especially at high P_0

These final results are intended to be picked up by a standard development organization, such as ISO/TC 197 (WG24) or the SAE FCEV Interface Task Force, to standardize, see PRHYDE Deliverables D6.2 (Dissemination and Exploitation Plan) and D6.8 (Topics for further work).

APPENDIX A: Fuelling Protocol Algorithms

A.1 Fuelling Control

The fuelling control described is a minimum set of instructions required to implement these fuelling concepts. The primary purpose of this section is to provide sufficient documentation to facilitate the implementation of the fuelling concepts for laboratory testing. There are many things important for a complete fuelling protocol that are left out or not considered here, such as a description of the startup sequence, and a detailed description of the communication between the vehicle and the station. For a higher level overview of each fuelling concept, refer to the Section 3.

The fuelling control is based on an advanced version of the MC Formula protocol found in SAE J2601. The control is structured by utilizing subroutines which describe a certain function within the overall control structure. These subroutines are labelled based on their function and are ordered by their sequence within the control structure. Most of the subroutines are common to all of the fuelling concepts presented in this report. However, there are some subroutines that are utilized only for a specific fuelling concepts. Furthermore, within some of the common subroutines, there may be elements which are only activated for certain fuelling concepts, in which case, these are called out in the subroutine. Although these subroutines are described below generally in the order they are executed, refer to Section 6 for the flow diagram for each fuelling concept, which definitively describes the order of operation of these subroutines.

A.1.1 Advanced MC Formula Control Subroutines

A.1.1.1 Subroutine – Determine Initial Parameters

A.1.1.1.1 Initial Pressure

The dispenser must determine the initial pressure. This may be done by dispensing a small amount of hydrogen into the CHSS until the dispenser pressure and CHSS pressure equalize. Alternatively, the initial pressure in the CHSS may be communicated to the dispenser. The initial pressure is recorded as $P_{initial}$.

A.1.1.1.2 Ambient Temperature

The dispenser must measure the ambient temperature. The ambient temperature is recorded as T_{amb}.

A.1.1.1.3 MAT Expected

The dispenser must determine the expected mass average fuel delivery temperature (MAT). This should be based on the fuel delivery temperature control setpoint, i.e., the fuel delivery temperature that the cooling system is targeting during the fill. MAT Expected is recorded as $MAT_{expected}$.

A.1.1.2 Subroutine – Parameter Initialization

A.1.1.2.1 Initialization of Parameters with Non-Discretionary Settings

The settings of the parameters in this subsection do not allow for discretion. The parameters shall be set and/or calculated as indicated.

The initial step is to set the time step counters to zero. The time step *j* is used to calculate all control parameters, as defined in Subroutines "Mass Average Calculation", "Calculation of t_{final}" , "Calculation of *PRR* and P_{ramp}", "Determination of Pressure Targets and Limits", "Evaluate End of Fill Criteria ", and "Process Check". The time step *j* shall be set to 1 second, meaning that the calculations are performed every second.

(Eq. A.1)

$$Set\ \ j = 0$$

The counter *n* is used to determine the point in the fill after which a total of 30 seconds of mass flow have elapsed. The counter *n* advances at the same frequency as time step counter *j*, but only advances if there is mass flow. It is utilized to determine the point in the fill at which the calculation of MAT_{30} commences.

(Eq. A.2)

$$Set\ \ n = 0$$

P_{final} is a parameter utilized in the variable pressure ramp rate equation. It represents the pressure at which the hot case fuelling scenario will reach 85 °C when starting the fill from the minimum pressure P_{min}. The unit of measure for P_{final} is MPa.

(Eq. A.3)

$$Set\ \ P_{final} = 1.25 \times NWP$$

P_{trans} is a parameter used in the mass average fuel delivery temperature control (MAT_C) equation. The unit of measure for P_{trans} is MPa.

(Eq. A.4)

$$Set\ \ P_{trans} = \frac{P_{final}+P_{initial}}{2}$$

$P_{initial}$ is used to set the initial ramp pressure P_{ramp}. The unit of measure for P_{ramp} is MPa.

(Eq. A.5)

$$Set\ P_{ramp} = P_{initial}$$

RR_{min} is the minimum calculated pressure ramp rate throughout the fill. It is utilized in the equation for α. The unit of measure for RR_{min} is MPa/sec.

(Eq. A.6)

$$Set\ \ RR_{min} = 1$$

RR_{max} is the maximum calculated pressure ramp rate throughout the fill. It is utilized in the equation for α (Equation A.34). The unit of measure for RR_{max} is MPa/sec.

(Eq. A.7)

$$Set\ \ RR_{max} = 0$$

α is a parameter which is multiplied by t_{final} to compensate for non-linearity in the pressure ramp rate during the fill (see Equations A.33 and A.34). See Section H.2.6.1 of SAE J2601 for a detailed explanation of α. The higher the difference between RR_{max} and RR_{min} the higher α becomes. α is calculated for each time step j. The unit of measure for α is dimensionless.

(Eq. A.8)

$$Set\ \alpha = 1$$

ΔP_{tol_high} is an upper tolerance on the ramp pressure P_{ramp}. ΔP_{tol_high} is a value which is added to P_{ramp} to provide an upper limit pressure P_{limit_high} which the dispenser pressure $P_{station}$ shall not exceed (see Process Check Subroutine in Section A.1.1.13). The unit of measure for ΔP_{tol_high} is MPa.

(Eq. A.9)

$$Set\ \Delta P_{tol\_high} = 7$$

Equation A.10 defines T_{hot_soak} as a function of T_{amb}. The hot soak temperature is a function of the ambient temperature and is defined in Figure A5 and Table A4 of SAE J2601.

(Eq. A.10)

If T_{amb} ≤ 0 °C, Then T_{hot_soak} = 15 °C

Else If 35 °C ≤ T_{amb} < 40 °C, Then T_{hot_soak} = 40 °C

Else If T_{amb} ≥ 40 °C, Then T_{hot_soak} = T_{amb}

Else If 0 °C < T_{amb} ≤ 10 °C, Then T_{hot_soak} = 15 + T_{amb}

Else If 10 °C < T_{amb} ≤ 20 °C, Then T_{hot_soak} = 25 + 0.5 (T_{amb} – 10)*

Else T_{hot_soak} = 30 + 2 (T_{amb} – 20)/3*

A.1.1.2.2 Initialization of Parameters with Discretionary Settings

The settings for the parameters in this subsection shall be determined by the discretion of the dispenser manufacturer or testing lab within the acceptable range provided. Some of the discretionary settings have recommended values.

A parameter SOC_{target} is used to define the target SOC, where SOC_{target} = 100 represents a target density of 40.2 g/l for the H70 pressure class and 24.0 g/l for H35 pressure class. Communication fills should achieve a final SOC in the CHSS of ≥ 95% and ≤ 100%. Thus, SOC_{target} shall be set between 95 and 100, where the value 95 represents 95% SOC and the value 100 represents 100% SOC. The unit of measure for SOC_{target} is percent (%).

(Eq. A.11)

$$Set\ SOC_{target}$$

A.1.1.2.2.1 Initialization of SOC Taper Parameters

The following parameters are settings for the SOC Taper method which is used to reduce the PRR so that the target SOC can be achieved without the ramp pressure exceeding the maximum dispenser pressure (or a lower value). **The SOC Taper method is utilized for all fuelling concepts**.

The target ramp pressure P_{ramp_target} is the value of the ramp pressure that the SOC Taper method will target to achieve the SOC_{target} value. This value cannot be set higher than the MAWP of the dispenser (e.g., 87.5 MPa for an H70 dispenser). It can be set at the MAWP or at a value slightly lower to account for a needed tolerance to avoid exceeding the MAWP. The unit of measure of P_{ramp_target} is MPa.

(Eq. A.12)

$$Set\ P_{ramp\_target}$$

The lookback period $t_{lookback\_SOC}$ is a parameter use to compare the current SOC with the SOC a certain number of prior timesteps . The number of timesteps is determined by $t_{lookback\_SOC}$. For example, if $t_{lookback\_SOC}$ is set to 30, then the current SOC is compared to the SOC 30 timesteps (or 30 seconds) ago.

(Eq. A.13)

$Set\ t_{lookback\_SOC}$ (recommended value → 30)

The pressure difference between the ramp pressure and the CHSS pressure is used to dynamically calculate the threshold pressure $P_{threshold}$ used in the SOC Taper approach. At each time step, this pressure difference is calculated, and the maximum pressure drop is recorded as ΔP_{max}. To start this process, ΔP_{max} must be initialized to zero, which is done in Equation A.14.

(Eq. A.14)

$$\Delta P_{max} = 0$$

A.1.1.2.2.2 Initialization of Tgas Throttle Parameters

The following parameters are settings for the T_{gas} Throttle method which is used to reduce the pressure ramp rate so that the CHSS gas temperature does not exceed a maximum value. **The T_{gas} Throttle method is an independent fuelling concept and is not to be used with the Static, T_{gas} Initial and T_{gas} Initial+ fuelling concepts**. . It is activated by a flag variable set to True or False.

Equation A.15 sets the flag variable TGASTHROTTLE to TRUE, which indicates that the T_{gas} Throttle pressure ramp rate calculations shall be conducted in the Calculation of PRR and P_{ramp} Subroutine.

(Eq. A.15)

$$Set\ TGASTHROTTLE = TRUE\ or\ FALSE$$

Equation A.16 sets the flag variable SELFADJUST to TRUE or FALSE, which indicates whether the T_{gas} Throttle control should self-adjust the parameters (TRUE) or not (FALSE) based on the noise in the T_{gas_high} data.

(Eq. A.16)

$$Set\ SELFADJUST = TRUE\ or\ FALSE$$

Equations A.17, A.18 and A.19 set parameters for T_{gas} Throttle (these are the minimum number of parameters needed to operate T_{gas} Throttle when SELFADJUST = FALSE). **These parameters should have user adjustable values (for testing).**

The unit of measure for the target gas temperature (T_{gas_target}) is Kelvin.

(Eq. A.17)

$Set\ T_{gas\_target}$ (recommended value → 358.15)

(Eq. A.18)

$Set\ a$ (recommended values → IF $T_{gas\_initial} < T_{hot\_soak}$ AND $P_{initial} \geq 10$ THEN $a = 3$, ELSE $a = 4$)

(Eq. A.19)

$Set\ b$ (recommended value → 4)

Equations A.20 through A.24 are settings for additional parameters that are only used when SELFADJUST = TRUE. **These parameters should have user adjustable values (for testing).**

The unit of measure for the maximum gas temperature (T_{gas_max}) is Kelvin.

(Eq. A.20)

$Set\ T_{gas\_max}$ (recommended value → 358.15)

(Eq. A.21)

$Set\ T_{gas\_diff\_factor}$ (recommended value → 0.6)

(Eq. A.22)

$Set\ T_{gas\_offset\_multiplier}$ (recommended value → 5)

(Eq. A.23)

$Set\ T_{gas\_smooth\_threshold}$ (recommended value → T_{gas_max} – 7.5)

(Eq. A.24) T_{gas_smooth} Triple Moving Average Length (TMAL)

$Set\ TMAL$ (recommended value → 10)

Equation A.25 is the initialization of one of the self-adjusting parameters. This value should always be initialized to zero (i.e. it is not a user adjustable value).

(Eq. A.25)

$$T_{gas\_diff\_max} = 0$$

A.1.1.3 Subroutine – Selection of t_{final} Table for Static Fuelling Concept

This subroutine applies only to the Type-2-PR-S Static Fuelling concept.

t_{final} tables store a derived t_{final} value which is a function of the ambient temperature T_{amb} and the mass average fuel delivery temperature used for control, MAT_C. The t_{final} table contains discrete values of T_{amb} and MAT_C. The t_{final} value is stored in minutes to the tenth (one significant digit), i.e. xx.x.

There are two t_{final} tables to choose from. Table A.1 utilizes a P_{min} value of 1 MPa. Table A.2 utilizes a P_{min} value of 6 MPa.

Table A.1: t_{final} as a function of MAT_C: P_{min} = 1 MPa

MAT_C / T_{amb}	-40	-38	-36	-34	-32	-30	-28	-26	-24	-22	-20	-18	-16	-14	-12	-10
50	xx.x	xx.x	xx.x	xx.x	xx.x	xx.x	xx.x	xx.x	xx.x	xx.x	xx.x	xx.x	xx.x	xx.x	xx.x	xx.x
45	xx.x	xx.x	xx.x	xx.x	xx.x	xx.x	xx.x	xx.x	xx.x	xx.x	xx.x	xx.x	xx.x	xx.x	xx.x	xx.x
40	xx.x	xx.x	xx.x	xx.x	xx.x	xx.x	xx.x	xx.x	xx.x	xx.x	xx.x	xx.x	xx.x	xx.x	xx.x	xx.x
35	xx.x	xx.x	xx.x	xx.x	xx.x	xx.x	xx.x	xx.x	xx.x	xx.x	xx.x	xx.x	xx.x	xx.x	xx.x	xx.x
30	xx.x	xx.x	xx.x	xx.x	xx.x	xx.x	xx.x	xx.x	xx.x	xx.x	xx.x	xx.x	xx.x	xx.x	xx.x	xx.x
25	xx.x	xx.x	xx.x	xx.x	xx.x	xx.x	xx.x	xx.x	xx.x	xx.x	xx.x	xx.x	xx.x	xx.x	xx.x	xx.x
20	xx.x	xx.x	xx.x	xx.x	xx.x	xx.x	xx.x	xx.x	xx.x	xx.x	xx.x	xx.x	xx.x	xx.x	xx.x	xx.x
15	xx.x	xx.x	xx.x	xx.x	xx.x	xx.x	xx.x	xx.x	xx.x	xx.x	xx.x	xx.x	xx.x	xx.x	xx.x	xx.x
10	xx.x	xx.x	xx.x	xx.x	xx.x	xx.x	xx.x	xx.x	xx.x	xx.x	xx.x	xx.x	xx.x	xx.x	xx.x	xx.x
5	xx.x	xx.x	xx.x	xx.x	xx.x	xx.x	xx.x	xx.x	xx.x	xx.x	xx.x	xx.x	xx.x	xx.x	xx.x	xx.x
0	xx.x	xx.x	xx.x	xx.x	xx.x	xx.x	xx.x	xx.x	xx.x	xx.x	xx.x	xx.x	xx.x	xx.x	xx.x	xx.x
-10	xx.x	xx.x	xx.x	xx.x	xx.x	xx.x	xx.x	xx.x	xx.x	xx.x	xx.x	xx.x	xx.x	xx.x	xx.x	xx.x
-20	xx.x	xx.x	xx.x	xx.x	xx.x	xx.x	xx.x	xx.x	xx.x	xx.x	xx.x	xx.x	xx.x	xx.x	xx.x	xx.x
-30	xx.x	xx.x	xx.x	xx.x	xx.x	xx.x	xx.x	xx.x	xx.x	xx.x	xx.x	xx.x	xx.x	xx.x	xx.x	xx.x
-40	xx.x	xx.x	xx.x	xx.x	xx.x	xx.x	xx.x	xx.x	xx.x	xx.x	xx.x	xx.x	xx.x	xx.x	xx.x	xx.x

Table A.2: t_{final} as a function of MAT_C: P_{min} = 6 MPa

MAT_C / T_{amb}	-40	-38	-36	-34	-32	-30	-28	-26	-24	-22	-20	-18	-16	-14	-12	-10
50	xx.x	xx.x	xx.x	xx.x	xx.x	xx.x	xx.x	xx.x	xx.x	xx.x	xx.x	xx.x	xx.x	xx.x	xx.x	xx.x
45	xx.x	xx.x	xx.x	xx.x	xx.x	xx.x	xx.x	xx.x	xx.x	xx.x	xx.x	xx.x	xx.x	xx.x	xx.x	xx.x
40	xx.x	xx.x	xx.x	xx.x	xx.x	xx.x	xx.x	xx.x	xx.x	xx.x	xx.x	xx.x	xx.x	xx.x	xx.x	xx.x
35	xx.x	xx.x	xx.x	xx.x	xx.x	xx.x	xx.x	xx.x	xx.x	xx.x	xx.x	xx.x	xx.x	xx.x	xx.x	xx.x
30	xx.x	xx.x	xx.x	xx.x	xx.x	xx.x	xx.x	xx.x	xx.x	xx.x	xx.x	xx.x	xx.x	xx.x	xx.x	xx.x
25	xx.x	xx.x	xx.x	xx.x	xx.x	xx.x	xx.x	xx.x	xx.x	xx.x	xx.x	xx.x	xx.x	xx.x	xx.x	xx.x
20	xx.x	xx.x	xx.x	xx.x	xx.x	xx.x	xx.x	xx.x	xx.x	xx.x	xx.x	xx.x	xx.x	xx.x	xx.x	xx.x
15	xx.x	xx.x	xx.x	xx.x	xx.x	xx.x	xx.x	xx.x	xx.x	xx.x	xx.x	xx.x	xx.x	xx.x	xx.x	xx.x
10	xx.x	xx.x	xx.x	xx.x	xx.x	xx.x	xx.x	xx.x	xx.x	xx.x	xx.x	xx.x	xx.x	xx.x	xx.x	xx.x
5	xx.x	xx.x	xx.x	xx.x	xx.x	xx.x	xx.x	xx.x	xx.x	xx.x	xx.x	xx.x	xx.x	xx.x	xx.x	xx.x
0	xx.x	xx.x	xx.x	xx.x	xx.x	xx.x	xx.x	xx.x	xx.x	xx.x	xx.x	xx.x	xx.x	xx.x	xx.x	xx.x
-10	xx.x	xx.x	xx.x	xx.x	xx.x	xx.x	xx.x	xx.x	xx.x	xx.x	xx.x	xx.x	xx.x	xx.x	xx.x	xx.x
-20	xx.x	xx.x	xx.x	xx.x	xx.x	xx.x	xx.x	xx.x	xx.x	xx.x	xx.x	xx.x	xx.x	xx.x	xx.x	xx.x
-30	xx.x	xx.x	xx.x	xx.x	xx.x	xx.x	xx.x	xx.x	xx.x	xx.x	xx.x	xx.x	xx.x	xx.x	xx.x	xx.x
-40	xx.x	xx.x	xx.x	xx.x	xx.x	xx.x	xx.x	xx.x	xx.x	xx.x	xx.x	xx.x	xx.x	xx.x	xx.x	xx.x

(Eq. A.26)

If $P_{initial}$ < 6 MPa, select Table A.1 and store P_{min} = 1

Else select Table A.2 and store P_{min} = 6

Once P_{min} has been determined, the parameter β can be calculated. β is a parameter which is multiplied by t_{final} to allow for the pressure tolerance ΔP_{tol_high}. See Section H.2.6.2 of SAE J2601 for a detailed explanation of β. The unit of measure for β is dimensionless.

(Eq. A.27)

$$Set\ \beta = \frac{P_{final} - P_{min}}{P_{final} - P_{min} - \Delta P_{tol\_high}}$$

A.1.1.4 Subroutine – Selection of t_{final} Table for T_{gas} Initial Fuelling Concept

This subroutine applies only to the T_{gas} Initial Fuelling concept.

t_{final} tables store a derived t_{final} value which is a function of the ambient temperature T_{amb} and the mass average fuel delivery temperature used for control, MAT_C. The t_{final} table contains discrete values of T_{amb} and MAT_C. The t_{final} value is stored in minutes to the tenth (one significant digit), i.e. xx.x.

In this example implementation, there are five t_{final} tables to choose from:
Table A.3 utilizes a P_{min} value of 1 MPa. Table A.4 utilizes a P_{min} value of 6 MPa. Table A.5 utilizes a P_{min} value of 11 MPa. Table A.6 utilizes a P_{min} value of 16 MPa. Table A.7 utilizes a P_{min} value of 21 MPa.
(The P_{min} values here are examples, their choice is left to the OEM).

Table A.3: t_{final} as a function of MAT_C: P_{min} = 1 MPa

MAT_C / T_{amb}	-40	-38	-36	-34	-32	-30	-28	-26	-24	-22	-20	-18	-16	-14	-12	-10
50	xx.x	xx.x	xx.x	xx.x	xx.x	xx.x	xx.x	xx.x	xx.x	xx.x	xx.x	xx.x	xx.x	xx.x	xx.x	xx.x
45	xx.x	xx.x	xx.x	xx.x	xx.x	xx.x	xx.x	xx.x	xx.x	xx.x	xx.x	xx.x	xx.x	xx.x	xx.x	xx.x
40	xx.x	xx.x	xx.x	xx.x	xx.x	xx.x	xx.x	xx.x	xx.x	xx.x	xx.x	xx.x	xx.x	xx.x	xx.x	xx.x
35	xx.x	xx.x	xx.x	xx.x	xx.x	xx.x	xx.x	xx.x	xx.x	xx.x	xx.x	xx.x	xx.x	xx.x	xx.x	xx.x
30	xx.x	xx.x	xx.x	xx.x	xx.x	xx.x	xx.x	xx.x	xx.x	xx.x	xx.x	xx.x	xx.x	xx.x	xx.x	xx.x
25	xx.x	xx.x	xx.x	xx.x	xx.x	xx.x	xx.x	xx.x	xx.x	xx.x	xx.x	xx.x	xx.x	xx.x	xx.x	xx.x
20	xx.x	xx.x	xx.x	xx.x	xx.x	xx.x	xx.x	xx.x	xx.x	xx.x	xx.x	xx.x	xx.x	xx.x	xx.x	xx.x
15	xx.x	xx.x	xx.x	xx.x	xx.x	xx.x	xx.x	xx.x	xx.x	xx.x	xx.x	xx.x	xx.x	xx.x	xx.x	xx.x
10	xx.x	xx.x	xx.x	xx.x	xx.x	xx.x	xx.x	xx.x	xx.x	xx.x	xx.x	xx.x	xx.x	xx.x	xx.x	xx.x
5	xx.x	xx.x	xx.x	xx.x	xx.x	xx.x	xx.x	xx.x	xx.x	xx.x	xx.x	xx.x	xx.x	xx.x	xx.x	xx.x
0	xx.x	xx.x	xx.x	xx.x	xx.x	xx.x	xx.x	xx.x	xx.x	xx.x	xx.x	xx.x	xx.x	xx.x	xx.x	xx.x
-10	xx.x	xx.x	xx.x	xx.x	xx.x	xx.x	xx.x	xx.x	xx.x	xx.x	xx.x	xx.x	xx.x	xx.x	xx.x	xx.x
-20	xx.x	xx.x	xx.x	xx.x	xx.x	xx.x	xx.x	xx.x	xx.x	xx.x	xx.x	xx.x	xx.x	xx.x	xx.x	xx.x
-30	xx.x	xx.x	xx.x	xx.x	xx.x	xx.x	xx.x	xx.x	xx.x	xx.x	xx.x	xx.x	xx.x	xx.x	xx.x	xx.x
-40	xx.x	xx.x	xx.x	xx.x	xx.x	xx.x	xx.x	xx.x	xx.x	xx.x	xx.x	xx.x	xx.x	xx.x	xx.x	xx.x

Table A.4: t_{final} **as a function of** MAT_C**:** P_{min} **= 6 MPa**

MAT_C / T_{amb}	-40	-38	-36	-34	-32	-30	-28	-26	-24	-22	-20	-18	-16	-14	-12	-10
50	xx.x	xx.x	xx.x	xx.x	xx.x	xx.x	xx.x	xx.x	xx.x	xx.x	xx.x	xx.x	xx.x	xx.x	xx.x	xx.x
45	xx.x	xx.x	xx.x	xx.x	xx.x	xx.x	xx.x	xx.x	xx.x	xx.x	xx.x	xx.x	xx.x	xx.x	xx.x	xx.x
40	xx.x	xx.x	xx.x	xx.x	xx.x	xx.x	xx.x	xx.x	xx.x	xx.x	xx.x	xx.x	xx.x	xx.x	xx.x	xx.x
35	xx.x	xx.x	xx.x	xx.x	xx.x	xx.x	xx.x	xx.x	xx.x	xx.x	xx.x	xx.x	xx.x	xx.x	xx.x	xx.x
30	xx.x	xx.x	xx.x	xx.x	xx.x	xx.x	xx.x	xx.x	xx.x	xx.x	xx.x	xx.x	xx.x	xx.x	xx.x	xx.x
25	xx.x	xx.x	xx.x	xx.x	xx.x	xx.x	xx.x	xx.x	xx.x	xx.x	xx.x	xx.x	xx.x	xx.x	xx.x	xx.x
20	xx.x	xx.x	xx.x	xx.x	xx.x	xx.x	xx.x	xx.x	xx.x	xx.x	xx.x	xx.x	xx.x	xx.x	xx.x	xx.x
15	xx.x	xx.x	xx.x	xx.x	xx.x	xx.x	xx.x	xx.x	xx.x	xx.x	xx.x	xx.x	xx.x	xx.x	xx.x	xx.x
10	xx.x	xx.x	xx.x	xx.x	xx.x	xx.x	xx.x	xx.x	xx.x	xx.x	xx.x	xx.x	xx.x	xx.x	xx.x	xx.x
5	xx.x	xx.x	xx.x	xx.x	xx.x	xx.x	xx.x	xx.x	xx.x	xx.x	xx.x	xx.x	xx.x	xx.x	xx.x	xx.x
0	xx.x	xx.x	xx.x	xx.x	xx.x	xx.x	xx.x	xx.x	xx.x	xx.x	xx.x	xx.x	xx.x	xx.x	xx.x	xx.x
-10	xx.x	xx.x	xx.x	xx.x	xx.x	xx.x	xx.x	xx.x	xx.x	xx.x	xx.x	xx.x	xx.x	xx.x	xx.x	xx.x
-20	xx.x	xx.x	xx.x	xx.x	xx.x	xx.x	xx.x	xx.x	xx.x	xx.x	xx.x	xx.x	xx.x	xx.x	xx.x	xx.x
-30	xx.x	xx.x	xx.x	xx.x	xx.x	xx.x	xx.x	xx.x	xx.x	xx.x	xx.x	xx.x	xx.x	xx.x	xx.x	xx.x
-40	xx.x	xx.x	xx.x	xx.x	xx.x	xx.x	xx.x	xx.x	xx.x	xx.x	xx.x	xx.x	xx.x	xx.x	xx.x	xx.x

Table A.5: t_{final} **as a function of** MAT_C**:** P_{min} **= 11 MPa**

MAT_C / T_{amb}	-40	-38	-36	-34	-32	-30	-28	-26	-24	-22	-20	-18	-16	-14	-12	-10
50	xx.x	xx.x	xx.x	xx.x	xx.x	xx.x	xx.x	xx.x	xx.x	xx.x	xx.x	xx.x	xx.x	xx.x	xx.x	xx.x
45	xx.x	xx.x	xx.x	xx.x	xx.x	xx.x	xx.x	xx.x	xx.x	xx.x	xx.x	xx.x	xx.x	xx.x	xx.x	xx.x
40	xx.x	xx.x	xx.x	xx.x	xx.x	xx.x	xx.x	xx.x	xx.x	xx.x	xx.x	xx.x	xx.x	xx.x	xx.x	xx.x
35	xx.x	xx.x	xx.x	xx.x	xx.x	xx.x	xx.x	xx.x	xx.x	xx.x	xx.x	xx.x	xx.x	xx.x	xx.x	xx.x
30	xx.x	xx.x	xx.x	xx.x	xx.x	xx.x	xx.x	xx.x	xx.x	xx.x	xx.x	xx.x	xx.x	xx.x	xx.x	xx.x
25	xx.x	xx.x	xx.x	xx.x	xx.x	xx.x	xx.x	xx.x	xx.x	xx.x	xx.x	xx.x	xx.x	xx.x	xx.x	xx.x
20	xx.x	xx.x	xx.x	xx.x	xx.x	xx.x	xx.x	xx.x	xx.x	xx.x	xx.x	xx.x	xx.x	xx.x	xx.x	xx.x
15	xx.x	xx.x	xx.x	xx.x	xx.x	xx.x	xx.x	xx.x	xx.x	xx.x	xx.x	xx.x	xx.x	xx.x	xx.x	xx.x
10	xx.x	xx.x	xx.x	xx.x	xx.x	xx.x	xx.x	xx.x	xx.x	xx.x	xx.x	xx.x	xx.x	xx.x	xx.x	xx.x
5	xx.x	xx.x	xx.x	xx.x	xx.x	xx.x	xx.x	xx.x	xx.x	xx.x	xx.x	xx.x	xx.x	xx.x	xx.x	xx.x
0	xx.x	xx.x	xx.x	xx.x	xx.x	xx.x	xx.x	xx.x	xx.x	xx.x	xx.x	xx.x	xx.x	xx.x	xx.x	xx.x
-10	xx.x	xx.x	xx.x	xx.x	xx.x	xx.x	xx.x	xx.x	xx.x	xx.x	xx.x	xx.x	xx.x	xx.x	xx.x	xx.x
-20	xx.x	xx.x	xx.x	xx.x	xx.x	xx.x	xx.x	xx.x	xx.x	xx.x	xx.x	xx.x	xx.x	xx.x	xx.x	xx.x
-30	xx.x	xx.x	xx.x	xx.x	xx.x	xx.x	xx.x	xx.x	xx.x	xx.x	xx.x	xx.x	xx.x	xx.x	xx.x	xx.x
-40	xx.x	xx.x	xx.x	xx.x	xx.x	xx.x	xx.x	xx.x	xx.x	xx.x	xx.x	xx.x	xx.x	xx.x	xx.x	xx.x

Table A.6: t_{final} **as a function of** MAT_C**:** P_{min} **= 16 MPa**

MAT_C / T_{amb}	-40	-38	-36	-34	-32	-30	-28	-26	-24	-22	-20	-18	-16	-14	-12	-10
50	xx.x	xx.x	xx.x	xx.x	xx.x	xx.x	xx.x	xx.x	xx.x	xx.x	xx.x	xx.x	xx.x	xx.x	xx.x	xx.x
45	xx.x	xx.x	xx.x	xx.x	xx.x	xx.x	xx.x	xx.x	xx.x	xx.x	xx.x	xx.x	xx.x	xx.x	xx.x	xx.x
40	xx.x	xx.x	xx.x	xx.x	xx.x	xx.x	xx.x	xx.x	xx.x	xx.x	xx.x	xx.x	xx.x	xx.x	xx.x	xx.x
35	xx.x	xx.x	xx.x	xx.x	xx.x	xx.x	xx.x	xx.x	xx.x	xx.x	xx.x	xx.x	xx.x	xx.x	xx.x	xx.x
30	xx.x	xx.x	xx.x	xx.x	xx.x	xx.x	xx.x	xx.x	xx.x	xx.x	xx.x	xx.x	xx.x	xx.x	xx.x	xx.x
25	xx.x	xx.x	xx.x	xx.x	xx.x	xx.x	xx.x	xx.x	xx.x	xx.x	xx.x	xx.x	xx.x	xx.x	xx.x	xx.x
20	xx.x	xx.x	xx.x	xx.x	xx.x	xx.x	xx.x	xx.x	xx.x	xx.x	xx.x	xx.x	xx.x	xx.x	xx.x	xx.x
15	xx.x	xx.x	xx.x	xx.x	xx.x	xx.x	xx.x	xx.x	xx.x	xx.x	xx.x	xx.x	xx.x	xx.x	xx.x	xx.x
10	xx.x	xx.x	xx.x	xx.x	xx.x	xx.x	xx.x	xx.x	xx.x	xx.x	xx.x	xx.x	xx.x	xx.x	xx.x	xx.x
5	xx.x	xx.x	xx.x	xx.x	xx.x	xx.x	xx.x	xx.x	xx.x	xx.x	xx.x	xx.x	xx.x	xx.x	xx.x	xx.x
0	xx.x	xx.x	xx.x	xx.x	xx.x	xx.x	xx.x	xx.x	xx.x	xx.x	xx.x	xx.x	xx.x	xx.x	xx.x	xx.x
-10	xx.x	xx.x	xx.x	xx.x	xx.x	xx.x	xx.x	xx.x	xx.x	xx.x	xx.x	xx.x	xx.x	xx.x	xx.x	xx.x
-20	xx.x	xx.x	xx.x	xx.x	xx.x	xx.x	xx.x	xx.x	xx.x	xx.x	xx.x	xx.x	xx.x	xx.x	xx.x	xx.x
-30	xx.x	xx.x	xx.x	xx.x	xx.x	xx.x	xx.x	xx.x	xx.x	xx.x	xx.x	xx.x	xx.x	xx.x	xx.x	xx.x
-40	xx.x	xx.x	xx.x	xx.x	xx.x	xx.x	xx.x	xx.x	xx.x	xx.x	xx.x	xx.x	xx.x	xx.x	xx.x	xx.x

Table A.7: t_{final} **as a function of** MAT_C**:** P_{min} **= 21 MPa**

MAT_C / T_{amb}	-40	-38	-36	-34	-32	-30	-28	-26	-24	-22	-20	-18	-16	-14	-12	-10
50	xx.x	xx.x	xx.x	xx.x	xx.x	xx.x	xx.x	xx.x	xx.x	xx.x	xx.x	xx.x	xx.x	xx.x	xx.x	xx.x
45	xx.x	xx.x	xx.x	xx.x	xx.x	xx.x	xx.x	xx.x	xx.x	xx.x	xx.x	xx.x	xx.x	xx.x	xx.x	xx.x
40	xx.x	xx.x	xx.x	xx.x	xx.x	xx.x	xx.x	xx.x	xx.x	xx.x	xx.x	xx.x	xx.x	xx.x	xx.x	xx.x
35	xx.x	xx.x	xx.x	xx.x	xx.x	xx.x	xx.x	xx.x	xx.x	xx.x	xx.x	xx.x	xx.x	xx.x	xx.x	xx.x
30	xx.x	xx.x	xx.x	xx.x	xx.x	xx.x	xx.x	xx.x	xx.x	xx.x	xx.x	xx.x	xx.x	xx.x	xx.x	xx.x
25	xx.x	xx.x	xx.x	xx.x	xx.x	xx.x	xx.x	xx.x	xx.x	xx.x	xx.x	xx.x	xx.x	xx.x	xx.x	xx.x
20	xx.x	xx.x	xx.x	xx.x	xx.x	xx.x	xx.x	xx.x	xx.x	xx.x	xx.x	xx.x	xx.x	xx.x	xx.x	xx.x
15	xx.x	xx.x	xx.x	xx.x	xx.x	xx.x	xx.x	xx.x	xx.x	xx.x	xx.x	xx.x	xx.x	xx.x	xx.x	xx.x
10	xx.x	xx.x	xx.x	xx.x	xx.x	xx.x	xx.x	xx.x	xx.x	xx.x	xx.x	xx.x	xx.x	xx.x	xx.x	xx.x
5	xx.x	xx.x	xx.x	xx.x	xx.x	xx.x	xx.x	xx.x	xx.x	xx.x	xx.x	xx.x	xx.x	xx.x	xx.x	xx.x
0	xx.x	xx.x	xx.x	xx.x	xx.x	xx.x	xx.x	xx.x	xx.x	xx.x	xx.x	xx.x	xx.x	xx.x	xx.x	xx.x
-10	xx.x	xx.x	xx.x	xx.x	xx.x	xx.x	xx.x	xx.x	xx.x	xx.x	xx.x	xx.x	xx.x	xx.x	xx.x	xx.x
-20	xx.x	xx.x	xx.x	xx.x	xx.x	xx.x	xx.x	xx.x	xx.x	xx.x	xx.x	xx.x	xx.x	xx.x	xx.x	xx.x
-30	xx.x	xx.x	xx.x	xx.x	xx.x	xx.x	xx.x	xx.x	xx.x	xx.x	xx.x	xx.x	xx.x	xx.x	xx.x	xx.x
-40	xx.x	xx.x	xx.x	xx.x	xx.x	xx.x	xx.x	xx.x	xx.x	xx.x	xx.x	xx.x	xx.x	xx.x	xx.x	xx.x

(Eq. A.28)

If $T_{gas\_high} > T_{hot\_soak}$, select Table A.3 and store $P_{min} = 1$

Else

If $P_{initial} < 6$ MPa, select Table A.3 and store $P_{min} = 1$

If $6 \leq P_{initial} < 11$ MPa, select Table A.4 and store $P_{min} = 6$

If $11 \leq P_{initial} < 16$ MPa, select Table A.5 and store $P_{min} = 11$

If $16 \leq P_{initial} < 21$ MPa, select Table A.6 and store $P_{min} = 16$

If $P_{initial} \geq 21$ MPa, select Table A.7 and store $P_{min} = 21$

End If

Once P_{min} has been determined, the parameter β can be calculated. β is a parameter which is multiplied by t_{final} to allow for the pressure tolerance ΔP_{tol_high}. See Section H.2.6.2 of SAE J2601 for a detailed explanation of β. The unit of measure for β is dimensionless.

(Eq. A.29)

$$Set\ \beta = \frac{P_{final} - P_{min}}{P_{final} - P_{min} - \Delta P_{tol\_high}}$$

A.1.1.5 Subroutine – Selection of t_{final} Table for T_{gas} Initial+ Fuelling Concept

This subroutine applies only to the T_{gas} Initial+ Fuelling concept.

t_{final} tables store a derived t_{final} value which is a function of the ambient temperature T_{amb} and the mass average fuel delivery temperature used for control, MAT_C. The t_{final} table contains discrete values of T_{amb} and MAT_C. The t_{final} value is stored in minutes to the tenth (one significant digit), i.e. xx.x.

In this example implementation, there are fifteen t_{final} tables to choose from. The t_{final} tables are labelled below ((The P_{min} and T_{soak} values here are examples, their choice is left to the OEM).

Table A.8: **t_{final} as a function of MAT_C: P_{min} = 1 MPa, CHSS soak temp = T_{hot_soak}**

MAT_C / T_{amb}	-40	-38	-36	-34	-32	-30	-28	-26	-24	-22	-20	-18	-16	-14	-12	-10
50	xx.x	xx.x	xx.x	xx.x	xx.x	xx.x	xx.x	xx.x	xx.x	xx.x	xx.x	xx.x	xx.x	xx.x	xx.x	xx.x
45	xx.x	xx.x	xx.x	xx.x	xx.x	xx.x	xx.x	xx.x	xx.x	xx.x	xx.x	xx.x	xx.x	xx.x	xx.x	xx.x
40	xx.x	xx.x	xx.x	xx.x	xx.x	xx.x	xx.x	xx.x	xx.x	xx.x	xx.x	xx.x	xx.x	xx.x	xx.x	xx.x
35	xx.x	xx.x	xx.x	xx.x	xx.x	xx.x	xx.x	xx.x	xx.x	xx.x	xx.x	xx.x	xx.x	xx.x	xx.x	xx.x
30	xx.x	xx.x	xx.x	xx.x	xx.x	xx.x	xx.x	xx.x	xx.x	xx.x	xx.x	xx.x	xx.x	xx.x	xx.x	xx.x
25	xx.x	xx.x	xx.x	xx.x	xx.x	xx.x	xx.x	xx.x	xx.x	xx.x	xx.x	xx.x	xx.x	xx.x	xx.x	xx.x
20	xx.x	xx.x	xx.x	xx.x	xx.x	xx.x	xx.x	xx.x	xx.x	xx.x	xx.x	xx.x	xx.x	xx.x	xx.x	xx.x
15	xx.x	xx.x	xx.x	xx.x	xx.x	xx.x	xx.x	xx.x	xx.x	xx.x	xx.x	xx.x	xx.x	xx.x	xx.x	xx.x
10	xx.x	xx.x	xx.x	xx.x	xx.x	xx.x	xx.x	xx.x	xx.x	xx.x	xx.x	xx.x	xx.x	xx.x	xx.x	xx.x
5	xx.x	xx.x	xx.x	xx.x	xx.x	xx.x	xx.x	xx.x	xx.x	xx.x	xx.x	xx.x	xx.x	xx.x	xx.x	xx.x
0	xx.x	xx.x	xx.x	xx.x	xx.x	xx.x	xx.x	xx.x	xx.x	xx.x	xx.x	xx.x	xx.x	xx.x	xx.x	xx.x
-10	xx.x	xx.x	xx.x	xx.x	xx.x	xx.x	xx.x	xx.x	xx.x	xx.x	xx.x	xx.x	xx.x	xx.x	xx.x	xx.x
-20	xx.x	xx.x	xx.x	xx.x	xx.x	xx.x	xx.x	xx.x	xx.x	xx.x	xx.x	xx.x	xx.x	xx.x	xx.x	xx.x
-30	xx.x	xx.x	xx.x	xx.x	xx.x	xx.x	xx.x	xx.x	xx.x	xx.x	xx.x	xx.x	xx.x	xx.x	xx.x	xx.x
-40	xx.x	xx.x	xx.x	xx.x	xx.x	xx.x	xx.x	xx.x	xx.x	xx.x	xx.x	xx.x	xx.x	xx.x	xx.x	xx.x

Table A.9: **t_{final} as a function of MAT_C: P_{min} = 6 MPa, CHSS soak temp = T_{hot_soak}**

MAT_C / T_{amb}	-40	-38	-36	-34	-32	-30	-28	-26	-24	-22	-20	-18	-16	-14	-12	-10
50	xx.x	xx.x	xx.x	xx.x	xx.x	xx.x	xx.x	xx.x	xx.x	xx.x	xx.x	xx.x	xx.x	xx.x	xx.x	xx.x
45	xx.x	xx.x	xx.x	xx.x	xx.x	xx.x	xx.x	xx.x	xx.x	xx.x	xx.x	xx.x	xx.x	xx.x	xx.x	xx.x
40	xx.x	xx.x	xx.x	xx.x	xx.x	xx.x	xx.x	xx.x	xx.x	xx.x	xx.x	xx.x	xx.x	xx.x	xx.x	xx.x
35	xx.x	xx.x	xx.x	xx.x	xx.x	xx.x	xx.x	xx.x	xx.x	xx.x	xx.x	xx.x	xx.x	xx.x	xx.x	xx.x
30	xx.x	xx.x	xx.x	xx.x	xx.x	xx.x	xx.x	xx.x	xx.x	xx.x	xx.x	xx.x	xx.x	xx.x	xx.x	xx.x
25	xx.x	xx.x	xx.x	xx.x	xx.x	xx.x	xx.x	xx.x	xx.x	xx.x	xx.x	xx.x	xx.x	xx.x	xx.x	xx.x
20	xx.x	xx.x	xx.x	xx.x	xx.x	xx.x	xx.x	xx.x	xx.x	xx.x	xx.x	xx.x	xx.x	xx.x	xx.x	xx.x
15	xx.x	xx.x	xx.x	xx.x	xx.x	xx.x	xx.x	xx.x	xx.x	xx.x	xx.x	xx.x	xx.x	xx.x	xx.x	xx.x
10	xx.x	xx.x	xx.x	xx.x	xx.x	xx.x	xx.x	xx.x	xx.x	xx.x	xx.x	xx.x	xx.x	xx.x	xx.x	xx.x
5	xx.x	xx.x	xx.x	xx.x	xx.x	xx.x	xx.x	xx.x	xx.x	xx.x	xx.x	xx.x	xx.x	xx.x	xx.x	xx.x
0	xx.x	xx.x	xx.x	xx.x	xx.x	xx.x	xx.x	xx.x	xx.x	xx.x	xx.x	xx.x	xx.x	xx.x	xx.x	xx.x
-10	xx.x	xx.x	xx.x	xx.x	xx.x	xx.x	xx.x	xx.x	xx.x	xx.x	xx.x	xx.x	xx.x	xx.x	xx.x	xx.x
-20	xx.x	xx.x	xx.x	xx.x	xx.x	xx.x	xx.x	xx.x	xx.x	xx.x	xx.x	xx.x	xx.x	xx.x	xx.x	xx.x
-30	xx.x	xx.x	xx.x	xx.x	xx.x	xx.x	xx.x	xx.x	xx.x	xx.x	xx.x	xx.x	xx.x	xx.x	xx.x	xx.x
-40	xx.x	xx.x	xx.x	xx.x	xx.x	xx.x	xx.x	xx.x	xx.x	xx.x	xx.x	xx.x	xx.x	xx.x	xx.x	xx.x

Table A.10: t_{final} **as a function of** MAT_C**:** P_{min} **= 11 MPa, CHSS soak temp =** T_{hot_soak}

MAT_C / T_{amb}	-40	-38	-36	-34	-32	-30	-28	-26	-24	-22	-20	-18	-16	-14	-12	-10
50	xx.x	xx.x	xx.x	xx.x	xx.x	xx.x	xx.x	xx.x	xx.x	xx.x	xx.x	xx.x	xx.x	xx.x	xx.x	xx.x
45	xx.x	xx.x	xx.x	xx.x	xx.x	xx.x	xx.x	xx.x	xx.x	xx.x	xx.x	xx.x	xx.x	xx.x	xx.x	xx.x
40	xx.x	xx.x	xx.x	xx.x	xx.x	xx.x	xx.x	xx.x	xx.x	xx.x	xx.x	xx.x	xx.x	xx.x	xx.x	xx.x
35	xx.x	xx.x	xx.x	xx.x	xx.x	xx.x	xx.x	xx.x	xx.x	xx.x	xx.x	xx.x	xx.x	xx.x	xx.x	xx.x
30	xx.x	xx.x	xx.x	xx.x	xx.x	xx.x	xx.x	xx.x	xx.x	xx.x	xx.x	xx.x	xx.x	xx.x	xx.x	xx.x
25	xx.x	xx.x	xx.x	xx.x	xx.x	xx.x	xx.x	xx.x	xx.x	xx.x	xx.x	xx.x	xx.x	xx.x	xx.x	xx.x
20	xx.x	xx.x	xx.x	xx.x	xx.x	xx.x	xx.x	xx.x	xx.x	xx.x	xx.x	xx.x	xx.x	xx.x	xx.x	xx.x
15	xx.x	xx.x	xx.x	xx.x	xx.x	xx.x	xx.x	xx.x	xx.x	xx.x	xx.x	xx.x	xx.x	xx.x	xx.x	xx.x
10	xx.x	xx.x	xx.x	xx.x	xx.x	xx.x	xx.x	xx.x	xx.x	xx.x	xx.x	xx.x	xx.x	xx.x	xx.x	xx.x
5	xx.x	xx.x	xx.x	xx.x	xx.x	xx.x	xx.x	xx.x	xx.x	xx.x	xx.x	xx.x	xx.x	xx.x	xx.x	xx.x
0	xx.x	xx.x	xx.x	xx.x	xx.x	xx.x	xx.x	xx.x	xx.x	xx.x	xx.x	xx.x	xx.x	xx.x	xx.x	xx.x
-10	xx.x	xx.x	xx.x	xx.x	xx.x	xx.x	xx.x	xx.x	xx.x	xx.x	xx.x	xx.x	xx.x	xx.x	xx.x	xx.x
-20	xx.x	xx.x	xx.x	xx.x	xx.x	xx.x	xx.x	xx.x	xx.x	xx.x	xx.x	xx.x	xx.x	xx.x	xx.x	xx.x
-30	xx.x	xx.x	xx.x	xx.x	xx.x	xx.x	xx.x	xx.x	xx.x	xx.x	xx.x	xx.x	xx.x	xx.x	xx.x	xx.x
-40	xx.x	xx.x	xx.x	xx.x	xx.x	xx.x	xx.x	xx.x	xx.x	xx.x	xx.x	xx.x	xx.x	xx.x	xx.x	xx.x

Table A.11: t_{final} **as a function of** MAT_C**:** P_{min} **= 16 MPa, CHSS soak temp =** T_{hot_soak}

MAT_C / T_{amb}	-40	-38	-36	-34	-32	-30	-28	-26	-24	-22	-20	-18	-16	-14	-12	-10
50	xx.x	xx.x	xx.x	xx.x	xx.x	xx.x	xx.x	xx.x	xx.x	xx.x	xx.x	xx.x	xx.x	xx.x	xx.x	xx.x
45	xx.x	xx.x	xx.x	xx.x	xx.x	xx.x	xx.x	xx.x	xx.x	xx.x	xx.x	xx.x	xx.x	xx.x	xx.x	xx.x
40	xx.x	xx.x	xx.x	xx.x	xx.x	xx.x	xx.x	xx.x	xx.x	xx.x	xx.x	xx.x	xx.x	xx.x	xx.x	xx.x
35	xx.x	xx.x	xx.x	xx.x	xx.x	xx.x	xx.x	xx.x	xx.x	xx.x	xx.x	xx.x	xx.x	xx.x	xx.x	xx.x
30	xx.x	xx.x	xx.x	xx.x	xx.x	xx.x	xx.x	xx.x	xx.x	xx.x	xx.x	xx.x	xx.x	xx.x	xx.x	xx.x
25	xx.x	xx.x	xx.x	xx.x	xx.x	xx.x	xx.x	xx.x	xx.x	xx.x	xx.x	xx.x	xx.x	xx.x	xx.x	xx.x
20	xx.x	xx.x	xx.x	xx.x	xx.x	xx.x	xx.x	xx.x	xx.x	xx.x	xx.x	xx.x	xx.x	xx.x	xx.x	xx.x
15	xx.x	xx.x	xx.x	xx.x	xx.x	xx.x	xx.x	xx.x	xx.x	xx.x	xx.x	xx.x	xx.x	xx.x	xx.x	xx.x
10	xx.x	xx.x	xx.x	xx.x	xx.x	xx.x	xx.x	xx.x	xx.x	xx.x	xx.x	xx.x	xx.x	xx.x	xx.x	xx.x
5	xx.x	xx.x	xx.x	xx.x	xx.x	xx.x	xx.x	xx.x	xx.x	xx.x	xx.x	xx.x	xx.x	xx.x	xx.x	xx.x
0	xx.x	xx.x	xx.x	xx.x	xx.x	xx.x	xx.x	xx.x	xx.x	xx.x	xx.x	xx.x	xx.x	xx.x	xx.x	xx.x
-10	xx.x	xx.x	xx.x	xx.x	xx.x	xx.x	xx.x	xx.x	xx.x	xx.x	xx.x	xx.x	xx.x	xx.x	xx.x	xx.x
-20	xx.x	xx.x	xx.x	xx.x	xx.x	xx.x	xx.x	xx.x	xx.x	xx.x	xx.x	xx.x	xx.x	xx.x	xx.x	xx.x
-30	xx.x	xx.x	xx.x	xx.x	xx.x	xx.x	xx.x	xx.x	xx.x	xx.x	xx.x	xx.x	xx.x	xx.x	xx.x	xx.x
-40	xx.x	xx.x	xx.x	xx.x	xx.x	xx.x	xx.x	xx.x	xx.x	xx.x	xx.x	xx.x	xx.x	xx.x	xx.x	xx.x

Table A.12: t_{final} **as a function of** MAT_C**:** P_{min} **= 21 MPa, CHSS soak temp =** T_{hot_soak}

MAT_C / T_{amb}	-40	-38	-36	-34	-32	-30	-28	-26	-24	-22	-20	-18	-16	-14	-12	-10
50	xx.x	xx.x	xx.x	xx.x	xx.x	xx.x	xx.x	xx.x	xx.x	xx.x	xx.x	xx.x	xx.x	xx.x	xx.x	xx.x
45	xx.x	xx.x	xx.x	xx.x	xx.x	xx.x	xx.x	xx.x	xx.x	xx.x	xx.x	xx.x	xx.x	xx.x	xx.x	xx.x
40	xx.x	xx.x	xx.x	xx.x	xx.x	xx.x	xx.x	xx.x	xx.x	xx.x	xx.x	xx.x	xx.x	xx.x	xx.x	xx.x
35	xx.x	xx.x	xx.x	xx.x	xx.x	xx.x	xx.x	xx.x	xx.x	xx.x	xx.x	xx.x	xx.x	xx.x	xx.x	xx.x
30	xx.x	xx.x	xx.x	xx.x	xx.x	xx.x	xx.x	xx.x	xx.x	xx.x	xx.x	xx.x	xx.x	xx.x	xx.x	xx.x
25	xx.x	xx.x	xx.x	xx.x	xx.x	xx.x	xx.x	xx.x	xx.x	xx.x	xx.x	xx.x	xx.x	xx.x	xx.x	xx.x
20	xx.x	xx.x	xx.x	xx.x	xx.x	xx.x	xx.x	xx.x	xx.x	xx.x	xx.x	xx.x	xx.x	xx.x	xx.x	xx.x
15	xx.x	xx.x	xx.x	xx.x	xx.x	xx.x	xx.x	xx.x	xx.x	xx.x	xx.x	xx.x	xx.x	xx.x	xx.x	xx.x
10	xx.x	xx.x	xx.x	xx.x	xx.x	xx.x	xx.x	xx.x	xx.x	xx.x	xx.x	xx.x	xx.x	xx.x	xx.x	xx.x
5	xx.x	xx.x	xx.x	xx.x	xx.x	xx.x	xx.x	xx.x	xx.x	xx.x	xx.x	xx.x	xx.x	xx.x	xx.x	xx.x
0	xx.x	xx.x	xx.x	xx.x	xx.x	xx.x	xx.x	xx.x	xx.x	xx.x	xx.x	xx.x	xx.x	xx.x	xx.x	xx.x
-10	xx.x	xx.x	xx.x	xx.x	xx.x	xx.x	xx.x	xx.x	xx.x	xx.x	xx.x	xx.x	xx.x	xx.x	xx.x	xx.x
-20	xx.x	xx.x	xx.x	xx.x	xx.x	xx.x	xx.x	xx.x	xx.x	xx.x	xx.x	xx.x	xx.x	xx.x	xx.x	xx.x
-30	xx.x	xx.x	xx.x	xx.x	xx.x	xx.x	xx.x	xx.x	xx.x	xx.x	xx.x	xx.x	xx.x	xx.x	xx.x	xx.x
-40	xx.x	xx.x	xx.x	xx.x	xx.x	xx.x	xx.x	xx.x	xx.x	xx.x	xx.x	xx.x	xx.x	xx.x	xx.x	xx.x

Table A.13: t_{final} **as a function of** MAT_C**:** P_{min} **= 1 MPa, CHSS soak temp = (**T_{hot_soak} **– 5 °C)**

MAT_C / T_{amb}	-40	-38	-36	-34	-32	-30	-28	-26	-24	-22	-20	-18	-16	-14	-12	-10
50	xx.x	xx.x	xx.x	xx.x	xx.x	xx.x	xx.x	xx.x	xx.x	xx.x	xx.x	xx.x	xx.x	xx.x	xx.x	xx.x
45	xx.x	xx.x	xx.x	xx.x	xx.x	xx.x	xx.x	xx.x	xx.x	xx.x	xx.x	xx.x	xx.x	xx.x	xx.x	xx.x
40	xx.x	xx.x	xx.x	xx.x	xx.x	xx.x	xx.x	xx.x	xx.x	xx.x	xx.x	xx.x	xx.x	xx.x	xx.x	xx.x
35	xx.x	xx.x	xx.x	xx.x	xx.x	xx.x	xx.x	xx.x	xx.x	xx.x	xx.x	xx.x	xx.x	xx.x	xx.x	xx.x
30	xx.x	xx.x	xx.x	xx.x	xx.x	xx.x	xx.x	xx.x	xx.x	xx.x	xx.x	xx.x	xx.x	xx.x	xx.x	xx.x
25	xx.x	xx.x	xx.x	xx.x	xx.x	xx.x	xx.x	xx.x	xx.x	xx.x	xx.x	xx.x	xx.x	xx.x	xx.x	xx.x
20	xx.x	xx.x	xx.x	xx.x	xx.x	xx.x	xx.x	xx.x	xx.x	xx.x	xx.x	xx.x	xx.x	xx.x	xx.x	xx.x
15	xx.x	xx.x	xx.x	xx.x	xx.x	xx.x	xx.x	xx.x	xx.x	xx.x	xx.x	xx.x	xx.x	xx.x	xx.x	xx.x
10	xx.x	xx.x	xx.x	xx.x	xx.x	xx.x	xx.x	xx.x	xx.x	xx.x	xx.x	xx.x	xx.x	xx.x	xx.x	xx.x
5	xx.x	xx.x	xx.x	xx.x	xx.x	xx.x	xx.x	xx.x	xx.x	xx.x	xx.x	xx.x	xx.x	xx.x	xx.x	xx.x
0	xx.x	xx.x	xx.x	xx.x	xx.x	xx.x	xx.x	xx.x	xx.x	xx.x	xx.x	xx.x	xx.x	xx.x	xx.x	xx.x
-10	xx.x	xx.x	xx.x	xx.x	xx.x	xx.x	xx.x	xx.x	xx.x	xx.x	xx.x	xx.x	xx.x	xx.x	xx.x	xx.x
-20	xx.x	xx.x	xx.x	xx.x	xx.x	xx.x	xx.x	xx.x	xx.x	xx.x	xx.x	xx.x	xx.x	xx.x	xx.x	xx.x
-30	xx.x	xx.x	xx.x	xx.x	xx.x	xx.x	xx.x	xx.x	xx.x	xx.x	xx.x	xx.x	xx.x	xx.x	xx.x	xx.x
-40	xx.x	xx.x	xx.x	xx.x	xx.x	xx.x	xx.x	xx.x	xx.x	xx.x	xx.x	xx.x	xx.x	xx.x	xx.x	xx.x

Table A 14: t_{final} **as a function of** MAT_C**:** P_{min} **= 6 MPa, CHSS soak temp = (**T_{hot_soak} **– 5 °C)**

MAT_C / T_{amb}	-40	-38	-36	-34	-32	-30	-28	-26	-24	-22	-20	-18	-16	-14	-12	-10
50	xx.x	xx.x	xx.x	xx.x	xx.x	xx.x	xx.x	xx.x	xx.x	xx.x	xx.x	xx.x	xx.x	xx.x	xx.x	xx.x
45	xx.x	xx.x	xx.x	xx.x	xx.x	xx.x	xx.x	xx.x	xx.x	xx.x	xx.x	xx.x	xx.x	xx.x	xx.x	xx.x
40	xx.x	xx.x	xx.x	xx.x	xx.x	xx.x	xx.x	xx.x	xx.x	xx.x	xx.x	xx.x	xx.x	xx.x	xx.x	xx.x
35	xx.x	xx.x	xx.x	xx.x	xx.x	xx.x	xx.x	xx.x	xx.x	xx.x	xx.x	xx.x	xx.x	xx.x	xx.x	xx.x
30	xx.x	xx.x	xx.x	xx.x	xx.x	xx.x	xx.x	xx.x	xx.x	xx.x	xx.x	xx.x	xx.x	xx.x	xx.x	xx.x
25	xx.x	xx.x	xx.x	xx.x	xx.x	xx.x	xx.x	xx.x	xx.x	xx.x	xx.x	xx.x	xx.x	xx.x	xx.x	xx.x
20	xx.x	xx.x	xx.x	xx.x	xx.x	xx.x	xx.x	xx.x	xx.x	xx.x	xx.x	xx.x	xx.x	xx.x	xx.x	xx.x
15	xx.x	xx.x	xx.x	xx.x	xx.x	xx.x	xx.x	xx.x	xx.x	xx.x	xx.x	xx.x	xx.x	xx.x	xx.x	xx.x
10	xx.x	xx.x	xx.x	xx.x	xx.x	xx.x	xx.x	xx.x	xx.x	xx.x	xx.x	xx.x	xx.x	xx.x	xx.x	xx.x
5	xx.x	xx.x	xx.x	xx.x	xx.x	xx.x	xx.x	xx.x	xx.x	xx.x	xx.x	xx.x	xx.x	xx.x	xx.x	xx.x
0	xx.x	xx.x	xx.x	xx.x	xx.x	xx.x	xx.x	xx.x	xx.x	xx.x	xx.x	xx.x	xx.x	xx.x	xx.x	xx.x
-10	xx.x	xx.x	xx.x	xx.x	xx.x	xx.x	xx.x	xx.x	xx.x	xx.x	xx.x	xx.x	xx.x	xx.x	xx.x	xx.x
-20	xx.x	xx.x	xx.x	xx.x	xx.x	xx.x	xx.x	xx.x	xx.x	xx.x	xx.x	xx.x	xx.x	xx.x	xx.x	xx.x
-30	xx.x	xx.x	xx.x	xx.x	xx.x	xx.x	xx.x	xx.x	xx.x	xx.x	xx.x	xx.x	xx.x	xx.x	xx.x	xx.x
-40	xx.x	xx.x	xx.x	xx.x	xx.x	xx.x	xx.x	xx.x	xx.x	xx.x	xx.x	xx.x	xx.x	xx.x	xx.x	xx.x

Table A.15: t_{final} **as a function of** MAT_C**:** P_{min} **= 11 MPa, CHSS soak temp = (**T_{hot_soak} **– 5 °C)**

MAT_C / T_{amb}	-40	-38	-36	-34	-32	-30	-28	-26	-24	-22	-20	-18	-16	-14	-12	-10
50	xx.x	xx.x	xx.x	xx.x	xx.x	xx.x	xx.x	xx.x	xx.x	xx.x	xx.x	xx.x	xx.x	xx.x	xx.x	xx.x
45	xx.x	xx.x	xx.x	xx.x	xx.x	xx.x	xx.x	xx.x	xx.x	xx.x	xx.x	xx.x	xx.x	xx.x	xx.x	xx.x
40	xx.x	xx.x	xx.x	xx.x	xx.x	xx.x	xx.x	xx.x	xx.x	xx.x	xx.x	xx.x	xx.x	xx.x	xx.x	xx.x
35	xx.x	xx.x	xx.x	xx.x	xx.x	xx.x	xx.x	xx.x	xx.x	xx.x	xx.x	xx.x	xx.x	xx.x	xx.x	xx.x
30	xx.x	xx.x	xx.x	xx.x	xx.x	xx.x	xx.x	xx.x	xx.x	xx.x	xx.x	xx.x	xx.x	xx.x	xx.x	xx.x
25	xx.x	xx.x	xx.x	xx.x	xx.x	xx.x	xx.x	xx.x	xx.x	xx.x	xx.x	xx.x	xx.x	xx.x	xx.x	xx.x
20	xx.x	xx.x	xx.x	xx.x	xx.x	xx.x	xx.x	xx.x	xx.x	xx.x	xx.x	xx.x	xx.x	xx.x	xx.x	xx.x
15	xx.x	xx.x	xx.x	xx.x	xx.x	xx.x	xx.x	xx.x	xx.x	xx.x	xx.x	xx.x	xx.x	xx.x	xx.x	xx.x
10	xx.x	xx.x	xx.x	xx.x	xx.x	xx.x	xx.x	xx.x	xx.x	xx.x	xx.x	xx.x	xx.x	xx.x	xx.x	xx.x
5	xx.x	xx.x	xx.x	xx.x	xx.x	xx.x	xx.x	xx.x	xx.x	xx.x	xx.x	xx.x	xx.x	xx.x	xx.x	xx.x
0	xx.x	xx.x	xx.x	xx.x	xx.x	xx.x	xx.x	xx.x	xx.x	xx.x	xx.x	xx.x	xx.x	xx.x	xx.x	xx.x
-10	xx.x	xx.x	xx.x	xx.x	xx.x	xx.x	xx.x	xx.x	xx.x	xx.x	xx.x	xx.x	xx.x	xx.x	xx.x	xx.x
-20	xx.x	xx.x	xx.x	xx.x	xx.x	xx.x	xx.x	xx.x	xx.x	xx.x	xx.x	xx.x	xx.x	xx.x	xx.x	xx.x
-30	xx.x	xx.x	xx.x	xx.x	xx.x	xx.x	xx.x	xx.x	xx.x	xx.x	xx.x	xx.x	xx.x	xx.x	xx.x	xx.x
-40	xx.x	xx.x	xx.x	xx.x	xx.x	xx.x	xx.x	xx.x	xx.x	xx.x	xx.x	xx.x	xx.x	xx.x	xx.x	xx.x

Table A.16: t_{final} **as a function of** MAT_C**:** P_{min} **= 16 MPa, CHSS soak temp = (**T_{hot_soak} **– 5 °C)**

MAT_C / T_{amb}	-40	-38	-36	-34	-32	-30	-28	-26	-24	-22	-20	-18	-16	-14	-12	-10
50	xx.x	xx.x	xx.x	xx.x	xx.x	xx.x	xx.x	xx.x	xx.x	xx.x	xx.x	xx.x	xx.x	xx.x	xx.x	xx.x
45	xx.x	xx.x	xx.x	xx.x	xx.x	xx.x	xx.x	xx.x	xx.x	xx.x	xx.x	xx.x	xx.x	xx.x	xx.x	xx.x
40	xx.x	xx.x	xx.x	xx.x	xx.x	xx.x	xx.x	xx.x	xx.x	xx.x	xx.x	xx.x	xx.x	xx.x	xx.x	xx.x
35	xx.x	xx.x	xx.x	xx.x	xx.x	xx.x	xx.x	xx.x	xx.x	xx.x	xx.x	xx.x	xx.x	xx.x	xx.x	xx.x
30	xx.x	xx.x	xx.x	xx.x	xx.x	xx.x	xx.x	xx.x	xx.x	xx.x	xx.x	xx.x	xx.x	xx.x	xx.x	xx.x
25	xx.x	xx.x	xx.x	xx.x	xx.x	xx.x	xx.x	xx.x	xx.x	xx.x	xx.x	xx.x	xx.x	xx.x	xx.x	xx.x
20	xx.x	xx.x	xx.x	xx.x	xx.x	xx.x	xx.x	xx.x	xx.x	xx.x	xx.x	xx.x	xx.x	xx.x	xx.x	xx.x
15	xx.x	xx.x	xx.x	xx.x	xx.x	xx.x	xx.x	xx.x	xx.x	xx.x	xx.x	xx.x	xx.x	xx.x	xx.x	xx.x
10	xx.x	xx.x	xx.x	xx.x	xx.x	xx.x	xx.x	xx.x	xx.x	xx.x	xx.x	xx.x	xx.x	xx.x	xx.x	xx.x
5	xx.x	xx.x	xx.x	xx.x	xx.x	xx.x	xx.x	xx.x	xx.x	xx.x	xx.x	xx.x	xx.x	xx.x	xx.x	xx.x
0	xx.x	xx.x	xx.x	xx.x	xx.x	xx.x	xx.x	xx.x	xx.x	xx.x	xx.x	xx.x	xx.x	xx.x	xx.x	xx.x
-10	xx.x	xx.x	xx.x	xx.x	xx.x	xx.x	xx.x	xx.x	xx.x	xx.x	xx.x	xx.x	xx.x	xx.x	xx.x	xx.x
-20	xx.x	xx.x	xx.x	xx.x	xx.x	xx.x	xx.x	xx.x	xx.x	xx.x	xx.x	xx.x	xx.x	xx.x	xx.x	xx.x
-30	xx.x	xx.x	xx.x	xx.x	xx.x	xx.x	xx.x	xx.x	xx.x	xx.x	xx.x	xx.x	xx.x	xx.x	xx.x	xx.x
-40	xx.x	xx.x	xx.x	xx.x	xx.x	xx.x	xx.x	xx.x	xx.x	xx.x	xx.x	xx.x	xx.x	xx.x	xx.x	xx.x

Table A 17: t_{final} **as a function of** MAT_C**:** P_{min} **= 21 MPa, CHSS soak temp = (**T_{hot_soak} **– 5 °C)**

MAT_C / T_{amb}	-40	-38	-36	-34	-32	-30	-28	-26	-24	-22	-20	-18	-16	-14	-12	-10
50	xx.x	xx.x	xx.x	xx.x	xx.x	xx.x	xx.x	xx.x	xx.x	xx.x	xx.x	xx.x	xx.x	xx.x	xx.x	xx.x
45	xx.x	xx.x	xx.x	xx.x	xx.x	xx.x	xx.x	xx.x	xx.x	xx.x	xx.x	xx.x	xx.x	xx.x	xx.x	xx.x
40	xx.x	xx.x	xx.x	xx.x	xx.x	xx.x	xx.x	xx.x	xx.x	xx.x	xx.x	xx.x	xx.x	xx.x	xx.x	xx.x
35	xx.x	xx.x	xx.x	xx.x	xx.x	xx.x	xx.x	xx.x	xx.x	xx.x	xx.x	xx.x	xx.x	xx.x	xx.x	xx.x
30	xx.x	xx.x	xx.x	xx.x	xx.x	xx.x	xx.x	xx.x	xx.x	xx.x	xx.x	xx.x	xx.x	xx.x	xx.x	xx.x
25	xx.x	xx.x	xx.x	xx.x	xx.x	xx.x	xx.x	xx.x	xx.x	xx.x	xx.x	xx.x	xx.x	xx.x	xx.x	xx.x
20	xx.x	xx.x	xx.x	xx.x	xx.x	xx.x	xx.x	xx.x	xx.x	xx.x	xx.x	xx.x	xx.x	xx.x	xx.x	xx.x
15	xx.x	xx.x	xx.x	xx.x	xx.x	xx.x	xx.x	xx.x	xx.x	xx.x	xx.x	xx.x	xx.x	xx.x	xx.x	xx.x
10	xx.x	xx.x	xx.x	xx.x	xx.x	xx.x	xx.x	xx.x	xx.x	xx.x	xx.x	xx.x	xx.x	xx.x	xx.x	xx.x
5	xx.x	xx.x	xx.x	xx.x	xx.x	xx.x	xx.x	xx.x	xx.x	xx.x	xx.x	xx.x	xx.x	xx.x	xx.x	xx.x
0	xx.x	xx.x	xx.x	xx.x	xx.x	xx.x	xx.x	xx.x	xx.x	xx.x	xx.x	xx.x	xx.x	xx.x	xx.x	xx.x
-10	xx.x	xx.x	xx.x	xx.x	xx.x	xx.x	xx.x	xx.x	xx.x	xx.x	xx.x	xx.x	xx.x	xx.x	xx.x	xx.x
-20	xx.x	xx.x	xx.x	xx.x	xx.x	xx.x	xx.x	xx.x	xx.x	xx.x	xx.x	xx.x	xx.x	xx.x	xx.x	xx.x
-30	xx.x	xx.x	xx.x	xx.x	xx.x	xx.x	xx.x	xx.x	xx.x	xx.x	xx.x	xx.x	xx.x	xx.x	xx.x	xx.x
-40	xx.x	xx.x	xx.x	xx.x	xx.x	xx.x	xx.x	xx.x	xx.x	xx.x	xx.x	xx.x	xx.x	xx.x	xx.x	xx.x

Table A 18: t_{final} **as a function of** MAT_C**:** P_{min} **= 1 MPa, CHSS soak temp = (**T_{hot_soak} **– 10 °C)**

MAT_C / T_{amb}	-40	-38	-36	-34	-32	-30	-28	-26	-24	-22	-20	-18	-16	-14	-12	-10
50	xx.x	xx.x	xx.x	xx.x	xx.x	xx.x	xx.x	xx.x	xx.x	xx.x	xx.x	xx.x	xx.x	xx.x	xx.x	xx.x
45	xx.x	xx.x	xx.x	xx.x	xx.x	xx.x	xx.x	xx.x	xx.x	xx.x	xx.x	xx.x	xx.x	xx.x	xx.x	xx.x
40	xx.x	xx.x	xx.x	xx.x	xx.x	xx.x	xx.x	xx.x	xx.x	xx.x	xx.x	xx.x	xx.x	xx.x	xx.x	xx.x
35	xx.x	xx.x	xx.x	xx.x	xx.x	xx.x	xx.x	xx.x	xx.x	xx.x	xx.x	xx.x	xx.x	xx.x	xx.x	xx.x
30	xx.x	xx.x	xx.x	xx.x	xx.x	xx.x	xx.x	xx.x	xx.x	xx.x	xx.x	xx.x	xx.x	xx.x	xx.x	xx.x
25	xx.x	xx.x	xx.x	xx.x	xx.x	xx.x	xx.x	xx.x	xx.x	xx.x	xx.x	xx.x	xx.x	xx.x	xx.x	xx.x
20	xx.x	xx.x	xx.x	xx.x	xx.x	xx.x	xx.x	xx.x	xx.x	xx.x	xx.x	xx.x	xx.x	xx.x	xx.x	xx.x
15	xx.x	xx.x	xx.x	xx.x	xx.x	xx.x	xx.x	xx.x	xx.x	xx.x	xx.x	xx.x	xx.x	xx.x	xx.x	xx.x
10	xx.x	xx.x	xx.x	xx.x	xx.x	xx.x	xx.x	xx.x	xx.x	xx.x	xx.x	xx.x	xx.x	xx.x	xx.x	xx.x
5	xx.x	xx.x	xx.x	xx.x	xx.x	xx.x	xx.x	xx.x	xx.x	xx.x	xx.x	xx.x	xx.x	xx.x	xx.x	xx.x
0	xx.x	xx.x	xx.x	xx.x	xx.x	xx.x	xx.x	xx.x	xx.x	xx.x	xx.x	xx.x	xx.x	xx.x	xx.x	xx.x
-10	xx.x	xx.x	xx.x	xx.x	xx.x	xx.x	xx.x	xx.x	xx.x	xx.x	xx.x	xx.x	xx.x	xx.x	xx.x	xx.x
-20	xx.x	xx.x	xx.x	xx.x	xx.x	xx.x	xx.x	xx.x	xx.x	xx.x	xx.x	xx.x	xx.x	xx.x	xx.x	xx.x
-30	xx.x	xx.x	xx.x	xx.x	xx.x	xx.x	xx.x	xx.x	xx.x	xx.x	xx.x	xx.x	xx.x	xx.x	xx.x	xx.x
-40	xx.x	xx.x	xx.x	xx.x	xx.x	xx.x	xx.x	xx.x	xx.x	xx.x	xx.x	xx.x	xx.x	xx.x	xx.x	xx.x

Table A.19: t_{final} **as a function of** MAT_C**:** P_{min} **= 6 MPa, CHSS soak temp = (**T_{hot_soak} **– 10 °C)**

MAT_C / T_{amb}	-40	-38	-36	-34	-32	-30	-28	-26	-24	-22	-20	-18	-16	-14	-12	-10
50	xx.x	xx.x	xx.x	xx.x	xx.x	xx.x	xx.x	xx.x	xx.x	xx.x	xx.x	xx.x	xx.x	xx.x	xx.x	xx.x
45	xx.x	xx.x	xx.x	xx.x	xx.x	xx.x	xx.x	xx.x	xx.x	xx.x	xx.x	xx.x	xx.x	xx.x	xx.x	xx.x
40	xx.x	xx.x	xx.x	xx.x	xx.x	xx.x	xx.x	xx.x	xx.x	xx.x	xx.x	xx.x	xx.x	xx.x	xx.x	xx.x
35	xx.x	xx.x	xx.x	xx.x	xx.x	xx.x	xx.x	xx.x	xx.x	xx.x	xx.x	xx.x	xx.x	xx.x	xx.x	xx.x
30	xx.x	xx.x	xx.x	xx.x	xx.x	xx.x	xx.x	xx.x	xx.x	xx.x	xx.x	xx.x	xx.x	xx.x	xx.x	xx.x
25	xx.x	xx.x	xx.x	xx.x	xx.x	xx.x	xx.x	xx.x	xx.x	xx.x	xx.x	xx.x	xx.x	xx.x	xx.x	xx.x
20	xx.x	xx.x	xx.x	xx.x	xx.x	xx.x	xx.x	xx.x	xx.x	xx.x	xx.x	xx.x	xx.x	xx.x	xx.x	xx.x
15	xx.x	xx.x	xx.x	xx.x	xx.x	xx.x	xx.x	xx.x	xx.x	xx.x	xx.x	xx.x	xx.x	xx.x	xx.x	xx.x
10	xx.x	xx.x	xx.x	xx.x	xx.x	xx.x	xx.x	xx.x	xx.x	xx.x	xx.x	xx.x	xx.x	xx.x	xx.x	xx.x
5	xx.x	xx.x	xx.x	xx.x	xx.x	xx.x	xx.x	xx.x	xx.x	xx.x	xx.x	xx.x	xx.x	xx.x	xx.x	xx.x
0	xx.x	xx.x	xx.x	xx.x	xx.x	xx.x	xx.x	xx.x	xx.x	xx.x	xx.x	xx.x	xx.x	xx.x	xx.x	xx.x
-10	xx.x	xx.x	xx.x	xx.x	xx.x	xx.x	xx.x	xx.x	xx.x	xx.x	xx.x	xx.x	xx.x	xx.x	xx.x	xx.x
-20	xx.x	xx.x	xx.x	xx.x	xx.x	xx.x	xx.x	xx.x	xx.x	xx.x	xx.x	xx.x	xx.x	xx.x	xx.x	xx.x
-30	xx.x	xx.x	xx.x	xx.x	xx.x	xx.x	xx.x	xx.x	xx.x	xx.x	xx.x	xx.x	xx.x	xx.x	xx.x	xx.x
-40	xx.x	xx.x	xx.x	xx.x	xx.x	xx.x	xx.x	xx.x	xx.x	xx.x	xx.x	xx.x	xx.x	xx.x	xx.x	xx.x

Table A.20: t_{final} **as a function of** MAT_C**:** P_{min} **= 11 MPa, CHSS soak temp = (**T_{hot_soak} **– 10 °C)**

MAT_C / T_{amb}	-40	-38	-36	-34	-32	-30	-28	-26	-24	-22	-20	-18	-16	-14	-12	-10
50	xx.x	xx.x	xx.x	xx.x	xx.x	xx.x	xx.x	xx.x	xx.x	xx.x	xx.x	xx.x	xx.x	xx.x	xx.x	xx.x
45	xx.x	xx.x	xx.x	xx.x	xx.x	xx.x	xx.x	xx.x	xx.x	xx.x	xx.x	xx.x	xx.x	xx.x	xx.x	xx.x
40	xx.x	xx.x	xx.x	xx.x	xx.x	xx.x	xx.x	xx.x	xx.x	xx.x	xx.x	xx.x	xx.x	xx.x	xx.x	xx.x
35	xx.x	xx.x	xx.x	xx.x	xx.x	xx.x	xx.x	xx.x	xx.x	xx.x	xx.x	xx.x	xx.x	xx.x	xx.x	xx.x
30	xx.x	xx.x	xx.x	xx.x	xx.x	xx.x	xx.x	xx.x	xx.x	xx.x	xx.x	xx.x	xx.x	xx.x	xx.x	xx.x
25	xx.x	xx.x	xx.x	xx.x	xx.x	xx.x	xx.x	xx.x	xx.x	xx.x	xx.x	xx.x	xx.x	xx.x	xx.x	xx.x
20	xx.x	xx.x	xx.x	xx.x	xx.x	xx.x	xx.x	xx.x	xx.x	xx.x	xx.x	xx.x	xx.x	xx.x	xx.x	xx.x
15	xx.x	xx.x	xx.x	xx.x	xx.x	xx.x	xx.x	xx.x	xx.x	xx.x	xx.x	xx.x	xx.x	xx.x	xx.x	xx.x
10	xx.x	xx.x	xx.x	xx.x	xx.x	xx.x	xx.x	xx.x	xx.x	xx.x	xx.x	xx.x	xx.x	xx.x	xx.x	xx.x
5	xx.x	xx.x	xx.x	xx.x	xx.x	xx.x	xx.x	xx.x	xx.x	xx.x	xx.x	xx.x	xx.x	xx.x	xx.x	xx.x
0	xx.x	xx.x	xx.x	xx.x	xx.x	xx.x	xx.x	xx.x	xx.x	xx.x	xx.x	xx.x	xx.x	xx.x	xx.x	xx.x
-10	xx.x	xx.x	xx.x	xx.x	xx.x	xx.x	xx.x	xx.x	xx.x	xx.x	xx.x	xx.x	xx.x	xx.x	xx.x	xx.x
-20	xx.x	xx.x	xx.x	xx.x	xx.x	xx.x	xx.x	xx.x	xx.x	xx.x	xx.x	xx.x	xx.x	xx.x	xx.x	xx.x
-30	xx.x	xx.x	xx.x	xx.x	xx.x	xx.x	xx.x	xx.x	xx.x	xx.x	xx.x	xx.x	xx.x	xx.x	xx.x	xx.x
-40	xx.x	xx.x	xx.x	xx.x	xx.x	xx.x	xx.x	xx.x	xx.x	xx.x	xx.x	xx.x	xx.x	xx.x	xx.x	xx.x

Table A.21: t_{final} **as a function of** MAT_C**:** P_{min} **= 16 MPa, CHSS soak temp = (**T_{hot_soak} **– 10 °C)**

MAT_C / T_{amb}	-40	-38	-36	-34	-32	-30	-28	-26	-24	-22	-20	-18	-16	-14	-12	-10
50	xx.x	xx.x	xx.x	xx.x	xx.x	xx.x	xx.x	xx.x	xx.x	xx.x	xx.x	xx.x	xx.x	xx.x	xx.x	xx.x
45	xx.x	xx.x	xx.x	xx.x	xx.x	xx.x	xx.x	xx.x	xx.x	xx.x	xx.x	xx.x	xx.x	xx.x	xx.x	xx.x
40	xx.x	xx.x	xx.x	xx.x	xx.x	xx.x	xx.x	xx.x	xx.x	xx.x	xx.x	xx.x	xx.x	xx.x	xx.x	xx.x
35	xx.x	xx.x	xx.x	xx.x	xx.x	xx.x	xx.x	xx.x	xx.x	xx.x	xx.x	xx.x	xx.x	xx.x	xx.x	xx.x
30	xx.x	xx.x	xx.x	xx.x	xx.x	xx.x	xx.x	xx.x	xx.x	xx.x	xx.x	xx.x	xx.x	xx.x	xx.x	xx.x
25	xx.x	xx.x	xx.x	xx.x	xx.x	xx.x	xx.x	xx.x	xx.x	xx.x	xx.x	xx.x	xx.x	xx.x	xx.x	xx.x
20	xx.x	xx.x	xx.x	xx.x	xx.x	xx.x	xx.x	xx.x	xx.x	xx.x	xx.x	xx.x	xx.x	xx.x	xx.x	xx.x
15	xx.x	xx.x	xx.x	xx.x	xx.x	xx.x	xx.x	xx.x	xx.x	xx.x	xx.x	xx.x	xx.x	xx.x	xx.x	xx.x
10	xx.x	xx.x	xx.x	xx.x	xx.x	xx.x	xx.x	xx.x	xx.x	xx.x	xx.x	xx.x	xx.x	xx.x	xx.x	xx.x
5	xx.x	xx.x	xx.x	xx.x	xx.x	xx.x	xx.x	xx.x	xx.x	xx.x	xx.x	xx.x	xx.x	xx.x	xx.x	xx.x
0	xx.x	xx.x	xx.x	xx.x	xx.x	xx.x	xx.x	xx.x	xx.x	xx.x	xx.x	xx.x	xx.x	xx.x	xx.x	xx.x
-10	xx.x	xx.x	xx.x	xx.x	xx.x	xx.x	xx.x	xx.x	xx.x	xx.x	xx.x	xx.x	xx.x	xx.x	xx.x	xx.x
-20	xx.x	xx.x	xx.x	xx.x	xx.x	xx.x	xx.x	xx.x	xx.x	xx.x	xx.x	xx.x	xx.x	xx.x	xx.x	xx.x
-30	xx.x	xx.x	xx.x	xx.x	xx.x	xx.x	xx.x	xx.x	xx.x	xx.x	xx.x	xx.x	xx.x	xx.x	xx.x	xx.x
-40	xx.x	xx.x	xx.x	xx.x	xx.x	xx.x	xx.x	xx.x	xx.x	xx.x	xx.x	xx.x	xx.x	xx.x	xx.x	xx.x

Table A.22: **t_{final} as a function of MAT_C: P_{min} = 21 MPa, CHSS soak temp = (T_{hot_soak} – 10 °C)**

MAT_C / T_{amb}	-40	-38	-36	-34	-32	-30	-28	-26	-24	-22	-20	-18	-16	-14	-12	-10
50	xx.x	xx.x	xx.x	xx.x	xx.x	xx.x	xx.x	xx.x	xx.x	xx.x	xx.x	xx.x	xx.x	xx.x	xx.x	xx.x
45	xx.x	xx.x	xx.x	xx.x	xx.x	xx.x	xx.x	xx.x	xx.x	xx.x	xx.x	xx.x	xx.x	xx.x	xx.x	xx.x
40	xx.x	xx.x	xx.x	xx.x	xx.x	xx.x	xx.x	xx.x	xx.x	xx.x	xx.x	xx.x	xx.x	xx.x	xx.x	xx.x
35	xx.x	xx.x	xx.x	xx.x	xx.x	xx.x	xx.x	xx.x	xx.x	xx.x	xx.x	xx.x	xx.x	xx.x	xx.x	xx.x
30	xx.x	xx.x	xx.x	xx.x	xx.x	xx.x	xx.x	xx.x	xx.x	xx.x	xx.x	xx.x	xx.x	xx.x	xx.x	xx.x
25	xx.x	xx.x	xx.x	xx.x	xx.x	xx.x	xx.x	xx.x	xx.x	xx.x	xx.x	xx.x	xx.x	xx.x	xx.x	xx.x
20	xx.x	xx.x	xx.x	xx.x	xx.x	xx.x	xx.x	xx.x	xx.x	xx.x	xx.x	xx.x	xx.x	xx.x	xx.x	xx.x
15	xx.x	xx.x	xx.x	xx.x	xx.x	xx.x	xx.x	xx.x	xx.x	xx.x	xx.x	xx.x	xx.x	xx.x	xx.x	xx.x
10	xx.x	xx.x	xx.x	xx.x	xx.x	xx.x	xx.x	xx.x	xx.x	xx.x	xx.x	xx.x	xx.x	xx.x	xx.x	xx.x
5	xx.x	xx.x	xx.x	xx.x	xx.x	xx.x	xx.x	xx.x	xx.x	xx.x	xx.x	xx.x	xx.x	xx.x	xx.x	xx.x
0	xx.x	xx.x	xx.x	xx.x	xx.x	xx.x	xx.x	xx.x	xx.x	xx.x	xx.x	xx.x	xx.x	xx.x	xx.x	xx.x
-10	xx.x	xx.x	xx.x	xx.x	xx.x	xx.x	xx.x	xx.x	xx.x	xx.x	xx.x	xx.x	xx.x	xx.x	xx.x	xx.x
-20	xx.x	xx.x	xx.x	xx.x	xx.x	xx.x	xx.x	xx.x	xx.x	xx.x	xx.x	xx.x	xx.x	xx.x	xx.x	xx.x
-30	xx.x	xx.x	xx.x	xx.x	xx.x	xx.x	xx.x	xx.x	xx.x	xx.x	xx.x	xx.x	xx.x	xx.x	xx.x	xx.x
-40	xx.x	xx.x	xx.x	xx.x	xx.x	xx.x	xx.x	xx.x	xx.x	xx.x	xx.x	xx.x	xx.x	xx.x	xx.x	xx.x

(Eq. A.30)

If $P_{initial}$ < 6 MPa

THEN

If (T_{hot_soak} – 10) ≤ T_{gas_high}, select Table A.8 and store P_{min} = 1

Else if (T_{hot_soak} – 20) ≤ T_{gas_high} < (T_{hot_soak} – 10), select Table A.13 and store P_{min} = 1

Else if T_{gas_high} < (T_{hot_soak} – 20), select Table A.18 and store P_{min} = 1

End If

If 6 ≤ $P_{initial}$ < 11 MPa

THEN

If T_{gas_high} > T_{hot_soak}, select Table A.8 and store P_{min} = 1

Else if (T_{hot_soak} – 10) ≤ T_{gas_high} ≤ T_{hot_soak}, select Table A.9 and store P_{min} = 6

Else if (T_{hot_soak} – 20) ≤ T_{gas_high} < (T_{hot_soak} – 10), select Table A.14 and store P_{min} = 6

Else if T_{gas_high} < (T_{hot_soak} – 20), select Table A.19 and store P_{min} = 6

End If

If 11 ≤ $P_{initial}$ < 16 MPa

THEN

If T_{gas_high} > T_{hot_soak}, select Table A.8 and store P_{min} = 1

Else if (T_{hot_soak} – 10) ≤ T_{gas_high} ≤ T_{hot_soak}, select Table A.10 and store P_{min} = 11

Else if (T_{hot_soak} – 20) ≤ T_{gas_high} < (T_{hot_soak} – 10), select Table A.15 and store P_{min} = 11

Else if T_{gas_high} < (T_{hot_soak} – 20), select Table A.20 and store P_{min} = 11

End If

If 16 ≤ $P_{initial}$ < 21 MPa

THEN

If T_{gas_high} > T_{hot_soak}, select Table A.8 and store P_{min} = 1

Else if (T_{hot_soak} – 10) ≤ T_{gas_high} ≤ T_{hot_soak}, select Table A.11 and store P_{min} = 16

Else if (T_{hot_soak} – 20) ≤ T_{gas_high} < (T_{hot_soak} – 10), select Table A.16 and store P_{min} = 16

Else if T_{gas_high} < (T_{hot_soak} – 20), select Table A.21 and store P_{min} = 16

End If

If $P_{initial}$ > 21 MPa

THEN

If T_{gas_high} > T_{hot_soak}, select Table A.8 and store P_{min} = 1

Else if (T_{hot_soak} – 10) ≤ T_{gas_high} ≤ T_{hot_soak}, select Table A.12 and store P_{min} = 21

Else if (T_{hot_soak} – 20) ≤ T_{gas_high} < (T_{hot_soak} – 10), select Table A.17 and store P_{min} = 21

Else if T_{gas_high} < (T_{hot_soak} – 20), select Table A.22 and store P_{min} = 21

End If

Once P_{min} has been determined, the parameter β can be calculated. β is a parameter which is multiplied by t_{final} to allow for the pressure tolerance ΔP_{tol_high}. See Section H.2.6.2 of SAE J2601 for a detailed explanation of β. The unit of measure for β is dimensionless.

(Eq. A.31)

$$Set\ \beta = \frac{P_{final} - P_{min}}{P_{final} - P_{min} - \Delta P_{tol\_high}}$$

A.1.1.6 Subroutine – Selection of t_{final} Table for T_{gas} Throttle Fuelling Concept

This subroutine applies only to the T_{gas} Throttle Fuelling concept.

t_{final} tables store a derived t_{final} value which is a function of the ambient temperature T_{amb} and the mass average fuel delivery temperature used for control, MAT_C. The t_{final} table contains discrete values of T_{amb} and MAT_C. The t_{final} value is stored in minutes to the tenth (one significant digit), i.e. xx.x.

There is one t_{final} table to choose from. Table A.23 utilizes a P_{min} value of 1 MPa.

Table A 23: t_{final} as a function of MAT_C: P_{min} = 1 MPa

T_{amb} \ MAT_C	-40	-38	-36	-34	-32	-30	-28	-26	-24	-22	-20	-18	-16	-14	-12	-10
50	xx.x	xx.x	xx.x	xx.x	xx.x	xx.x	xx.x	xx.x	xx.x	xx.x	xx.x	xx.x	xx.x	xx.x	xx.x	xx.x
45	xx.x	xx.x	xx.x	xx.x	xx.x	xx.x	xx.x	xx.x	xx.x	xx.x	xx.x	xx.x	xx.x	xx.x	xx.x	xx.x
40	xx.x	xx.x	xx.x	xx.x	xx.x	xx.x	xx.x	xx.x	xx.x	xx.x	xx.x	xx.x	xx.x	xx.x	xx.x	xx.x
35	xx.x	xx.x	xx.x	xx.x	xx.x	xx.x	xx.x	xx.x	xx.x	xx.x	xx.x	xx.x	xx.x	xx.x	xx.x	xx.x
30	xx.x	xx.x	xx.x	xx.x	xx.x	xx.x	xx.x	xx.x	xx.x	xx.x	xx.x	xx.x	xx.x	xx.x	xx.x	xx.x
25	xx.x	xx.x	xx.x	xx.x	xx.x	xx.x	xx.x	xx.x	xx.x	xx.x	xx.x	xx.x	xx.x	xx.x	xx.x	xx.x
20	xx.x	xx.x	xx.x	xx.x	xx.x	xx.x	xx.x	xx.x	xx.x	xx.x	xx.x	xx.x	xx.x	xx.x	xx.x	xx.x
15	xx.x	xx.x	xx.x	xx.x	xx.x	xx.x	xx.x	xx.x	xx.x	xx.x	xx.x	xx.x	xx.x	xx.x	xx.x	xx.x
10	xx.x	xx.x	xx.x	xx.x	xx.x	xx.x	xx.x	xx.x	xx.x	xx.x	xx.x	xx.x	xx.x	xx.x	xx.x	xx.x
5	xx.x	xx.x	xx.x	xx.x	xx.x	xx.x	xx.x	xx.x	xx.x	xx.x	xx.x	xx.x	xx.x	xx.x	xx.x	xx.x
0	xx.x	xx.x	xx.x	xx.x	xx.x	xx.x	xx.x	xx.x	xx.x	xx.x	xx.x	xx.x	xx.x	xx.x	xx.x	xx.x
-10	xx.x	xx.x	xx.x	xx.x	xx.x	xx.x	xx.x	xx.x	xx.x	xx.x	xx.x	xx.x	xx.x	xx.x	xx.x	xx.x
-20	xx.x	xx.x	xx.x	xx.x	xx.x	xx.x	xx.x	xx.x	xx.x	xx.x	xx.x	xx.x	xx.x	xx.x	xx.x	xx.x
-30	xx.x	xx.x	xx.x	xx.x	xx.x	xx.x	xx.x	xx.x	xx.x	xx.x	xx.x	xx.x	xx.x	xx.x	xx.x	xx.x
-40	xx.x	xx.x	xx.x	xx.x	xx.x	xx.x	xx.x	xx.x	xx.x	xx.x	xx.x	xx.x	xx.x	xx.x	xx.x	xx.x

(Eq. A.32)

Select Table A.23 and store P_{min} = 1

Once P_{min} has been determined, the parameter β can be calculated. β is a parameter which is multiplied by t_{final} to allow for the pressure tolerance ΔP_{tol_high}. See Section H.2.6.2 of SAE J2601 for a detailed explanation of β. The unit of measure for β is dimensionless.

(Eq. A.33)

$$Set\ \beta = \frac{P_{final} - P_{min}}{P_{final} - P_{min} - \Delta P_{tol\_high}}$$

A.1.1.7 Subroutine - t_{final} Vector Interpolation

From the t_{final} table selected in the "Selection of t_{final} Table Subroutine" (for the fuelling concept being utilized), select the row of t_{final} values above and below T_{amb}. For example, if T_{amb} = 27 °C, select the row of t_{final} values in the t_{final} table at a T_{amb} of 30 °C (above) and the row of t_{final} values in the t_{final} table at a T_{amb} of 25 °C (below). Then use Equation A.34 to interpolate t_{final} for each MAT_C value. Each t_{final} value is associated with its MAT_C value, i.e. $t_{final(MATC)}$. For example, $t_{final(-40)}$ is the t_{final} value when MAT_C is equal to -40 °C, $t_{final(-38)}$ is the t_{final} value when MAT_C is equal to -38 °C, etc, see Table A 24.

Table A 24: Example of interpolating t_{final} values

	T_{amb} \ MAT_C	-40	-38	-36	-34	…..
t_{final} Values →	T_{amb_above}	$t_{final(-40)}$	$t_{final(-38)}$	$t_{final(-36)}$	$t_{final(-34)}$	$t_{final(.....)}$
New Interpolated Values →	T_{amb}	$t_{final(-40)}$	$t_{final(-38)}$	$t_{final(-36)}$	$t_{final(-34)}$	$t_{final(.....)}$
t_{final} Values →	T_{amb_below}	$t_{final(-40)}$	$t_{final(-38)}$	$t_{final(-34)}$	$t_{final(-34)}$	$t_{final(.....)}$

(Eq. A.34)

$$t_{final(MATC)} = t_{final(MATC)(T_{amb\_below})} + \frac{\left[t_{final(MATC)(T_{amb\_above})} - t_{final(MATC)(T_{amb\_below})}\right] \times \left[T_{amb} - T_{amb\_below}\right]}{\left[T_{amb\_above} - T_{amb\_below}\right]}$$

After interpolation, a t_{final} vector is stored, i.e. a t_{final} value for each MAT_C value in the t_{final} table.

t_{final} vector → $t_{final(-40)}$ = *xx.x*, $t_{final(-38)}$ = *xx.x*, $t_{final(-36)}$ = *xx.x*, $t_{final(-34)}$ = *xx.x*, $t_{final(-32)}$ = *xx.x*, $t_{final(-28)}$ = *xx.x*, $t_{final(-26)}$ = *xx.x*, $t_{final(-24)}$ = *xx.x*, $t_{final(-22)}$ = *xx.x*, $t_{final(-20)}$ = *xx.x*, $t_{final(-18)}$ = *xx.x*, $t_{final(-16)}$ = *xx.x*, $t_{final(-14)}$ = *xx.x*, $t_{final(-12)}$ = *xx.x*, $t_{final(-10)}$ = *xx.x*

A.1.1.8 Subroutine - Mass Average Calculation of the Fuel Delivery Temperature

A key control input for determining the pressure ramp rate is the mass average of the fuel delivery temperature measured at the dispenser outlet. There are two mass average calculations, MAT_0 and MAT_{30}. MAT_0 begins the calculation at the beginning of the main fuelling time from t = 0 seconds. MAT_{30} begins the calculation after a total of 30 seconds of mass flow have elapsed. See Section H.2.4 of SAE J2601 for a detailed explanation of how the mass average of the fuel delivery temperature is used in the pressure ramp rate control. The unit of measure for MAT_0 and MAT_{30} is Kelvin (K).

In the equations in this subroutine, T_{fuel_inst} is the fuel delivery temperature measured at the dispenser outlet, and m represents the total mass dispensed from the beginning of the main fuelling time. $T_{fuel\_instl(j)}$ represents the temperature measured at the current time step j. $T_{fuel\_inst(j-1)}$ represents the temperature measured at the previous time step j-1. $T_{fuel\_inst\_A}$ and $T_{fuel\_inst\_B}$ represent two separate measurements when redundancy is employed. $m_{(j)}$ represents the total mass dispensed up to the current time step j. $m_{(j-1)}$ represents the total mass dispensed up to the previous time step j-1. Thus, $m_{(j)}$ - $m_{(j-1)}$ represents the change in mass over the last time step j. It is important that the denominator in Equations A.35 and A.36 be calculated as the sum of $m_{(j)}$ - $m_{(j-1)}$, rather than just using the value m. This is because the mass average is a weighting function, and thus the change in mass for the numerator and denominator must be summed in the same way. The unit of measure for T_{fuel_inst} is Kelvin (K). The unit of measure for m is grams.

(Eq. A.35)

$$IF\ j = 0,\ THEN\ MAT_{0\_A(j)} = T_{fuel\_inst\_A(0)},\ ELSE\ \ MAT_{0\_A(j)} = \frac{\sum_0^j\left[\left(m_{(j)} - m_{(j-1)}\right) \times 0.5\left(T_{fuel\_inst\_A(j)} + T_{fuel\_inst\_A(j-1)}\right)\right]}{\sum_0^j\left(m_{(j)} - m_{(j-1)}\right)}$$

(Eq. A.36)

$$IF\ j = 0,\ THEN\ MAT_{0\_B(j)} = T_{fuel\_inst\_B(0)},\ ELSE\ \ MAT_{0\_B(j)} = \frac{\sum_0^j[(m_{(j)}-m_{(j-1)})\times 0.5(T_{fuel\_inst\_B(j)}+T_{fuel\_inst\_B(j-1)})]}{\sum_0^j(m_{(j)}-m_{(j-1)})}$$

(Eq. A.37)

$$MAT_{0(j)} = MAXIMUM\left[MAT_{0\_A(j)}, MAT_{0\_B(j)}\right]$$

In Equations A.38 and A.39 for MAT_{30}, and Equation A.41, which utilizes MAT_{30} , a parameter named *n* (a counter), is utilized for determining the point in the fill at which these calculations shall commence. The calculation of MAT_{30} begins after a total of 30 seconds of mass flow have elapsed. Because the time step counter *j* advances every second, regardless of whether there is mass flow or not, a separate counter *n*, which updates at the same frequency as *j*, is utilized. The difference between *n* and *j* is that *n* only updates when there is mass flow during the calculation cycle, which means that *n* does not advance during an intended non-fuelling event such as a leak check or bank switch. Since, by definition, the calculation of MAT_{30} begins after a total of 30 seconds of mass flow, the calculation of MAT_{30} begins when *n*=30. Since the summation terms in the numerator and denominator of Equations A.38 and A.39 utilize the time step *j*, the time at which the calculation begins is denoted by *j* at *n*=30, which represents the value of *j* when the counter *n* reaches 30. If there are no intended non-fuelling events during the first 30 seconds of the fill, then *j* and *n* will reach 30 at the same time.

If an intended non-fuelling event occurs when $20 \leq n \leq 30$, then subtract 10 seconds from *n*. In this case, a total of 40 seconds of mass flow are allowed prior to the MAT_{30} calculation beginning. The purpose of subtracting 10 seconds is to allow the fuel delivery temperature T_{fuel_inst} to get cold again after the warming which occurs during the intended non-fuelling event.

It is important that the denominator in Equations A.38 and A.39 be calculated as the sum of $m_{(j)}$ - $m_{(j-1)}$, rather than just using the value m - $m_{(j@n=30)}$. This is because the mass average is a weighting function, and thus the change in mass for the numerator and denominator must be summed in the same way.

(Eq. A.38)

$$IF\ n \geq 30,\ THEN\ MAT_{30\_A(j)} = \frac{\sum_{j@n=30}^{j}[(m_{(j)}-m_{(j-1)})\times 0.5(T_{fuel\_inst\_A(j)}+T_{fuel\_inst\_A(j-1)})]}{\sum_{j@n=30}^{j}(m_{(j)}-m_{(j-1)})}$$

(Eq. A.39)

$$IF\ n \geq 30,\ THEN\ MAT_{30\_B(j)} = \frac{\sum_{j@n=30}^{j}[(m_{(j)}-m_{(j-1)})\times 0.5(T_{fuel\_inst\_B(j)}+T_{fuel\_inst\_B(j-1)})]}{\sum_{j@n=30}^{j}(m_{(j)}-m_{(j-1)})}$$

(Eq. A.40)

$$MAT_{30(j)} = MAXIMUM\left[MAT_{30\_A(j)}, MAT_{30\_B(j)}\right]$$

The mass average of the fuel delivery temperature which is utilized as the control input for the t_{final} equation is labelled as MAT_C. MAT_C is calculated from either $MAT_{expected}$, MAT_{30}, or a combination of MAT_{30} and MAT_0. The logic for making this determination is explained in Section H.2.4. of SAE J2601. Equation 5.26 is utilized to calculate MAT_C.

(Eq. A.41)

$$IF$$

$$n \leq 30$$

$$THEN$$

$$MAT_{C(j)} = MAT_{expected}$$

$$ELSE$$

$$IF\ P_{ramp(j)} \leq P_{trans}$$

$$THEN$$

$$MAT_{C(j)} = MAT_{30(j)}$$

$$ELSE$$

$$IF\ P_{trans} < P_{ramp(j)} \leq P_{final}$$

$$THEN$$

$$MAT_{C(j)} = MAT_{30(j)} \times \left(\frac{P_{final} - P_{ramp(j)}}{P_{final} - P_{trans}}\right) + MAT_{0(j)} \times \left(1 - \frac{P_{final} - P_{ramp(j)}}{P_{final} - P_{trans}}\right)$$

A.1.1.9 Subroutine - Calculation of t_{final}

This Subroutine is used to calculate t_{final}, which is defined as the total time required to fill from P_{min} to P_{final}. t_{final} is the key control input to the pressure ramp rate equation. The unit of measure for t_{final} for the values from the t_{final} tables is minutes to the tenth or one significant digit.

The calculations in this subroutine shall be conducted using the time step *j*, which means they are calculated once every second.

To calculate t_{final} for each timestep, the t_{final} vector calculated in the t_{final} Vector Interpolation Subroutine (A.1.1.7) is utilized, along with the $MAT_{C(j)}$ from the Mass Average Calculation of the Fuel Delivery Temperature Subroutine. From the t_{final}

vector, the t_{final} value associated with the MAT_C value directly below (colder than) than $MAT_{C(j)}$ and the t_{final} value associated with the MAT_C value directly above (warmer than) than $MAT_{C(j)}$ are utilized. These values are referred to as $t_{final(MATC\_below)}$ & $MAT_{C(below)}$ and $t_{final(MATC\_above)}$ & $MAT_{C(above)}$, respectively.

As an example, a shortened t_{final} vector is defined as follows:
$t_{final(-40)} = 6.4$, $t_{final(-38)} = 7.1$, $t_{final(-36)} = 7.9$, $t_{final(-34)} = 8.7$, $t_{final(-32)} = 9.4$, etc.
In this example, $MAT_{C(j)}$ for the current timestep is -33.1 °C / 240.05 K. Therefore, $t_{final(MATC\_below)}$ is $t_{final(-34)} = 8.7$, $MAT_{C(below)}$ is -34 °C / 239.15 K,
$t_{final(MATC\_above)}$ is $t_{final(-32)} = 9.4$, and $MAT_{C(above)}$ is -32 °C / 241.15 K.

(Eq. A.42)

$$t_{final(j)} = t_{final(MATC\_below)} + \frac{\left[t_{final(MATC\_above)} - t_{final(MATC\_below)}\right] \times \left[MATC_{(j)} - MATC_{(below)}\right]}{\left[MATC_{(above)} - MATC_{(below)}\right]}$$

The pressure ramp rate equation utilizes a t_{final} value with the units of seconds instead of minutes. In Equation A.43, t_{final} is converted into seconds using the convention t_{final_sec}. Additionally, t_{final} is multiplied by the factors α and β.

(Eq. A.43)

$$t_{final\_sec(j)} = 60 \times \alpha \times \beta \times t_{final(j)}$$

A.1.1.10 Subroutine - Calculation of PRR and P_{ramp}

This subroutine is used to calculate the pressure ramp rate PRR, ramp pressure P_{ramp}, the limit pressure P_{limit_high}, and the factor α, used in the t_{final} equation. The ramp pressure is the pressure targeted by the dispenser control at any time during the fill. The upper limit pressure defines a boundary or limit on the station pressure that is not to be exceeded. See Section H.2.3 and Section H.2.5 of SAE J2601 for a detailed explanation of the variable pressure ramp rate PRR, and Section H.2.6 for a detailed explanation of α, and P_{limit_high}.

The calculations in this subroutine shall be conducted based on a time step j, which is advanced every one second. Thus, each calculation in this subroutine is conducted once every second.

Equation A.44 is used to calculate α. α is a factor which accounts for variability in the pressure ramp rate during the fill. α is multiplied by the t_{final} equation to extend the fuelling time based on the amount of variability in the pressure ramp rate. The unit of measure for α is dimensionless. The unit of measure for RR_{min} and RR_{max} is MPa/sec.

Note that in Equation A.44, for the first calculation cycle when $j = 0$, α is not calculated and the initialization value of 1 is utilized. Also note that if the mass flow rate is zero for longer than 5 seconds (for example, during an intended non-fuelling event), the minimum pressure ramp rate RR_{min} is set to zero.

(Eq. A.44)

$$IF\ j > 0$$

$$THEN$$

$$IF\ \ PRR < RR_{min},\ THEN\ RR_{min} = PRR$$

$$IF\ \ PRR > RR_{max},\ THEN\ RR_{max} = PRR$$

$$IF\ \dot{m} = 0\ for\ greater\ than\ 5\ seconds, \qquad THEN\ RR_{min} = 0$$

$$\alpha\ = \left[\frac{100+18.5(RR_{max}-RR_{min})}{100}\right]$$

Equation A.45 is used to calculate the State of Charge (SOC) of the CHSS. The SOC is a function of the density, which can be calculated using an equation of state for hydrogen with sufficient accuracy (±0.5%). An example of an equation of state is provided, although alternate equations may be used. The units of measure for density ρ is g/l.

(Eq. A.45)

$$\rho = f\left(MP, T_{gas\_low}\right)$$

where MP is the gas pressure in the CHSS and T_{gas_low} is the lowest bulk average gas temperature in the CHSS

Example equation of state referenced from Equation J96 in 2020 SAE J2601 (in this equation P = MP and T = T_{gas_low}):

$$\begin{aligned}\rho = (&-1.1671\text{E}-16 \times P^4 + 0.000000000000035429 \times P^3 \\ &- 0.00000000000380467 \times P^2 + 0.000000000151947 \times P \\ &- 0.00000000000376254) \times T^4 \\ &+ (0.000000000000159364 \times P^4 - 0.0000000000491286 \times P^3 \\ &+ 0.00000000538378 \times P^2 - 0.000000222007 \times P \\ &+ 0.00000000512189) \times T^3 \\ &+ (-0.0000000000826768 \times P^4 + 0.000000026014 \times P^3 \\ &- 0.00000293356 \times P^2 + 0.00012714 \times P - 0.00000263185) \times T^2 \\ &+ (0.0000000195877 \times P^4 - 0.00000634261 \times P^3 \\ &+ 0.0007478 \times P^2 - 0.0354828 \times P + 0.000608078) \times T \\ &+ (-0.0000018437 \times P^4 + 0.000623884 \times P^3 - 0.0798237 \times P^2 \\ &+ 4.77618 \times P - 0.0536549)\end{aligned}$$

$$IF\ NWP = H70$$

$$SOC_{(j)} = 100 \times \frac{\rho_{(j)}}{40.2}$$

$$IF\ NWP = H35$$

$$SOC_{(j)} = 100 \times \frac{\rho_{(j)}}{24.0}$$

Equation A.46 is used to calculate the pressure ramp rate PRR. See Section H.2.3 and Section H.2.5 of SAE J2601 for a detailed explanation of pressure ramp rate control and equations. The unit of measure for *PRR* is MPa/sec.

(Eq. A.46) *(Note: see Section B.2.1 for changes proposed after test campaign.)*

$$IF\ \ t_{final\_sec\,(j)} \times \left(\frac{P_{final} - P_{initial}}{P_{final} - P_{min}}\right) - t > 10\ \ AND\ P_{ramp(j)} < 0.99 \times P_{final}$$

$$THEN$$

$$PRR_{\mathrm{MC}(j)} = \frac{P_{final} - P_{ramp(j)}}{t_{final\_sec\,(j)} \times \left(\frac{P_{final} - P_{initial}}{P_{final} - P_{min}}\right) - t}$$

$$ELSE$$

$$PRR_{\mathrm{MC}(j)} = PRR_{\mathrm{MC}(j-1)}$$

$$END\ IF$$

$$PRR_{(j)} = PRR_{\mathrm{MC}(j)}$$

Equation A.47 calculates the pressure drop between the ramp pressure P_{ramp} and the CHSS gas pressure. This pressure drop is used to dynamically calculate the threshold pressure $P_{threshold}$ in Equation A.48 and the temperature threshold $T_{threshold}$ for T_{gas} Throttle when this fuelling concept is utilized.

(Eq. A.47)

$$\Delta P_{(j)} = P_{ramp(j)} - MP_{(j)}$$

Where MP is the CHSS gas pressure communicated from the vehicle to the dispenser.

$$IF\ \Delta P_{(j)} \geq \Delta P_{max}\ \ THEN\ \Delta P_{max} = \Delta P$$

$$END\ IF$$

Equation A.48 implements the SOC Taper concept. It calculates a pressure ramp rate based the ramp pressure reaching P_{ramp_target} at the same time that SOC reaches SOC_{target}. This pressure ramp rate is termed PRR_{SOC}, and when it is smaller than the PRR calculated in Equation A.46, it is used as the PRR instead.

(Eq. A.48) *(Note: see Section B.2.2 for changes proposed after test campaign.)*

$P_{threshold} = P_{ramp\_target} - \Delta P_{(j)}$

$IF\ P_{ramp(j)} \geq P_{threshold}\ AND\ j > \ t_{lookback\_SOC}$

$THEN$

Calculate lookback SOC ramp rate:

$$SOCRR_{lookback(j)} = \frac{\left(SOC_{(j)} - SOC_{(j - t_{lookback})}\right)}{t_{lookback\_SOC}}$$

Calculate time remaining based on lookback SOC ramp rate:

$IF\ \ Press\ Class = H70, \mathrm{THEN}$

$$SOC_{max} = 69.444 \times \left[\frac{\left(P_{ramp\_target} + 0.1\right)}{\left(0.2782 \times T_{gas\_low} - 4.7145E - 05 \times T_{gas\_low}^2 - 6.18\right)} + 0.439\right]$$

$SOC_{end} = \mathrm{MINIMUM}\left[SOC_{max}\ , SOC_{target}\right]$

$$t_{remainSOC(j)} = \frac{\left(SOC_{end} - SOC_{(j)}\right)}{SOCRR_{lookback}(j)}$$

$ELSE\ IF\ \ Press\ Class = H35, \mathrm{THEN}$

$$SOC_{max} = 81.3 \times \left[\frac{\left(P_{ramp\_target} + 0.12\right)}{\left(0.1346 \times T_{gas_{low}} - 1.3637E - 05 \times T_{gas_{low}}^2 - 2.65\right)} + 0.227\right]$$

$SOC_{end} = \mathrm{MINIMUM}\left[SOC_{max}\ , SOC_{target}\right]$

$$t_{remainSOC(j)} = \frac{\left(SOC_{end} - SOC_{(j)}\right)}{SOCRR_{lookback}(j)}$$

$END\ IF$

Calculate PRR_{SOC}:

$IF\ \ t_{remainSOC(j)} > 0$

$THEN$

$$PRR_{SOC(j)} = \frac{\left(P_{ramp\_target} - \ P_{ramp(j)}\right)}{t_{remainSOC(j)}}$$

$ELSE$

$PRR_{SOC(j)} = 0$

$END\ IF$

$PRR_{(j)} = MINIMUM\left[PRR_{(j)}, PRR_{SOC(i)}\right]$

$END\ IF$

Equations A.49 and A.50 apply only to the T_{gas} Throttle fuelling concept. Only one of these equations is used, depending on the flag variable SELFADJUST. These equations calculate the pressure ramp rate $PRR_{throttle}$.

(Eq. A.49) *(Note: see Section B.2.3 for changes proposed after test campaign.)*

$IF\ TGASTHROTTLE = TRUE\ \ AND\ \ SELFADJUST = FALSE$

$THEN$

$T_{threshold} = T_{gas\_target} - a\Delta P_{max}$

$IF\ T_{gas\_high(j)} \geq T_{threshold}$

$THEN$

$$PRR_{threshold(j)} = \frac{(P_{final} - P_{min})}{t_{final\_sec(j)}}$$

$AD_{(j)} = MAXIMUM[b, a\Delta P_{(j)}]$

$$PRR_{throttle(j)} = \ MAXIMUM\left[0, \frac{PRR_{threshold(j)} x \left(T_{gas\_target} - T_{gas\_high_{(j)}}\right)}{AD_{(j)}}\right]$$

$PRR_{(j)} = MINIMUM[PRR_{(j)}, PRR_{throttle(j)}]$

$END\ IF$

$END\ IF$

(Eq. A.50) *(Note: see Section B.2.4 for changes proposed after test campaign.)*

$IF\ TGASTHROTTLE = TRUE\ \ AND\ \ SELFADJUST = TRUE$

$THEN$

$$T_{gas\_MA\_1(j)} = \frac{\sum_{(j-TMAL)}^{j} T_{gas\_high(j)}}{TMAL}$$

$$T_{gas\_MA\_2(j)} = \frac{\sum_{(j-TMAL)}^{j} T_{gas\_MA\_1(j)}}{TMAL}$$

$$T_{gas\_smooth(j)} = \frac{\sum_{(j-TMAL)}^{j} T_{gas\_MA\_2(j)}}{TMAL}$$

Note: in the above equations if j-TMAL < 0, then j-TMAL = 0

$T_{threshold} = T_{gas\_target} - a\Delta P_{max}$

$IF\ T_{gas\_smooth(j)} \geq T_{threshold}$

$THEN$

$$PRR_{threshold(j)} = \frac{(P_{final} - P_{min})}{t_{final\_sec(j)}}$$

$IF\ T_{gas\_smooth(j)} \geq T_{gas\_smooth\_threshold}$

$THEN\ \ T_{gas\_diff(j)} = \ T_{gas\_high(j)} - \ T_{gas\_smooth(j)}$

$ELSE\ \ T_{gas\_diff(j)} = 0$

$END\ IF$

$IF\ T_{gas\_diff(j)} \geq T_{gas\_diff\_max}\ \ THEN\ \ T_{gas\_diff\_max} = T_{gas\_diff(j)}$

$END\ IF$

$T_{gas\_offset} = T_{gas\_diff\_factor} \times T_{gas\_diff\_max}$

$T_{gas\_target} = T_{gas\_max} - T_{gas\_offset}$

$b = MAXIMUM\left[4, T_{gas\_offset\_multiplier} \times T_{gas\_offset}\right]$

$AD_{(j)} = MAXIMUM[b, a\Delta P_{(j)}]$

$$PRR_{throttle(j)} = MAXIMUM\left[0, \frac{PRR_{threshold(j)} x \left(T_{gas\_target} - T_{gas\_smooth_{(j)}}\right)}{AD_{(j)}}\right]$$

$PRR_{(j)} = MINIMUM[PRR_{(j)}, PRR_{throttle(j)}]$

$END\ IF$

$END\ IF$

Equation A.51 and A.52 apply to all fuelling concepts. Equation A.51 calculates the ramp pressure P_{ramp} for the next time step *j+1*.

(Eq. A.51)

$P_{ramp(j+1)} = P_{ramp(j)} + PRR_{(j)}$

$IF\ P_{ramp(j+1)} > P_{ramp_{target}}\ THEN\ P_{ramp(j+1)} = P_{ramp\_target}\ \ END\ IF$

Equation A.52 calculates the upper pressure corridor limit pressure P_{limit_high}.

(Eq. A.52)

$P_{limit\_high(j+1)} = P_{ramp(j+1)} + \Delta P_{tol\_high}$

$IF\ P_{limit\_high(j+1)} > P_{final}, THEN\ P_{limit\_high(j+1)} = P_{final}\ \ END\ IF$

A.1.1.11 Subroutine - Determine Communication Pressure Target

A pressure target is calculated for communication fills based on an end of fill target density of 40.2 g/l for the H70 pressure class and 24.0 g/l for the H35 pressure class, which has been discounted by SOC_{target} (i.e., pressure target = *f*(density * SOC_{target})). SOC_{target} is set in the Parameter Initialization Subroutine (A.1.1.2). The unit of measure for P_{target_comm} is MPa, the unit of measure for T_{gas_low} is Kelvin (K), and the unit of measure for SOC_{target} is % (e.g., 100% is expressed as 100). Equation A.53 has an accuracy of + 0/-0.08 MPa over the range of temperatures 233.15 K ≤ T_{gas_low} ≤ 358.15 K and range of target SOC 95 ≤ SOC_{target} ≤ 100, referencing data from the National Institute of Standards and Technology (NIST).

(Eq. A.53) *(Note: see Section B.2.5 for changes proposed after test campaign.)*

$$IF\ \ Press\ Class = H70,$$

$$P_{target\_comm} = \mathrm{MINIMUM}\big[P_{ramp\_target}, (0.0144 \times SOC_{target} - 0.439) \times (0.2782 \times T_{gas\_low} - 4.7145E - 05 \times T^2_{gas\_low} - 6.18) - 0.1\big]$$

$$ELSE\ IF\ \ Press\ Class = H35,$$

$$P_{target_{comm}} = \mathrm{MINIMUM}\left[P_{ramp_{target}}, (0.0123 \times SOC_{target} - 0.227) \times (0.1346 \times T_{gas_{low}} - 1.3637E - 05 \times T^2_{gas_{low}} - 2.65) - 0.12\right]$$

$$END\ IF$$

A.1.1.12 Subroutine - Evaluate End of Fill Criteria

This subroutine is utilized to determine if the end of fill criteria is met, which will then end the fill. The calculations in this subroutine shall be conducted at a frequency of no less than 10 Hz (10 calculations per second).

Note: When these fuelling concepts are implemented into a fuelling protocol standard, a P_{limit_comm} value will also be specified. The end of fill criteria will then be based on the minimum of P_{target_comm} and P_{limit_comm}. This is to ensure that the CHSS cannot be overfilled to an unsafe state of charge. P_{limit_comm} may be determined by a common set of values in a lookup table, or it may be communicated by the vehicle as one of the parameters. This needs further discussion in the during the development of the fuelling protocol standard, see PRHYDE Deliverable D6.8.

(Eq. A.54)

$$IF\ \ P_{station} \geq P_{target\_comm}\,,\ \ THEN\ \ END\ FILL$$

A.1.1.13 Subroutine - Process Check

This subroutine is used to check if temperature, pressure, and mass flow rate are within the process limits. If any of the process condition checks are not satisfied, the Process Check Subroutine fails, and the fill shall terminate as soon as possible, but within five seconds.

The unit of measure for $P_{station}$, and P_{limit_high} is MPa. The unit of measure of T_{amb} is ℃. The unit of measure for T_{gas_high}, T_{fuel}, and MAT_{30} is Kelvin (K). The unit of measure for t is seconds, and the unit of measure for $\dot{m}$ is g/s.

The calculations in this subroutine shall be conducted based on a time step *j*, which is advanced every one second. Thus, each calculation in this subroutine is conducted once every second.

(Eq. A.55)

$$IF\ P_{station} \leq 87.5,\ \ THEN\ \ PASS,\ \ \ ELSE\ \ FAIL$$

(Eq. A.56)

$$IF\ t > 15\ AND\ IF\ P_{station} \leq P_{limit\_high},\ \ THEN\ \ PASS,\ \ \ ELSE\ \ FAIL^{\dagger}$$

(Eq. A.57)

$$IF\ \ \text{-}40 \leq T_{amb} \leq 50,\ \ THEN\ \ PASS,\ \ \ ELSE\ \ FAIL$$

(Eq. A.58)

$$IF\ T_{gas\_high} < 358.15,\ \ THEN\ \ PASS,\ \ \ ELSE\ \ FAIL$$

(Eq. A.59)

$$IF\ T_{fuel} \geq 233.15,\ \ THEN\ \ PASS,\ \ \ ELSE\ \ FAIL$$

(Eq. A.60) - Applicable to Single Tank Tests Only

$$IF\ \dot{m} \leq 300,\ \ THEN\ \ PASS,\ \ \ ELSE\ \ FAIL$$

(Eq. A.61) - Applicable to Full Scale CHSS Tests Only

$$IF\ \dot{m} \leq 300,\ \ THEN\ \ PASS,\ \ \ ELSE\ \ FAIL$$

† Note to Eq. A.56: If the station pressure exceeds the upper pressure limit by 5 MPa or less, it shall come back within the limit within 5 seconds of the initial excursion or shall stop fuelling within 5 seconds of the initial excursion. If the magnitude of the excursion is greater than 5 MPa, the station shall stop fuelling within 5 seconds of the initial excursion.

A.1.1.14 Subroutine - Advance Counters

Advance the counter *j* by 1.

(Eq. A.62)

$$j = j + 1$$

The counter *n* is only advanced if mass is flowing, as represented in Equation A.63. During an intended non-fuelling event, the counter *n* does not advance.

(Eq. A.63)

$$IF\ \dot{m} > 0,\ \ n = n + 1$$

APPENDIX B: Learnings from protocol implementation

B.1 Learnings from testing

In additional to proving out the PRHYDE fuelling concepts and demonstrating their expected fuelling performance, a third objective of the testing regime was to determine if there were any issues with the original protocol control specification, see APPENDIX A, and if so, to rectify them. While testing, a few issues were found and revisions made to the fuelling protocol control specification. This should fix the problems identified and also improve performance. The changes made to the fuelling protocol control specification are described in the sections below.

B.2 Changes made to the fuelling protocol control specification

In the sections below, the changes made to the fuelling protocol specification are detailed. The original equation (as originally implemented for testing)is shown, the modified equation (as already incorporated in APPENDIX A) is shown, and the reasons for the modification are explained.

B.2.1 Changes made to Equation A.46

B.2.1.1 Original Equation

(Eq. A.46)

$$IF \quad t_{final\_\sec\,(j)} \times \left(\frac{P_{final} - P_{initial}}{P_{final} - P_{min}}\right) - t > 10 \quad AND\ P_{ramp(j)} < 0.99 \times P_{final}$$

$$THEN$$

$$PRR_{(j)} = \frac{P_{final} - P_{ramp(j)}}{t_{final\_\sec\,(j)} \times \left(\frac{P_{final} - P_{initial}}{P_{final} - P_{min}}\right) - t}$$

$$ELSE$$

$$PRR_{(j)} = PRR_{(j-1)}$$

B.2.1.2 Revised Equation

(Eq. A.46)

$$IF \quad t_{final\_\sec\,(j)} \times \left(\frac{P_{final} - P_{initial}}{P_{final} - P_{min}}\right) - t > 10 \quad AND\ P_{ramp(j)} < 0.99 \times P_{final}$$

$$THEN$$

$$PRR_{\mathrm{MC}(j)} = \frac{P_{final} - P_{ramp(j)}}{t_{final\_sec\,(j)} \times \left(\frac{P_{final} - P_{initial}}{P_{final} - P_{min}}\right) - t}$$

$ELSE$

$PRR_{\mathrm{MC}(j)} = PRR_{\mathrm{MC}(j-1)}$

$PRR_{(j)} = PRR_{\mathrm{MC}(j)}$

$END\ IF$

B.2.1.3 Explanation of changes

With the PRHYDE fuelling concepts, a number of pressure ramp rate values can be calculated. The MC Formula pressure ramp rate calculates the PRR as a function of t_{final}. The SOC Taper pressure ramp rate calculates PRR as a function of the *SOC*. The T_{gas} Throttle pressure ramp rate calculated PRR as a function of T_{gas_high}. The lowest PRR of these values is just named *PRR* and the value used in the ramp pressure control equation.

The original Equation A.46 utilized the nomenclature of PRR for the MC Formula calculated pressure ramp rate. For clarify, it should be named with a subscript like the other two *PRR* values, i.e. PRR_{SOC} and $PRR_{throttle}$. Therefore, in the second formula in equation A.46, *PRR* was changed to PRR_{MC}. There is an additional reason for making this change. When the first IF statement is false, the ELSE statement is used. Previously, $PRR_{(j)}$ was set to $PRR_{(j-1)}$. But $PRR_{(j-1)}$ may not have been the value calculated by the MC Formula pressure ramp rate since *PRR* is the lowest value of all three pressure ramp rates. When this happens, the PRR gets locked into the previous value and can no longer increase. That is not the intention, and this can cause the fill to slow down unnecessarily, hurting fuelling performance. Therefore, under the ELSE statement, $PRR_{MC(j)}$ is set to $PRR_{MC(j-1)}$ and then $PRR_{(j)}$ is set to $PRR_{MC(j)}$. This fixes the problem. Additionally, an END IF is added to the end of the equation for clarity.

B.2.2 Changes made to Equation A.48

B.2.2.1 Original Equation

(Eq. A.48)

$P_{threshold} = P_{ramp\_target} - \Delta P_{max}$

$IF\ P_{ramp(j)} \geq P_{threshold}\ AND\ j > t_{lookback}$

$THEN$

Calculate lookback SOC ramp rate:

$$IF\ j > t_{lookback}, THEN\ SOCRR_{lookback(j)} = \frac{\left(SOC_{(j)} - SOC_{(j-t_{lookback})}\right)}{t_{lookback}}$$

Calculate time remaining based on lookback SOC ramp rate:

$$t_{remainSOC(j)} = \frac{(SOC_{target} - SOC_{(j)})}{SOCRR_{lookback}(j)}$$

Calculate PRR_{SOC}:

$$PRR_{SOC(j)} = \frac{(P_{ramp\_target} - P_{ramp(j)})}{t_{remainSOC(j)}}$$

$$PRR_{(j)} = MINIMUM[PRR_{(j)}, PRR_{SOC(i)}]$$

B.2.2.2 Revised Equation

(Eq. A.48)

$$P_{threshold} = P_{ramp\_target} - \Delta P_{(j)}$$

$$IF\ P_{ramp(j)} \geq P_{threshold}\ AND\ j > t_{lookback\_SOC}$$

$$THEN$$

Calculate lookback SOC ramp rate:

$$SOCRR_{lookback(j)} = \frac{(SOC_{(j)} - SOC_{(j-t_{lookback})})}{t_{lookback\_SOC}}$$

Calculate time remaining based on lookback SOC ramp rate:

$$IF\ \ Press\ Class = H70, \mathrm{THEN}$$

$$SOC_{max} = 69.444 \times \left[\frac{(P_{ramp\_target} + 0.1)}{(0.2782 \times T_{gas\_low} - 4.7145E - 05 \times T_{gas\_low}^{2} - 6.18)} + 0.439\right]$$

$$SOC_{end} = \mathrm{MINIMUM}[SOC_{max}, SOC_{target}]$$

$$t_{remainSOC(j)} = \frac{(SOC_{end} - SOC_{(j)})}{SOCRR_{lookback}(j)}$$

$$ELSE\ IF\ \ Press\ Class = H35, \mathrm{THEN}$$

$$SOC_{max} = 81.3 \times \left[\frac{(P_{ramp\_target} + 0.12)}{(0.1346 \times T_{gas_{low}} - 1.3637E - 05 \times T_{gas_{low}}^{2} - 2.65)} + 0.227\right]$$

$$SOC_{end} = \mathrm{MINIMUM}[SOC_{max}, SOC_{target}]$$

$$t_{remainSOC(j)} = \frac{(SOC_{end} - SOC_{(j)})}{SOCRR_{lookback}(j)}$$

$$END\ IF$$

Calculate PRR_{SOC}:

$$IF\ \ t_{remainSOC(j)} > 0$$

$$THEN$$

$$PRR_{SOC(j)} = \frac{(P_{ramp\_target} - P_{ramp(j)})}{t_{remainSOC(j)}}$$

$$ELSE$$

$$PRR_{SOC(j)} = 0$$

$$END\ IF$$

$$PRR_{(j)} = MINIMUM[PRR_{(j)}, PRR_{SOC(i)}]$$

$$END\ IF$$

B.2.2.3 Explanation of changes

The first change to equation A.48 is to replace ΔP_{max} with $\Delta P_{(j)}$ in the formula for $P_{threshold}$ on the first line. Testing showed that SOC Taper can be activated even when it is not needed. And once SOC Taper is activated, it only reduces the pressure ramp rate. The pressure ramp rate cannot increase, because a newly calculated PRR_{SOC} cannot be higher than the PRR_{SOC} calculated in the previous time step. This can especially be problematic when T_{gas} Throttle is active because T_{gas} Throttle modulates (decreases and increases) the pressure ramp rate according to T_{gas_high}, but SOC Taper constrains this modulation to only decreasing the pressure ramp rate. SOC Taper should only be active when it is needed, and when it is not needed, it should either not activate or deactivate. This is why ΔP_{max} is replaced with $\Delta P_{(j)}$ in the formula for $P_{threshold}$ on the first line of equation A.48. With this change, $P_{threshold}$ can float up and down according to the pressure drop $\Delta P_{(j)}$, which allows the SOC Taper function to activate and deactivate when needed, depending on the magnitude of the pressure drop and the current value of P_{ramp}.

Another issue which was discovered during testing is that it is possible for two parameters that have discretionary settings to be incompatible. These two parameters are P_{ramp_target} and SOC_{target}. These parameters are set in Subroutine A.1.1.2, Section A.1.1.2.2. As an example, if SOC_{target} is set to 99, and P_{ramp_target} is set to 85, P_{target_comm} (as calculated in equation A.53) will be above P_{ramp_target} if T_{gas_low} is greater than 80.3 °C. This means that many fills will never achieve the end of fill criteria. One solution to this would be to provide guidance on setting SOC_{target} and P_{ramp_target} so they are coordinated and not incompatible. However, it is challenging to make this infallible. Therefore, instead, SOC_{target} was replaced in the formula for t_{remain_SOC} with a new parameter called SOC_{end}, which is derived based on the lower of SOC_{target} and another new parameter SOC_{max}. SOC_{max} calculates the maximum SOC that is achievable based on the P_{ramp_target}. Because this is a function of the NWP, there are two separate formulas, one for H70 and another for H35. This ensures that SOC_{end} in the formula for t_{remain_SOC} is based on the highest possible SOC, regardless of the P_{ramp_target} setting. An additional change was made to equation A.53, so that P_{target_comm} cannot be calculated higher than P_{ramp_target}. This is explained in more detail below.

Although it is unlikely, there may be scenarios where t_{remain_SOC} is less than zero (this would likely only occur for a single time step just before the target pressure is reached). Therefore, to prevent either a division by zero or a negative PRR_{SOC} value, an IF statement was added which sets the PRR_{SOC} to zero under this circumstance.

Finally, END IF statements were added where appropriate for clarity.

B.2.3 Changes made to Equation A.49

B.2.3.1 Original Equation

(Eq. A.49)

$$IF\ TGASTHROTTLE = TRUE\ \ AND\ \ SELFADJUST = FALSE$$

$$THEN$$

$$T_{threshold} = T_{gas\_target} - a\Delta P_{max}$$

$$IF\ T_{gas\_high(j)} \geq T_{threshold}$$

$$IF\ T_{gas\_high(j)} \geq T_{threshold}\, for\ first\ time, THEN\ Set\ PRR_{threshold} = PRR_{(j)}$$

$$THEN$$

$$AD_{(j)} = MAXIMUM[b, a\Delta P_{(j)}]$$

$$PRR_{throttle(j)} = \frac{PRR_{threshold}x\left(T_{gas\_target} - T_{gas\_high_{(i)}}\right)}{AD_{(j)}}$$

$$PRR_{(j)} = MINIMUM[PRR_{(j)}, PRR_{throttle(j)}]$$

B.2.3.2 Revised Equation

(Eq. A.49)

$$IF\ TGASTHROTTLE = TRUE\ \ AND\ \ SELFADJUST = FALSE$$

$$THEN$$

$$T_{threshold} = T_{gas\_target} - a\Delta P_{max}$$

$$IF\ T_{gas\_high(j)} \geq T_{threshold}$$

$$THEN$$

$$PRR_{threshold(j)} = \frac{(P_{final} - P_{min})}{t_{final\_sec(j)}}$$

$$AD_{(j)} = MAXIMUM[b, a\Delta P_{(j)}]$$

$$PRR_{throttle(j)} = \ MAXIMUM\left[0, \frac{PRR_{threshold(j)}x\left(T_{gas\_target} - T_{gas\_high_{(j)}}\right)}{AD_{(j)}}\right]$$

$$PRR_{(j)} = MINIMUM[PRR_{(j)}, PRR_{throttle(j)}]$$

$$END\ IF$$

$$END\ IF$$

B.2.3.3 Explanation of changes

The method for calculating $PRR_{threshold}$ was changed. Originally, $PRR_{threshold}$ was calculated as the pressure ramp rate $PRR_{(j)}$ at the first instance that T_{gas_high} exceeded $T_{threshold}$. However, during testing, there were some tests where the fuel delivery temperature was still not at the target value when T_{gas_high} exceeded $T_{threshold}$. PRR is a function of t_{final}, which depends on the value of MAT_C, and at this point in the fill, MAT_C was still substantially warmer than it would eventually become later in the fill. The term $PRR_{threshold}$ / AD in the $\mathrm{PRR_{throttle}}$ equation acts like the proportional coefficient "K_p" in the proportional term of a PID control equation. Therefore, when $PRR_{threshold}$ is smaller than it should be, the $PRR_{throttle}$ calculated will also be smaller than it should be, resulting in a lower T_{gas_high} temperature and a longer fuelling time. To correct this issue, the method for calculating $PRR_{threshold}$ was changed so that it is a function of t_{final}. This way, $PRR_{threshold}$ changes during the fill. When MAT_C is warmer, t_{final} will be larger, and when MAT_C is colder, t_{final} will be shorter, causing $PRR_{threshold}$ to be lower and higher, respectively. Another rationale for this is that the temperature development in the CHSS is a function of MAT_C. The colder MAT_C is, the lower T_{gas_high} will be, everything else being equal, and visa versa. It is therefore logical that the coefficient $PRR_{threshold}$ / AD in the $\mathrm{PRR_{throttle}}$ equation should effectively be a function of MAT_C, because $PRR_{threshold}$ / AD is the driving force that pushes T_{gas_high} towards T_{gas_target}, so when MAT_C is colder, this driving force should be higher, and visa versa.

The $\mathrm{PRR_{throttle}}$ equation was also changed so that it cannot be a negative value. Previously, if T_{gas_high} exceeded T_{gas_target}, $PRR_{throttle}$ would be a negative value, causing the ramp pressure to decrease. It is undesirable for the ramp pressure to decrease, so $PRR_{throttle}$ is now set as the maximum of zero or the calculated value.

Finally, END IF statements were added where appropriate for clarity.

B.2.4 Changes made to Equation A.50

B.2.4.1 Original Equation

(Eq. A.50)

$$IF\ TGASTHROTTLE = TRUE\ \ AND\ \ SELFADJUST = TRUE$$

$$THEN$$

$$T_{gas\_MA\_1(j)} = \frac{\sum_{(j-TMAL)}^{j} T_{gas\_high(j)}}{TMAL}$$

$$T_{gas\_MA\_2(j)} = \frac{\sum_{(j-TMAL)}^{j} T_{gas\_MA\_1(j)}}{TMAL}$$

$$T_{gas\_smooth(j)} = \frac{\sum_{(j-TMAL)}^{j} T_{gas\_MA\_2(j)}}{TMAL}$$

Note: in the above equations if j-TMAL < 0, then j-TMAL = 0

$$T_{threshold} = T_{gas\_target} - a\Delta P_{max}$$

$$IF\ T_{gas\_smooth(j)} \geq T_{threshold}$$

$$IF\ T_{gas\_smooth(j)} \geq T_{threshold}\ for\ first\ time, THEN\ Set\ PRR_{threshold} = PRR_{(j)}$$

$$THEN$$

$$IF\ T_{gas\_smooth(j)} \geq T_{gas\_smooth\_threshold}$$

$$THEN\ \ T_{gas\_diff(j)} = T_{gas\_high(j)} - T_{gas\_smooth(j)}$$

$$ELSE\ \ T_{gas\_diff(j)} = 0$$

$$IF\ T_{gas\_diff(j)} \geq T_{gas\_diff\_max}\ \ THEN\ \ T_{gas\_diff\_max} = T_{gas\_diff(j)}$$

$$T_{gas\_offset} = T_{gas\_diff\_factor} \times T_{gas\_diff\_max}$$

$$T_{gas\_target} = T_{gas\_max} - T_{gas\_offset}$$

$$b = MAXIMUM\left[4, T_{gas\_offset\_multiplier} \times T_{gas\_offset}\right]$$

$$AD_{(j)} = MAXIMUM[b, a\Delta P_{(j)}]$$

$$PRR_{throttle(j)} = \frac{PRR_{threshold} x \left(T_{gas\_target} - T_{gas\_smooth_{(i)}}\right)}{AD_{(j)}}$$

$$PRR_{(j)} = MINIMUM[PRR_{(j)}, PRR_{throttle(j)}]$$

B.2.4.2 Revised Equation

(Eq. A.50)

$$IF\ TGASTHROTTLE = TRUE\ \ AND\ \ SELFADJUST = TRUE$$

$$THEN$$

$$T_{gas\_MA\_1(j)} = \frac{\sum_{(j-TMAL)}^{j} T_{gas\_high(j)}}{TMAL}$$

$$T_{gas\_MA\_2(j)} = \frac{\sum_{(j-TMAL)}^{j} T_{gas\_MA\_1(j)}}{TMAL}$$

$$T_{gas\_smooth(j)} = \frac{\sum_{(j-TMAL)}^{j} T_{gas\_MA\_2(j)}}{TMAL}$$

Note: in the above equations if j-TMAL < 0, then j-TMAL = 0

$$T_{threshold} = T_{gas\_target} - a\Delta P_{max}$$

$$IF\ T_{gas\_smooth(j)} \geq T_{threshold}$$

$$THEN$$

$$PRR_{threshold(j)} = \frac{(P_{final} - P_{min})}{t_{final\_sec(j)}}$$

$$IF\ T_{gas\_smooth(j)} \geq T_{gas\_smooth\_threshold}$$

$$THEN\ \ T_{gas\_diff(j)} = T_{gas\_high(j)} - T_{gas\_smooth(j)}$$

$$ELSE\ \ T_{gas\_diff(j)} = 0$$

$$END\ IF$$

$$IF\ T_{gas\_diff(j)} \geq T_{gas\_diff\_max}\ \ THEN\ \ T_{gas\_diff\_max} = T_{gas\_diff(j)}$$

$$END\ IF$$

$$T_{gas\_offset} = T_{gas\_diff\_factor} \times T_{gas\_diff\_max}$$

$$T_{gas\_target} = T_{gas\_max} - T_{gas\_offset}$$

$$b = MAXIMUM\left[4, T_{gas\_offset\_multiplier} \times T_{gas\_offset}\right]$$

$$AD_{(j)} = MAXIMUM[b, a\Delta P_{(j)}]$$

$$PRR_{throttle(j)} = MAXIMUM\left[0, \frac{PRR_{threshold(j)} x \left(T_{gas\_target} - T_{gas\_smooth_{(j)}}\right)}{AD_{(j)}}\right]$$

$$PRR_{(j)} = MINIMUM[PRR_{(j)}, PRR_{throttle(j)}]$$

$$END\ IF$$

$$END\ IF$$

B.2.4.3 Explanation of changes

The same changes that were made to equation A.49 were also made to equation A.50. For an explanation of these changes, see B.2.2.3.

B.2.5 Changes made to Equation A.53

B.2.5.1 Original Equation

(Eq. A.53)

$$IF\ \ Press\ Class = H70,$$

$$P_{target\_comm} = (0.0144 \times SOC_{target} - 0.439) \times (0.2782 \times T_{gas\_low} - 4.7145E - 05 \times T_{gas\_low}^2 - 6.18) - 0.1$$

$$IF\ \ Press\ Class = H35,$$

$$P_{target\_comm} = (0.0123 \times SOC_{target} - 0.227) \times (0.1346 \times T_{gas\_low} - 1.3637E - 05 \times T_{gas\_low}^2 - 2.65) - 0.12$$

B.2.5.2 Revised Equation

(Eq. A.53)

$$IF\ \ Press\ Class = H70,$$

$$P_{target\_comm} = \text{MINIMUM}\big[P_{ramp\_target}, (0.0144 \times SOC_{target} - 0.439) \times (0.2782 \times T_{gas\_low} - 4.7145E - 05 \times T_{gas\_low}^2 - 6.18) - 0.1\big]$$

$$ELSE\ IF\ \ Press\ Class = H35,$$

$$P_{target_{comm}} = \text{MINIMUM}\left[P_{ramp_{target}}, (0.0123 \times SOC_{target} - 0.227) \times (0.1346 \times T_{gas_{low}} - 1.3637E - 05 \times T_{gas_{low}}^2 - 2.65) - 0.12\right]$$

$$END\ IF$$

B.2.5.3 Explanation of changes

As explained in the changes made to equation A.48 (see B.2.1), it was previously possible to set values for SOC_{target} and P_{ramp_target} which were incompatible. In these cases, the fill would never reach the end of fill criteria due to P_{ramp_target} being lower than P_{target_comm}. Therefore, equation A.53 was changed so that P_{target_comm} is lower of the calculated value and P_{ramp_target}. This ensures that P_{target_comm} can be reached so that the end of fill criteria in equation A.54 can be satisfied.

Finally, ELSE IF and END IF statements were added for clarity.

APPENDIX C: Test facilities and equipment utilised during the PRHYDE project

C.1 General

The following is a short overview of the test equipment used during the project.

C.2 Test layout at ZBT HYDROGEN TESTFIELD

The following figure shows the simplified P&ID of experimental setup of the HYDROGEN TESTFIELD at ZBT in Duisburg, Germany. .

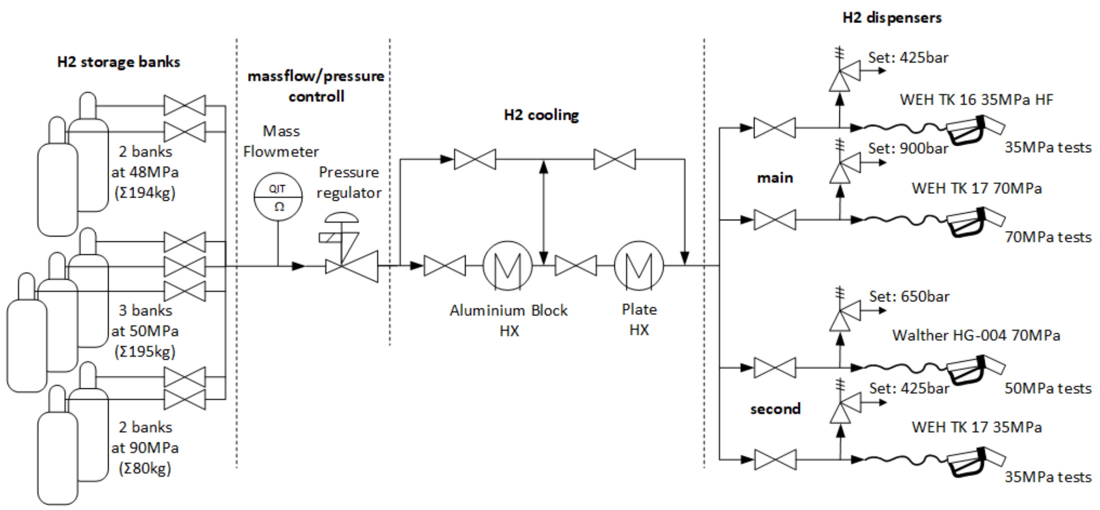

Figure 55: **Experimental setup ZBT test site (Source: ZBT)**

The setup consists out of 7 pressure storage banks from 48 up to 90 MPa, a Coriolis mass flowmeter, a pressure regulator, a hydrogen precooling unit and different dispenser lines.

Contrary to what is shown here in simplified form, the structure has a large number of additional sensors for pressure and temperature at all relevant points.

The following figures show the measuring points layout for the 35, 50 and 70MPa highly instrumented tanks tested at ZBT and the dispenser instrumentation.

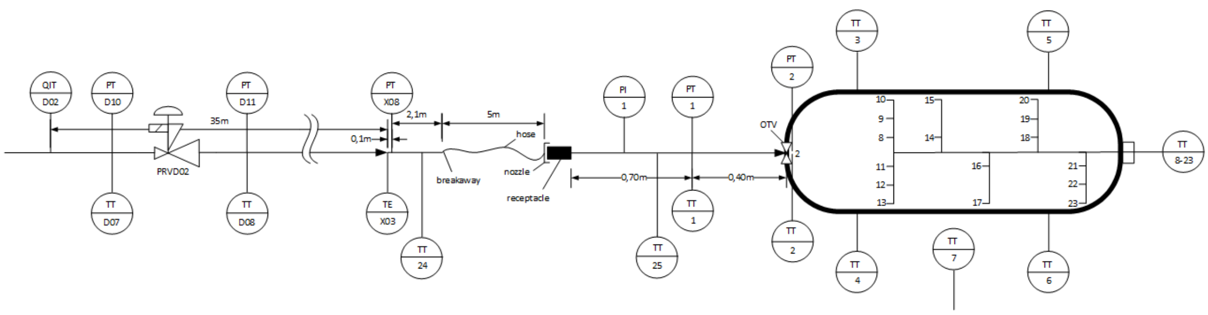

Figure 56: **35MPa type 3 tank (322L) (Source: ZBT)**

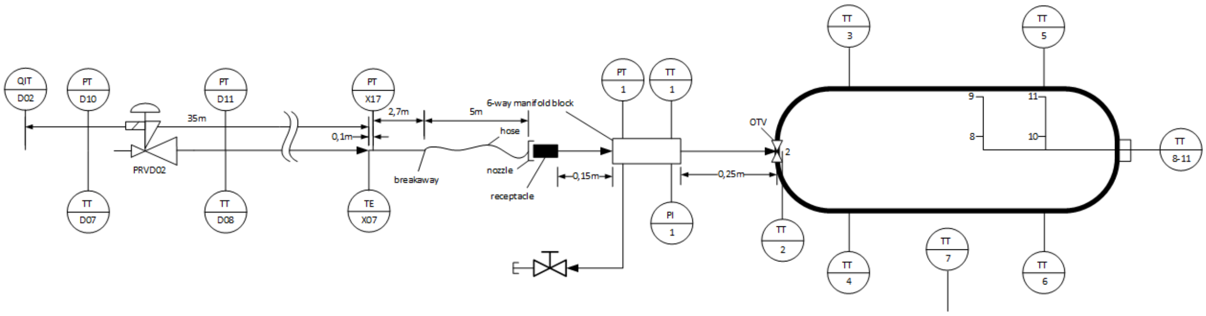

Figure 57: **50MPa type 4 tank (341L) (Source: ZBT)**

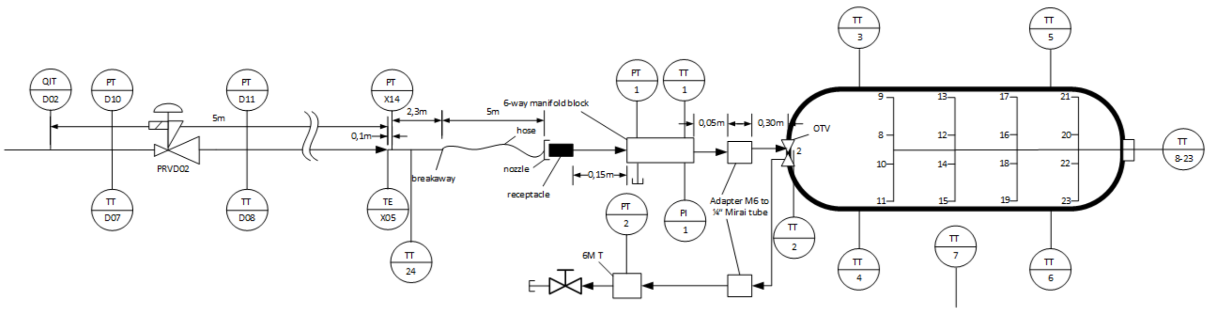

Figure 58: **70MPa type 4 tank (240L) (Source: ZBT)**

During a fuelling all test data are logged at a frequency of 2 Hz via the central PLC of the HYDROGEN TESTFIELD. After the test, the fuelled hydrogen was returned to the storage banks in a controlled manner.

C.3 Summary of Nikola's Contracted Test Facility (TesTneT Gmbh)

Nikola tested a Type IV, 165L, H70 vessel instrumented with a thermocouple tree and pressure sensor. Pressure, temperature, and mass-flow rate measurements were also attained upstream of the vessel. The vessel was tested inside an environmental chamber which allowed for temperature control of the ambient temperature, initial gas temperature, and vessel soak temperature.

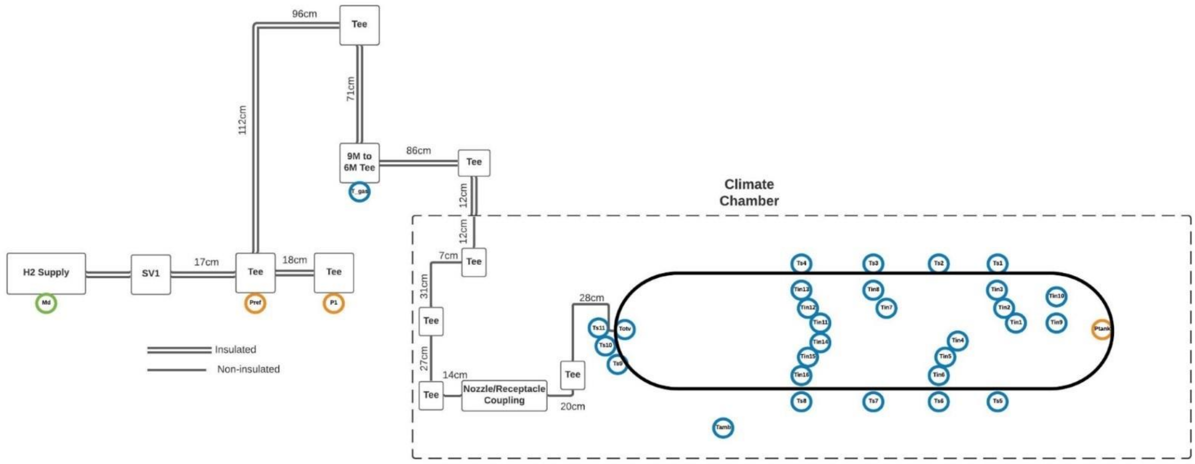

Figure 59: Experimental Set-up Nikola test site (Source: Nikola)

APPENDIX D: Test Results

D.1 ZBT Phase 1 testing results

Due to the very large number of tests, only one exemplary measurement for each 70, 50 and 35 MPa tank is presented here.

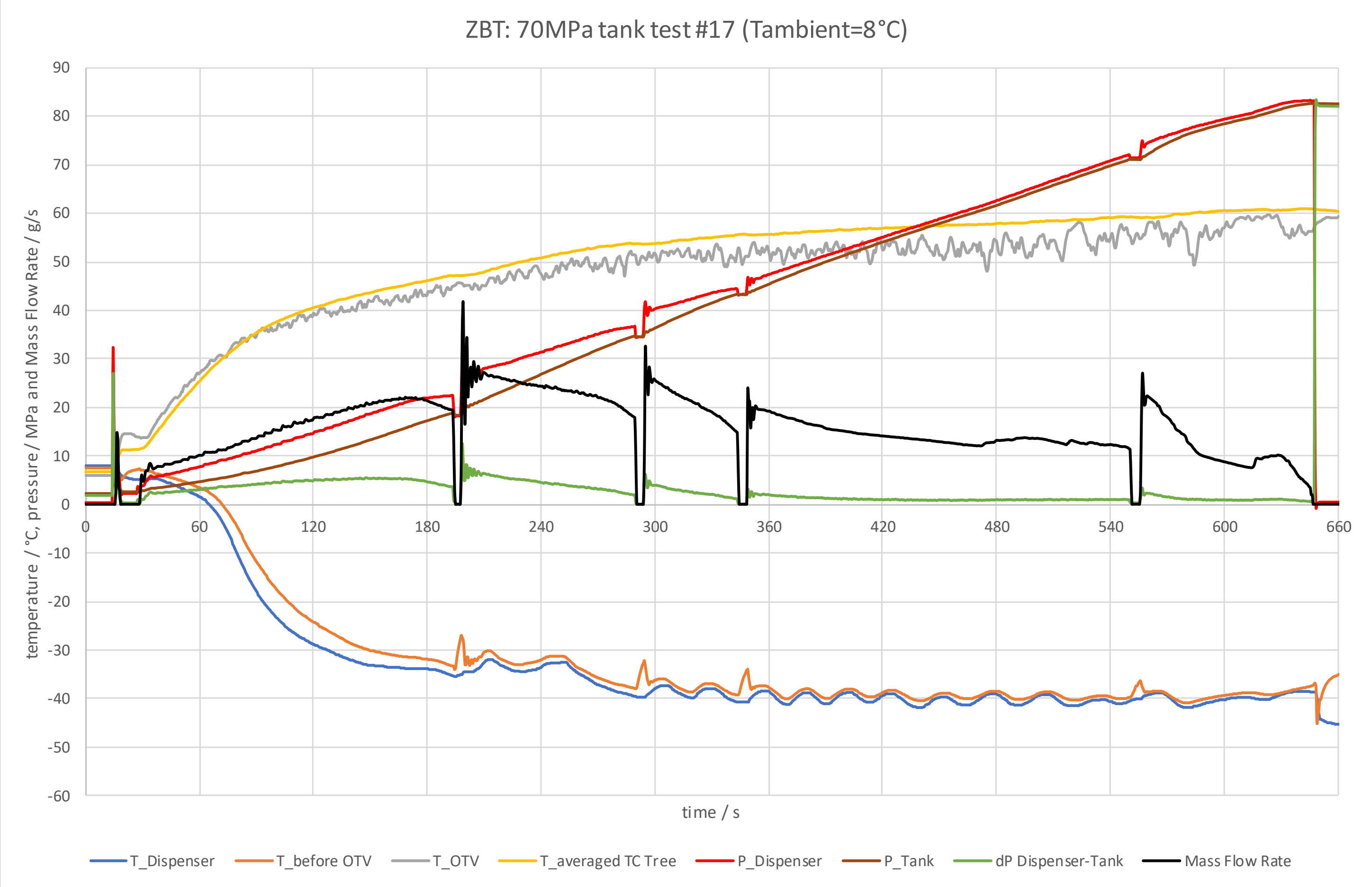

Figure 60: ZBT Tank Test #17

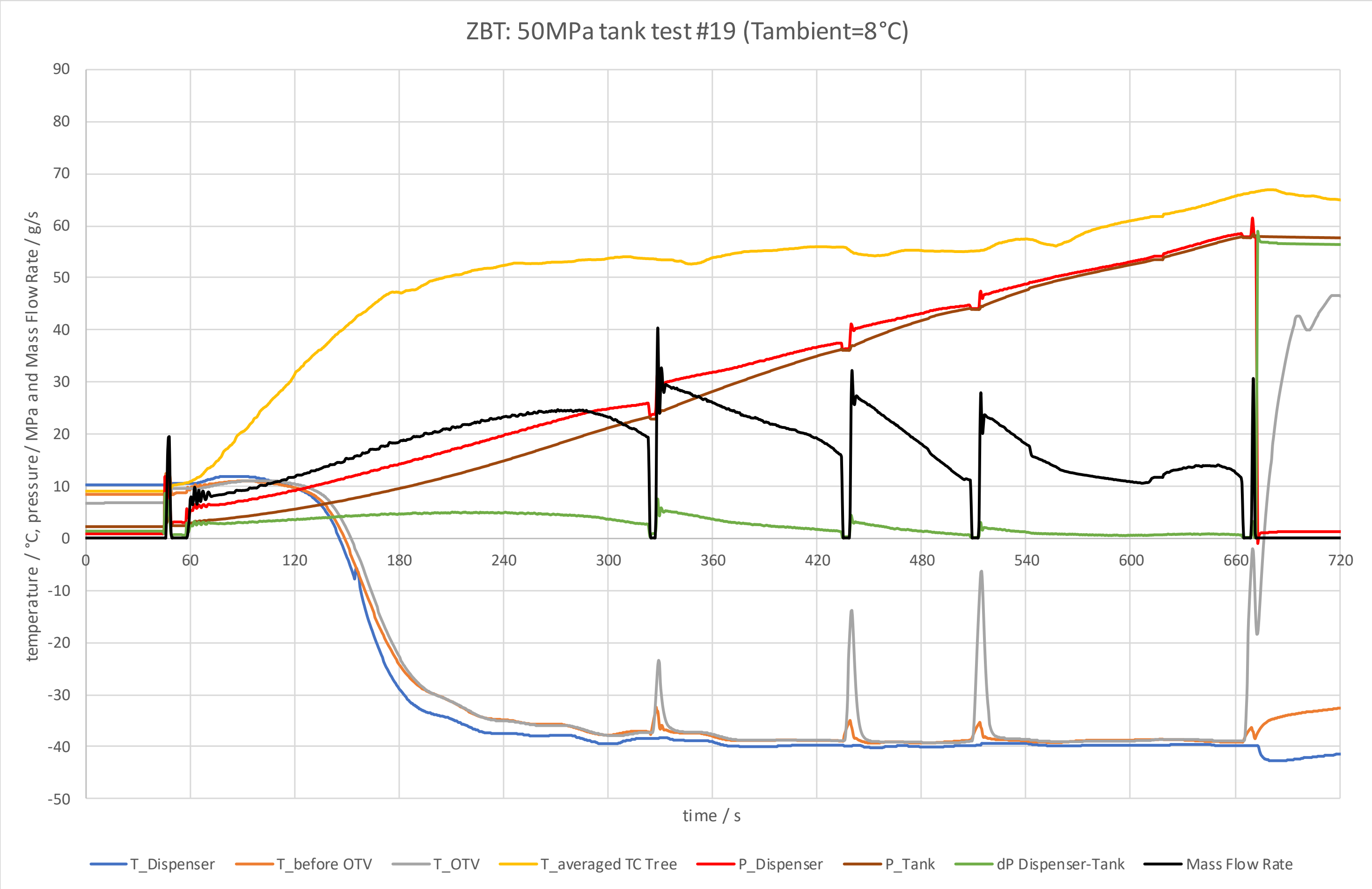

Figure 61: ZBT Tank Test #19

Annotation to Figure 61: The TC Tree consists out of only four remaining temperature sensors in the upper part of the vessel (the four in the lower part of the vessel were destroyed during assembly), the OTV temperature sensor is totally dominated by the injected precooled hydrogen and the P_{Tank} is for this vessel the Pressure before OTV (no pressure measure in the tank).

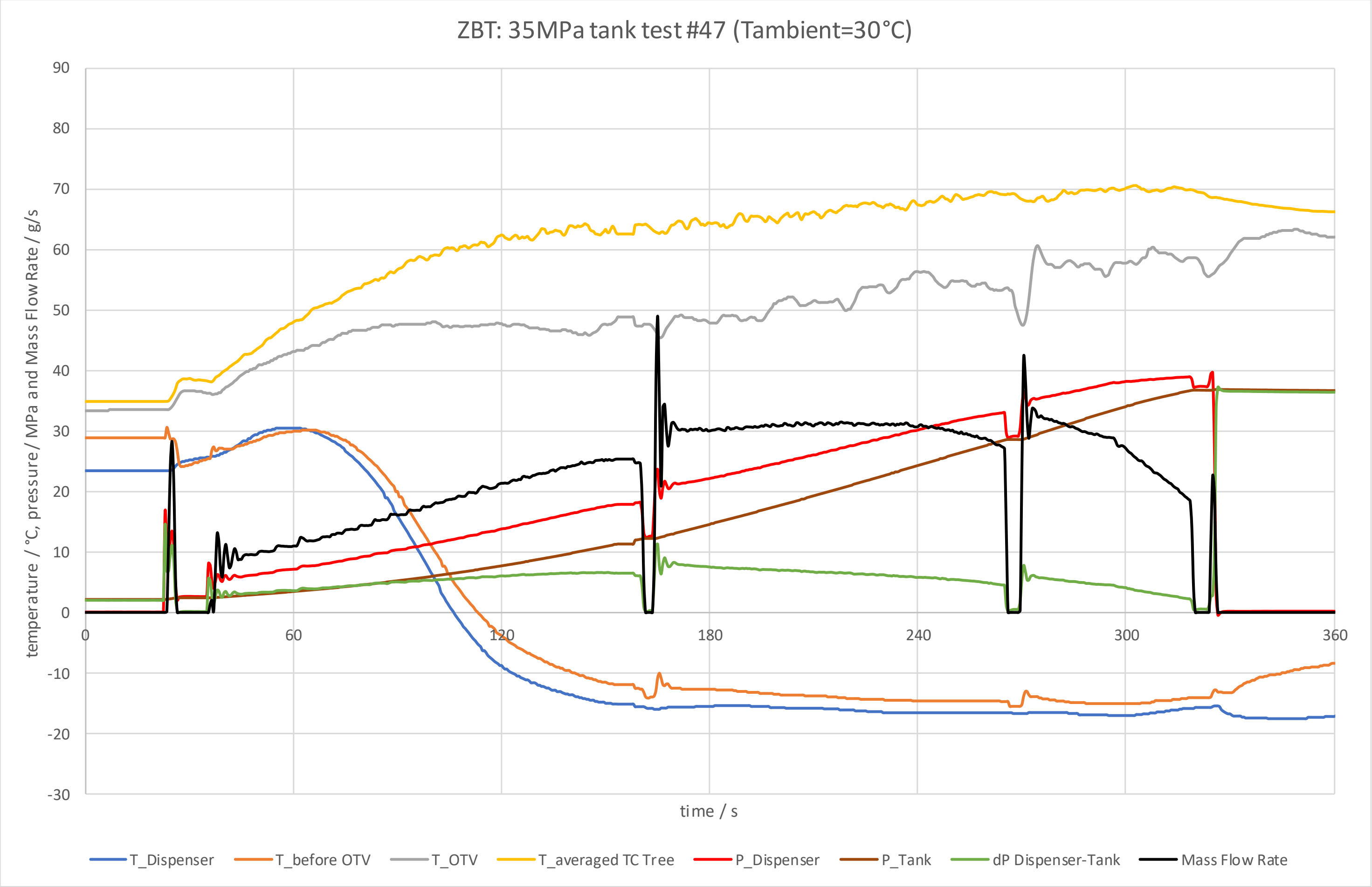

Figure 62: ZBT Tank Test #47

Annotation to Figure 62: The TC Tree consists out of only of 15 remaining temperature sensors in the vessel and the OTV temperature sensor shows high deviation to the averaged TC Tree temperatures.

D.2 Nikola Phase 1 testing results

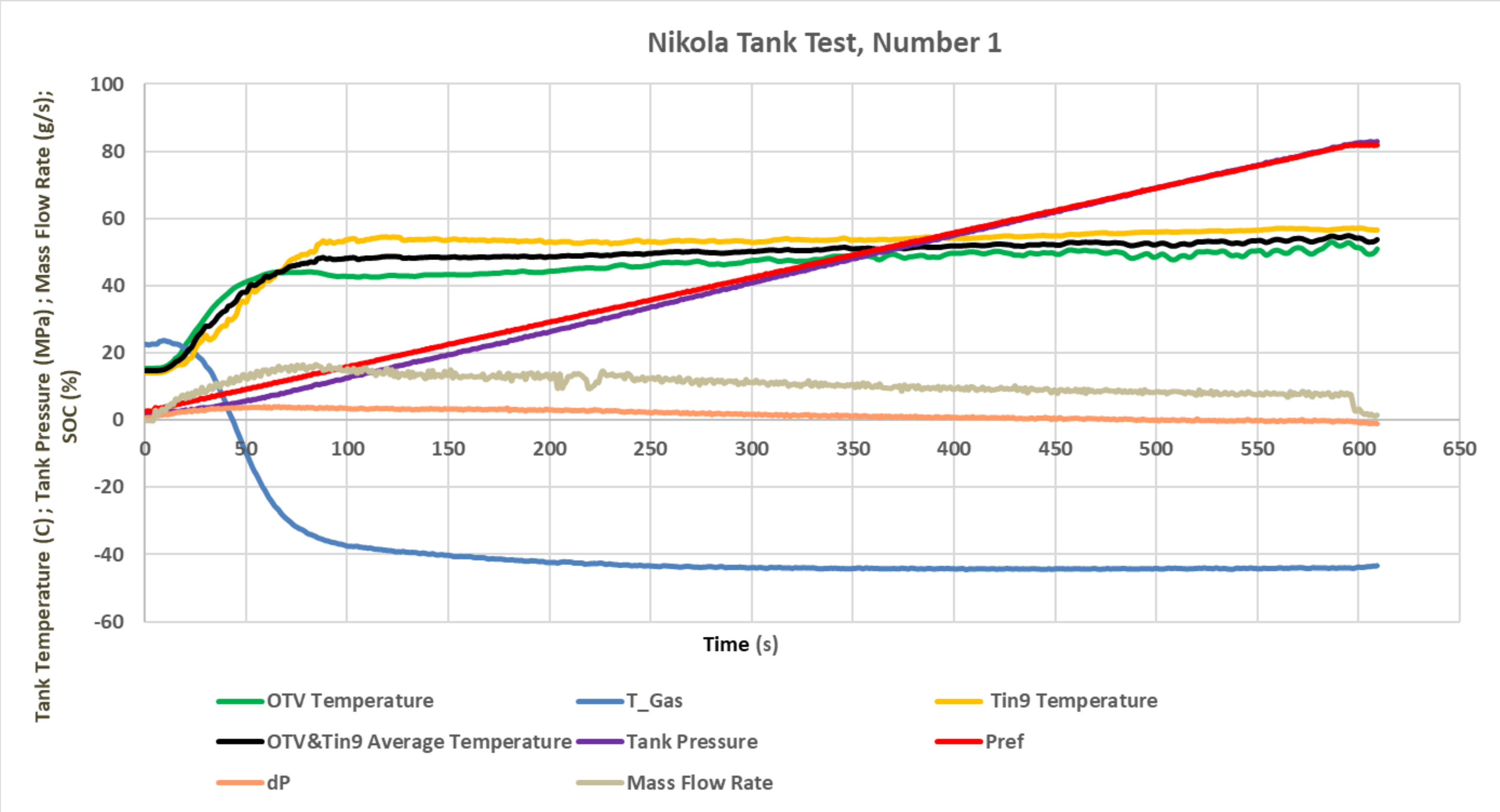

Figure 63: Nikola Test #1

D.3 ZBT Phase 2 testing results

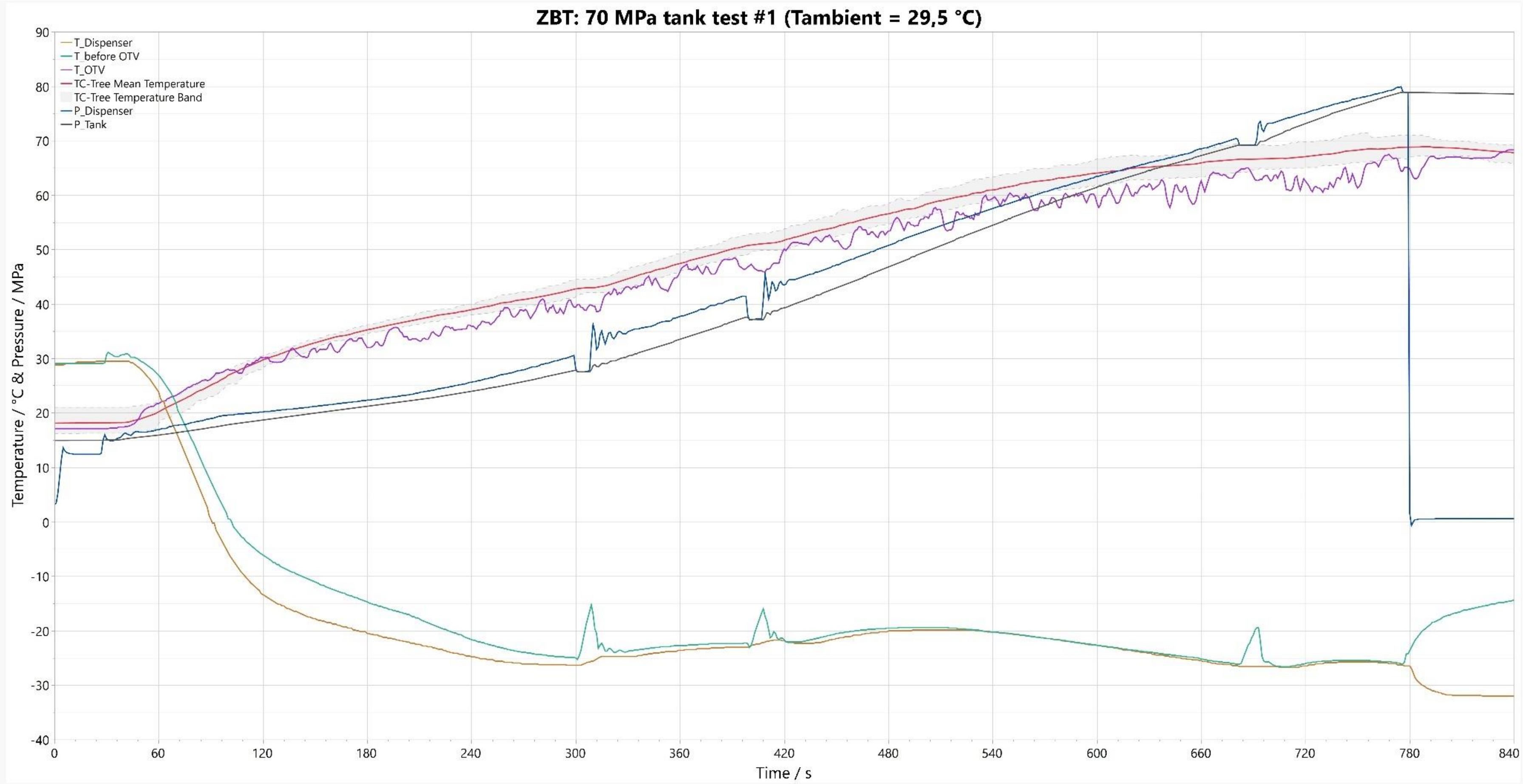

Figure 64: ZBT Tank Test #1

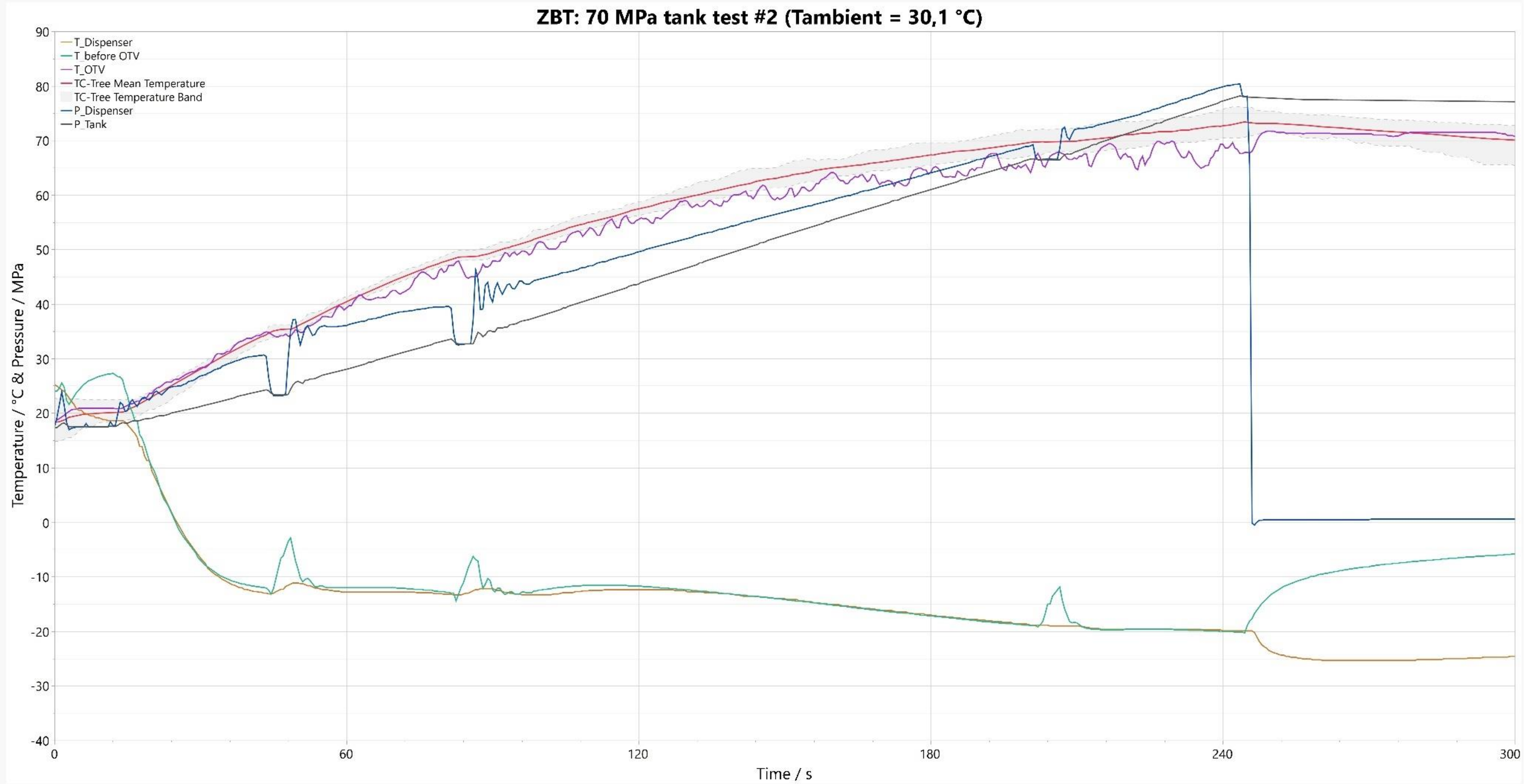

Figure 65: **ZBT Tank Test #2**

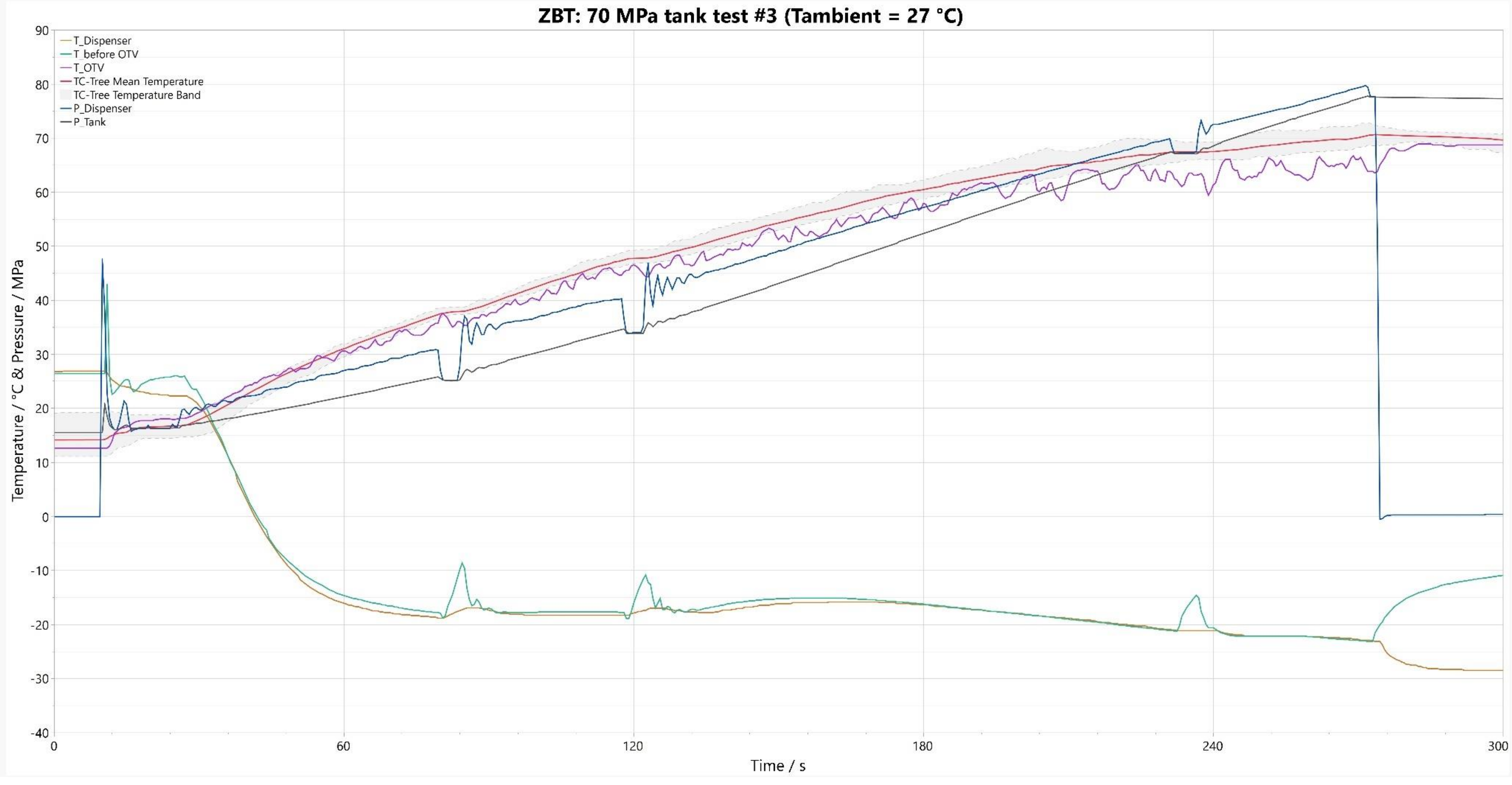

Figure 66: **ZBT Tank Test #3**

Figure 67: **ZBT Tank Test #4**

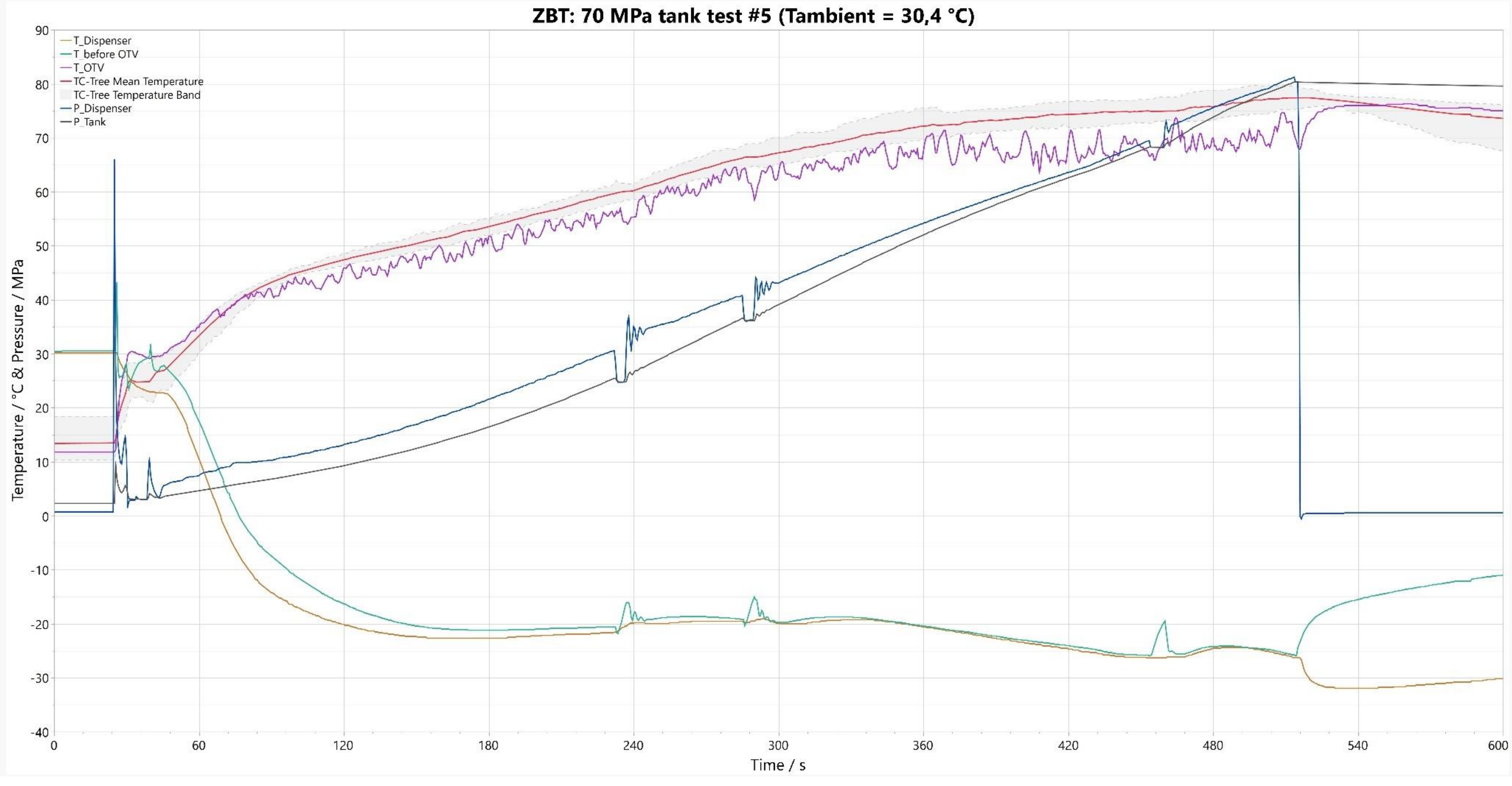

Figure 68: ZBT Tank Test #5

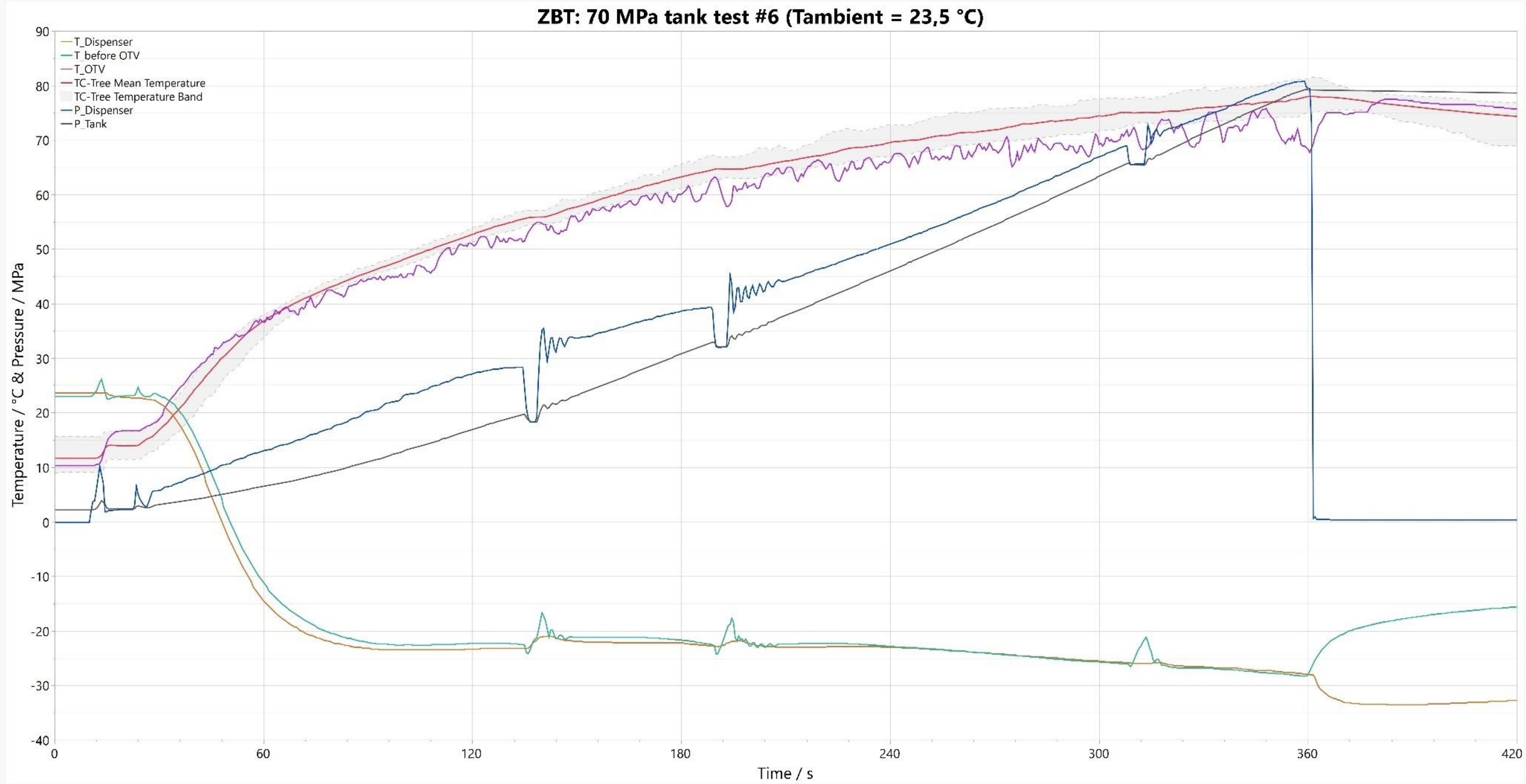

Figure 69: **ZBT Tank Test #6**

D.4 Nikola Phase 2 testing results

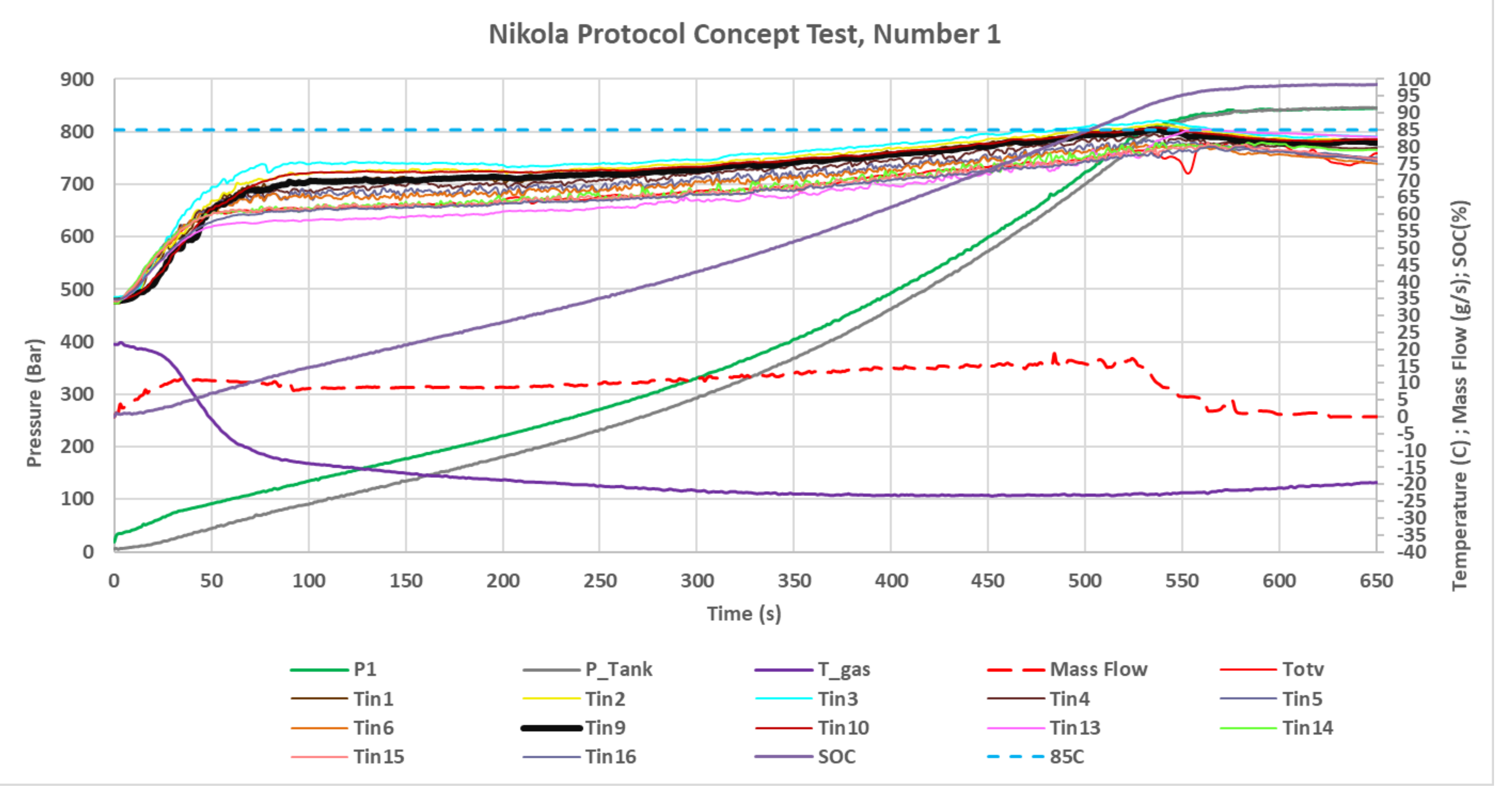

Figure 70: Nikola Protocol Concept Test #1

APPENDIX E: Risk Assessment

Please note: This chapter is an extract from a confidential PRHYDE document.

The original PRHYDE report was written by: Claus Due Sinding, Bjarne Vig (Nel Hydrogen), Steve Mathison (First Element Fuel, external Expert), Spencer Quong (Quong & associates, Inc. On behalf of Toyota Motor North America), Ethan Metsger, Todd Comins (Shell), James Sneddon (RiskTec Solutions Ltd., external Expert).

The PRHYDE Risk Assessment on novel fuelling concepts was done to the best of our abilities with help from external experts. The performed Risk Assessment is the first milestone in assessing the risks arising from the novel fuelling concepts. End-implementation should include separate Risk Assessment by the individual station manufacturers and OEMs for most accurate mitigation of risk.

E.1 Executive Summary

PRYHDE Work Package Three (WP3) held risk assessment sessions between May 2021 and March 2022. WP3 consisted of a team of experts from PRHYDE partner companies and external experts from invited organizations. The primary objective of the risk assessment was to identify the hazards associated with use of the PRHYDE fuelling concepts and corresponding prevention and mitigation barriers. This work extends prior risk assessments made by EIGA and others **see PRHYDE Deliverable D2.2**, taking special care to focus on threats and initiating events particular to the PRHYDE fuelling protocols.

Risk assessment was performed using standard Bowtie and LOPA frameworks.

The threat identified for all the fuelling concepts was following a wrong pressure ramp rate (PRR) that results in the gas temperature in the CHSS exceeding the limit. Initiating events identified which can lead to this threat are: T_{fuel} error, mass flow error, station pressure error, ambient temperature error for all of the fuelling concepts, and T_{gas} vehicle error for the Type 3 fuelling concepts. In addition to identifying the initiating events, consideration was also given to enabling factors.

Preventive barriers were identified for each initiating event, along with an associated PFD value. Some preventive barriers were identified but not utilized, either due to the WP3 experts not being able to assess a correct PFD value or due to the barrier not being desirable.

Because the probability of loss of containment at temperatures above the CHSS qualification temperature is unknown, the PRHYDE WP3 risk assessment decided to assign a probability distribution as a function of the temperature exceedance. Since no data is available, the probability distribution was considered under three cases: Very Conservative, Medium Conservative, Less Conservative

Once the probability distributions were determined, the other consideration was the determination of the overtemperature potential for the initiating events under consideration. To determine this, WP4 conducted fuelling simulations with a wrong fuel delivery temperature, a wrong ambient temperature, a wrong mass flow rate, and the wrong CHSS T_{gas} temperature. The fuelling simulations showed that the maximum temperature development due to any of these initiating events is 95 °C. Therefore, the probability of loss of containment was based on this maximum temperature. For repeated exposures, the maximum CHSS gas temperature due to an initiating event in the T_{gas} temperature (for the Type 3 fuelling concepts) was also determined to be 95 °C, in this case by the design of the t_{final} tables which inherently limit the maximum gas temperature development to 95 °C.

Mitigative barriers were identified but no credit was taken for them on the right side of the bowtie because the station designs where the protocol is being used could vary significantly.

The risk assessment is centered around the potential impact to personnel in the vicinity of a loss of containment event and, as such, focus has been placed upon the tolerability criteria as applicable to H&S. Based on the above, and consistent with a previous EIGA risk acceptance criteria (June 2019), the following Target Consequence Frequencies were utilized:

1) Jet fire from the vehicle leading to single fatality, 1,0E-5 pr year; and
2) Flash fire / explosion leading to multiple fatalities, 1,0E-6 pr year.

The consequence frequency was determined for Jet Fire, and Flash Fire / Explosion for each fuelling concept. These were based on the worst-case initiating event with preventative barriers applied. For the Static (Type 2), T_{gas} Initial (Type 3), and T_{gas} Initial+ (Type 3) fuelling concepts, the residual frequency of occurrence met the target consequence frequency for both Jet Fire and Flash Fire under the Less Conservative case, but not for the Medium Conservative case and Very Conservative case. For the T_{gas} Throttle (Type 3) fuelling concept, the residual frequency of occurrence did not meet the target consequence frequency for either Jet Fire and Flash Fire under any of the cases. However, with the application of additional preventative barriers or a lower PFD (higher SIL/ASIL rank) on the existing barriers, the frequency of occurrence can potentially meet the targets.

Certain threats pertinent to the vehicle (e.g., wrong programming of the ECU with t_{final} table values, improper maintenance, etc) could not be scored within the Bowtie / LOPA approach and these were addressed separately. Further discussion and consideration of these threats and preventive barriers should be conducted during the fuelling protocol standards development process.

In conclusion, these new and novel PRHYDE fuelling concepts with appropriate preventive barriers applied, can meet the targeted consequence frequencies. The threats and initiating events identified on the station are similar to those for the MC Formula protocol in SAE J2601. Initiating events on the vehicle stem from the use of the T_{gas} measurement, which is new and differentiates the PRHYDE fuelling protocols from previous fuelling protocols.

E.2 Acronyms and Abbreviations

Abbreviations and symbols related to the MC Formula Framework are defined in SAE SAE J2601_202005.
Additional symbols not defined in SAE J2601 are listed below:

T_{gas_high}	The highest value of the bulk average gas temperature in a multi-tank CHSS
T_{gas_low}	The lowest value of the bulk average gas temperature in a multi-tank CHSS

Further acronyms and abbreviations found in this report:

ASIL	Automotive Safety Integrity Level
BPCS	Basic Process Control System
CCPS	Center for Chemical Process Safety
CHSS	Compressed Hydrogen Storage System
EIGA	European Industrial Gases Association
ECU	Electronic Control Unit
H_2	Hydrogen
HRS	Hydrogen Refuelling Station
H&S	Health & Safety
IEF	Initiating Event Frequency
IPL	Independent Protection Layer
LOPA	Layers of Protection Analysis
MT	Measured Temperature
OEM	Original Equipment Manufacturer
PFD	Probability of Failure on Demand
PRR	Pressure Ramp Rate
SIF	Safety Instrumented Function
SIL	Safety Integrity Level
SIS	Safety Instrumented System
TMEL	Target Mitigated Event Likelihoods
WP3	PRHYDE Work Package Three

E.3 Introduction

The primary objective of the PRHYDE risk assessment is to identify the hazards associated with use of the PRHYDE fuelling methods discussed in Report D3.2 and corresponding protective and mitigative barriers.

Risk assessment sessions were carried out from May 2021 to March 2022 by a team of experts from PRHYDE partner companies and external experts from invited organizations. The team used a combination of frameworks “Bowtie” and “LOPA” described in more detail in the following sections. Previous work done by EIGA and others was embraced and is considered still true.

Although the spectrum of available expertise is broad, the Risk Assessment Team focused on threats and associated initiating events that arise from the novel fuelling concepts specifically.

E.4 Methodology

E.4.1 Scope

The scope of analysis was chosen to be in line with the newly introduced elements of the refuelling protocol. I.e. work previously done by EIGA and others is taken to be still true and the defined barriers to still stand.

The scope of the PRHYDE risk assessment task was to focus on risks arising from the new fuelling approaches and leaving out common fuelling risks (example: leaks from a worn hose).

Advanced communications is assumed to be available, therefore communications based loops with final elements on the station side can be rated.

Generally, any newly-introduced initiating events were considered and analysed, and mitigations were proposed using well-established Bowtie and LOPA methodologies.

Vehicle and station errors (e.g., programming the ECU with incorrect implementation of Tfinal table values, improper maintenance, etc.) were not considered in this risk assessment.

E.4.2 Bowtie Framework

The PRHYDE risk assessment uses a standard bowtie framework to maintain continuity with the risk assessment performed by EIGA for ISO Technical Committee 197, Workgroup 24.

A bowtie diagram illustrates how a hazard can arise, how it can escalate, and how it is controlled. It defines the barriers required to effectively manage the hazard and prevent or mitigate harmful consequences. See Figure 71 below for an example.

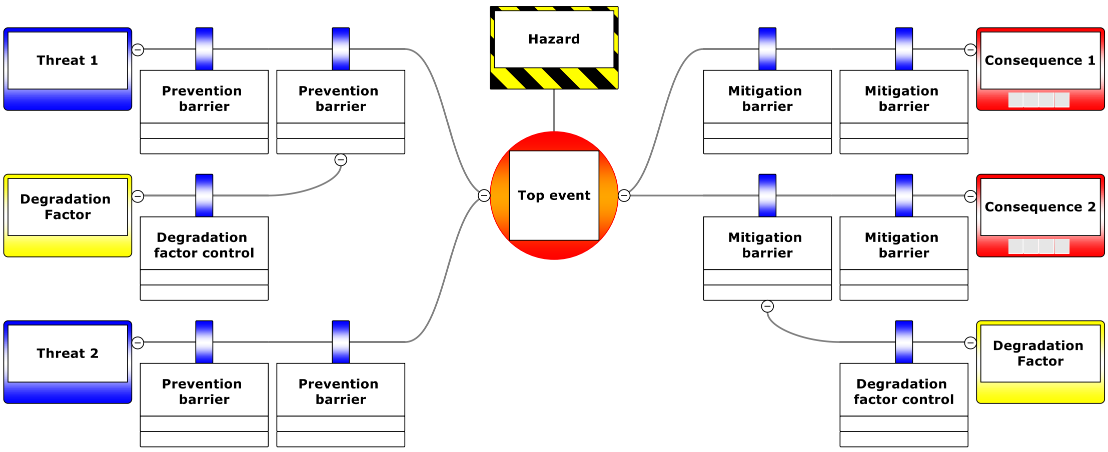

Figure 71: An example bowtie

Key components of the bowtie are defined below. The bowtie was generated using industry best practices as documented in the CCPS guidance document “Bow Ties in Risk Management: A Concept Book for Process Safety”.

Top Event:	At the center of the bowtie diagram is the top event, which represents the moment when control of a hazard is lost (e.g. loss of control / containment of the hazard).
Threats:	Threats are the potential causes which could directly and independently result in the top event and are listed on the left-hand side of the bowtie diagram.
Consequences:	Consequences are the negative events which could result from the top event and lead to harm or damage. These are listed on the right-hand side of the bowtie diagram.
Prevention Barriers:	A prevention barrier is a barrier that prevents the top event from occurring and is located between the applicable threat and top event on the left-hand side of the bowtie diagram.
Mitigation Barriers:	Mitigation barriers are employed after the top event occurs and will reduce the magnitude of the consequence. These barriers are located on the right-hand side of the bowtie diagram.
Degradation Factors:	Factors that may defeat or reduce the effectiveness of a barrier are termed degradation factors. These are applied as necessary throughout the bowtie diagram.

E.4.3 LOPA Framework

Layers of Protection Analysis (LOPA) is a semi-quantitative form of risk assessment that uses order-of-magnitude categories for Initiating Event Frequencies (IEF), consequence severity, and the likelihood of failure of Independent Protection Layers (IPL) to approximate the risk of a scenario.

LOPA allowed the risk assessment team to determine whether the risk for each identified scenario was appropriately managed. See Figure 72 for a high-level overview of the process.

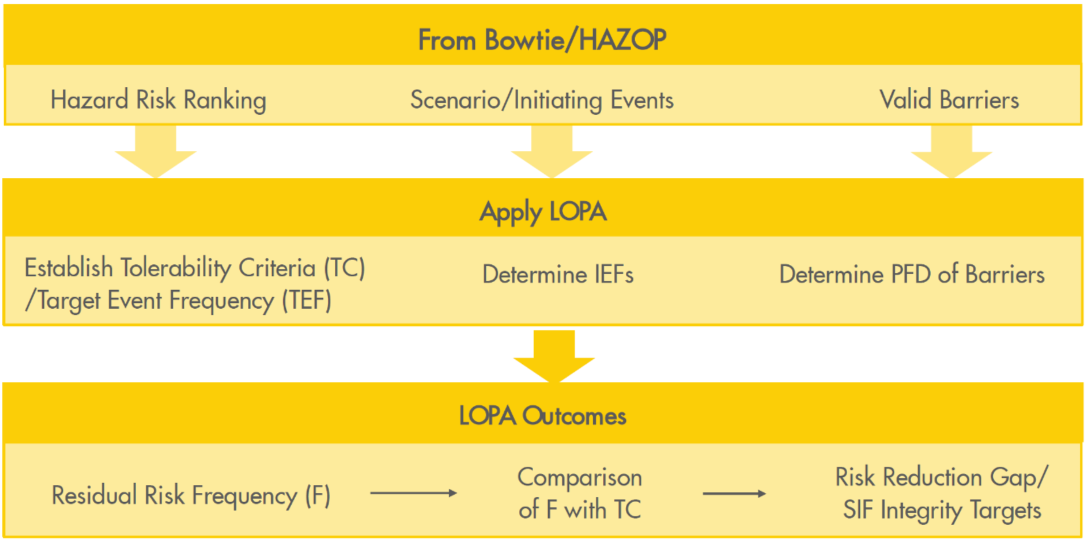

Figure 72: LOPA methodology

The Residual Risk Frequency (F) was calculated using the method shown in Figure 73.

$F = \Sigma(IEF \times P_e \times PFD_1 \times PFD_2 \times PFD_n) \times P_c \times PFD_{RHS}$ **OR** $F = \Sigma MEF \times P_c \times PFD_{RHS}$

IEF = Initiating Event Frequency
P_e = Enabling Factor
P_c = Conditional Modifier
PFD_n = Probability of Failure on Demand for Valid Barriers (n being the total number of valid barriers for each IE)
PFD_{RHS} = Probability of Failure on Demand for Valid Barriers on the right hand side of the bowtie

Figure 73: LOPA residual risk frequency calculation

Key components of the LOPA are defined below:

Initiating Event Frequency (IEF):	Statistical representation of the frequency that a cause is expected to occur on a station per year basis.
Enabling Factor (P_e):	A dimensionless probability that represents the fraction of the time that there is potential for an initiating event to lead to a top event. The enabling condition describes the required condition under which the event could occur.
Conditional Modifier (P_c):	A dimensionless probability that provides a numerical adjustment to residual risk associated with the right-hand side of a bowtie (i.e. control of ignition, control of personnel).
Probability of Failure on Demand (PFD):	Dimensionless parameter that provides a statistical representation of the probability that the safety function does not work when required to.

E.5 Output

The following section discusses the results of the PRHYDE risk assessment. It includes the threats, preventive barriers, top event, mitigative barriers, modifiers, tolerability, and final results.

E.5.1 Threat – Wrong Pressure Ramp Rate resulting in high tank temperature

The primary threat considered for the fuelling concepts is a high ramp rate which causes overheating in the CHSS. Generic vehicle and station threats unrelated to the applied fuelling protocol (such as a vehicle ECU programming error or hose leak) were not part of the analysis because they are not essential to what is being developed within PRHYDE.

This sub-section discusses the potential initiating events for this threat. Each one includes a table which shows potential barriers for each initiating event and its specific PFD. In some cases, a barrier was not used and no credit was taken because the team was unable to determine an appropriate PFD or the barrier was unlikely to be adopted by the industry. Details of the barriers are discussed in Section E.5.2

Table 28: Overview of applicable Initiating Events for each of the Fuelling Concepts

			Fuelling Concepts			
			Type2-PR-S	Type3-PR-S		
			Static	**T_{gas} Initial**	**T_{gas} Initial+**	**T_{gas} Throttle**
Initiating Events	**E.5.1.1**	**T_{Fuel} Error**	X	X	X	X
	E.5.1.2	**Mass Flow Error**	X	X	X	X
	E.5.1.3	**Station Pressure Error**	X	X	X	X
	E.5.1.4	**Ambient Temperature Error**	X	X	X	X
	E.5.1.5	**T_{gas} (vehicle) for fuelling history Error**		X		
	E.5.1.6	**T_{gas} (vehicle) for fuelling history and T_{soak} Error**			X	
	E.5.1.7	**Tgas (vehicle) Error**				X

E.5.1.1 T_{Fuel} Error

Applicable to: All Fuelling Concepts

Initiating Event Frequency: 1,00E-1 events / year

IEF Justification: T_{Fuel} Sensor is within the BPCS loop, hence IEF as per CCPS

Event Description

The T_{Fuel} sensor provides wrong fuel delivery temperature readings, causing a mismatch between the fuelling rate and the fuel delivery temperature.

Enabling factor(s)

Event is only dangerous if Actual Fuel Delivery Temperature is warmer than erroneous T_{Fuel} measurement.

Preventive Barriers identified

Table 29: Preventive barriers identified for Fuel Temperature Error

Barriers	Domain	PFD value used	Comments
Redundant Sensor Monitoring	SIS	1,00E-01	
High MT / Vehicle Abort Signal	SIS /BPCS	1,00E-01	
Shut-off Valve (Vehicle)	Vehicle ECU	1,00E-00	No credit taken
Safety Max PRR Limit	SIS	1,00E-00	No credit taken

E.5.1.2 Mass Flow Error

Applicable to: All Fuelling Concepts

Initiating Event Frequency: 1,00E-1 events / year

IEF Justification: Mass Flow Sensor is within the BPCS loop, hence IEF as per CCPS.

Event Description

The mass flow meter has a fault causing it to report the mass flow incorrectly (outside its accuracy tolerance). This can cause the mass average of the fuel delivery temperature to be calculated incorrectly. The mass average calculation weights the fuel delivery temperature by the amount of mass dispensed at each time step. A faulty mass flow meter could cause the mass average calculation to weigh the cold fuel delivery temperature more than it should be, causing the MAT value to be colder than it actually is. This can cause the pressure ramp rate to be higher than it should be.

Enabling factor(s)

MC Formula is insensitive to wrong mass flow measurement, especially when T_{Fuel} is consistent. Therefore, two failures must happen simultaneously to enable a mass flow error to cause a problem:

1 T_{Fuel} must be relatively warm for most of the fill, but dip momentarily to a very cold temperature in the early to mid-part of the fill.

2 The mass flow meter must read a very high mass flow during the time the temperature is cold.

These two conditions taken together will cause the calculated MAT value to be colder than it actually is. This may lead to an over-temperature condition in the CHSS.

Preventive Barriers identified

Table 30: Preventive barriers identified for Mass Flow Error

Barrier	Domain	PFD value used	Comments
Redundant Sensor Monitoring	SIS	1,00E-01	
Integrity barrier	BPCS	1,00E-00	No credit taken
High MT / Vehicle Abort Signal	SIS	1,00E-01	
Shut-off Valve (Vehicle)	Vehicle ECU	1,00E-00	No credit taken
Safety Max PRR Limit	SIS	1,00E-00	No credit taken

E.5.1.3 Station Pressure Error

Applicable to: All Fuelling Concepts

Initiating Event Frequency: 1,00E-1 events / year

IEF Justification: Station Pressure Sensor is within the BPCS loop, hence IEF as per CCPS

Event Description

An error on station pressure sensor provides wrong pressure measurements, such that the feedback to regulator will cause the regulator to open further in an attempt to close the artificial gap between measured pressure and the setpoint.

Enabling factor(s)

Event is only dangerous if $P_{Station}$ measurement is lower than actual Station Pressure

Preventive Barriers identified

Table 31: Preventive barriers identified for Station Pressure Error

Barrier	Domain	PFD value used	Comments
Redundant Sensor Monitoring	SIS	1,00E-01	
Integrity barrier	BPCS	1,00E-00	No credit taken
High MT / Vehicle Abort Signal	SIS	1,00E-01	
Shut-off Valve (Vehicle)	Vehicle ECU	1,00E-00	No credit taken
Safety Max PRR Limit	SIS	1,00E-00	No credit taken

E.5.1.4 Ambient Temperature Error

Applicable to: All Fuelling Concepts

Initiating Event Frequency: 1,00E-1 events / year

IEF Justification: Ambient Temperature Sensor is within the BPCS loop, hence IEF as per CCPS

Event Description

An error on T_{Amb} sensor provides wrong ambient temperature readings such that the interpolation of t-final tables lead to higher than intended ramp rates.

Enabling factor(s)

Event is only dangerous if T_{amb} measurement is lower than actual ambient temperature.

Preventive Barriers identified

Table 32: Preventive barriers identified for Ambient Temperature Error

Barrier	Domain	PFD value used	Comments
Redundant Sensor Monitoring	SIS	1,00E-01	
High MT / Vehicle Abort Signal	SIS	1,00E-01	
Shut-off Valve (Vehicle)	Vehicle ECU	1,00E-00	No credit taken
Safety Max PRR Limit	SIS	1,00E-00	No credit taken

E.5.1.5 T_{gas} (Vehicle) for fuelling history error

Applicable to: T_{gas} Initial

Initiating Event Frequency: 1,00E-1 events / year

IEF Justification: T_{gas} value from vehicle ECU, assumed equivalent to BPCS loop, hence IEF as per CCPS

Event Description

An error on T_{gas} value provides wrong estimate of fuelling history leading to the wrong selection of t-final table.

Enabling factor(s)

Event is only dangerous if T_{gas} measurement is lower than actual CHSS Tank temperature

Preventive Barriers identified

Table 33: Preventive barriers identified for Gas Temperature for Fuelling History Error

Barrier	Domain	PFD value used	Comments
Redundant Sensor Monitoring	Vehicle ECU	1,00E-01	
Vehicle record last refuelling	Vehicle ECU	1,00E-01	
Qualify CHSS to 95°	CHSS	1,00E-00	No credit taken

E.5.1.6 T_{gas} (Vehicle) for fuelling history and T_{soak} error

Applicable to: T_{Gas} Initial+

Initiating Event Frequency: 1,00E-1 events / year

IEF Justification: T_{gas} value from vehicle ECU, assumed equivalent to BPCS loop, hence IEF as per CCPS

Event Description

An error on T_{gas} value provides wrong estimate of fuelling history and soak temperature leading to the wrong selection of t-final table.

Enabling factor(s)

Event is only dangerous if T_{gas} measurement is lower than actual CHSS Tank temperature

Preventive Barriers identified

Table 34: Preventive Barriers Identified for Gas Temperature for Fuelling History and Soak Error

Barrier	Domain	PFD value used	Comments
Redundant Sensor Monitoring	Vehicle ECU	1,00E-01	
Vehicle record last refuelling	Vehicle ECU	1,00E-01	
Qualify CHSS to 95°C	CHSS	1,00E-00	No credit taken

E.5.1.7 T_{gas} (Vehicle) error

Applicable to: T_{Gas} throttle

Initiating Event Frequency: 1,00E-1 events / year

IEF Justification: T_{gas} value from vehicle ECU, assumed equivalent to BPCS loop, hence IEF as per CCPS

Event Description

An error on T_{gas} value provides wrong input to throttling feature, leading to missing throttling near max CHSS temperature limit

Enabling factor(s)

Event is only dangerous if T_{gas} measurement is lower than actual CHSS gas temperature

Preventive Barriers identified

Table 35: Preventive Barriers Identified for Gas Temperature Error

Barrier	Domain	PFD value used	Comments
Redundant Sensor Monitoring	Vehicle ECU	1,00E-01	
Qualify CHSS to 95°C	CHSS	1,00E-00	No credit taken

E.5.2 Preventive Barriers

In this section is a description of each of the preventive barriers considered for this assignment. The effectiveness of each preventive barrier varies with threat circumstances and how the barrier is built up.

Most barriers may be tuned for better effectiveness at the expense of heightened requirements.

E.5.2.1 Redundant Sensor Monitoring (Station)

This type of barrier features a redundant independent loop of sensor, logic and final element, which can detect if a BPCS sensor transmits erroneous measurements.

E.5.2.2 Redundant Sensor Monitoring (Vehicle)

This type of barrier features a redundant independent loop of sensor, logic and final element, which can detect if a sensor in the vehicle ECU loop transmits erroneous measurements.

E.5.2.3 High MT / Vehicle Abort Signal

This barrier features a loop from the vehicle to station where an abnormality is detected by the vehicle temperature sensor (or other sensors) which triggers an abort signal which the station shall observe and enforce a failsafe state preventing further flow of hydrogen.

E.5.2.4 Shut-off Valve (Vehicle)

This barrier features a loop on vehicle featuring a final element on the vehicle to stop the hydrogen flow into the CHSS in case the station or vehicle detects a potential scenario.

E.5.2.5 Safety Max PRR Limit

This barrier is a secondary t-final table stored in the station PLC or safety PLC. This t-final table is derived using a conservative reference CHSS design and with a maximum gas temperature of 100 °C. A pressure ramp is calculated using this t-final table independently and concurrent to the pressure ramp calculated from the t-final table communicated from the vehicle. The primary purpose of this barrier is to limit the over temperature risk due to a fault in the communication of the t-final table(s) from the vehicle to the station. The temperature for the derivation of this safety t-final table is set to 100 °C so that it does not override the normal function of a correctly communicated t-final table from the vehicle, which for the Type 3 fuelling concepts utilize t-final tables derived with maximum temperature of 95 °C.

E.5.2.6 Qualify the CHSS to 95°C

This barrier consists of qualifying the CHSS in a manner which makes it robust to bulk average gas temperatures in the CHSS up to 95 °C. Although the UN GTR 13 and associated container standards (ISO 19881 and 19882) do not provide an explicit pathway for qualification of the CHSS to 95 °C, they do provide minimum requirements, and therefore, the vehicle OEM may conduct the CHSS qualification at temperatures above these minimum requirements (for example, replacing temperatures specified at 85 °C with a temperature of 95 °C).

As discussed in Section E.5.2.5, the t-final tables can be derived so that even if the CHSS gas temperatures is grossly wrong, the maximum temperature cannot exceed 95 °C. If the CHSS has been qualified to 95 °C, the PFD of this preventative barrier is zero, meaning that is prevents the risk of loss of containment due to the CHSS gas temperature being wrong.

E.5.2.7 Vehicle record last refuelling

This barrier is an independent means for the vehicle to determine if there has been fuelling history or not. Fuelling history is typically determined by comparing the initial CHSS gas temperature (prior to fuelling) to a hot soak temperature. However, this barrier uses a different approach. The vehicle ECU records the date and time when the CHSS gas pressure last increased above a threshold criterion (e.g. 5 MPa). A pressure rise above this criterion can only be caused by fuelling of the vehicle. If the elapsed time between this last fuelling event and the current time is greater than a threshold criterion (e.g. 15 minutes), then fuelling history is determined not to be present.

E.5.2.8 Integrity barrier

This barrier is a means to detect a fault in the mass flow measurement or the station pressure measurement. This barrier works by comparing the mass dispensed from the flow meter to a calculated mass dispensed based on the change in density and CHSS volume. At the initial leak check (prior to the main fuelling time), the station calculates the mass in the CHSS by using the station pressure and T_{gas} temperature and CHSS volume communicated from the vehicle ($m_{calculated(0)} = \sigma_0$ x TV). During the main fuelling time, the station periodically stops the flow of hydrogen long enough for the mass flow rate to go to zero (e.g. 3 to 5 seconds) and again calculates the mass dispensed ($m_{calculated(i)} = \sigma_i$ x TV). The difference in mass ($m_{calculated(i)} - m_{calculated(0)}$) is compared to the mass dispensed by the flow meter ($m_{(i)} – m_{(0)}$) and the difference between these two measurements is expressed as a percent error. An error band is established that accounts for a distribution of “normal” or “expected” error due to inaccuracies in the various input parameters. If the percent error exceeds this normal error band, this indicates there is a fault in one or more of the input parameters (i.e. station pressure, mass flow measurement, vehicle tank volume, or vehicle T_{gas} measurement). This barrier can therefore effectively detect faults in the mass flow meter or station pressure measurement. Although this barrier is currently defined in the 2020 SAE J2601 Appendix L, its effectiveness has not been sufficiently evaluated, so an appropriate PFD could not be assigned.

E.5.3 Modifiers (Left Side of Bowtie)

An initiating event will not automatically lead to a loss of containment. A loss of containment is contingent upon the severity and frequency of occurrence. The UN GTR 13 does not include tests for temperature excursions above the qualification temperature. Therefore, the probability of the CHSS leaking upon temperature excursions above the qualification temperature is unknown.

E.5.3.1 Probability of loss of containment for single event exposures

PRHYDE WP3 utilized a distribution for the probability of loss of containment, based on the magnitude of the temperature exposure above the CHSS qualification temperature. Because this distribution of probabilities is unknown, and limited data exists, WP3 made an assumption for three cases: (1) Less Conservative; (2) Medium Conservative; and (3) Very Conservative. The assumed probabilities for each case are shown in the table below.

Case 1: Less Conservative --an exponential increase in probability starting at 10 °C above certification and reaching 100% probability at 55 °C above the certification temperature.

Case 2: Medium Conservative — a linear increase in probability of 20% for every 5 °C above certification temperature starting at 10 °C above certification and reaching 100% probability at 30 °C above the certification temperature.

Case 3: Very Conservative — a linear increase in probability of 50% for every 5 °C above certification, starting at 10 °C above certification

Table 36: Probabilities of Loss of Containment for three cases

Case 1: Less Conservative		Case 2: Medium Conservative		Case 3: Very Conservative	
Temperature above Certification	Probability of loss of containment	Temperature above Certification	Probability of loss of containment	Temperature above Certification	Probability of loss of containment
0	0.0%	0	0.00%	0	0.00%
5	0.0%	5	0.00%	5	0.00%
10	0.4%	10	10.00%	10	50.00%
15	0.7%	15	20.00%	15	100.00%
20	1.2%	20	40.00%		
25	2.3%	25	60.00%		
30	4.3%	30	80.00%		

Case 1: Less Conservative		Case 2: Medium Conservative		Case 3: Very Conservative	
Temperature above Certification	Probability of loss of containment	Temperature above Certification	Probability of loss of containment	Temperature above Certification	Probability of loss of containment
35	8.1%	35	100.00%		
40	15.2%				
45	28.5%				
50	53.4%				
55	100.0%				

Single event exposures are based on faults of the station such as the ambient temperature or fuel delivery temperature being wrong. In these cases, if the initiating event leads to the gas temperature exceeding the maximum gas temperature rating of the CHSS, the vehicle will send both T_{gas_high} and an abort signal via communications to the station. Because the fuelling protocol is designed such that the gas temperature should never exceed the maximum gas temperature rating of the CHSS, WP3 assumes that if a station receives from the vehicle an abort signal and T_{gas_high} above or near the maximum temperature, the station will be taken out of service to investigate if this was caused by a fault in a component. Therefore, these events are classified as single event exposures.

E.5.3.2 Maximum CHSS Gas Temperature due to Initiating Events

At the request of WP3, WP4 conducted fuelling simulations using the SOFIL model to determine the expected worst case gas temperature development in the CHSS due to the following initiating events: T_{fuel} Error, T_{amb} Error, and Mass Flow Error. An error in the station pressure was deemed much more difficult to bound, and therefore, simulations were not conducted for this initiating event. Furthermore, this initiating event is not unique to the PRHYDE fuelling concepts, since any fuelling protocol that utilizes pressure control will encounter the threat of a wrong pressure ramp rate due to a station pressure error.

A reference CHSS from Report D4.3, Section 2.1 was utilized to conduct these simulations.

For the initiating events under consideration, the error case is defined below.

a. Error on T_{fuel}: actual T_{fuel} (-10 °C) is hotter than measured (-40 °C)

b. Error on T_{amb}: actual T_{amb} is hotter (two cases of 30 and 50 °C) than measured (15 °C)

c. Error on Mass Flow: temperature potential deemed similar to error on T_{fuel}

d. Error on $P_{station}$: not considered (see justification above)

e. Error on T_{gas}: considered in Section E.5.3.3

Error on T_{fuel} and Mass Flow:

This simulation was conducted with a fuel delivery temperature of -10 °C and an average pressure ramp rate derived with a fuel delivery temperature of - 40 °C. This simulates a condition where the fuel delivery temperature reads 30 °C colder than it actually is. This simulation was also utilized as a worst-case condition for an error in the mass flow because T_{fuel} and mass flow are combined to calculate a mass average fuel delivery temperature. Under these conditions, the maximum gas temperature was 93.4 °C. See Figure 74:

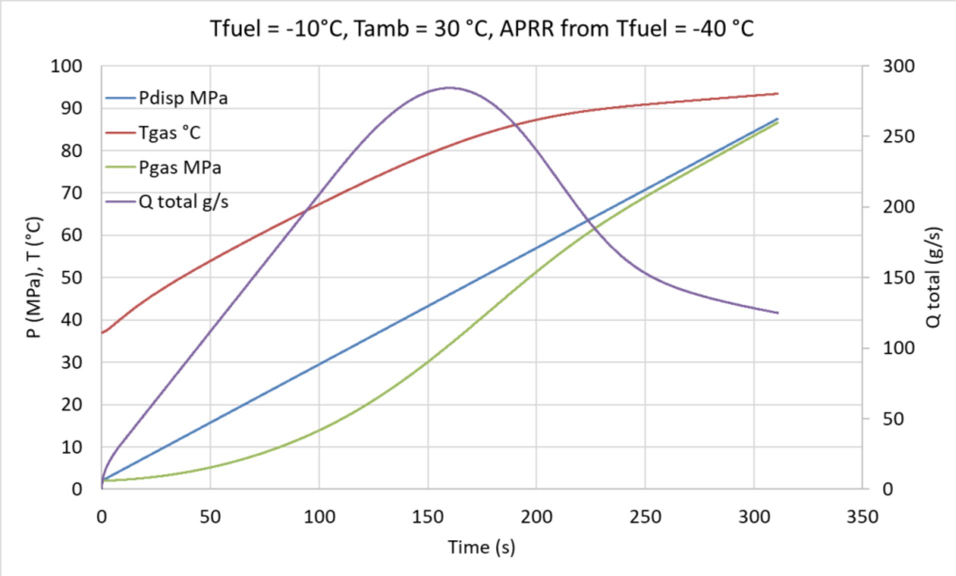

Figure 74: **Effect of error on T_{fuel} (or Mass Flow)**

Error on T_{amb}:

The first simulation was conducted with a fuel delivery temperature of -10 °C and an ambient temperature of 30 °C. The average pressure ramp rate was derived at an ambient temperature of 15 °C. Therefore, this simulates a condition where the ambient temperature reads 15 °C colder than it actually is. Under these conditions, the maximum gas temperature was 88.9 °C. See Figure 75 below:

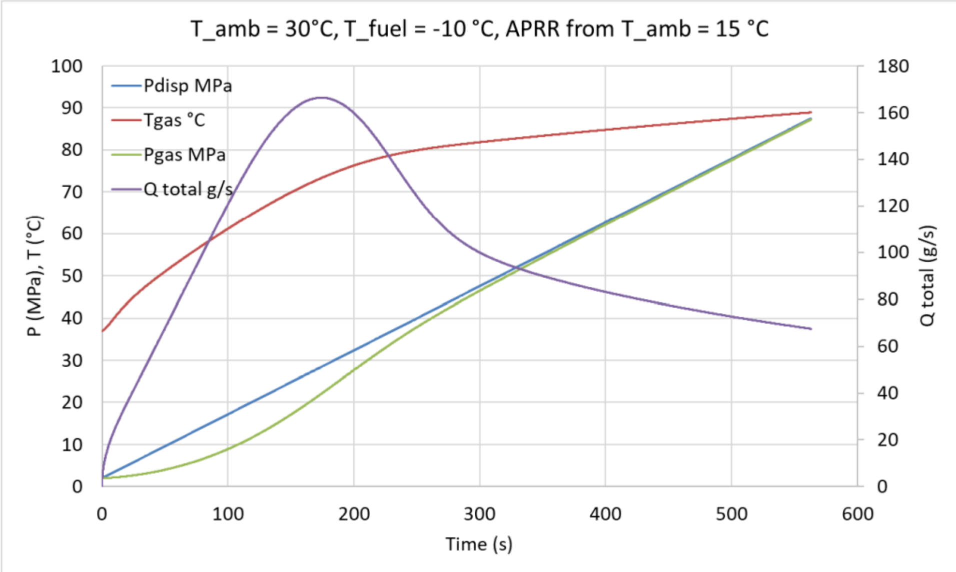

Figure 75: Effect of error on T_{amb} measurement 15°C, but actual is 30°C

The second simulation was conducted with a fuel delivery temperature of -10 °C and an ambient temperature of 50 °C. The average pressure ramp rate was derived at an ambient temperature of 15 °C. Therefore, this simulates a condition where the ambient temperature reads 35 °C colder than it actually is. Under these conditions, the maximum gas temperature was 94.7 °C. See Figure 76 below:

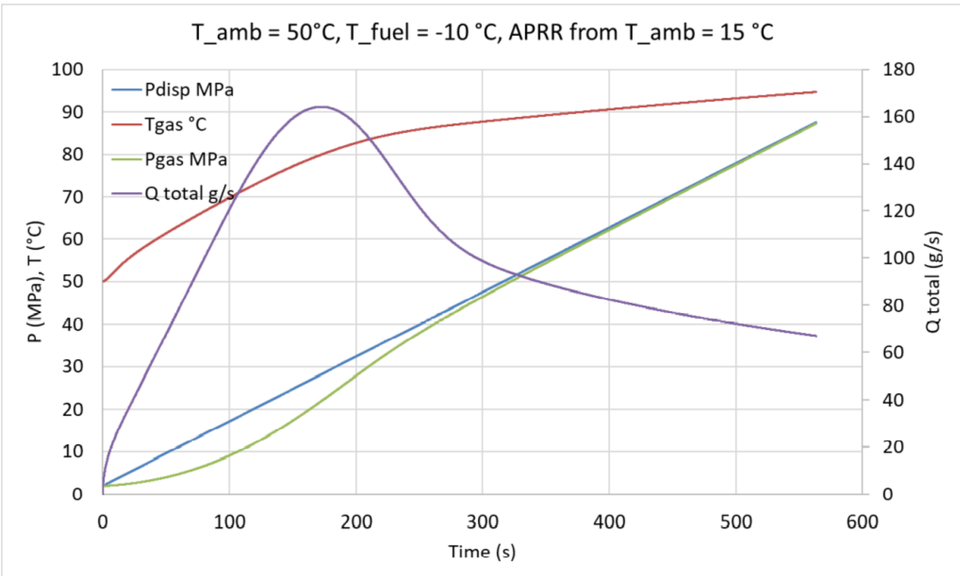

Figure 76: Effect of error on T_{amb} measurement 15°C, but actual is 50°C

As a result of these simulations, the maximum gas temperature considered due to the initiating events under considerations is 95 °C or 10 °C above the certification temperature.

E.5.3.3 Probability of loss of containment for repeated exposures

If the CHSS gas temperature is wrong (has a fault) and the vehicle does not detect it, the station will not be able to detect it. For the Type 3 fuelling concepts, this can potentially lead to repeated exposures to gas temperatures above the CHSS qualification temperature over the life of the vehicle.

Again, due to lack of data, assigning probabilities to the loss of containment for repeated events where the gas temperature exceeds the CHSS qualification temperature is difficult. An approach similar to the single exposure events is utilized whereby probabilities are assigned based on the Very Conservative, Medium Conservative, and Less Conservative cases.

Most fuelling events do not have the potential for the gas temperature to exceed the CHSS qualification temperature. This is because the initial conditions must be at or near the worst case for several factors.

An additional challenge of repeated exposures over single event exposures is that both the magnitude of over temperature and frequency of occurrence affect the loss of containment probability distribution. For example, in the event of a fault in the T_{gas} measurement, over the life of the vehicle the frequency of exposures to 88 °C may be 150 times vs 40 times for exposures to 93 °C. Which has a higher probability of causing a loss of containment? To limit the complexity of the risk assessment, WP3 assumed that less frequent exposures to higher gas temperatures above the CHSS qualification temperature is more severe than more frequent exposures to lower gas temperatures above the CHSS qualification temperature.

In the derivation of the t-final tables for the Type 3 fuelling concepts, the t-final values can be constrained (see barrier discussed in Section E.5.2.5) so that even under worst case initial conditions and a wrong CHSS gas temperature, the maximum CHSS gas temperature will not exceed 95 °C.

Therefore, WP3 assumed that 95 °C is the maximum gas temperature that can be reached for all Type 3 fuelling concepts due to a fault in the CHSS gas temperature. Therefore, the approach utilized is to determine the number of fuelling events that can potentially reach 95 °C over the life of the vehicle.

The first step in determining the probability of loss of containment is to consider the conditions necessary for the gas temperature to reach 95 °C. These conditions are dependent upon the fuelling concept utilized. For the Tgas Initial and Tgas Initial+ fuelling concepts, the vehicle must have been recently fuelled (e.g. approximately within the last 5 minutes) using the t-final tables. This is called fuelling history. In addition to the CHSS having fuelling history, the conditions during the previous fill must have also been conducive to achieving 95 °C. To achieve 95 °C, the initial CHSS pressure must be at the minimum operating pressure, and the CHSS temperature must be at the hot soak temperature. Additionally, the t-final values must be temperature constrained, meaning that under the conditions that influence the t-final value (ambient temperature and fuel delivery temperature), the t-final value is derived based on a fuelling speed that will constrain the gas temperature from exceeding the maximum gas temperature. If all these conditions are not present, then the gas temperature cannot reach 95 °C. Data obtained from hundreds of thousands of light duty fuelling events, indicates that fuelling from minimum pressure and hot soak temperatures occurs less than 1.25% of the time. Fuelling events with fuelling history (i.e. where the initial measured temperature MT is greater than the SAE J2601 defined hot soak temperature) occur less than 1.9% of the time. Based on this data WP3 assumed that fuelling from minimum pressure and hot soak temperature has a frequency of occurrence of 1.5% and fuelling where fuelling history is present has a frequency of occurrence of 2%. Therefore, the probability of the gas temperature reaching 95 °C for T_{gas} Initial and T_{gas} Initial+ is 0.015 x 0.02 = 0.0003. The frequency of occurrence of these conditions for heavy duty vehicle fuelling could be different from light duty vehicle fuelling, but this is the best data we have available.

For the T_{gas} Throttle fuelling concept, the initial CHSS pressure must be at the minimum operating pressure, and the initial CHSS temperature must be at the hot soak temperature for the end CHSS gas temperature to reach 95 °C. Therefore, the probability of the gas temperature reaching 95 °C for T_{gas} Throttle is 0.015.

The next step is to determine the number of 95 °C temperature exposures over the life of the vehicle. The life of the vehicle (and CHSS) is assumed to be one million miles, and the minimum range of the vehicle is assumed to be 250 miles, resulting in the potential for 4,000 full (minimum SOC to maximum SOC) fills over the life of the vehicle. To determine the number of potential exposures of the CHSS to 95 °C over the life of the vehicle, the number of full fills is multiplied by the probability. For T_{gas} Initial and T_{gas} Initial+, this is 4,000 x 0.0003 = 1.2 fills, which is rounded to 1 fill. For T_{gas} Throttle, this is 4,000 x 0.015 = 60 fills.

With the potential number of exposures determined, the final step in assigning a probability of loss of containment is to relate the number of exposures to a probability. Again, due to lack of data and published studies, the confidence level in these probabilities is relatively low.

- For the Very Conservative case, if a single exposure has a 50% probability at +10 °C (95 °C), then repeated exposures should be higher than this. For the T_{gas} Initial and T_{gas} Initial+ fuelling concepts, there is only a single exposure over the life of the CHSS, so the probability of loss of containment is 50%. For T_{gas} Throttle, there are 60 exposures over the life of the CHSS, so the probability of loss of containment is 100%.

- For the Less Conservative case, the single exposure probability at +10 °C is 0.4%. Therefore, for the T_{gas} Initial and T_{gas} Initial+ fuelling concepts, there is only a single exposure over the life of the CHSS, so the probability of loss of containment is 0.4% or 0.004. Multiple exposures must result in a probability higher than this. For the T_{gas} Throttle fuelling concept, the approach utilized is to multiply the single exposure probability by the number of potential exposures over the life of the vehicle and then reduce this value by a factor of 4. This results in a probability of 6% or 0.06 (0.004 x 60 ÷ 4).

- For the Medium Conservative case, the single exposure probability at +10 °C is 10%. Therefore, for the T_{gas} Initial and T_{gas} Initial+ fuelling concepts, there is only a single exposure over the life of the CHSS, so the probability of loss of containment is 10% or 0.1 For the T_{gas} Throttle fuelling concept a value of 0.5 is utilized, which is approximately halfway between the Very Conservative and Less Conservative.

The table below summarizes the approach described above.

Table 37: Enabling factors for fuelling concepts

Enabling Factors	**T_{gas} Initial**	**T_{gas} Initial+**	**T_{gas} Throttle**
Conditions required for gas temperature to achieve 95 °C	Fuelling history – a previous fill must have just occurred from a minimum initial pressure, high T_{amb} or high T_{fuel}, and CHSS at hot soak T	Fuelling history – a previous fill must have just occurred from a minimum initial pressure, high T_{amb} or high T_{fuel}, and CHSS at hot soak T	Minimum initial pressure and high T_{amb} or high T_{fuel} and CHSS at hot soak T
Probability of hitting 95 °C	Fuelling history – 0.02 Other conditions – 0.015 Total – 0.0003	Fuelling history – 0.02 Other conditions – 0.015 Total – 0.0003	Conditions – 0.015
Frequency of hitting 95 °C (over life of vehicle)	4,000 x 0.000015 = 0.06, rounded to **1**	4,000 x 0.000015 = 0.06, rounded to **1**	4,000 x 0.015 = 6**0**
Probability of loss of containment (Very Conservative)	**50%**	**50%**	**100%**
Probability of loss of containment (Medium Conservative)	**10%**	**10%**	**50%**
Probability of loss of containment (Less Conservative)	**0.4%**	**0.4%**	**6%**

E.5.4 Mitigative Barriers, Modifiers

E.5.4.1 Mitigative Barriers general

Mitigative barriers are employed after the top event - here after vehicle tank has start leaking. The mitigative barriers cannot hinder the top event, but reduce the consequence, or hinder an escalation of the consequence.

In several risk assessment scenarios, it was discussed if these mitigative barriers would be effective at all. Do they come so late that the final consequence has already been escalated as much at it could? Based on that and on the fact that other known risk assessment for this type of scenarios did not take credit for mitigative barriers it was decided to remove any mitigation credit.

The mitigative barriers considered in this study were:

E.5.4.2 Hydrogen detector (Station)

Domain: SIS

PFD Value: 1

Description

This barrier features a loop from detection of hydrogen above the refuelling area/dispenser to the final element to stopping the hydrogen flow / terminate refuelling.

E.5.4.3 Hydrogen detector (Vehicle)

Domain: Vehicle ECU - SIS/BPCS on station

PFD Value: 1

Description

This barrier features a loop from a hydrogen detector on the vehicle to the final element on station stopping the hydrogen flow / terminate refuelling.

E.5.4.4 Ultrasonic leak detector (Station)

Domain: SIS

PFD Value: 1

Description

This barrier features a loop from detection of hydrogen leak through an ultrasonic leak detector covering the refuelling area to the final element stopping the hydrogen flow / terminate refuelling.

E.5.5 Tolerability

Tolerability criteria, or Target Mitigated Event Likelihoods (TMEL), are generally dependent on a number of factors, including;

- Company risk appetite;
- Classification of severity in company Risk Matrix, and;
- Consequence type (e.g. H&S, Environment, Asset Damage).

The UK HSE "*Process Safety Leadership Group. Safety and environmental standards for fuel storage sites: Process Safety Leadership Group Final Report*" document outlines a baselined approached to the definition of criteria, based on typical industry application (see below)

Table 38: Excerpt of UK HSE Process Safety Leadership Group Final Report

Consequence Category		Risk Type: Safety	Risk Type: Environment	Risk Type: Commercial (Asset & Loss of Production)	Target Consequence Frequency (per year)
C1	Minor	Medical case or First Aid with return to duty by the next shift, recordable but with no LWDC/RWDC.	Nuisance on-site only (i.e. no off-site effects). No outside complaints.	Impact less than US$10k due to loss of assets or earnings, production delays, contract violations and/or HSE fines.	10^{-2}
C2	Noticeable	Temporary disabling injuries with more than 1 but less than 100 recordable LWDC/RWDC.	Noticeable nuisance off-site, e.g. discernible odours. Minor breach of permitted emission limits, no environmental harm. One or two complaints from the public.	Impact between US$10k and US$100k due to loss of assets or earnings, production delays, contract violations and/or HSE fines.	10^{-3}
C3	Significant	Long-term disabling injuries with more than 100 recordable LWDC/RWDC.	Severe and sustained nuisance, e.g. strong offensive odours or noise disturbance. Major breach of permitted emission limits with the possibility of prosecution. Numerous public complaints.	Impact between US$100k and US$1m due to loss of assets or earnings, production delays, violation of local laws, contractual violations and/or HSE fines.	10^{-4}
C4	Severe	1 fatality or permanent disability. Intervention by a regulatory body.	Hospital treatment required. Public warning and off-site emergency plan invoked. Hazardous substance releases into water course, ½-mile effect.	Impact between US$1m and US$10m due to loss of assets or earnings, production delays, FCPA/Class Action, contract violations and/or HSE fines.	10^{-5}
C5	Major	2 - 10 fatalities. Intervention by a regulatory body.	Evacuation of local populace. Temporary disabling & hospitalisation. Serious toxic effect on beneficial or protected species.	Impact between US$10m and US$100m due to loss of assets or earnings, production delays, contract violations, SEC violation and/or HSE fines.	10^{-6}

Consequence Category		Risk Type			Target Consequence Frequency (per year)
		Safety	Environment	Commercial (Asset & Loss of Production)	
			Widespread but not persistent damage to land. Significant fish-kill over a 5-mile range.		
C6	Catastrophic	11 – 50 fatalities. Intervention by a regulatory body.	Major airborne release with serious off-site effects. Major release to sea, damage to coastal waters and aquatic life. Serious contamination of groundwater or watercourse with extensive loss of aquatic life.	Impact exceeding US$100m due to loss of assets or earnings, production delays, contract violations, SEC violation and/or HSE fines.	10^{-7}

The PRHYDE risk assessment is centered around the potential impact to personnel in the vicinity due to a loss of containment event and, as such, focus has been placed upon the tolerability criteria as applicable to H&S. Based on the above, and consistent with pervious EIGA risk acceptance criteria (June 2019), the following tolerability criteria was agreed:

- Scenario resulting in single fatality (employees, contractors etc.): 10^{-4}
- Scenario resulting in single fatality (member of public): 10^{-5}

- Scenario resulting in multiple fatalities (employees, contractors etc.): 10^{-5}
- Scenario resulting in multiple fatalities (member of public): 10^{-6}

E.5.5.1 Modifiers (Consequence):

An ignition modifier has been added to the consequences where equal credit has been taken for the two dangerous outcomes –

A. Jetfire from the vehicle leading to single fatality
B. Flash fire / Explosion leading to multiple fatality

E.5.5.2 Consequences:

The consequences are the harming or damaging event coming after the Top Event, or an event which is initiated by the Top Event.

Using the table in the tolerability section, the severity of the consequence will give a Target Consequence Frequency which is the target for the LOPA calculation in the risk assessment.

In this risk assessment there has been identified two consequences

E.5.5.3 Jet fire from the vehicle tank leading to single fatality

Target consequence frequency: 1,0E-5

Description:
Jet fire scenario: A scenario with a leak in the vehicle tank which is instantly ignited (early ignition). This jet will be extremely hot and the length will vary according to pressure and leak size. In severity this was rated to one fatality.

E.5.5.4 Flash fire / explosion leading to multiple fatalities

Target consequence frequency: 1,0E-6

Description:
Flash fire scenario: A scenario with a leak in the vehicle tank. This leak will generate a gas cloud before it ignites (late ignition). Depending on the leak size and the vehicle design this could also give outcome as an explosion. This flash fire will be site specific and therefore difficult to rate the potential worse case. It was agreed to rate this as an multi fatality severity.

E.6 Output of Bowtie-LOPA

The following section summarizes the results of the Bowtie-LOPA. A table in each of the sub-sections below show the frequency of occurrence for the Top event and the two consequence scenarios under each case. The text in *red italics* shows where the target is not met.

E.6.1 Static

For the static fuelling protocol approach, the initiating events for this approach are discussed in Section E.5.1, and the frequency of occurrence for all of them are the same.

Table 39: Bowtie-LOPA output for Fuelling Concept: Static

Frequency of Occurrence	Less Conservative	Medium Conservative	Very Conservative	Target
Top Event	1,76 E-6	5,00 E-5	2,50 E-4	
Jetfire → Single Fatality	5,27 E-7	1,50 E-5	7,50 E-5	1,0E-5
Explosion → Multiple Fatalities	5,27 E-7	*1,50 E-5*	*7,50 E-5*	1,0E-6

E.6.2 T_{gas} initial

For the T_{gas} initial fuelling protocol approach, initiating events for this approach are discussed in Section E.5.1, and the probabilities for all of them are the same.

Table 40 Bowtie-LOPA output for Fuelling Concept: Tgas Initial

Frequency of Occurrence	Less Conservative	Medium Conservative	Very Conservative	Target
Top Event	1,76 E-6	5,00 E-5	2,50 E-4	
Jetfire → Single Fatality	5,27 E-7	1,50 E-5	7,50 E-5	1,0E-5
Explosion → Multiple Fatalities	5,27 E-7	*1,50 E-5*	*7,50 E-5*	1,0E-6

E.6.3 T_{gas} initial +

For the T_{gas} initial+ fuelling protocol approach, the initiating events for this approach are discussed in Section E.5.1, and the probabilities for all of them are the same.

Table 41 Bowtie-LOPA output for Fuelling Concept: Tgas Initial+

Frequency of Occurrence	Less Conservative	Medium Conservative	Very Conservative	Target
Top Event	1,76 E-6	5,00 E-5	2,50 E-4	
Jetfire → Single Fatality	5,27 E-7	1,50 E-5	7,50 E-5	1,0E-5
Explosion → Multiple Fatalities	5,27 E-7	*1,50 E-5*	*7,50 E-5*	1,0E-6

E.6.4 T_{gas} throttle

For the T_{gas} throttle fuelling concept, the probabilities for T_{fuel}, mass flow, station pressure, and ambient temperature errors are all the same.

The T_{gas} vehicle error however, is significantly different and with the standard preventive barriers in place, even the Less Conservative cannot meet the frequency of occurrence target.

Table 42 Bowtie-LOPA output for Fuelling Concept: Tgas throttle

Frequency of Occurrence	Less Conservative	Medium Conservative	Very Conservative	Target
Top Event	3,00 E-4	2,50 E-3	5,00 E-3	
Jetfire → Single Fatality	*9,00 E-5*	*7,50 E-4*	*1,50 E-3*	1,0E-5
Explosion → Multiple Fatalities	*9,00 E-5*	*7,50 E-4*	*1,50 E-3*	1,0E-6

E.6.4.1 Additional barriers to achieve the target probability

For the Static, Tgas initial, and Tgas initial + the target frequency was not achieved under the Medium Conservative and Very Conservative cases for the explosion scenario. To achieve the target under the Medium Conservative case, an additional barrier with a PFD value of 1,00E-1 pr year is needed. Under the Very Conservative case, the PFD for the one barrier would need to be increased to 1,00E-2 pr year or a second barrier with a PFD of 1,00E-1 pr year would need to be added. There are several options to accomplish this, as discussed in Section E.5.2. For example, the PFD of the redundant sensor monitoring could be increased to 1,0 E-2 pr year.

The Tgas throttle approach does not meet the target frequency for both scenarios under any cases. The table below shows the additional PFD needed to achieve the target probability for both scenarios under each case. Again, this can be done by increasing the PFD of a single barrier or adding additional barriers.

The most effective preventive barrier of those identified is to qualify the CHSS to 95 °C, which has an effective PFD of zero. This barrier is effective and applicable to all the fuelling concepts, especially the Type 3.

Table 43 Required additional PFD to achieve target for fuelling concept: Tgas Throttle

Required additional PFD to achieve target for Throttle protocol	Less Conservative	Medium Conservative	Very Conservative
Jetfire → Single Fatality	1,00 E-1	1,00 E-2	1,00 E-3
Explosion → Multiple Fatalities	1,00 E-2	1,00 E-3	1,00 E-4

E.7 Non-scored threats

E.7.1 Development, implementation and maintenance of Fuelling Parameters

The fuelling concepts under consideration within PRHYDE are unique in many aspects and change the current approach to refuelling by allowing vehicle information to be utilized as an input into the fuelling protocol control functions which dictate the pressure ramp rate. This vehicle information consists of static parameters for the Type 2 fuelling concept and both static and dynamic parameters for the Type 3 fuelling concepts. More specifically, the static parameters consist of t_{final} values from tables stored in the vehicle ECU and the dynamic parameters consist of the gas temperature within the CHSS. The threat of a wrong value in the gas temperature is considered within the Bowtie-LOPA framework. However, the threat of wrong t_{final} values are not considered within the Bowtie-LOPA and thus are not scored. Of course, it is important that the t_{final} values correctly reflect the allowable fuelling rate into the vehicle.

Several scenarios which could cause the t_{final} values to be incorrect are conceivable:

- Wrong derivation of t_{final} values
- Wrong implementation or communication of t_{final} values
- Replacement parts changing the assumptions used in the original derivation of the t_{final} values

The table below shows the potential threats and potential mitigative barriers identified for these scenarios. Additional consideration should be given to these threats and mitigative barriers during the fuelling protocol standards development process.

Table 44 T-final implementation - Potential Threats and Potential Mitigative Barriers

Potential Threats	Potential Mitigative Barriers
t_{final} values are derived incorrectly	• Use of a validated and industry accepted fuelling model, ideally with the automatic generation of t_{final} tables built into its functionality ✓ NREL's H2FillS fuelling model is one such candidate • Validation testing – testing should be defined in the fuelling protocol standard and should be conducted at defined conditions to ensure that: A) Flow rate constrained t_{final} values do not exceed the mass flow limit defined in the fuelling protocol standard (e.g. 300 g/s) B) Temperature constrained t_{final} values do not exceed the maximum T_{gas} temperature utilized to derive the t_{final} values in the fuelling model

t_{final} vector or t t_{final} tables are implemented or communicated incorrectly	• t_{final} vector verification ✓ A testing regimen / validation process may be defined in the fuelling protocol standard which provides guidance and recommendations to the vehicle OEM for validating that the vehicle communicates the appropriate t_{final} table and/or calculates and communicates the correct t_{final} vector based on a set of inputs. This should be done in a comprehensive manner to verify the calculation logic, table selection, and stored table values over the range of possible inputs.
Incorrect CHSS parts replaced during repair or maintenance	• OEM to require replacement with original equipment parts. • Communication ECU requires connections to each tank in the CHSS to confirm it is the correct specification. ✓ Tank could have an IC (for wired connection) or RFID chip (for wireless connection) integrated into the outer layer of the tank winding during manufacturing. ✓ ECU needs signal from each chip to function

E.8 Highlights of specific risks

Touching on focus points from PRHYDE Deliverable D2.2

This risk assessment focused on the overtemperature of the vehicle tank. Overfill protections can be handled in a manner similar to that used in SAE J2601. The consequence of overflow, or of a pressure regulator not working or failing was not deemed unique to the PRHYDE fuelling protocols and thus was not considered. In regard to the avoidance of overpressure, tank design has pressure margin built in for fault management via the CHSS qualification standards and GTR 13. The previously conducted EIGA risk assessment showed that this, in combination with a SIF and mechanical pressure relief valve as mandated by ISO 19880-1, results in a Top Event probability of < 1,0E-6 and a residual risk of fire or explosion of < 2,0E-7. This residual risk is at an acceptable level and is independent of the fuelling protocol utilized, thus PRHYDE did not consider the overpressure scenario in its risk assessment.

E.9 Conclusion

An important aspect of this risk assessment is the approach utilized for modifiers applied to the left of the Top Event in the Bowtie, i.e. the realization that an initiating event will not automatically lead to a loss of containment. This risk assessment utilized a methodical process to quantify the probabilities of loss of containment due to gas temperature exposures above the CHSS qualification temperature, instead of assuming a 100% likelihood of failure. Additionally, the overtemperature potential of the various initiating events was quantified so that an appropriate probability could be applied. This approach considered both single- and multiple-event exposures.

Except for a failure in monitoring station pressure, modelling showed all initiating events led to a maximum gas temperature of less than 95 °C. This bounding of the overtemperature potential has important implications because it facilitates two things: a) the ability to conduct testing on CHSS qualified to existing standards / regulations to better understand their inherent robustness to gas temperature excursions of this magnitude; and b) it facilitates several new approaches to preventive barriers.

The probability of a loss of containment due to over-temperature conditions is hard to estimate due to the lack of data. WP3 chose to provide three estimates (Very Conservative, Medium Conservative, and Less Conservative) to account for this gap and to encourage industry to develop test procedures and publish data for use in future risk assessments.

Many preventive barriers were identified during this risk assessment but were not utilized in the Bowtie / LOPA, or were utilized with a conservative estimate of the PFD. For example, qualifying the CHSS to 95 °C would make it resistant to all the considered initiating events based upon modelling. Some preventive barriers were identified as being effective but not desirable (due to cost, durability or other factors), such as a shut-off valve on the vehicle. An example of an easy to implement barrier that could potentially be quite effective is the integrity barrier described in Section 3.2.8. Some of the preventive barriers, especially the redundant sensor monitoring, could potentially be utilized with a lower PFD, but this would require a higher SIL / ASIL rank (which must consider the complete loop, including communications). As noted in Section E.6.4.1, with these additional preventive barriers or lower PFDs on the utilized barriers, the target frequencies of occurrence can be reached for all of the fuelling protocols, even under the Medium Conservative and Very Conservative cases.

PRHYDE fuelling protocols assume a safety-critical communications channel between the vehicle and dispenser. WP3 could not assess the impact of such a channel to the risks of fuelling since it did not exist at the time of the assessment. The communications system and protocol must undergo a separate assessment to ensure their suitability for use with PRHYDE fuelling protocols.

Overall, the PRHYDE risk analysis showed that the fuelling protocols in this project can meet safety targets when appropriate preventive barriers are in place.

What is PRHYDE?

With funding from the Fuel Cells and Hydrogen 2 Joint Undertaking (FCH 2 JU, now CHJU) under Grant Agreement No 874997, the PRHYDE project aimed to develop recommendations for a non-proprietary heavy duty refuelling protocol used for future standardization activities for trucks and other heavy duty transport systems applying hydrogen technologies.

Based on existing fuelling protocols and current state of the art for compressed (gaseous) hydrogen fuelling, different hydrogen fuelling protocols concepts were developed for large tank systems with 35, 50, and 70 MPa nominal working pressures using simulations as well as experimental verification. A broad industry perspective was captured via an intense stakeholder participation process throughout the project.

The work enables the widespread deployment of hydrogen for heavy duty applications in road, train, and maritime transport. The results are a valuable guidance for station design but also the prerequisite for the deployment of a standardized, cost-effective hydrogen infrastructure.

Further information can be found on the project website (https://prhyde.eu). For feedback on the PRHYDE project or the published deliverables, please contact info@prhyde.eu.

PRHYDE Project Coordinator

Ludwig-Boelkow-Systemtechnik GmbH
Daimlerstr. 15, 85521 Ottobrunn/Munich, Germany
http://www.lbst.de

Members of the PRHYDE Consortium:

Further linked third partner to the project are MAN and Toyota North America.

We also thank the following companies and institutions for their contribution to the project (in alphabetical order): Bennet Pump, Daimler, FirstElement Fuel, Hexagon Purus, Honda, LifteH2, Luxfer, National Renewable Energy Laboratory (NREL), National Technology & Engineering Solutions of Sandia, LLC (NESS), NPROXX, Risktec, Savannah River National Laboratory (SRNL) and TÜV SÜD Rail.